THE UNIVERSITY OF HULL

Investigations into the influence and role of tissue factor in the pathogenesis of myocardial hypertrophy

being a thesis submitted for the Degree of Doctor of philosophy

in the University of Hull

by

Georgia Alkistis Frentzou, MSc, BSc

April 2007

I. Declaration

The contents of this thesis have not been submitted in whole or part for any other academic award at the University of Hull or any other institution.

Georgia Alkistis Frentzou

20 April 2006

II. Abstract

Recently it has been demonstrated that tissue factor (TF) plays an important role in the induction and/or progression of cardiac hypertrophy. The aim of this thesis was to examine the relationship between TF and the onset of cardiac hypertrophy. Cardiac hypertrophy was achieved by aortic constriction in male Sprague-Dawely rats. TF levels increased in cardiac tissue but not in isolated cardiomyocytes suggesting another cellular site of TF expression. In contrast, tissue factor pathway inhibitor, (TFPI), was transiently up-regulated in cardiomyocytes potentially to counteract the effects of TF.

Stimulation of H9c2 cardiomyocytes with exogenous TF resulted in the up-regulation of mechano growth factor. Incubation of the cells with TF alone up-regulated atrial natriuretic factor (ANF) expression, whilst the presence of the TF-associated proteases, factor VIIa and factor Xa, suppressed this effect, suggesting that contact between TF and blood within the heart can exacerbates the hypertrophic response.

Moderate concentrations of TF were found to induce proliferation in H9c2 cardiomyocytes, while high concentrations of TF resulted in increased cellular apoptosis as detected by caspase-3 activation but via a p53-independent mechanism. In addition, supplementation of TF with proteolytically active factors, VIIa and Xa, partially abrogated this apoptotic effect. These data suggest that the expression of moderate concentrations of TF, induced by pressure overload observed during early hypertrophy, result in an enhanced rate of cellular turnover, and combined with hypertrophic growth, leads to alterations in heart structure. In contrast, higher concentrations of TF at later stages of disease can deplete the cardiomyocytes. In conclusion, TF appears to function as a pro-inflammatory mediator which is up-regulated at the onset of hypertrophy and is capable of influencing the progression of the disease through altering the function of cardiomyocytes.

III. Published work

Abstracts

G.A. Frentzou, A-M.L. Seymour, C. Ettelaie (2004). The expression of tissue factor and tissue factor pathway inhibitor in cardiac hypertrophy (abstract/poster). *British Society for Cardiovascular Research, Spring 2004 Meeting, University of Manchester*

G.A. Frentzou, C. Ettelaie, A-M.L. Seymour (2004). Exogenous tissue factor suppresses the expression of atrial natriuretic factor in H9c2 rat cardiomyocytes (abstract/poster). *British Society for Cardiovascular Research, Autumn 2004 Meeting, Kings College London*

G.A. Frentzou, C. Ettelaie, A-M.L. Seymour (2005). The expression of tissue factor and tissue factor pathway inhibitor in cardiac hypertrophy (abstract/poster). *International Society for Heart Research, 25th European Meeting, Tromso, Norway* (Supported by a travel grant awarded by the Heart Research UK). J Mol Cell Cardiol 38(6):1022

G.A. Frentzou, A-M.L. Seymour, C. Ettelaie (2005). The expression of atrial natriuretic factor in H9c2 cardiomyocytes in response to exogenous tissue factor (abstract/poster). *British Society of Thrombosis and Haemostasis, Autumn Meeting, Chester*

G.A. Frentzou, C. Ettelaie, A-M.L. Seymour (2006). Alterations in the expression of tissue factor and tissue factor pathway inhibitor induced by the onset of cardiac hypertrophy (abstract/poster). *International Society for Heart Research, 26th European Meeting, Manchester, UK.* J Mol Cell Cardiol 40(6):945

G.A. Frentzou, C. Ettelaie, A-M.L. Seymour (2006). Induction of cellular apoptosis in H9c2 cells by tissue factor (abstract/poster). *International Society for Heart Research, 26th European Meeting, Manchester, UK.* J Mol Cell Cardiol 40(6):998

IV. Contents

V. List of tables

VI. List of figures

VII. Acknowledgments

Doing a PhD is a roller-coaster of work and emotions, but when a thesis is about to be submitted, it defines the end of an era. For the completion of this project a lot of people played important roles. My appreciation and thanks goes to my supervisors, Dr Camille Ettelaie and Dr Anne-Marie L. Seymour for their continued guidance, and for always making time available. Their encouragement and friendship have helped to make this project thoroughly enjoyable. I am indebted to both of them for their endless support throughout. My gratitude goes to Heart Research UK for making this project possible.

Many thanks go to Ms Jenny Foster, Ms Kath Bulmer and Ms Rhonda Green for their greatly appreciated help, support and friendship throughout the past three years. Also a special word of thanks goes to my colleagues, now friends, from my two labs: Amandine, Chao, Mary, Ashwin, Jessica, Veena and Dunja. "Thank you guys for always being there, and for your fantastic company at conferences". I will never forget the time in Birmingham- *'Lakeside, near the lake'*, Tromso – *'There and back again'*, Chester- *'Cocktail nights'* and Manchester – *'Because, we are such good travellers'* - I will always cherish them! To my colleague and friend Valentina, from the MRL, many thanks for our endless conversations, coffees and fun during the past three years.

On a personal note I am very grateful to my friends back in Preston: Ria and Chris and Leanne and Mark for supporting me throughout this study and for always finding the time to make the journey across. A special word of thanks goes to my Fiancé Simon, whose dedication, love and support have been so important for the completion of this thesis. "Thank you Simon, for your useful advice and your unquestionable faith in me". Last but not least I would like to express my appreciation to my Mum and Step-Dad for believing in me. "Thank you Mum for always been so supportive and thank you Vasili for been my pc wizard for the past seven years". On a special note, I would also like to thank my dad, his memory kept me going.

VIII. Abbreviations

ACE:	angiotensin converting enzyme
ACE inhibitors:	angiotensin converting enzyme inhibitors
ANF:	atrial natriuretic factor
Ang II:	angiotensin II
Ala-Glu:	alanine-glutamine
A_{260}:	absorbance at 260 nm
AT_1:	angiotensin II receptor 1
AT_2:	angiotensin II receptor 2
BNP:	brain natriuretic peptide
BDM:	butanedione monoxime
BSA:	bovine serum albumin
bp:	base pairs
bWt:	body weight
cDNA:	complementary deoxyribonucleic acid
cGMP:	cyclic 3', 5' –guanosine monophosphate
CO_2:	carbon dioxide
cm^2:	square centimetres
°C:	centigrade
Ca^{2+}:	calcium ions
CE:	cardiac efficiency
CNP:	C-type natriuretic peptide
dH_2O:	distilled water
DMSO:	di-methyl sulphoxide
DMEM:	Dulbeco's modified essential medium
ET-1:	endothelin 1
ET_A:	endothelin type A
EDTA:	ethylenediaminetetraacetic acid
FasL:	Fas ligand
FCS:	foetal calf serum
FVII:	factor VII
FVIIa:	activated factor VII

FX:	factor X
FXa:	activated factor X
FIX:	factor IX
FIXa:	activated factor IX
FXII:	factor XII
FXIIa:	activated factor XII
FXI:	factor XI
FXI:	activated factor XI
FVIII:	factor VIII
FXIII:	factor XIII
FXIIIa:	activated factor XIII
FSC:	Forward scatter
g:	grams
G_q:	G coupled protein q
GAP3DH:	glyceraldehyde-3-phosphate dehydrogenase
GTP:	guanidine triphosphate
h:	hour
H^+:	hydrogen ions
HRP:	horse radish peroxidase
IGF-I:	insulin-like growth factor-I
IgG:	immunoglobulin G
IL-1β:	interleukin 1β
IAPs:	inhibitors of apoptosis proteins
JAK:	Janus kinase
KHB:	Krebs Hensleit bicarbonate Buffer
LVDP:	left ventricular developed pressure
mA:	milliamps
MAPK:	mitogen activated protein kinase
MGF:	mechano growth factor
l/h:	litres per hour
min:	minutes
MMPs:	matrix metaloproteinases
mRNA:	messenger ribonucleic acid
MLP:	cytoskeletal-associated muscle L_1M protein

MHCβ:	myosin heavy chain beta
MVO_2:	oxygen consumption
NF-κB:	nuclear factor κB
nMHC:	neonatal myosin heavy chain
NPs:	natriuretic peptides
NPR-A:	natriuretic peptide receptor A
NPA-B:	natriuretic peptide receptor B
NPA-C:	natriuretic peptide receptor C
OD:	outer diameter
PAR:	protease activated receptor
PBS:	phosphate buffer saline
PCR:	polymerase chain reaction
PI3 kinase:	phosphotidylinositide-3-(OH) kinase
PKC:	protein kinase C
PKC-β:	protein kinase cytokine β
PLC:	phospholipase C
pO_2:	partial pressure of oxygen
rpm:	revolutions per minute
RAS:	renin-angiotensin system
rTdT:	recombinant terminal Deoxynucleotidyl Transferase
RT-PCR:	reverse transcription-polymerase chain reaction
RPP:	Rate pressure product
SD:	standard deviation
SDS-PAGE:	sodium dodecyl polyacrylamide gel electrophoresis
SERCA-2a:	sarcoplasmic reticular calcium ATPase type 2a
SEM:	standard error of the mean
shRNA:	short hairpin ribonucleic acid
SMCs:	smooth muscle cells
SSc:	side scatter
TBE:	tris borate –EDTA
TBST:	tris-buffered saline Tween 20
TEMED:	tetramethylethylenediamine
TFPI:	tissue factor pathway inhibitor
TGF:	transforming growth factor

TIMPs:	inhibitors of matrix metaloproteinases
TMB:	3,3',5,5'tetramethylbenzidine
TNF:	tumour necrosis factor
TF:	tissue factor
TF/FVIIa:	tissue factor/activated factor VII complex
TF/FVIIa/FXa:	tissue factor/activated factor VII/activated factor X complex
TF/FVIIa/FXa/TFPI:	tissue factor/activated factor VII/activated factor X/tissue factor pathway inhibitor complex
TK:	tyrosine kinase
TUNEL:	TdT-mediated dUTP nick and labelling
2D:	two dimensional
V:	volts

To My Mum

Thank you Nefeli, for teaching me to always aim higher

"The only true wisdom is in knowing you know nothing."

- Socrates -

CHAPTER 1

Introduction

1. Introduction

1.1 Heart failure

Cardiovascular disease and heart failure are primary causes of global morbidity and mortality, and are responsible for one in three deaths worldwide. Every year 32 million individuals suffer heart attacks and strokes. The major risk factors for cardiovascular disease, include hypertension, hypertrophy, diabetes, smoking, high blood lipids and physical inactivity (Figure 1.1) (WHO, 2002).

Heart failure is defined as the inability of the heart to meet the demands of the body (Katz, 2003). It is a progressive condition that can be defined by cellular and molecular abnormalities, leading to remodelling of the heart when chronic mechanical overload stimulates adult cardiomyocytes to undergo hypertrophy (Katz 2003, Katz 1994). These cells are terminally differentiated and have little or no capacity to divide (Katz 2003, Katz 1994). Initially the hypertrophic response is compensatory, however, at later stages, it becomes pathological, representing the limited adaptive capacity of cardiomyocytes (Katz 2003, Katz 1994, Meerson 1969). Cardiac hypertrophy is itself an independent risk factor in the development of heart failure (Figure 1.1) (Katz 2003, Frey & Olson 2003).

Heart failure is a combination of symptoms, of which contractile dysfunction is considered a major element. A defect in sarcomere shortening in cardiomyocytes has been shown in a number of experimental animal models and clinical studies (Koide *et al.* 1997). Ventricular assist devices have been found to partially reverse this contractile dysfunction (Dipla *et al.* 1998). In cases of chronic systolic heart failure,

Figure 1.1: Major risk factors leading to heart failure.

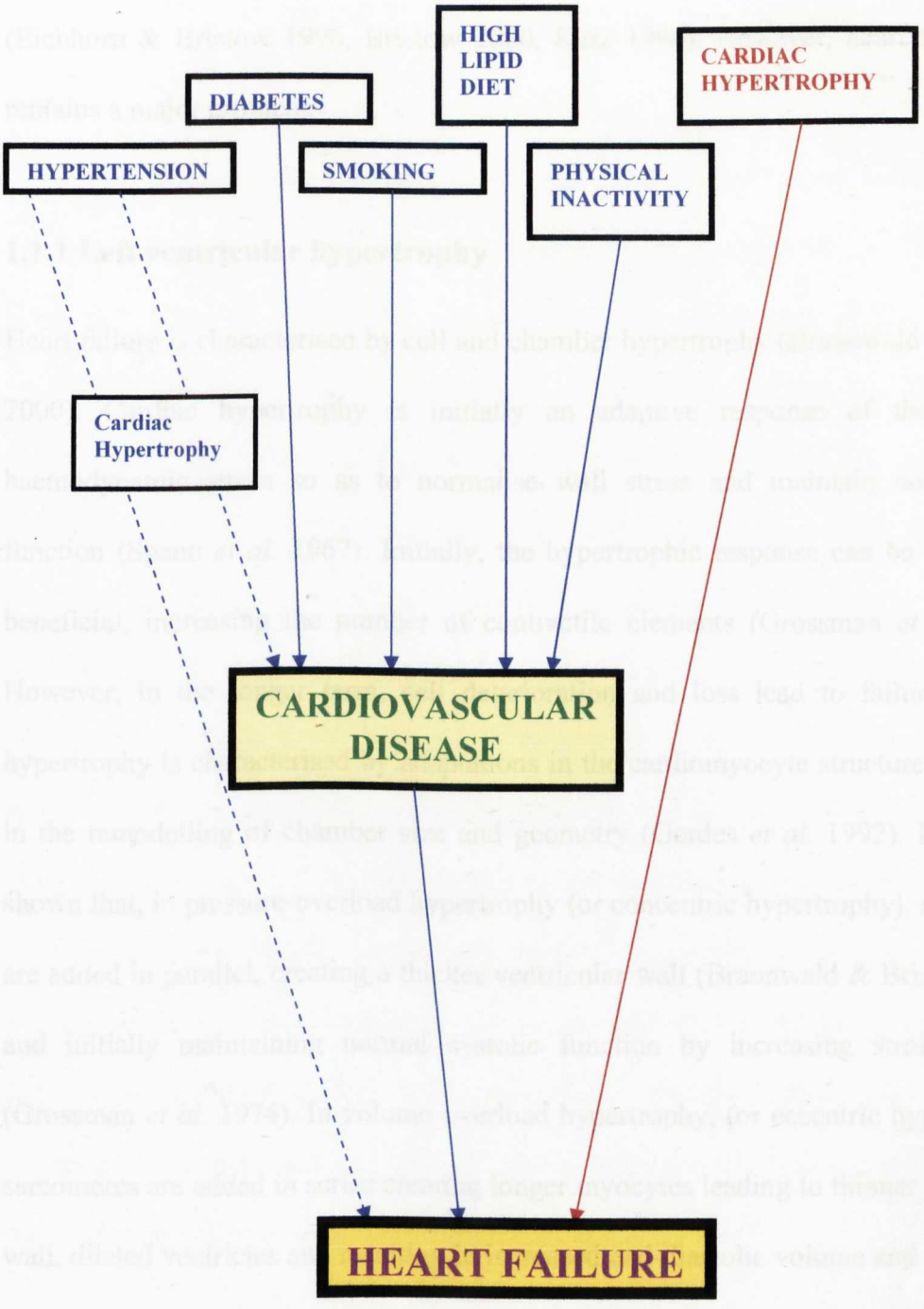

A schematic representation showing the risk factors that can lead to cardiovascular disease and ultimately to heart failure. Cardiac hypertrophy is itself an independent risk factor in the development of heart failure.

β-adrenergic blocking agents such as propranolol and metoprolol and ACE inhibitors such as enalapril, captopril and benazepril which can lower the blood pressure, have been shown to improve systolic function and potentially may reverse remodelling (Eichhorn & Bristow 1996, Bristow 2000, Katz 1994). However, heart failure still remains a major problem.

1.1.1 Left ventricular hypertrophy

Heart failure is characterised by cell and chamber hypertrophy (Braunwald & Bristow 2000). Cardiac hypertrophy is initially an adaptive response of the heart to haemodynamic stress so as to normalise wall stress and maintain normal heart function (Spann *et al.* 1967). Initially, the hypertrophic response can be considered beneficial, increasing the number of contractile elements (Grossman *et al.* 1974). However, in the longer term, cell deterioration and loss lead to failure. Cardiac hypertrophy is characterised by adaptations in the cardiomyocyte structure that result in the remodelling of chamber size and geometry (Gerdes *et al.* 1992). It has been shown that, in pressure-overload hypertrophy (or concentric hypertrophy), sarcomeres are added in parallel, creating a thicker ventricular wall (Braunwald & Bristow 2000) and initially maintaining normal systolic function by increasing stroke volume (Grossman *et al.* 1974). In volume overload hypertrophy, (or eccentric hypertrophy), sarcomeres are added in series creating longer myocytes leading to thinner ventricular wall, dilated ventricles and resulting in increased end-diastolic volume and ventricular dysfunction (Braunwald & Bristow 2000, Grossman *et al.* 1974, Frey & Olson 2003). As the heart contains a number of different cell types, pathophysiologic hypertrophy leads to alterations in other cell types such as fibroblasts (Braunwald & Bristow 2000). Increased expression of extracellular matrix associated proteins in fibroblasts,

including collagen, fibronectin, matrix metalloproteinases (MMPs) and their inhibitors (TIMPs) lead to interstitial fibrosis that stiffen the ventricles and impair contraction and relaxation (Li *et al.* 1998, Shirwany & Weber 2006, Weber 2005).

1.1.1.1 Signal transduction in hypertrophy

A number of signalling pathways have been demonstrated to be involved in the development of hypertrophy (Frey & Olson 2003). Changes in myocardial gene expression occur as a result of increased haemodynamic overload and stretch. A number of different agonists, including norepinephrine, angiotensin II (Ang II), endothelin 1 (ET-1), fibroblasts growth factor, transforming growth factor β (TGF- β), tumour necrosis factor α (TNF-α), interleukin 1β (IL-1β) and G-protein 130-signalling cytokines are also thought to trigger signalling leading to hypertrophy (Braunwald & Bristow 2000). These triggers involve a sequence of signal transduction proteins/receptors, including α- and β- adrenergic receptors, AT_1 receptors, ET_A receptors, TNF receptors, IL-1 receptors, ras, Ga_q and Ga_s proteins according to the initial stimulus (table 1.1) (Frey & Olson 2003). Subsequently, protein kinase C, mitogen-activated protein kinase and Raf-1 kinases, CAM kinase, calcineurin pathway, may be activated causing the re-expression of foetal genes (Figure 1.2) (Braunwald & Bristow 2000). It has been shown that the activation of G-coupled isoforms of protein kinase C can initiate hypertrophy, leading to a fibrotic cardiomyopathy (D' Angelo *et al.* 1997, Wakasaki *et al.* 1997).

Of great interest and one of the most characterised trigger is the renin-angiotensin system (RAS). The RAS has Ang II as its active component, which is responsible for regulating blood pressure, plasma volume and sympathetic nervous activity under

Table 1.1: Triggers, receptors and signal transduction pathways that are involved in pathological hypertrophy.

TRIGGER	RECEPTORS/ SIGNAL TRANSDUCTION PATHWAY
Stretch/ wall stress	G_q/PLC/PKC, sarcolemmal ion channels
Angiotensin II	AT_1 receptor- G_q/PKCβ, TK pathways, MAPK pathways, JAK/STAT pathways, others
Norephinephrine	α-, β- Adrenergic pathways, oxidative signaling
Endothelin	ET_A receptor- G_q/PKCβ pathway, calcineurin and CAMK pathways
TNF-α	TNF receptors, MAPK, PKC
IL 1β	IL 1β receptors, MAPK, TK pathways
Cardiotropin-1	Gp 130 pathways

PLC: phospholipase C, PKC: protein kinase C, G_q: G coupled protein q, AT_1: angiotensin 1, MAPK: mitogen activated protein kinase, ET_A: endothelin type A, TNF: tumour necrosis factor, TK: tyrosine kinase, IL 1β: interleukin 1 β *(Adapted from Braunwald & Bristow 2000).*

Figure 1.2: Different pathways that could lead to cardiac hypertrophy.

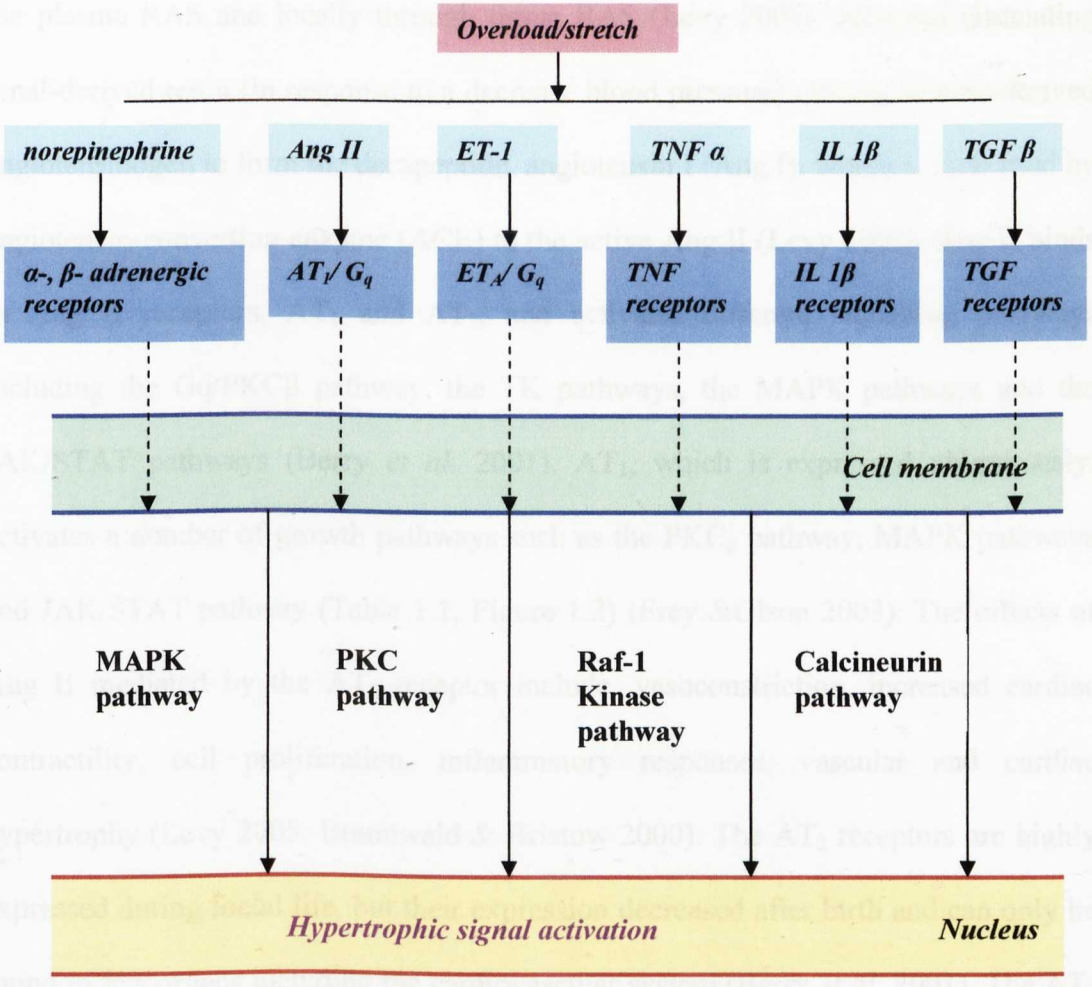

A schematic representation showing the signalling pathways involved in the induction of cardiac hypertrophy. Ang II, TGF β, TNF α, IL β, etc could bind to membrane receptors, leading to the activation of MAPK, PKC, Raf-1 kinase and/or Calcineurin pathways. Subsequently, initiation of a hypertrophic response occurs, leading ultimately to heart failure (Braunwald & Bristow 2000). For simplicity, interactions between the different pathways are not shown.

physiological conditions (Levy 2005). However Ang II can also play a role in pathophysiological cardiac hypertrophy, myocardial infarction, hypertension and atherosclerosis (Ichihara *et al.* 2001, Huriuchi *et al.* 1999). Ang II is synthesised by the plasma RAS and locally through tissue RAS (Levy 2005). Elevated circulating renal-derived renin (in response to a decrease blood pressure) cleaves hepatic-derived angiotensinogen to form the decapeptide, angiotensin I (Ang I), which is converted by angiotensin-converting enzyme (ACE) to the active Ang II (Levy 2005). Ang II binds to Ang II receptors, AT_1 and AT_2, and activates different signalling pathways including the Gq/PKCβ pathway, the TK pathways, the MAPK pathways and the JAK/STAT pathways (Berry *et al.* 2001). AT_1, which is expressed ubiquitously, activates a number of growth pathways such as the PKC_β pathway, MAPK pathways and JAK/STAT pathway (Table 1.1, Figure 1.2) (Frey &Olson 2003). The effects of Ang II mediated by the AT_1 receptor include, vasoconstriction, increased cardiac contractility, cell proliferation, inflammatory responses, vascular and cardiac hypertrophy (Levy 2005, Braunwald & Bristow 2000). The AT_2 receptors are highly expressed during foetal life, but their expression decreased after birth and can only be found in few organs including the cardiovascular system (Berry *et al.* 2001). The AT_2 receptors are re-expressed during adulthood after cardiac damaged and wound healing, suggesting that they may play a role in tissue remodelling (Otsuka *et al.* 1998). AT_2 receptor is believed to induce opposing effects to the AT_1 receptor, such as vasodilation and antigrowth and antihypertrophic effects (Siragy 2000), and to play a role in blood pressure regulation (Carey *et al.* 2001).

1.1.1.1.1 The role of calcium and calcineurin in the development of cardiac hypertrophy

Sarcolemmal ion channels are thought to be activated via stretch and transmit signals via the cytoskeleton to the nuclear membrane to trigger hypertrophy (Komuro & Yazaki 1994). Calcineurin is a potential trigger of hypertrophy. Intracellular calcium is involved in the calcineurin pathway and calmodulin kinase pathway and when increased via this pathway is thought to play a role in hypertrophic responses due to neurohormonal-cytokine signalling (Molkentin *et al.* 1998, Lim *et al.* 2000, Zhu *et al.* 2000).

The serine-threonine calcineurin is expressed in multiple tissues and has been identified as a central pro-hypertrophic signalling molecule in the heart (Heineke & Molkentin 2006, Frey & Olson 2003). Calcineurin consist of a catalytic subunit (CnA) and a regulatory subunit (CnB), and becomes active through the direct binding of the Ca^{+2}-binding adaptor protein calmodulin (Heineke & Molkentin 2006). Further to this, calcineurin phosphorylates transcription factors of the nuclear factor of activated T-cells (NFAT), resulting in the translocation of NFAT proteins to the nucleus and the prohypertrophic gene expression (Wilkins & Molkentin 2004, Frey & Olson 2003). NFAT transcription factors are classified as the primary calcineurin effectors in the heart and have been found to sufficiently mediate cardiac hypertrophy (Molkentin *et al.* 1998, Wilkins *et al.* 2002). Calcineurin is also regulated by structural proteins found to the Z-disc in cardiomyocytes in an area that also contains NFAT (Knoll *et al.* 2002, Frey *et al.* 2004). Furthermore, the calcineurin-NFAT signalling is controlled by specific kinases such as GSK3β, p38 and JNK, which direct phosphorylate the regulatory domain of NFAT (Antos *et al.* 2002, Braz *et al.* 2003, Liang *et al.* 2003).

1.1.1.2 Adaptation in hypertrophy: Early changes

The main response of the myocardium as it undergoes the hypertrophic response, is the activation of the immediate early genes (Lee *et al.* 1988), the re-expression of foetal genes (Izumo *et al.* 1987, Schwartz *et al.* 1986, Izumo *et al.* 1988) and changes in the expression of contractile (Swynghedauw 1986, Nadal-Ginard & Mahdavi 1989, Lowers *et al.* 1997, Miyata *et al.* 2000) and calcium handling proteins (Chang *et al.* 1997, Feldman *et al.* 1993, Meyer *et al.* 1995, Braunwald & Bristow 2000), adaptations in cardiac metabolism (Stanley *et al.* 2005) and overall increases in protein synthesis (Frey & Olson 2003, Lee *et al.* 1988). A schematic representation of the early changes in cardiac hypertrophy can be seen in Figure 1.3. Alternatively, physiological cardiac hypertrophy (or exercise induce hypertrophy) has similarities with a mild condition of pathological hypertrophy but is typically not accompanied by collagen accumulation and usually does not exceed a modest increase in left ventricular wall (Frey & Olson 2003). A schematic representation underlying the fundamental differences of pathological hypertrophy and physiological hypertrophy is shown in Figure 1.4.

The induction of the immediate early genes is the earliest detectable effect of growth (Figure 1.3) and they are characterised by their rapid induction (Sheng & Greenberg 1990, Chien *et al.* 1991). The proto-oncogenes, c-fos and c-jun are two key members of the immediate early gene family (Chien *et al.* 1991). Studies have identified new members of the fos and jun gene family, as well as, a series of related zinc finger genes, including erg-1, krox-24, NGFa, tis 8, erg-2 (Sukhatme *et al.* 1988, Christy *et al.* 1988, Lemaire *et al.* 1988, Rangnekar *et al.* 1990), that have structural characteristics and are members of the steroid receptor superfamily (Lemaire *et al.*

Figure 1.3: Early changes in cardiac hypertrophy.

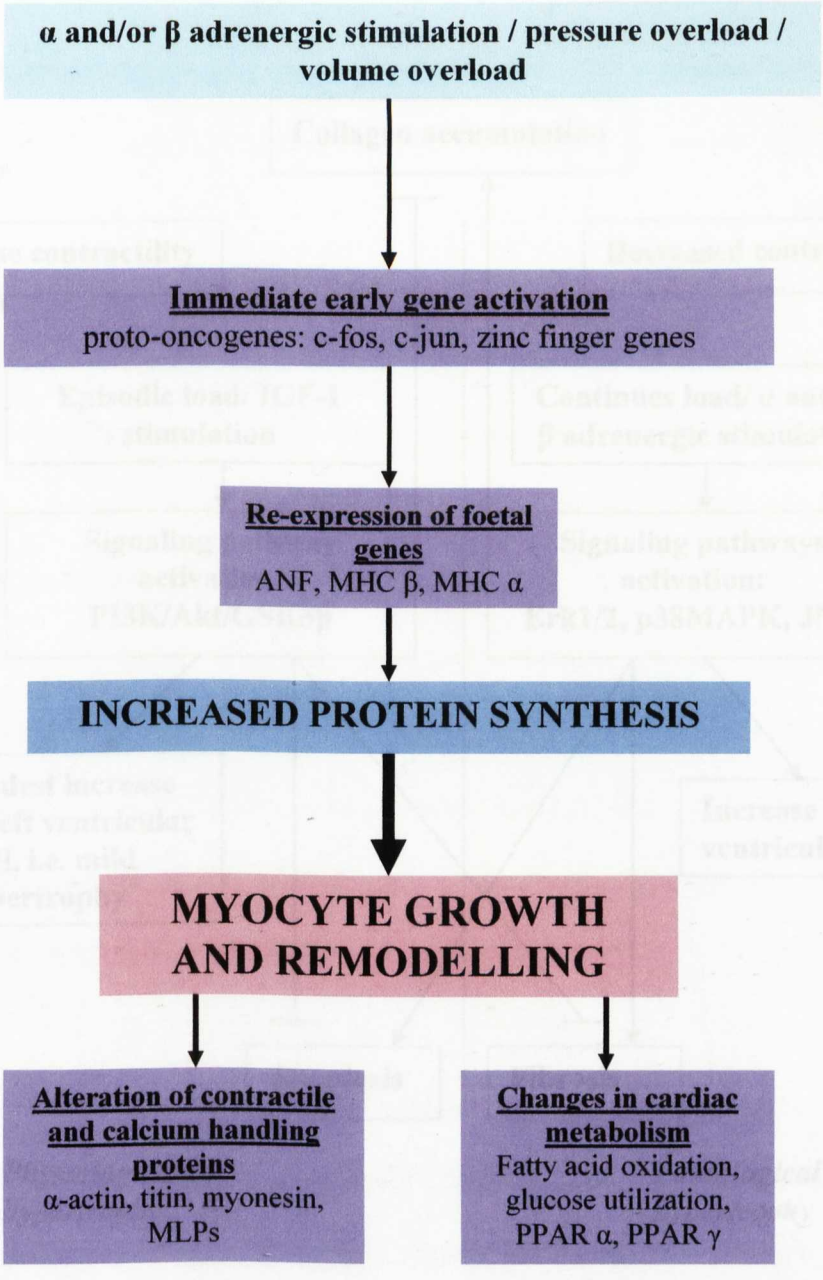

A simple schematic representation showing the early changes occurring in left ventricular cardiac hypertrophy. Upon stimulation, the immediate early genes are the first to be activated, following re-expression of the foetal genes and alterations in contractile and calcium handling proteins. Overall protein synthesis is increased and myocyte growth is observed.

Figure 1.4: A schematic representation showing the differences of pathological and physiological hypertrophy.

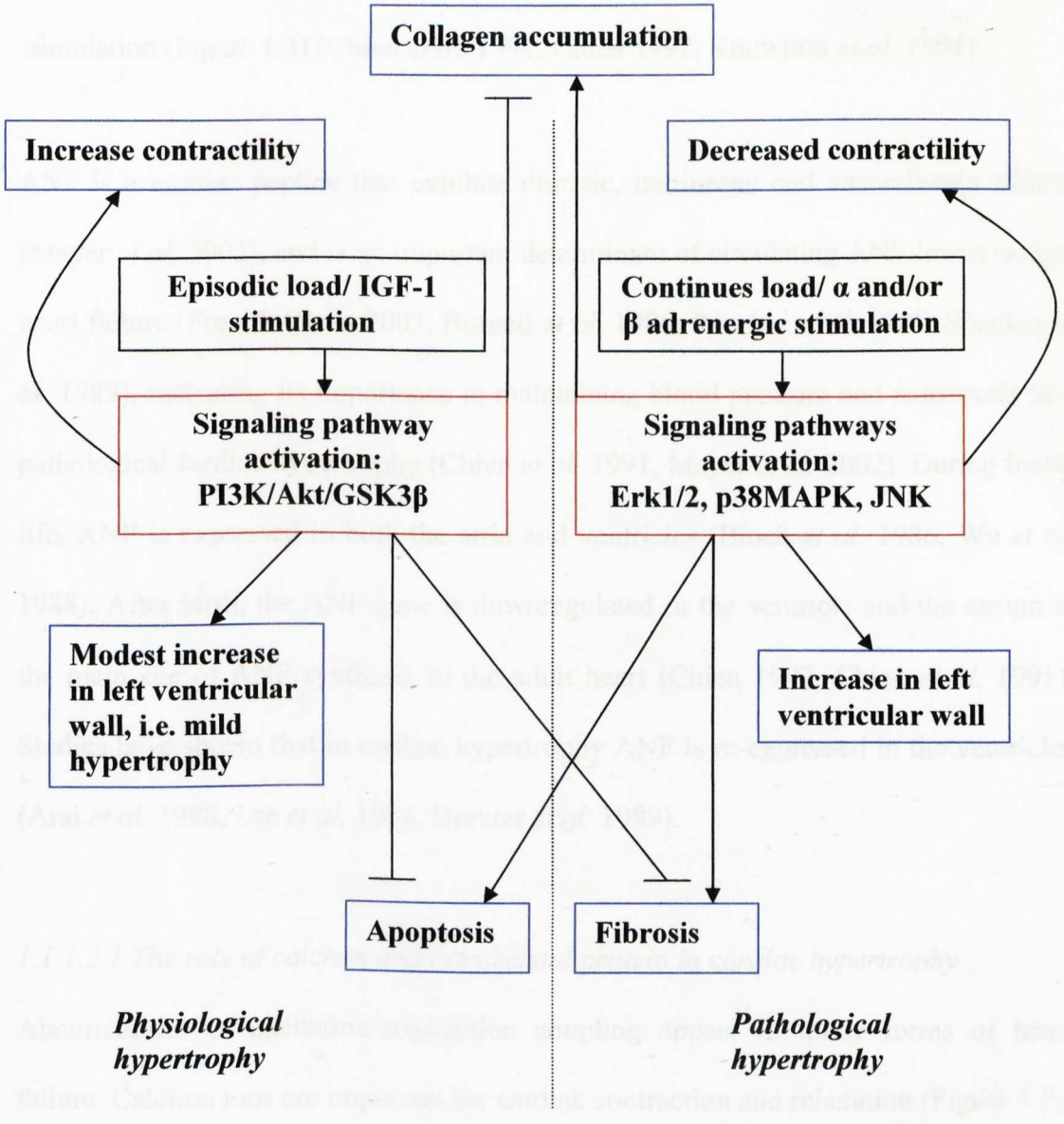

A simple schematic representation showing the differences of pathological and physiological hypertrophy. Upon activation of the signalling pathways, in pathological hypertrophy increased left ventricular wall, decrease contractility, collagen accumulation, fibrosis and myocyte apoptosis are observed. In contrast, physiological hypertrophy is accompanied by a modest increase in left ventricular wall and increase contractility without signs of collagen accumulation, fibrosis or apoptosis (Hart 2003, Tetsuro *et al.* 2004, Isumo 2006).

1988, Hazel *et al.* 1988). C-fos and c-jun early genes are induced upon α- and β-adrenergic stimulation, whereas Erg-1 is only induced upon α-adrenergic stimulus (LaMorte *et al.* 1994, Petersen *et al.* 2000). The induction of Erg-1 is thought to play an important role in the re-expression of ANF gene that is induced upon α-adrenergic stimulation (Figure 1.3) (Chien *et al.* 1991, Chien 1992, Knowlton *et al.* 1991).

ANF is a cardiac peptide that exhibits diuretic, natriuretic and vasorelaxant effects (Mayer *et al.* 2002), and is an important determinant of circulating ANF levels during heart failure (Frey & Olson 2003, Burnett *et al.* 1986, Rascher *et al.* 1985, Shenker *et al.* 1985), indicating its importance in maintaining blood pressure and natriuresis in a pathological cardiac hypertrophy (Chien *et al.* 1991, Mayer *et al.* 2002). During foetal life, ANF is expressed in both the atria and ventricles (Bloch *et al.* 1986, Wu *et al.* 1988). After birth, the ANF gene is downregulated in the ventricle and the atrium is the main site of ANF synthesis in the adult heart (Chien 1992, Chien *et al.* 1991). Studies have shown that in cardiac hypertrophy ANF is re-expressed in the ventricles (Arai *et al.* 1988, Lee *et al.* 1988, Drexter *et al.* 1989).

1.1.1.2.1 The role of calcium and cytoskeletal protein in cardiac hypertrophy

Abnormalities of excitation-contraction coupling appear in many forms of heart failure. Calcium ions are important for cardiac contraction and relaxation (Figure 1.5). Changes in trans-sarcolemmal and intra-cellular Ca^{2+} movements due to malfunction of receptors, pumps and proteins have been implicated in altered Ca^{2+} handling and consequent cardiac dysfunction (Houser & Margulies 2003, Beuckelmann *et al.* 1992). The outcome of these changes is elevated diastolic Ca^{2+} levels (Beuckelmann *et al.* 1992) and decreased systolic Ca^{2+} levels followed by a prolonged relaxation

Figure 1.5: Cardiac contraction and relaxation.

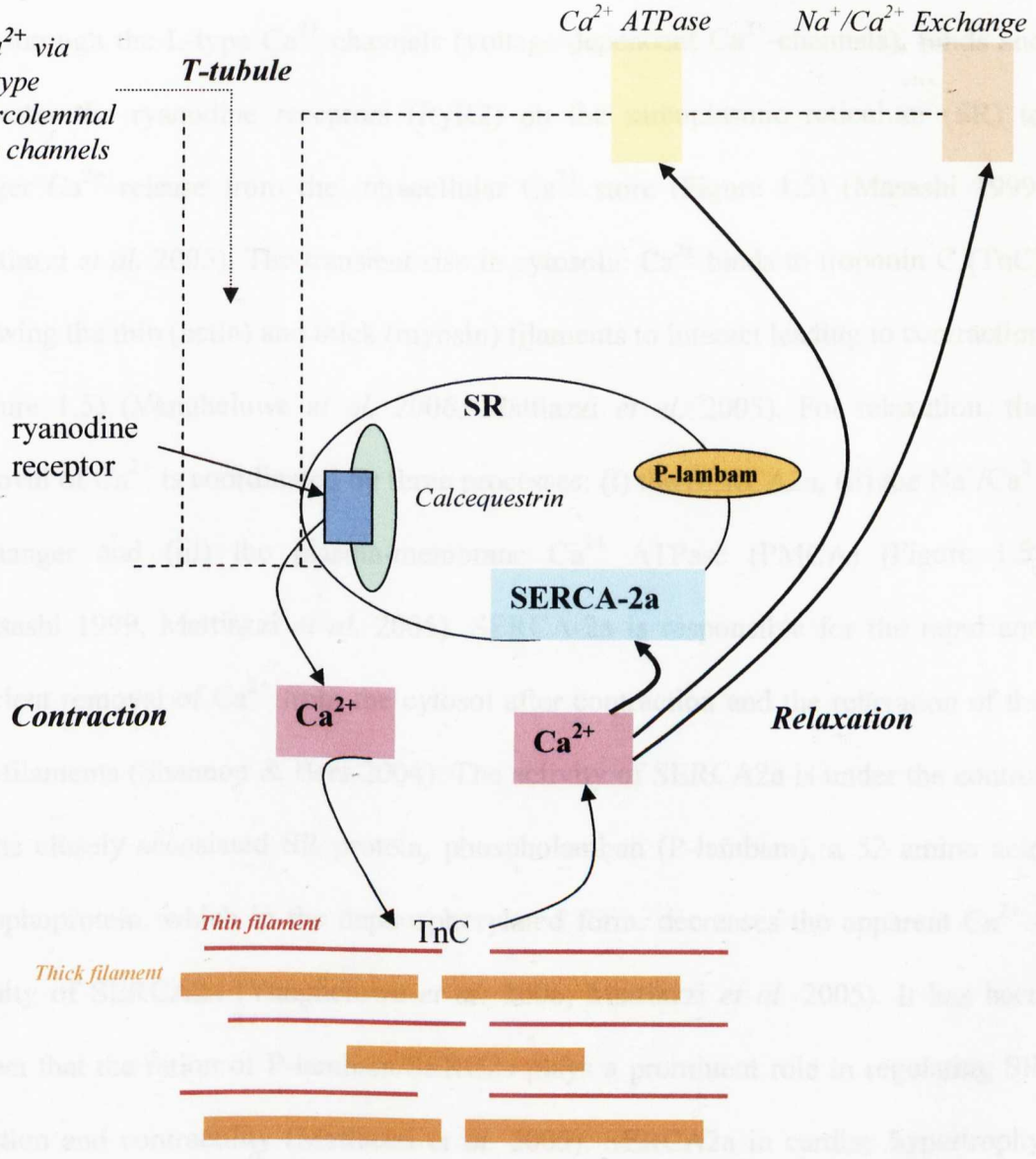

A schematic diagram showing the cycle of cardiac contraction and relaxation. Ca^{2+} influx via L-type sarcolemmal Ca^{2+} channels, activated during an action potential, triggers Ca^{2+} release from sarcoplasmic reticulum. Ca^{2+} binds to troponin C (TnC) and allows actinomyosin interaction resulting in cross bridge formation and contraction. Following systole, cytosolic Ca^{2+} is removed by the sarcoplasmic reticulum via SERCA2 or via Na^{+}/Ca^{2+} exchanger and Ca^{2+}ATPase (relaxation).

phase (Gwathmey & Morgan, 1985). These changes are caused by impairment in protein expression (Meyer *et al.* 1995) and function of sarcoplasmic reticular ATPase (SERCA-2a) (Schwinger *et al.* 1999). During cardiac action potential, Ca^{2+} enters the cell through the L-type Ca^{2+} channels (voltage-dependent Ca^{2+} channels), binds and activates the ryanodine receptors (RyR2) on the sarcoplasmic reticulum (SR) to trigger Ca^{2+} release from the intracellular Ca^{2+} store (Figure 1.5) (Masashi 1999, Mattiazzi *et al.* 2005). The transient rise in cytosolic Ca^{2+} binds to troponin C (TnC) allowing the thin (actin) and thick (myosin) filaments to interact leading to contraction (Figure 1.5) (Vangheluwe *et al.* 2006, Mattiazzi *et al.* 2005). For relaxation, the removal of Ca^{2+} is coordinated by three processes: (i) the SERCA2a, (ii) the Na^{+}/Ca^{2+} exchanger and (iii) the plasma-membrane Ca^{2+} ATPase (PMCA) (Figure 1.5) (Masashi 1999, Mattiazzi *et al.* 2005). SERCA-2a is responsible for the rapid and efficient removal of Ca^{2+} from the cytosol after contraction and the relaxation of the myofilaments (Shannon & Bers 2004). The activity of SERCA2a is under the control of the closely accosiated SR protein, phospholamban (P-lambam), a 52 amino acid phosphoprotein, which in the dephosphorylated form, decreases the apparent Ca^{2+} - affinity of SERCA2a (Vangheluwe *et al.* 2006, Mattiazzi *et al.* 2005). It has been shown that the ration of P-lambam/SERC2a plays a prominent role in regulating SR function and contractility (Mattiazzi *et al.* 2005). SERCA2a in cardiac hypertrophy has been shown to be downregulated resulting in impaired diastolic and systolic function (Houser & Margulies 2003).

Experimental studies have shown changes in the sarcomeric proteins in the failing heart (Lowers *et al.* 1997, Morano *et al.* 1977). These include the switch in the isoforms of myosin heavy chain β (MHCβ), troponin T and myosin light chain 1

isoforms (Lowers *et al.* 1997, Nakao *et al.* 1997, Miyata 2000, Anderson *et al.* 1995, Hitzel *et al.* 1985, Morano *et al.* 1977). Such changes are considered as a re-expression of foetal phenotype (Figure 1.3) (Frey & Olson 2003). The mRNA levels of the contractile protein, myosin light chain 2 have been found to be up-regulated, corresponding to accumulation of this contractile protein in myocardial cells (Lee *et al.* 1988). Furthermore, the induction of genes encoding for contractile protein normally expressed in foetal life, such as skeletal actin α and MHCβ, alters the contractile protein content in cardiac hypertrophy (Izumo *et al.* 1987, Schwartz K *et al.* 1986, Izumo *et al.* 1988). It has been shown that the induction of foetal genes for the thick and thin filament of the contractile proteins such as MHCβ and troponin T, slow myofibrillar ATPase activity and contractile function, (Braunwald & Bristow 2000, Pagani *et al.* 1988). These changes may thus make contractile function more efficient in the short term. Changes in myosin heavy chain α (MHCα) (down-regulated during hypertrophy and foetal development) and in MHCβ (up-regulated in hypertrophy and foetal development), result in decrease contractile function and an increase in cell growth (Braunwald & Bristow 2000). The end result of the induction of the foetal genes is stimulation of protein synthesis which results in the enlargement of cardiomyocytes to normalise wall stress (Frey & Olson 2003). Furthermore, possible maladaptation of neurohormonal/cytokine activation occurs resulting to progression of hypertrophy (Frey & Olson 2003, Braunwald & Bristow 2000). Subsequently, there is a reduction in stoke volume and increase in ventricular volume as hypertrophy moves from compensated to decompensate failure (Alpert *et al.* 1979).

Under pressure overload, excessive microtubular polymerisation impeding sarcomere motion, affects adversely the systolic function (Tsutsui *et al.* 1994). A number of

cytoskeletal proteins including desmin, tubulin, vinculin, dystrophin, talin and spectrin have been shown to increase in end-state heart failure (Hein *et al.* 2000). In addition, the sarcomeric skeletal proteins, α-actin, titin and myonesin have been shown to decrease (Hein *et al.* 2000). These adaptations are thought to modify the normal cardiomyocyte function and are part of the remodelling process (Figure 1.3) (Braunwald & Bristow 2000).

Mutations in cytoskeletal genes can give rise to the alterations which underlying different dilated cardiomyopathies (Towbin 1998), including dystrophin, desmin, sarcoglycans and nuclear envelope proteins, laminin A and laminin C (Towbin 1998, Li *et al.* 1999, Barresi *et al.* 2000, Fatkin *et al.* 1999, Brodsky *et al.* 2000). In the syrian hamster model of cardiomyopathy, a mutation in the δ-sarcoglycan gene resulting in the deficiency of δ-sarcoglycan transcripts and consequently in the loss of δ-sarcoglycan protein, has been identified as a primary cause of the heart failure (Sakamoto *et al.* 1997). Several studies have demonstrated that abnormalities of the cytoskeletal-associated muscle L_1M protein (MLP), in animals can cause dilated cardiomyopathy and its expression is decreased in the failing left ventricular myocardium (Arber *et al.* 1997, Zolk *et al.* 2000). MLP is essential for the regulation of the cytoarchitecture of cardiomyocytes and when decreased, can be responsible for impaired systolic function (Katz 2000). This evidence suggests that mutations in the genes responsible for cytoskeletal proteins can result in idiopathic dilated cardiomyopathy and may play a role in the development of other dilated cardiomyopathies (Figure 1.3) (Braunwald & Bristow 2000).

1.1.2 Natriuretic peptides and their involvement in cardiac hypertrophy

Natriuretic peptides (NPs) comprise a family of peptide hormones that have an important role in the regulation of cardiovascular, endocrine and renal homeostasis (Levin *et al.* 1998, Gardner 2003). The family includes the atrial natriuretic peptide (ANP), otherwise known as atrial natriuretic factor (ANF), the brain natriuretic peptide (BNP) and the C-type natriuretic peptide (CNP) (Yap *et al.* 2004, Gardner 2003). ANF and BNP are of cardiac origin while CNP is primarily produced in the vascular endothelium and in the nervous system (Yap *et al.* 2004, Gardner 2003). In general, the natriuretic peptides have a range of actions throughout the body, including fluid and pressure control and local neuroendocrine actions (Yap *et al.* 2004). ANF and BNP are primarily produced in the myocytes of the cardiac atria (Gardner 2003). However, synthesis in the ventricles is high in late foetal and early neonatal life and decreases to adult levels within the first few weeks to months after birth (Chien *et al.* 1993). Furthermore, both proteins are re-expressed in the adult ventricles, along with other foetal genes, in conditions associated with myocardial hypertrophy (Chien *et al.* 1993). Expression of the genes encoding ANF and BNP have been proven to be one of the most reliable markers for activation of the hypertrophic programme in clinical states and experimental models of cardiac hypertrophy and expression is maintained as the ventricles remodel and dilate with progression to heart failure (Mukoyama *et al.* 1991, Wei *et al.* 1993).

The ANF gene is located in chromosome 1 and is synthesized as a high molecular weight precursor with a 17-amino acid ring structure (that is also present in BNP) (Yap *et al.* 2004, Ogawa *et al.* 1995). Translation of the ANF mRNA produces a 150-amino acid precursor called pre-proANF (Yang-Feng *et al.* 1985). ANP expression is

increased upon hypovolemia, endothelin, vasopressin and catecholamine stimulation (Stein & Levin 1998), α1- and β2-adrenergic stimulation (Morisco *et al.* 2000, Sprenkle *et al.* 1995) and hypoxia (Chen *et al.* 1997). After synthesis the pre-proANF is enzymatically transformed into a 126-amino acid proprecursor (proANF) and stored in the atrial myocyte granules (Yap *et al.* 2004). Upon secretion, proANF is cleaved by corin (Yan *et al.* 2000) or prohormone convertase (PC1/3) (Wu *et al.* 2002) to give an N-terminal fragment (NT-ANF 1-98) and a biological active C-terminal ANF 28 hormone (ANF 99-126) (Kelly & Struthers 2001). A similar process occurs for the synthesis of BNP, where furin (an endoprotease) cleaves the BNP precursor into an active C-terminal BNP 32 and an N-terminal proBNP 1-76 (Sawada *et al.* 1997).

There are three main natiuretic peptide receptors, the NPR-A, NPR-B and NPR-C (Yap *et al.* 2004). All three receptors are guanylyl cyclase (GC)-linked transmembrane receptors which convert guanidine triphosphate (GTP) into cyclic 3', 5' –guanosine monophosphate (cGMP) as part of the intracellular messenger (Chinkers & Garbers 1991, Gardner 2003). NPR-A receptor can recapture both ANF and BNP, whereas NPR-B is specific for CNP, while NPR-C can bind to all the three natriuretic peptides (Figure 1.6) as it is involved in the natriuretic peptide degradation and clearance from the circulation (Gardner 2003, Engel & Lowe 1995, Matsukawa *et al.* 1999). Intracellular increase of cGMP following activation of the natriuretic peptide receptors modulates downstream proteins including phosphodiesterases, ion channels and cGMP –dependent protein kinases via phospatase phosphorylation of channel proteins which ultimately are able to modify cellular functions (Soderling & Beavo 2000, Lohmann *et al.* 1997, Yap *et al.* 2004).

Figure 1.6: Signal transduction pathways of natriuretic peptides.

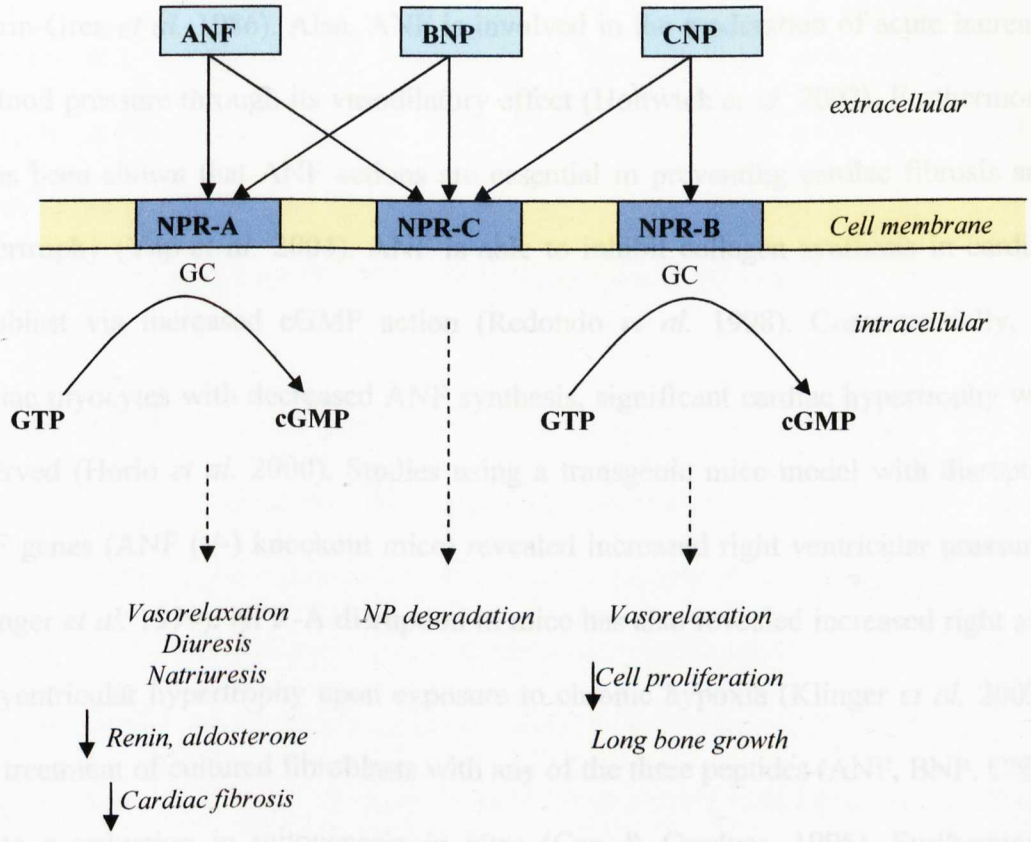

A simplified schematic diagram showing the signal transduction pathway for the natriuretic peptides. Binding of the natriuretic peptides to the receptor stimulates GC to convert GTP to cGMP. ANF and BNP bind to NPR-A and CNP to NPR-B resulting in different cellular actions. All the three natriuretic peptides bind to NPR-C receptor that acts as a clearance receptor *(Adapted from Yap et al. 2004)*.

The primary trigger for ANF release is an increase in either wall stretch or pressure (de Bold *et al.* 2001) but can also be affected by neurohormonal factors such as glucocorticoids, cathecholamines, arginine vasopressin, angiotensin II and endothelin (Ruskoaho 1992). The actions of ANF include vasodilation, inhibition of the renin-angiotensin-aldosterone and sympathetic systems (Brenner *et al.* 1990) and diuresis (Marin-Grez *et al.* 1986). Also, ANF is involved in the moderation of acute increase in blood pressure through its vasodilatory effect (Holtwick *et al.* 2002). Furthermore, it has been shown that ANF actions are essential in preventing cardiac fibrosis and hypertrophy (Yap *et al.* 2004). ANF is able to inhibit collagen synthesis in cardiac fibroblast via increased cGMP action (Redondo *et al.* 1998). Controversially, in cardiac myocytes with decreased ANF synthesis, significant cardiac hypertrophy was observed (Horio *et al.* 2000). Studies using a transgenic mice model with disrupted ANF genes (ANF (-/-) knockout mice) revealed increased right ventricular pressures (Klinger *et al.* 1999). NPR-A disruption in mice has also revealed increased right and left ventricular hypertrophy upon exposure to chronic hypoxia (Klinger *et al.* 2002). The treatment of cultured fibroblasts with any of the three peptides (ANF, BNP, CNP) led to a reduction in mitogenesis *in vitro* (Cao & Gardner, 1995). Furthermore, treatment of neonatal rat ventricular cardiomyocytes resulted in a reduction in the expression of the *Nnpa* gene (which encodes ANF) and inhibition of protein synthesis and cytoskeletal organisation that are characteristic of cardiac hypertrophy (Horio *et al.* 2000, Calderone *et al.* 1998, Silberbach *et al.* 1999). To conclude, ANF (and in general the natriuretic peptides) functions as a local brake to control myocyte growth and fibroblast proliferation in hearts exposed to hypertrophic stimuli and is an important marker and modulator of cardiac hypertrophy.

1.1.3 Mechano-growth factor and its possible involvement on cardiac muscle hypertrophy

Cardiac muscle is known to change its mass and phenotype in response to activity, involving quantitative and qualitative changes in gene expression such as the myosin heavy chain β isogenes (Goldspink 2002). The regulation of muscle mass involves autocrine and systemic factors; one autocrine factor of a particular interest is the mechano growth factor (Goldspink 2002). Mechano growth factor (or else MGF) is the splice variant of the insulin-like growth factor-I (IGF-I) and is usually detectable following injury and/or mechanical activity (Goldspink 2002, Yang *et al.* 1996).

MGF has been found to act in an autocrine/paracrine manner and is thought to be the end product of mechanotransduction signalling pathway in muscle cells (Goldspink 2002). Experiments have demonstrated that active muscles can undergo hypertrophy, characterised by the addition of new sarcomeres (Griffin *et al.* 1971, Williams & Goldspink 1971), up-regulation of protein synthesis (Goldspink & Goldspink 1986, Loughna *et al.* 1986) and changes in gene transcription (Goldspink *et al.* 1992). Studies using intramuscular injected with a plasmid gene construct, containing the MGF cDNA has revealed a significant increase in skeletal muscle mass (Goldspink 2002). In addition, overexpression of IGF-I gene in transgenic animals increased muscle mass (Matthews *et al.* 1988). Cardiac myocytes, isolated from hearts exhibiting hypertrophy are also shown to express elevated amounts of IGF-1 gene and protein (Dong *et al.* 2005). Other experiments have shown that MGF is capable of increasing myoblast proliferation (Yang & Goldspink, 2002). Two dimensional gel electrophoresis analysis of MGF-binding proteins, in combination with mass spectroscopy, showed an interaction with MGF but not the systemic type of IGF-I

(Goldspink 2002). Therefore, MGF is regarded as an autocrine growth/repair factor providing a link between mechanical stimulus and gene expression with a possible involvement in muscle hypertrophy (Goldspink 2002).

1.2 Apoptosis in the failing heart

The loss of cardiac myocytes in the heart is an important step during the progression of cardiac failure of either ischemic or non-ischemic origin (Olivetti *et al.* 1997). There are essentially two mechanisms that lead to cell death: (1) apoptosis, (2) oncosis, or a combination of both (Nadal-Ginard *et al.* 2003). Apoptosis and oncosis have several differences in the remodelling of the heart (Nadal-Ginard *et al.* 2003). Apoptosis is the process of cell death, which occurs naturally as part of normal development, maintenance and renewal of tissues within an organism. During apoptosis, the cells shrink and eventually are removed by the neighbouring cells without any visible change in tissue morphology, as tissue repair does not include collagen accumulation (Nadal-Ginard *et al.* 2003). In contrast to apoptosis, cellular oncosis is accompanied by inflammatory responses, vessel proliferation, macrophage infiltration, fibroblast activation and can lead to scar formation and collagen deposition in response to cell rupture (Nadal-Ginard *et al.* 2003).

Apoptosis is a distinct form of cell death that is characterized by alterations in cell morphology (Majno & Joris 1995). Early stages of apoptosis involve chromatin condensation and margination within the nucleus (Majno & Joris 1995) and are followed by impaired mitochondrial function (Petit *et al.* 1995, Zamzami *et al.* 1995), cytoskeletal alteration and membrane bleeding (Majino & Joris 1995, Martin & Green 1995). In later stages of apoptosis, nuclear fragmentation is observed, accompanied

with the condensation of cytoplasm, resulting in the fragmentation of one or more apoptotic bodies (Haunstetter & Izumo, 1998). The remainings of the cells are taken up by phagocytic cells (e.g. macrophages) or are engulfed by cells that are not specialised in phagocytosis, including vascular smooth muscle cells (Bennett *et al.* 1995).

There are numerous components associated with the apoptotic signalling pathways, including the cell surface receptors (such as the death receptors of the tumour necrosis factor receptor family), cell cycle regulators, proteolytic enzymes (such as casapses and calpain), Bcl-2 family of proteins, the inhibitors of apoptosis proteins (IAPs), stress-response proteins (such as heat shock proteins), and cell adhesion proteins (Clerk *et al.* 2003).

The cell apoptotic machinery can easily be divided into two distinct pathways; the intrinsic pathway and the extrinsic pathway (Figure 1.7) (Gopisetty *et al.* 2006). The intrinsic pathway involves p53 activation and stabilisation, resulting in mitochondrial cytocrome c release (Figure 1.7) (Cory & Adams 2002), ultimately leading to caspase activation, DNA damage and cellular apoptosis (Hockenbery *et al.* 1990). The intrinsic pathway involves the Bcl-2 family of proteins (Figure 1.7) which can be divided into three main subclasses (Gopisetty *et al.* 2006). The first subclass is the anti-apoptotic proteins which include Bcl-2, Bcl-x_l, Mcl-1, AI and Bcl-w (Hockenbery *et al.* 1990, Cory & Adams 2002, Gopisetty *et al.* 2006). The second subclass is the pro-apoptotic proteins which include Bax and Bak and can interact with Bcl-2 and Bcl-x_l, while the third subclass act by binding and inactivating the anti-apoptotic members, which include Bid, Bim, Bik, Bad, Hrk, Noxa and Puma

Figure 1.7: A schematic diagram showing the intrinsic and extrinsic pathways of cellular apoptosis.

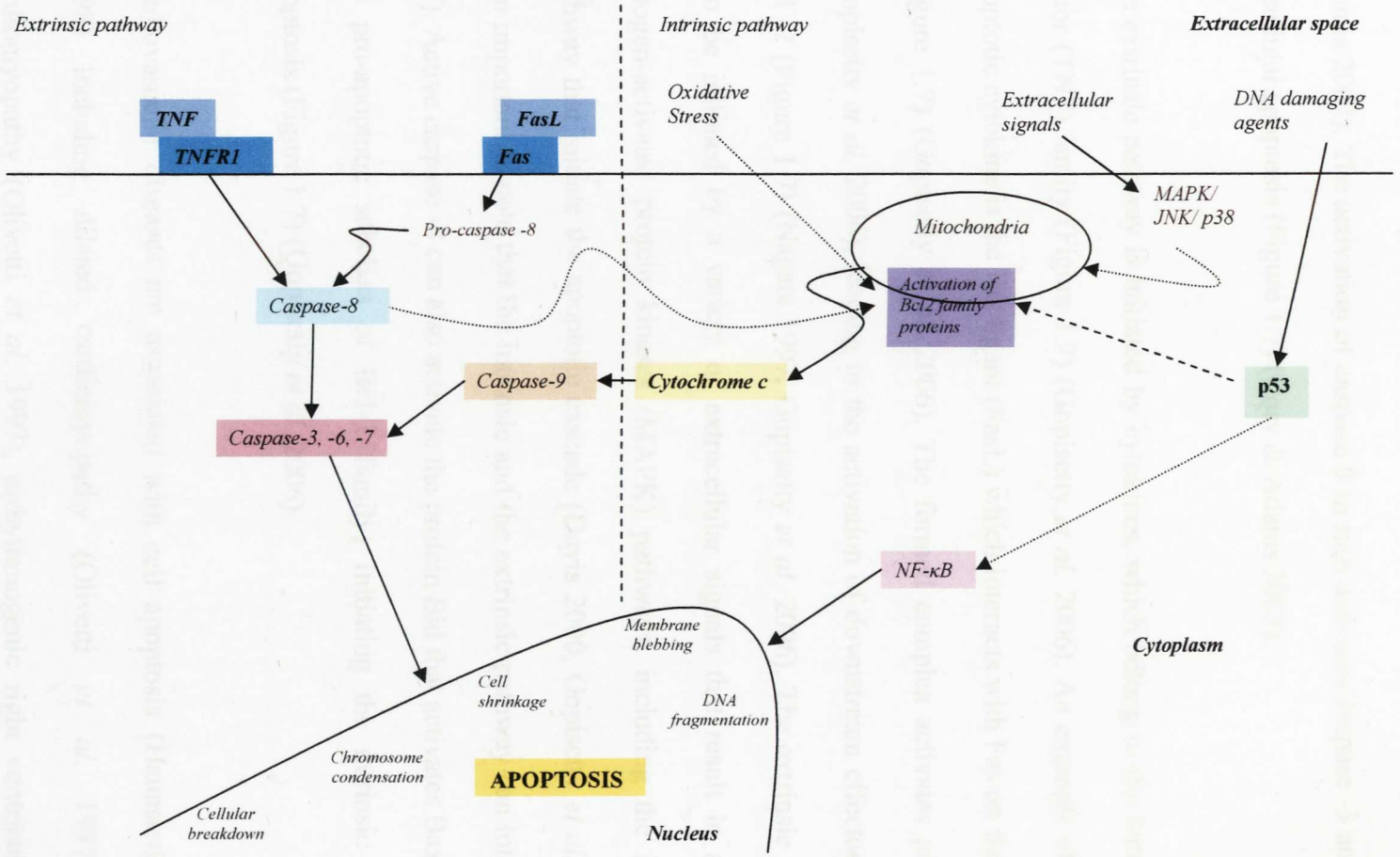

A schematic showing the intrinsic and extrinsic pathways involved in cellular apoptosis. Extracellular signals, DNA damaging agents, growth factors or stimulating antibodies, are capable of initiating apoptotic responses. For simplicity intermediate proteins and enzymes involved in apoptosis and further interactions between pathways are not shown.

(Hockenbery *et al.* 1990, Cory & Adams 2002, Gopisetty *et al.* 2006). The pro-apoptotic members are responsible for changes in the mitochondrial membrane permeability, resulting in cytochrome c release and caspase -9 activation (Cory & Adams 2002). The activation of caspase 9 in turn activates caspase -3 and -7 leading to cellular apoptosis (Figure 1.7) (Cory & Adams 2002).

The extrinsic pathway is initiated by cytokines, which belong to the tumour necrosis factor (TNF) family (Figure 1.7) (Gopisetty *et al.* 2006). An example of such a pro-apoptotic cytokine is the Fas ligant (FasL) which interacts with Fas on the cell surface (Figure 1.7) (Gopisetty *et al.* 2006). The formed complex activates pro-caspase-8, (Gopisetty *et al.* 2006), leading to the activation of downstream effector caspases -3 and -7 (Figure 1.7) (Nagata 1997, Gopisetty *et al.* 2006). The extrinsic pathway can also be initiated by a variety of extracellular signals that result in activation of mitogen-activated protein kinases (MAPK) pathways, including the JNK or p38 pathway that initiate the apoptotic cascade (Davis 2000, Gopisetty *et al.* 2006). It is also important to note that the intrinsic and the extrinsic pathway can interact (Figure 1.7). Active caspase -8 can also activate the protein Bid that activates Bax and Bad (of the pro-apoptotic subclass of Bcl-2 family) initiating the intrinsic pathway of apoptosis (Figure 1.7) (Gopisetty *et al.* 2006).

Cardiovascular diseases are associated with cell apoptosis (Haunstetter & Izumo 1998) including dilated cardiomyopathy (Olivetti *et al.* 1997), ischemic cardiomyopathy (Olivetti *et al.* 1997), arrhythmogenic right ventricular dysplasia (Mallat *et al.* 1996), acute myocardial infarction (Itoh *et al.* 1995), atherosclerosis (Kockx *et al.* 1994), myocarditis (Bachmaier *et al.* 1997), cardiac allograph rejection

(Szabolcs *et al.* 1996), preexcitation syndrome (James 1994), congenital atrioventricular block (James *et al.* 1996) and cardiac hypertrophy (Nadal-Ginard *et al.* 2003). Both apoptotic pathways have previously been implicated in the apoptosis of the cardiac myocytes and are currently considered to play a major role in heart failure (Haunstetter & Izumo 1998, Bromme & Holtz 1996).

1.2.1 Apoptosis and left ventricular hypertrophy

Cardiac hypertrophy results from the enlargement of pre-existing myocytes (Nadal-Ginard *et al.* 2003). It is believed that in the adult heart, myocytes are terminally differentiated and therefore cannot re-enter the cell cycle ((Bicknell *et al.* 2007, Nadal-Ginard *et al.* 2003). Approximately 85 % of the cardiomyocytes are arrested in the G0/G1-phases of the cell cycle and the remaining nuclei are blocked in G2/M phase (Bicknell *et al.* 2007). Also, the myocardium lacks a stem cell population capable of producing new myocytes (Nadal-Ginard *et al.* 2003). During heart disease as well as during ageing, the rate of cell death increases (Nadal-Ginard *et al.* 2003). As a result, the cardiomyocyte numbers decrease and as a consequence, myocyte hypertrophy is initiated to the heart muscle (Nadal-Ginard *et al.* 2003). Therefore, even a moderate rate of myocyte death can gradually lead to decrease in the myocardial mass and result in chronic heart failure (Nadal-Ginard *et al.* 2003).

Following an ischaemic event, 80 % of the affected cardiomyocytes are apoptotic whereas necrosis is visible in less than 20 % of the cells (Bardales *et al.* 1996). After coronary occlusion, single and double stranded DNA breaks are observed in the myocardial cells and are increased in the region around the dead tissue (Muller *et al.* 2000). This is indicative of increased rate of myocyte apoptosis (Nadal-Ginard *et al.*

2003). Single stranded DNA breaks may be visualised in healthy cells, as a result of mechanical overload (Nadal-Ginard *et al.* 2003). Primarily, repairable DNA damage is observed, and subsequently irreversible injury and apoptosis (Nadal-Ginard *et al.* 2003). Subsequently, the reorganisation of the myocytes in the ventricle may occur, resulting in a decrease in cardiac wall thickness and an increase in chamber volume (Li *et al.* 1997, Anversa *et al.* 1993). Another mechanism, by which myocytes can undergo apoptosis, is through the reduced rate of ATP synthesis following myocardial infarction, leading to electrolyte imbalance within the cells (Nadal-Ginard *et al.* 2003, Clerk *et al.* 2003). The ionic disruption triggers myocyte apoptosis and progressive impairment of myocyte function, leading to hypertrophy (Nadal-Ginard *et al.* 2003). A strong marker and putative modulator of cellular events in apoptosis is the pro-inflammatory protein tissue factor (TF) (Camerer *et al.*, 2000, Riewald & Ruf 2002).

1.3 Haemostasis and tissue factor

1.3.1 Tissue factor, haemostasis and blood coagulation

Haemostatic mechanisms are responsible for the maintenance of the normal blood circulatory system, following damage to the blood vessel. The activation of coagulation mechanisms together with the aggregation of the platelets at the injured site result in the formation of a haemostatic plug (Norris 2003, Hoffman 2003). The coagulation phase (Figure 1.8) is made up of two pathways; 1) the intrinsic pathway which is initiated when contact is made between blood and sub-endothelial surface and 2) the extrinsic pathway which is initiated upon vascular injury leading to the release of Tissue Factor (TF) (Norris 2003, Hoffman 2003). TF acts as a cofactor to factor VIIa to form the TF/FVIIa complex, which proteolytically digest factor X to

Figure 1.8: Coagulation cascades.

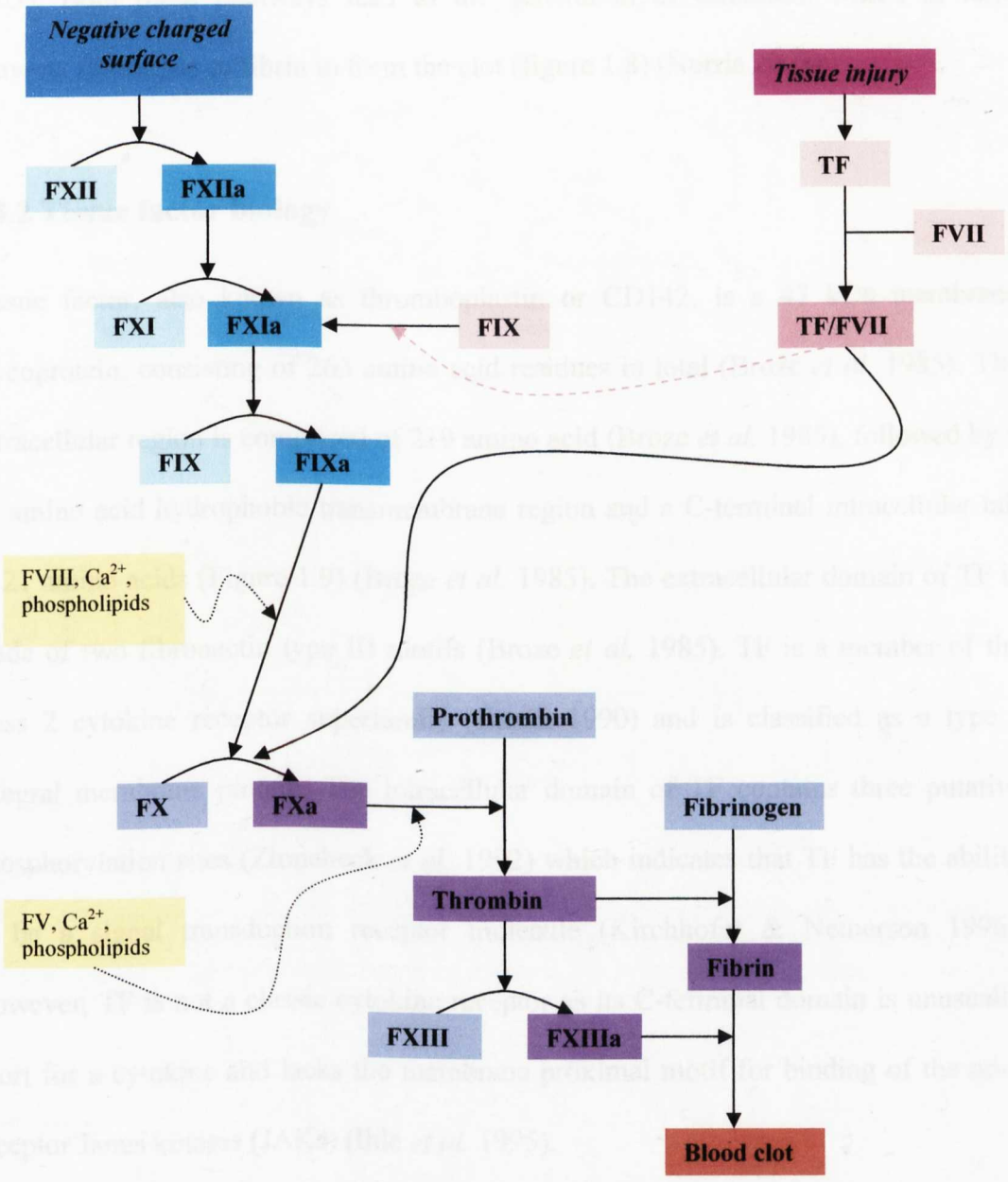

The intrinsic cascade, indicated in blue, is initiated when exposed negative charged surfaces and blood come into contact. The extrinsic pathway, indicated in pink, is initiated upon vascular injury leading to the release of TF. The pink dotted arrow indicates the cross-over point between the extrinsic and the intrinsic pathway. The two cascades lead to a common pathway indicated in purple and convert FX to its active form FXa. Active factor FXa hydrolyses and activates prothrombin to thrombin. Subsequently, thrombin converts fibrinogen to fibrin leading to a stable blood clot.

factor Xa. Additionally, TF/FVIIa also activates factor IX which can in turn activate factor X, ultimately feeding back on the intrinsic pathway (Norris 2003, Hoffman 2003). Both these pathways lead to the generation of thrombin, which in turn, converts fibrinogen to fibrin to form the clot (figure 1.8) (Norris 2003).

1.3.2 Tissue factor biology

Tissue factor, also known as thromboplastin or CD142, is a 47 kDa membrane glycoprotein, consisting of 263 amino acid residues in total (Broze *et al.* 1985). The extracellular region is comprised of 219 amino acid (Broze *et al.* 1985), followed by a 29 amino acid hydrophobic transmembrane region and a C-terminal intracellular tail of 21 amino acids (Figure 1.9) (Broze *et al.* 1985). The extracellular domain of TF is made of two fibronectin type III motifs (Broze *et al.* 1985). TF is a member of the class 2 cytokine receptor superfamily (Bazan 1990) and is classified as a type I integral membrane protein. The intracellular domain of TF contains three putative phosphorylation sites (Zioncheck *et al.* 1992) which indicates that TF has the ability to be a signal transduction receptor molecule (Kirchhofer & Nemerson 1996). However, TF is not a classic cytokine receptor as its C-terminal domain is unusually short for a cytokine and lacks the membrane proximal motif for binding of the non-receptor Janus kinases (JAKs) (Ihle *et al.* 1995).

The complete genomic sequence of TF spanning 12.4 kb was published in 1989 by Mackman *et al.* The gene for TF is localised on human chromosome 1 at 1p21-22 (Mackman *et al.* 1989) and is organised into six exons, whereby the second through fifth exons encode the extracellular domain of the protein and the sixth exon provides

Figure 1.9: Structure and amino acid sequence of tissue factor.

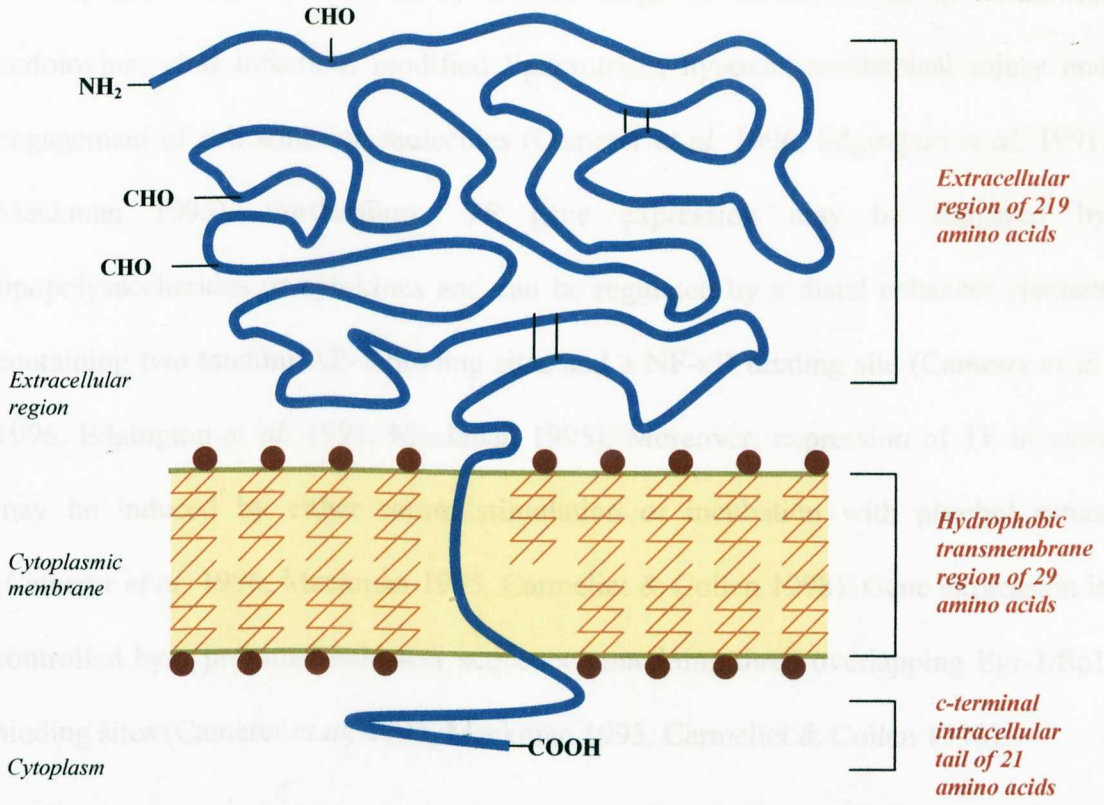

NH_2- 1metpawprvprpetavartlllgwvfaqvagasgttntvaaynltwkstnfktilewepkpvnqvytvqistksgdwk skcfyttdtecdltdeivkdvkqtylarvfsypagnvestgsageplyenspeftpyletnlgqptiqsfeqvgtkvnvtved ertlvrrnntflslrdvfgkdliytlyywkssssgkktaktntneflidvdkgenycfsvqavipsrtvnrkstdspvecmg qekgefreifyiigavvfvviilviilaislhkcrkagvgqswkensplnvs **-COOH**

Tissue factor consist of 263 amino acid residues in total. The extracellular region is comprised of 219 amino acid, followed by a 29 amino acid hydrophobic trans-membrane region and a c-terminal intracellular tail of 21 amino acids *(Broze et al. 1985)*. The TF amino acid sequence was taken from "NCBI" web site: "http://www.ncbi.nlm.nih.gov".

both the transmembrane and cytoplasmic domains (Camerer *et al.* 1996, Edgington *et al.* 1991, Mackman 1995, Ogino *et al.* 1996).

TF expression can be induced by a wide range of factors including hormones, endotoxins, viral infection, modified lipoproteins, hypoxia, mechanical injury and engagement of cell adhesion molecules (Camerer *et al.* 1996, Edgington *et al.* 1991, Mackman 1995). Furthermore, TF gene expression may be triggered by lipopolysaccharides or cytokines and can be regulated by a distal enhancer element containing two tandom AP-1 binding sites and a NF-κB binding site (Camerer *et al.* 1996, Edgington *et al.* 1991, Mackman 1995). Moreover, expression of TF *in vitro* may be induced by either serum stimulation or incubation with phorbol esters (Camerer *et al.* 1996, Mackman 1995, Carmeliet & Collen 1998). Gene expression is controlled by a proximal enhancer sequence containing three overlapping Egr-1/Sp1 binding sites (Camerer *et al.* 1996, Mackman 1995, Carmeliet & Collen 1998).

1.3.2.1 Tissue factor as a signalling molecule

TF is capable of inducing cell signalling as it has structural similarities to members of the cytokine receptor superfamily (Bazan 1990). There are two well documented mechanisms by which TF has been shown to initiate cell signalling: 1) via the protease activity of FVIIa and FXa which may involve the activity of protease activator receptors (PARs) and 2) via its cytoplasmic domain.

Previous studies have shown that the binding of TF to FVIIa can induce intracellular Ca^{2+} oscillations in a number of TF-expressing cells including myocytes (Rottingen *et al.* 1995, Camerer *et al.* 1996). This FVIIa-induced calcium signalling is brought

about by binding of catalytically active FVIIa to TF (Figure 1.10) but the presence of the cytoplasmic domain of TF was not necessary (Rottingen *et al.* 1995, Camerer *et al.* 1996). Furthermore, it has been shown that FVIIa binding to TF in BHK cells expressing TF, results in transient activation of p44/p42 MAPK which is also dependent on the presence of proteolytically active FVIIa but not on the cytoplasmic domain of TF (Figure 1.10) (Sorensen *et al.* 1999, Poulsen *et al.* 1998). In addition, stimulation of cells expressing TF such as fibroblasts and keratinocytes, with FVIIa resulted in the activation of p44/p42 MAPK pathway (Pendurthi *et al.* 1997, Camerer *et al.* 2000). Moreover, treatment of keratinocytes with FVIIa was shown to increase phosphorylation of key components of the p38 and JNK kinase pathways (Figure 1.10) (Camerer *et al.* 1999). A study by Versteeg *et al.* (2000) showed that FVIIa initiates signalling in fibroblasts through activation of the Src-like family members and subsequently PI3-kinase, leading to the activation of p44/p42 MAPK, Akt/protein kinase B and small GTPases, Rac and Cdc42 (Figure 1.10). Furthermore, it has been shown that FVIIa induces Ca^{2+} release in *Xenopus* oocytes expressing TF, together with activation of PAR1 or PAR2 but not PAR3 and PAR4 (Figure 1.10) (Camerer *et al.* 2000). Treatment of CHO cells transfected to express TF and PAR2, with FVIIa was shown to activate the p44/p42 MAPK (Figure 1.10) (Riewald & Ruf 2001). It has also been shown that PAR2 is essential for the TF/FVIIa-induced smooth muscle cell migration (Marutsuka *et al.* 2002). Moreover, it has been shown that binding of FXa to TF/FVIIa can form a transient ternary TF/FVIIa/FXa complex which is a potent signalling unit capable of efficient activation of PAR1 and PAR2 (Figure 1.10) (Riewald & Ruf 2002, Hjortoe *et al.* 2004).

Figure 1.10: TF-mediated signalling mechanisms.

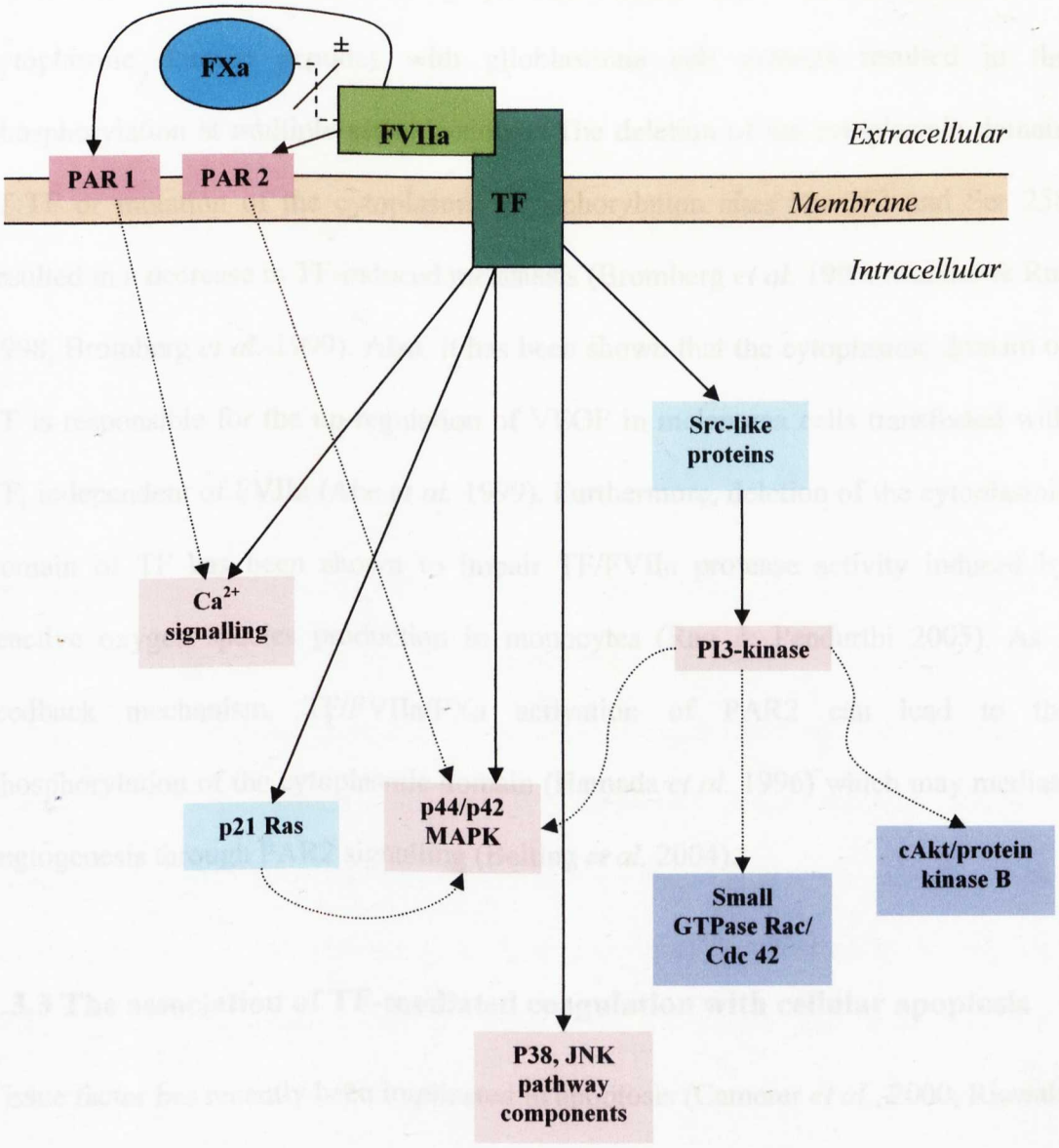

TF/FVIIa complex activates Ca^{2+} signalling, and other signalling pathways and protease activator receptor 1 and 2 with or without the addition of FXa. For simplicity the different cell types where these findings were observed are not shown.

The importance of the cytoplasmic domain of TF in TF/FVIIa-induced cell signalling has been shown by analysing the human TF protein sequence (Zioncheck *et al.* 1992). A study by Mody and Carson (1997) employing a synthetic peptide corresponding to residues 245-263 of the human TF cytoplasmic domain showed that incubation of TF cytoplasmic domain peptides with glioblastoma cell extracts resulted in the phosphorylation at multiple serine residues. The deletion of the cytoplasmic domain of TF or mutation of the cytoplasmic phosphorylation sites Ser 253 and Ser 258 resulted in a decrease in TF-induced metastasis (Bromberg *et al.* 1995, Mueller & Ruf 1998, Bromberg *et al.* 1999). Also, it has been shown that the cytoplasmic domain of TF is responsible for the up-regulation of VEGF in melanoma cells transfected with TF, independent of FVIIa (Abe *et al.* 1999). Furthermore, deletion of the cytoplasmic domain of TF has been shown to impair TF/FVIIa protease activity induced by reactive oxygen species production in monocytes (Rao & Pendurthi 2005). As a feedback mechanism, TF/FVIIa/FXa activation of PAR2 can lead to the phosphorylation of the cytoplasmic domain (Hamada *et al.* 1996) which may mediate angiogenesis through PAR2 signalling (Belting *et al.* 2004).

1.3.3 The association of TF-mediated coagulation with cellular apoptosis

Tissue factor has recently been implicated in apoptosis (Camerer *et al.*, 2000, Riewald & Ruf 2002). A variety of intracellular signal cascades, including p42/p44 mitogen-activated protein kinase pathway (Poulsen *et al.* 1998, Camerer *et al.* 1999, 2000, Pendurthi *et al.* 2000, Versteeg *et al.* 2000), Akt/ protein kinase B (PKB) pathways (Versteeg *et al.* 2000, 2002) are activated upon the binding of TF to factor VIIa (Versteeg *et al.* 2001). Both of these pathways are capable of inhibiting cell apoptosis (Kennedy *et al.* 1997, Kulik *et al.* 1997). Versteeg *et al.* (2003) observed that FVIIa

inhibits apoptosis and caspase-3 activation in BHK cell over-expressing TF. Furthermore, FVIIa-mediated activation of caspase-3 is suppressed by inhibitors of the phosphotidylinositide-3-(OH) kinase (PI3 kinase) and p42/p44 MAP kinase pathways (Versteeg *et al.* 2003). In addition, FXa generated by the binding of TF to FVIIa, dramatically increased cell survival (Versteeg *et al.* 2003). A study by Sorensen *et al.* (2003) also showed that FVIIa decreased the number of cells with apoptotic morphology and prevented DNA degradation as measured by means of TdT-mediated dUTP nick and labelling (TUNEL). Also, FVIIa induced cell survival was correlated with the activation of PI3-kinase/Akt pathway (Sorensen *et al.* 2003).

1.3.4 Tissue factor in atherosclerosis and thrombosis

In normal arteries TF is localised to the cells within the adventitia and only traces of the protein are detectable in the media or intima (Drake *et al.* 1989, Marmur *et al.* 1993). However, following injury, tissue factor is rapidly released into the aorta by smooth muscle cells (SMCs) acting as a procoagulant to induce thrombus formation (Marmur *et al.* 1993). In atherosclerotic plaques derived from human carotid and coronary arteries, a heavy deposit of TF antigen may be detected in macrophage-derived foam cells, vascular smooth muscle cells, endothelial cells as well as within the cell-free necrotic core (Wilcox *et al.* 1989, Toschi *et al.* 1997, Ardissino *et al.* 1997, Entman *et al.* 1991). Plaque-associated TF has been shown to be active and capable of activating factor VII (Marmur *et al.* 1996, Ardissino *et al.* 1997) and capable of triggering thrombosis following plaque rupture (Moons *et al.* 2002, Viles-Gonzalez & Badimon 2004), causing serious damage.

1.3.5 Tissue factor pathway inhibitor

The inhibition of the extrinsic pathway of coagulation is vital for the prevention of excessive clotting and thrombus formation. Tissue factor pathway inhibitor (TFPI) is a plasma protein that can inhibit the TF/FVIIa complex (Broze 1987). TFPI is composed of 3 tandem Kunitz-type domains (Figure 1.11) with a molecular weight of 38 kDa (Bajaj *et al.* 1999, Broze 1995). TFPI inhibits the action of TF in two ways. Firstly, TFPI can bind to the active site of FVIIa in the TF/FVIIa complex through the first Kunitz domain (Figure 1.11) (Broze 1995). Additionally, TFPI may directly bind to FXa through the second Kunitz domain (Figure 1.11) (Broze 1992). Once formed, the TFPI/FXa complex binds to TF/FVIIa with a higher affinity than the TFPI molecule alone, forming an inhibited tetramolecular complex TF/FVIIa/TFPI/FXa (Broze 1992). In both cases the inhibition results in the ablation of thrombin generation and fibrin formation (Huang *et al.* 1993).

The importance of TFPI in the living organism has been demonstrated in TFPI knock-out transgenic animals which on post-mortem were found to have developed disseminated intravascular coagulation (Sandset *et al.* 1991). Homozygous mice with TFPI gene distruption of the Kunitz 1 domain die in *utero* and 60 % of these animals die during the embryonic days E9.5-E11.5 with evidence of yolk sack bleeding (Huang *et al.* 1997). Those surviving beyond embryonic day E11.5, exhibited signs of bleeding in central nervous system and tail but still do not survival to neonatal period (Huang *et al.* 1997).

TFPI also have an important role in cellular apoptosis. A study by Hamuro *et al.* (1998) identified TFPI as an inducer of apoptosis in human endothelial cells.

Figure 1.11: Structure and amino acid sequence of TFPI.

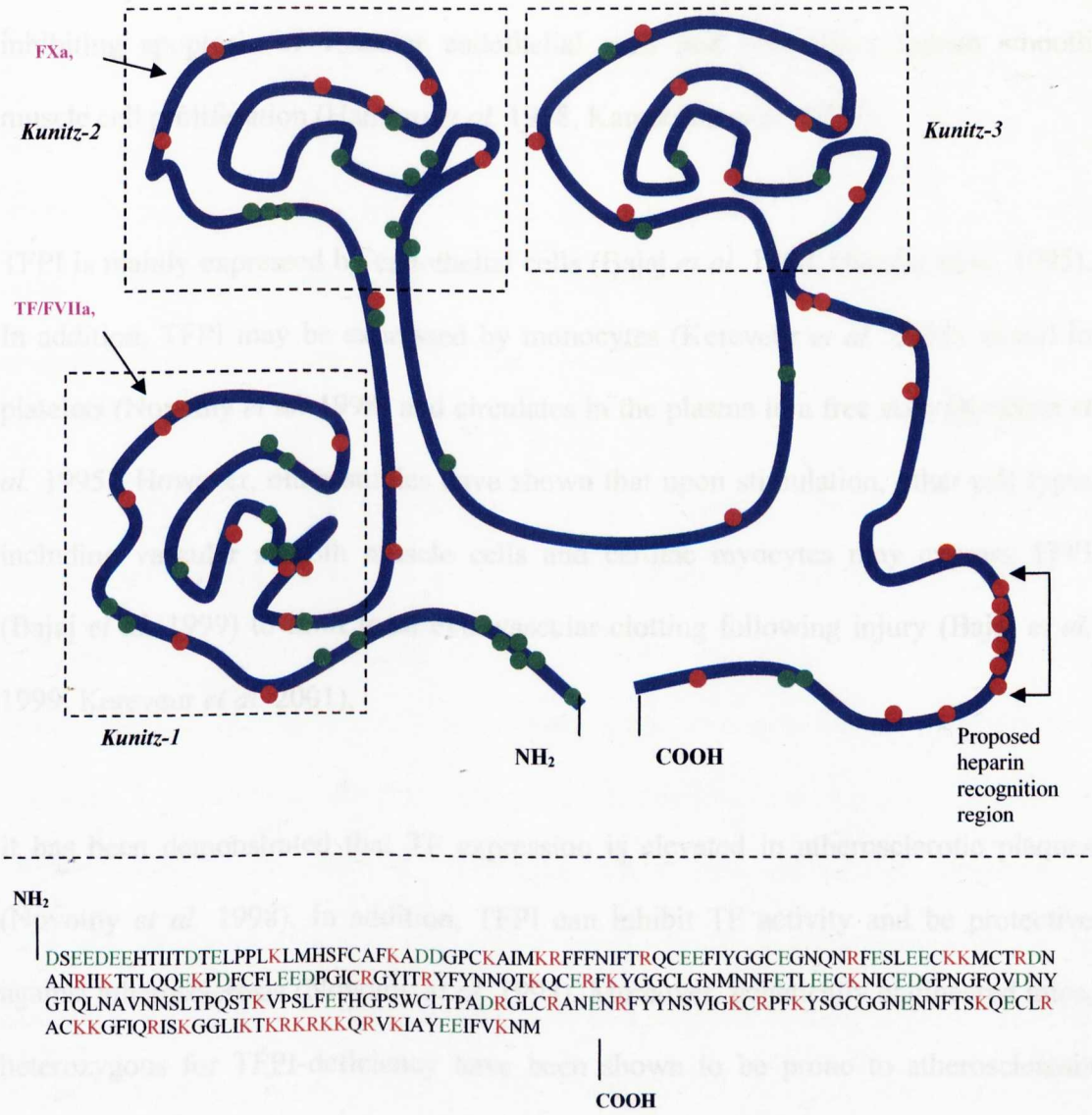

Model of tissue factor pathway inhibitor showing the Kunitz type domains and the positively (red) and negatively (green) charged amino acids groups. Kunitz 1 is responsible of binding in the active site of FVIIa of the TF/FVIIa complex and Kunitz 2 is responsible of binding to FXa. The arrows indicate the possible site of heparin binding at the C-terminal end of the TFPI. *(Adapted from Broze 1995)*

Furthermore, TFPI has been demonstrated to inhibit proliferation of human smooth muscle cells (Kamikubo *et al.* 1997). TFPI plays a physiologically important role in the establishment of the vascular system during development and angiogenesis by inhibiting apoptosis of vascular endothelial cells and controlling human smooth muscle cell proliferation (Hamuro *et al.* 1998, Kamikubo *et al.* 1997).

TFPI is mainly expressed by endothelial cells (Bajaj *et al.* 1990, Osterud *et al.* 1995). In addition, TFPI may be expressed by monocytes (Kereveur *et al.* 2001), stored in platelets (Novotny *et al.* 1998) and circulates in the plasma in a free state (Kokawa *et al.* 1995). However, other studies have shown that upon stimulation, other cell types including vascular smooth muscle cells and cardiac myocytes may express TFPI (Bajaj *et al.* 1999) to limit local extravascular clotting following injury (Bajaj *et al.* 1999, Kereveur *et al.* 2001).

It has been demonstrated that TF expression is elevated in atherosclerotic plaques (Novotny *et al.* 1998). In addition, TFPI can inhibit TF activity and be protective against atherosclerosis (Novotny *et al.* 1998). Moreover, genetically engineered mice, heterozygous for TFPI-deficiency have been shown to be prone to atherosclerosis (Westrick *et al.* 2001). These findings suggest that an imbalance between TF and TFPI can influence the progression of both atherosclerosis and thrombosis (Doshi & Marmur 2002). In cardiomyocytes TFPI may be expressed upon stimulation with interleukin 1 (Kereveur *et al.* 2001). Moreover, patients suffering from heart disease exhibit increased levels of TFPI antigen in their plasma (Falciani *et al.* 1998) which suggests that TFPI may have a protective role in the heart (Kereveur *et al.* 2001, Doshi & Marmur, 2002).

1.3.6 Tissue factor expression in the myocardium

Tissue factor is shown to be expressed in mouse and rabbit heart tissues mainly in the intercalated discs (Hartzell et al 1989, Luther *et al.* 2000, Mackman *et al.* 1993). Furthermore, TF antigen concentration, expressed in ng TF/mg protein, has been shown to be higher in cardiac muscle compared to skeletal muscle (Luther *et al.* 2000). TF activity has been estimated to be 17.5 fold greater in cardiac than in skeletal muscle (Drake *et al.* 1989). This difference is also reflected in the TF activity as indicated by the shorter prothrombin time (Drake *et al.* 1989).

Luther *et al.* (1996) showed that TF plays an important role in the developing myocardium by examining the expression of TF during mouse cardiogenesis in comparison to human post-implantation embryos and foetuses of corresponding gestational age. During the early embryonic period in murine (6.5-7.5 post-coitum) and stage 5 of human development, TF antigen is detected in ectodermal, mesodermal and endodermal cells whilst at later stages, TF antigen and mRNA expression is detectable in the developing heart (Luther *et al.* 1996). The expression of TF by cardiomyocytes during development suggests that it may have morphogenic functions in the developing heart (Luther & Mackman 2001). Studies, using genetically engineered mice with a TF deficiency (TF null mice) have shown 90 % lethality of embryos at 9.5-10.5 post-coitum (Toomey *et al.* 1996, Bugge *et al.* 1996, Carmeliet *et al.* 1996). Furthermore, transgenic mice exhibiting low TF levels (low-TF mice) have shortened life spans than the wild-type mice (Parry *et al.* 1998). Autopsy examination of these mice shows marked impairment of myocardium contractility. The level of this impairment is not sufficient to lead to heart failure (Pawlinski *et al.* 2002). However, the extensive fibrosis observed in low-TF mice may cause fatal arrhythmias

(Pawlinski *et al.* 2002). This may be a reason that TF may be characterised as a "lethal" gene, and either the absence or low levels of TF expression leads to bleeding, haemosiderin deposition and fibrosis, giving rise to cardiac dysfunction and probably heart failure (Pawlinski *et al.* 2002).

Immunohistochemical and ELISA studies have shown that TF is present within the transverse components of the intercalated discs (Figure 1.12) in human, rabbits and murine adult myocardium (Luther *et al.* 2000). This suggests that TF may be associated with the actin filament system, within the myocyte, in the fascial adherent of contractile fibres (Figure 1.12) (Luther *et al.* 2000). The same study also reported that TF antigen is increased in premature hearts as compared to adult hearts (Luther *et al.* 2000). Moreover, TF antigen is lower in the atrial compared to ventricular tissue, due to the increase in the number of contact site in ventricular cardiomyocytes (11.3-11.6 neighbours cells in ventricle as opposed to 4.8-6.4 neighbour cells in atria) (Luther *et al.* 2000). Hence, these findings suggest a structural as well as a haemostatic role for TF in cardiac muscle.

The role of TF has also been demonstrated during heart transplantation. TF has been detected in coronary intima and endothelium of cardiac allografts following transplantation (Holschermall *et al.* 1999). Moreover, the TF mRNA expression measured in coronary endothelial cells is localised in the transplanted heart tissue but not in the surrounding recipient tissue (Holschermall *et al.* 1999). Similar results produced by Nagasu *et al.* (2000) in guinea pig cells and whole tissue, showed that TF expression was observed, 3 h post-transplantation, in endothelial cells and smooth muscle cells whereas in rats, TF expression was observed after 16 h in the circulating

Figure 1.12: A schematic representation of the intercalated discs within cardiomyocytes and the associated TF.

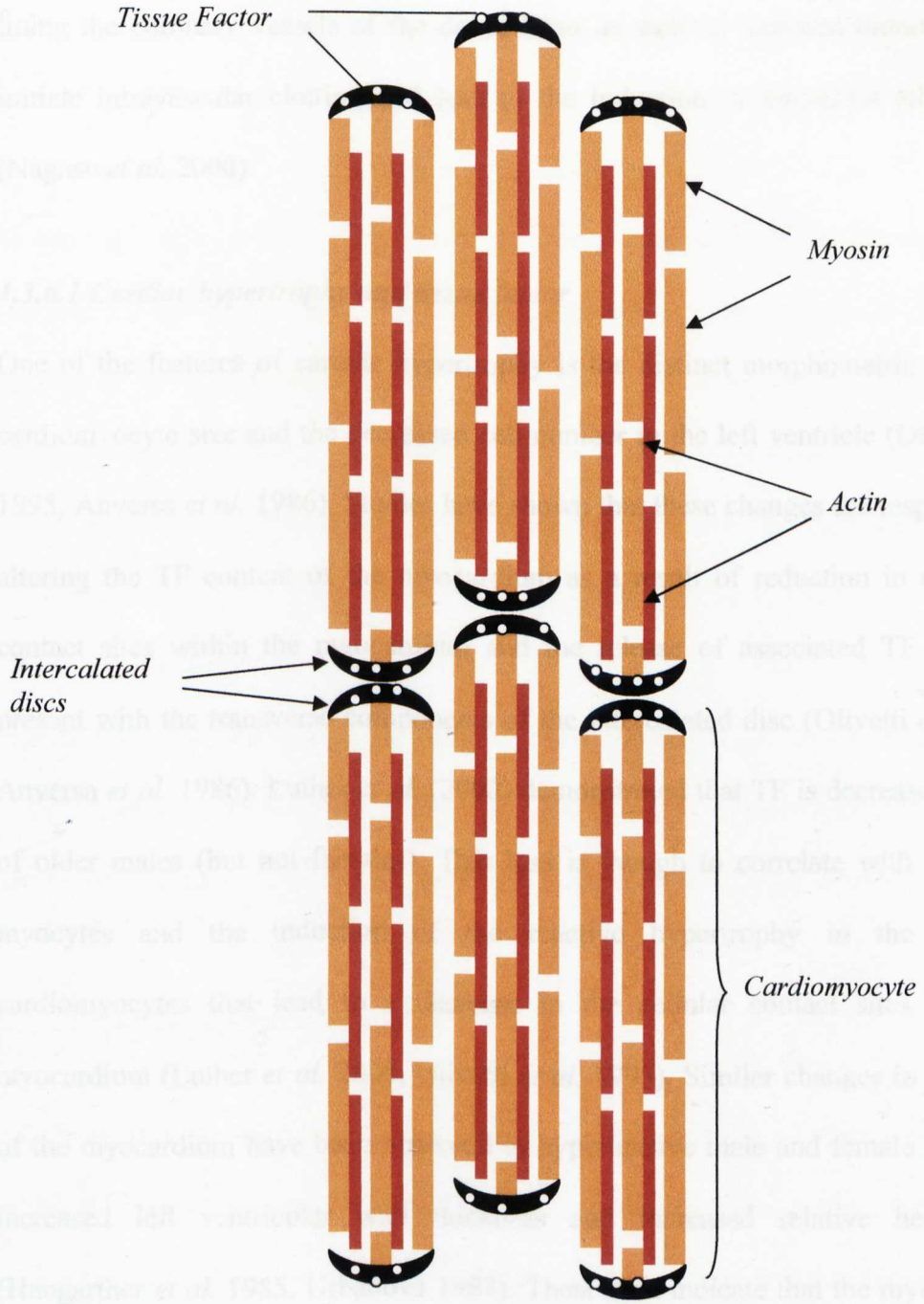

Tissue factor (white dots) is present in the intercalated discs of the myocytes and is associated with the actin-myosin filament system in the fascial adherent of contractile fibres (Luther *et al.* 2000).

monocytes. Holschermall *et al.* (2000) reported that TF mRNA was increased in the transplanted heart compared with recipient tissue 120 days post-transplantation in rats. Therefore, abnormal TF expression in the coronary intima and in endothelial cells lining the coronary vessels of the donor heart as well as recipient monocytes, may initiate intravascular clotting and lead to the induction of transplant atherogenesis (Nagasu *et al.* 2000).

1.3.6.1 Cardiac hypertrophy and tissue factor

One of the features of cardiac hypertrophy is the distinct morphometric changes in cardiomyocyte size and the decreased cell number in the left ventricle (Olivetti *et al.* 1995, Anversa *et al.* 1986). Studies have shown that these changes are responsible for altering the TF content of the myocardium as a result of reduction in the cellular contact sites within the myocardium and the release of associated TF have been present with the transverse components of the intercalated disc (Olivetti *et al.* 1995, Anversa *et al.* 1986). Luther *et al.* (2000) demonstrated that TF is decreased in hearts of older males (but not females). This loss is though to correlate with the loss of myocytes and the induction of the reactive hypertrophy in the remaining cardiomyocytes that lead to a decrease in the cellular contact sites within the myocardium (Luther *et al.* 2000, Olivetti *et al.* 1995). Similar changes in TF content of the myocardium have been observed in hypertensive male and female hearts with increased left ventricular wall thickness and increased relative heart weight (Hangarther *et al.* 1985, Urbanova 1983). These data indicate that the myocardial TF content is reduced in hypertrophic myocardium in comparison to normal heart tissue (Luther *et al.* 2000). Additionally, the number of myocyte contact sites per cardiac muscle mass is decreased and therefore, it is possible to associate the decrease in the TF expression with the hypertrophic myocardium (Luther *et al.* 2000).

Furthermore, a transgenic rat model has previously been employed to examine the pattern of TF expression during experimental hypertrophy (Muller *et al.* 2000). This genetically engineered strain of rat over-expressed human renin angiotensinogen genes and gave rise to hypertension and left ventricular hypertrophy, resulting in mortality at 7 weeks (Muller *et al.* 2000). The plasma and cardiac angiotensin II levels in the transgenic rats were 3-5 times higher than the Sprague-Dawley (SD) rats, used as control (Muller *et al.* 2000). A separate group of transgenic rats received an Ang II inhibitor, valsatant to normalise blood pressure and ameliorate cardiac hypertrophy (Muller *et al.* 2000). Measurement of TF mRNA levels in hearts of the transgenic group exhibited increased expression in comparison to SD control rats (Muller *et al.* 2000). Furthermore, the increase in the expression was concomitant with the presence of TF antigen in the endothelial layer of coronary vessels (Muller *et al.* 2000). However, on treatment with Valsatant, the TF mRNA levels and TF antigen in endothelial cells was reduced to normal levels (Muller *et al.* 2000). These findings suggest that TF expression by endothelial cells may lead to microvascular thrombosis and micro-infarction leading to cardiac hypertrophy (Muller *et al.* 2000).

1.4 Objectives of this study

The aim of this study was to investigate the involvement of tissue factor in the pathogenesis and/or development of cardiac hypertrophy. This could provide a better understanding of the disease and thus identify possible new approaches toward novel treatments.

The main objectives of this study were:

- To establish the pattern of TF and TFPI expression over a 14 day period post-induction of cardiac hypertrophy in adult rat heart through analysing the mRNA and protein expression.
- To investigate the role of TF on the expression of ANF in H9c2 cardiomyocytes *in vitro* by analysing ANF mRNA and protein levels upon treatment with exogenous TF.
- To assess the role of TF in cellular apoptosis in H9c2 cardiomyocyte *in vitro*, by analysing activation of the caspase-3 and cell viability, upon treatment with exogenous TF.

CHAPTER 2

Materials and methods

2. Materials and methods

2.1 Materials

The materials, reagents and equipment used throughout this project were purchased from the companies listed in table 2.1 below.

Table 2.1: A table showing the companies from which the materials, reagents and equipment used in this project were purchased.

COMPANY AND ADDRESS	PRODUCT(S)
Anachem Ltd., Luton, UK	Mouse monoclonal anti-GAP3DH [6C5]
Animal Care Ltd., York, UK	Sterile isotonic saline
Apple, Cupertino, Canada	MacLab recording system
ATCC-LGC/Promochem, Teddington, UK	H9c2 cells
Axis-Shield Diagnostics Ltd., Dundee, UK	Human factor Xa, recombinant human factor VIIa
BD Biosciences, Oxford, UK	Becton Dickinson FACSCalibur flow cytometer, CellQuest software program, 0.5 mm OD needles, Falcon microscope chamber slides, Falcon FACS tubes
BDH Laboratory supplies, Poole, UK	NaCl, KCl, $MgSO_4.7H_2O$, KH_2PO_4, Mannitol, Glucose, $CaCl_2.2H_2O$, $NaHCO_3$, Glysine, HCl
Bioline, London, UK	Molecular graded agarose, PCR ranger DNA ladder 1000bp
Charles Rivers, Kent, UK	Male Sprague-Dawley rats
Chemicon Europe Ltd., Chanders Ford, UK	Rabbit anti mouse IgG Rhodamine-linked antibody
Dade Behring, Marburg, Germany	Recombinant human tissue factor
DAKO Corporation, Carpinteria, USA	Fluorescent mounting medium
DAKO Ltd., Ely, UK	Normal rabbit serum, Normal swine serum Goat anti-rabbit TRITC-conjugated antibody Swine anti rabbit IgG TRITC conjugated
Ethicon, Somerville, USA	Mersilk O suture, Ethicon 3-0 Vicyl braided suture, Ethicon 3-0 blue monofilament suture

Fisher Scientific Ltd., Leicester, UK	Eppendorf miniSpin micro centrifuge, 1.5 ml ependorf nuclease free microfuge tubes, 1.5 microfuge tubes, Wollenberger tongs, Hawkleys crystallite Haematocytometer
Flowgen, Loughborough, UK	Bis-acrylamide solution [30 % (w/v) acrylamide: 0.8 % (w/v) bis acrylamide stock solution 37:5:1], Resolving buffer [1.5 M Tris-HCl, pH 8.8, 0.4 % (w/v) SDS], Tetramethylethylanediamine (TEMED)
GE Healthcare, Little Chalfont, UK	Ready-to-go RT-PCR beads
Gilmount Instruments, Barrington, USA	2.0 ml micrometer syringe
Greiner Bio-one, Longwood, USA	25 cm^3 tissue culture flasks, 75 cm^3 tissue culture flasks, 150 cm^3 tissue culture flasks, 30 ml sterilin tubes, 50 ml sterile tubes, 15 ml sterile tubes
Helena Laboratories, Sunderland, UK	Cascade-M coagulometer, Normal human plasma
Intervet Ltd., Milton Keynes, UK	Amfipen (150 mg/ml anhydrous ampicillin)
Janke & Kunkel KKA^R Labortechnick, Staufen, Germany	Ultra-turrex T25 homogeniser
Kingston Veterinary Group, Hull, UK	Halothane (prescribed by the veterinary doctor)
Leica Microsystems, Milton Keynes, UK	Fluorescent microscope
Leo Laboratories Ltd., Dublin, Ireland	Heparin Sodium (100 U/ml)
Media Cybernetics, Wokingham, UK	CoolSNAP-Pro, Color CCD camera, ImagePro software
Merck Pharmaceuticals, Notingham, UK	Mouse monoclonal anti-TF antibody (Calbiochem), Rabbit polyclonal anti-TFPI antibody (Calbiochem), Caspase-3 Activity Detection Kit (FITC-DEVD-FMK) (Oncogene), Taurine
MWG-Biotech AG, Ebersberg, Germany	Primer synthesis for: ANF GAP3DH, MGF, MHCβ, TF, TFPI
Nikon, Kingston-Upon-Thames, UK	Nikon TMS inverted microscope
Novartis Animal Health Ltd., Lifington/Royston, UK	Thiopentone sodium (0.025 g/ml)
Novocastra Ltd., Newcastle Upon Tyne, UK	Mouse anti human developmental myocin heavy chain antibody
Pfizer Ltd., Kent, UK	Rimadyl

Promega, Southampton, UK	10X TBE buffer, TMB stabilized substrate for horse-radish peroxidase, Cell Titer 96 Aqueous One solution reagent, DeadEnd™ Fluorometric Tunel System
PromoCell, Heidelberg, Germany	Heat inactivated foetal calf serum (FCS)
Radiometer, Copenhagen, Netherlands	ABL 77 Series blood gas analyser
Royal Free Hospital, London, UK	Rabbit anti human mgf (kindly provides by Prof. Goldspink)
Santa Cruz Biotechnology Inc, Heidelberg, Germany	Rabbit polyclonal anti-rat ANF antibody, Anti-rabbit IgG HRP conjugated antibody, Anti-mouse IgG HRP conjugated antibody, Rabbit anti-human p53 antibody, goat abti-rabbit IgGFITC conjugated antibody
SensoNor a.s., Horten, Norway	SensoNor 840 transducer
Sigma-Aldrich Inc, Poole, UK	Dulbecco's Modified Eagle's medium (without glutamine, with 4.5 g/l glucose and sodium bicarbonate), Ala-Glu solution, Antibiotic/antimycotic solution, Sterile PBS, Trypsin-EDTA, Sodium pyruvate, Sodium lactate, Hepes, Butanedion Monoxime (BDM), BSA A6003, BSA A7030, TRI-reagent, Chloroform minimum (99 %), 2-Propanol for molecular biology (minimum 99 %), Absolute ethanol 200proof for molecular biology, Nuclease free water, Bromophenol blue, Lipid-free BSA protein standards, 2X Laemmli's buffer, PMSF, Methanol, Tween-20, Formaldehyde, Anicomycin Triton X-100, Ammonium persulfate, Nucleic asid gel stain Sybergreen I, Mouse anti-human slow myosin heavy chain antibody
Sybron Ing., Chicago, USA	1.5 ml cryovials
Syngene, Cambridge, UK	UV transilluminator, "Gene Tools" software program
Techne Ltd., Stone, UK	Techgene thermal cycler
TCS Cellwork, Botolph Claydon, UK	Diamethyl sulfoxide (DMSO) freezing medium
Tocris Biosciences, Bristol, UK	2-Methoxyestradiol (2ME)
VWR, Poole, UK	Trypan blue
Wissenchafliche Software, Freberg, Germany	"B & L Menu" primer design software
Worthington Biochemical- Lorne Laboratories Ltd., Reading, UK	Worthington type 2 collagenase enzyme
WPA, Cambridge, UK	WPA lightwave UV/Vis Diobe array spectrophotometer

2.2 Methods

2.2.1 Culture and maintenance of H9c2 cells

The H9c2(2-1) cell line, is a sub-clone of the original clonal cell line derived from the embryonic BD1X rat heart tissue by B. Kimes and B. Brandt and excibits many of the properties of skeletal muscle and is ideal to be used for expression studies. Also, myoblastic cells in this line have the ability to fuse and form multinucleated myotubes and respond to acetylcholine stimulation. The myoblastic population becomes depleted rapidly if the cultures are allowed to become confluent. It is advisable to subculture the cells before reaching 100% confluence and the line should be recloned periodically with selection for myoblastic cells (ATCC-LGC/Promochem, UK).

2.2.1.1 Culture of H9c2 cells from frozen stock

All procedures were performed under sterile conditions. H9c2 cells stored in DMSO-freezing medium in liquid nitrogen (-80°C), were propagated in Dulbecco's Modified Eagle's medium (DMEM) supplemented with heat inactivated foetal calf serum (10 % v/v), 4 mM of Ala-Glu solution and antibiotic/antimycotic solution (1 % v/v). Cells were thawed by gentle agitation at 37°C for 2 min and 500 µl of complete DMEM medium was added to reduce the toxicity of the DMSO-freezing medium. A suspension of 2 x 10^5 cells were seeded in a 75 cm^2 tissue culture flask, containing 10 ml of complete DMEM medium and incubated at 37°C under 5 % CO_2 atmosphere. The medium was partially exchanged (3 ml) every 3 days.

2.2.1.2 Subculturing procedure

Cells were propagated, as specified by the manufacturer's instructions, to 80-90 % confluence before sub-culturing, so as to maintain the myoblastic component of the population. The medium was aspirated and retained at 37°C. Sterile pre-warmed phosphate buffer saline (PBS), pH 7.4, was used to rinse the cells to remove any trace of medium. Subsequently, trypsin-EDTA solution (5 ml for 25 cm^2 culture flask or 8 ml for 75 cm^2 culture flask) was added and incubated at 37°C for 5-10 min. Cells were observed using an inverted microscope to ensure detachment. The suspension was then aspirated into a 30 ml sterilin tube and the flask rinsed with an equal volume of the retained medium and pooled with the cell suspension (to neutralise the trypsin solution). Cell density was established using a haematocytometer. Cells were then centrifuged at 400 *g* for 10 min, and the pellet was re-suspended in fresh complete DMEM medium pre-warmed at 37°C. The cells were divided between new culture vessels as required (7.5 x 10^4 cells/ 25 cm^2 flask, 2 x 10^5 cells/ 75 cm^2 flask and/or 4.2 x 10^5 cells/ 150 cm^2 flask) and incubated at 37°C under 5 % CO_2 atmosphere. The medium was changed partially (1 ml for the 25 cm^2 flask, 3 ml for 75 cm^2 flask, 5 ml for 150 cm^2 flask) every 3 days.

2.2.1.3 Harvesting procedure

Cells were trypsinised and pelleted as described in section 2.2.1.2. The pellet was resuspended in prewarmed (37°C) sterile PBS pH 7.4 and divided into sterile 1.5 ml eppendorf microfuge tubes. Finally, the cells were centrifuged at 12,110 *g* in a microcentrifuge for 10 min, the supernatant was discarded and the pellet frozen at -20°C for protein and nucleic acid analysis.

2.2.1.4 Freezing procedure

Cells were harvested by trypsinisation as described above (section 2.2.1.2). Cells were resuspended in freezing medium containing DMSO, aliquoted in cryovials (4×10^5 cells/ cryovial and/or 1×10^6 cells/ cryovial), placed in a freezing chamber and stored at –70°C overnight. The vials were subsequently transferred to a liquid nitrogen container for long-term storage.

2.2.1.5 Cell counting procedure

The number of the cells was determined using a double chamber haematocytometer. 10 μl of the cell suspension was placed into the hematocytometer chamber and the cell density was determined, by counting cells within a set area of 10 squares. Concentration of cells was determined from the following equation:

Cell concentration (cells/ ml) = average cell count x 10^4 x dilution factor (where appropriate).

Cell viability was checked using Trypan blue stain and was assessed by the ratio of the stained cells (dead cells) versus the unstained cells (live cells). Cells in suspension were diluted 1:1 with 0.1 % (w/v) Trypan blue, were loaded in a haematocytometer chamber and were counted as described above.

2.2.2 The aortic constriction model of cardiac hypertrophy in rats

Male Sprague-Dawley rats were housed and maintained under conditions complying with Home Office regulations under the Animals (Scientific Procedures) Act 1986 and had ethical clearance. All procedures were carried out in an aseptic environment. The surgical procedure was performed as described by Boateng *et al.*, (1998). In brief, male Sprague-Dawley rats, weighing between 240-260 g were anaesthetised by

inhalation of 4 % halothane in oxygen (4 l/h), and 0.02 ml Rimadyl analgesic agent (5 % w/v Carprofen) administered subcutaneously prior to surgery. Animals were maintained under anaesthesia with 2-2.5 % halothane in oxygen (1 l/h). A laparotomy was performed, the abdominal aorta exposed between the left and the right renal branches and constricted with Ethicon suture (Mersilk 0 suture) and a blunted needle with an outer diameter of 0.5 mm. As an indication of successful constriction, the left kidney was blanched following constriction. The suture was then tied, the needle removed and the kidney allowed to re-colour. Prior to closure, approximately 5 ml of sterile isotonic saline was administered to re-hydrate the animal. The abdominal wall was closed using absorbable suture (Ethicon 3-0, Vicryl braided) and the skin layer with non-absorbable suture (Ethicon 3-0, blue monofilament). Subsequently, animals were given 100 % oxygen and 0.07 ml of antibiotic (42 mg/kg of body weight (bWt) (Ampifen) was administered subcutaneously. Sham-operated animals underwent the same procedure without constriction of the abdominal aorta. Animals were fed and watered *ad lib*. The hearts were harvested 1, 3, 7 and 14 days post surgery and used either for isolating adult ventricular cardiomyocytes (section 2.2.2.1) or for isolating the left ventricle (section 2.2.2.2).

2.2.2.1 Isolation of adult ventricular rat cardiomyocytes

The method was adapted by Smolenski *et al.* (1991). Briefly, male Sprague-Dawley rats, weighed between 240 and 260 g were anaesthetised with approximate 1 ml/100g BWt, sodium thiopentone (0.025 g/ml Thiopentone sodium), hearts excised and the aorta cannulated on a Langendorff perfusion apparatus. The left atrium was perforated and a small piece of plastic tubing inserted into the mitral valve to prevent closure. The heart was perfused in the Langendorff mode with non-circulating buffer

containing 60 mM NaCl, 16 mM KCl, 3.2 mM $MgSO_4$, 1.2 mM KH_2PO_4, 10 mM mannitol, 20 mM taurine, 11 mM glucose, 5 mM pyruvate, 10 mM BDM, 10 mM Hepes, pH 7.2, and oxygenated 100 %, at a flow rate of 11.5 ml/min, at 37°C for 10 min. Cells were isolated as described previously by Smolenski *et al.* 1991. Subsequently, the perfusion was switched to a re-circulating mode with 35 ml of non-circulating buffer containing 0.875 units of collagenase Worthington type 2 and 0.5 % (w/v) BSA (A6003). After 10 min, 7 x 5 µl aliquots of 1 M $CaCl_2$ were added to give a final concentration of 1 mM $CaCl_2$ to produce Ca-tolerant cardiomyocytes. The re-circulating perfusion was maintained for a further 30 min. The perfusion apparatus is illustrated in Figure 2.1.

Following removal of atria, the ventricles were placed in 25 ml of washing buffer containing 120 mM NaCl, 2.6 mM KCl, 1.2 mM $MgSO_4$, 1.2 mM KH_2PO_4, 1 mM $CaCl_2$, 11 mM glucose, 2 mM pyruvate, 4 % (w/v) BSA (A7030), 10 mM BDM, 10 mM, Hepes, pH 7.4, oxygenated with 100 % O_2, and gently agitated by repeating pipetting. The cell suspension was filtered through a nylon gauze and centrifuged at 15 *g* for 10 min. The cells were re-suspended in 5 ml of DMEM medium supplemented with 10 % (v/v) heat inactivated foetal calf serum, 1 % (v/v) antibiotic/antimycotic solution, and 2 mM Ala-Glu solution and transferred to a 75 cm^2 culture flask. The cells were incubated at 37°C with 5 % CO_2 atmosphere for 1 h, to remove other cell types such as fibroblasts. The purified population of cells was centrifuged at 400 *g* for 10 min and the pellet re-suspended in 1 ml of pre-warmed (37°C) sterile PBS, pH 7.4, centrifuged at 12,110 *g* in a microcentrifuge for 8 min and frozen at –20°C for molecular analysis.

Figure 2.1: A schematic representation of the procedure for the isolation of adult rat ventricular cardiomyocytes.

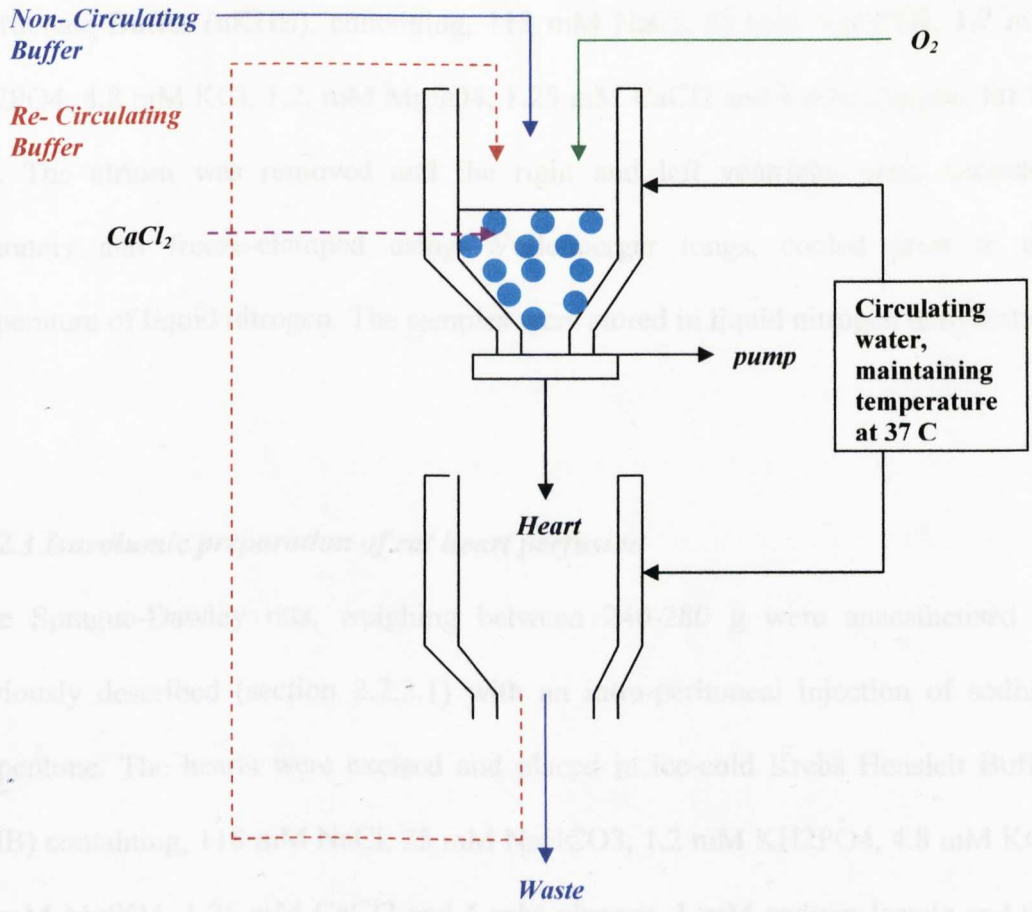

Hearts were perfused for 10 min with non-circulating buffer (blue line) 100 % oxygenated and pre-warmed at 37°C, which was subsequently discarded. The buffer was then switched to the re-circulating buffer (red dashed line) oxygenated 100 % for a further 10 min before the addition of $CaCl_2$ (violet dashed line). The re-circulating perfusion was maintained for a further 30 min.

2.2.2.2 Isolation of left ventricular rat heart tissue

Male Sprague-Dawley rats, weighing between 240-260 g were anaesthetised as described previously (section 2.2.2.1), the heart excised and the aorta cannulated in a Langendorff perfusion apparatus. The heart was rinsed with normal Krebs Hensleit bicarbonate Buffer (nKHB), containing, 118 mM NaCl, 25 mM NaHCO3, 1.2 mM KH2PO4, 4.8 mM KCl, 1.2. mM MgSO4, 1.25 mM CaCl2 and 5 mM glucose, for 10 min. The atrium was removed and the right and left ventricles were dissected separately and freeze-clamped using Wollenberger tongs, cooled prior to the temperature of liquid nitrogen. The samples were stored in liquid nitrogen until further use.

2.2.2.3 Isovolumic preparation of rat heart perfusion

Male Sprague-Dawley rats, weighing between 240-280 g were anaesthetised as previously described (section 2.2.2.1) with an intra-peritoneal injection of sodium thiopentone. The hearts were excised and placed in ice-cold Krebs Hensleit Buffer (KHB) containing, 118 mM NaCl, 25 mM NaHCO3, 1.2 mM KH2PO4, 4.8 mM KCl, 1.2 mM MgSO4, 1.25 mM CaCl2 and 5 mM glucose, 1 mM sodium lactate and 0.1 mM sodium pyruvate. The wet heart weight was recorded and the heart cannulated via the aorta and subjected to retrograde perfusion using a modified isovolumic Langendorff method (Ogino *et al.*, 1996). The heart was perfused at a flow rate of 14 ml/min with KHB, equilibrated with 95 % O2 and 5 % CO2, at 37°C using a specially constructed oxygenator (Gamesik *et al.*, 1996). The apex of the heart was pierced so as to prevent accumulation of fluid. A balloon, made of cling film, was inserted through the mitral valve into the left ventricle and inflated with water using a 2.0 ml micrometer syringe so as to maintain a diastolic pressure of 5 mmHg. Monitoring of

the left ventricular pressure was achieved using a SensoNor 840 physiological pressure transducer connected to the balloon via a fluid filled line to a MacLab recording system (AD Instruments) (Figure 2.2).

The heart was perfused with KHB at a constant flow rate of 14 ml/min for 20 min equilibration period (Figure 2.3). Subsequently, the heart was subjected to increasing doses of TF for 15 min as shown in Figure 2.3.

Effluent samples were collected at 5 min interval and oxygen content was determined using an ABL 77 series blood gas analyser. Oxygen consumption (MVO2) was determined by measuring the difference in partial pressure of oxygen in the buffer (pO2 perfusate) and the coronary effluent (pO2 effluent) and calculated using the following equation:

$$MVO_2 = \frac{[(pO_2 \text{ perfusate} - pO_2 \text{ effluent})/760 \text{ mmHg}] \times O_2 \text{ solubility at } 37^\circ C \times 5 \times \text{flow rate}}{\text{Wet hear weight}}$$

Where MVO_2 is measured in μmoles O_2/min/g wet heart weight, pO2 is measured in mmHg and flow rate is measured as ml/min. O_2 solubility at 37°C is equalled to 0.199 μmole/ml. At the end of the perfusion protocol, the balloon was removed and the heart was freeze-clamped and stored as previously described (section 2.2.2.2).

After excision of the heart, approx. 1 ml of blood from the thoracic cavity was collected in an 1.5 ml microfuge tube containing 100 μl of heparin and haematocrit was measured using a radiometer ABL 77 series blood gas analyser. At the same time, tibia length was measured and the kidneys were removed and weighed.

Figure 2.2: The perfusion rig for Langendorff heart perfusion

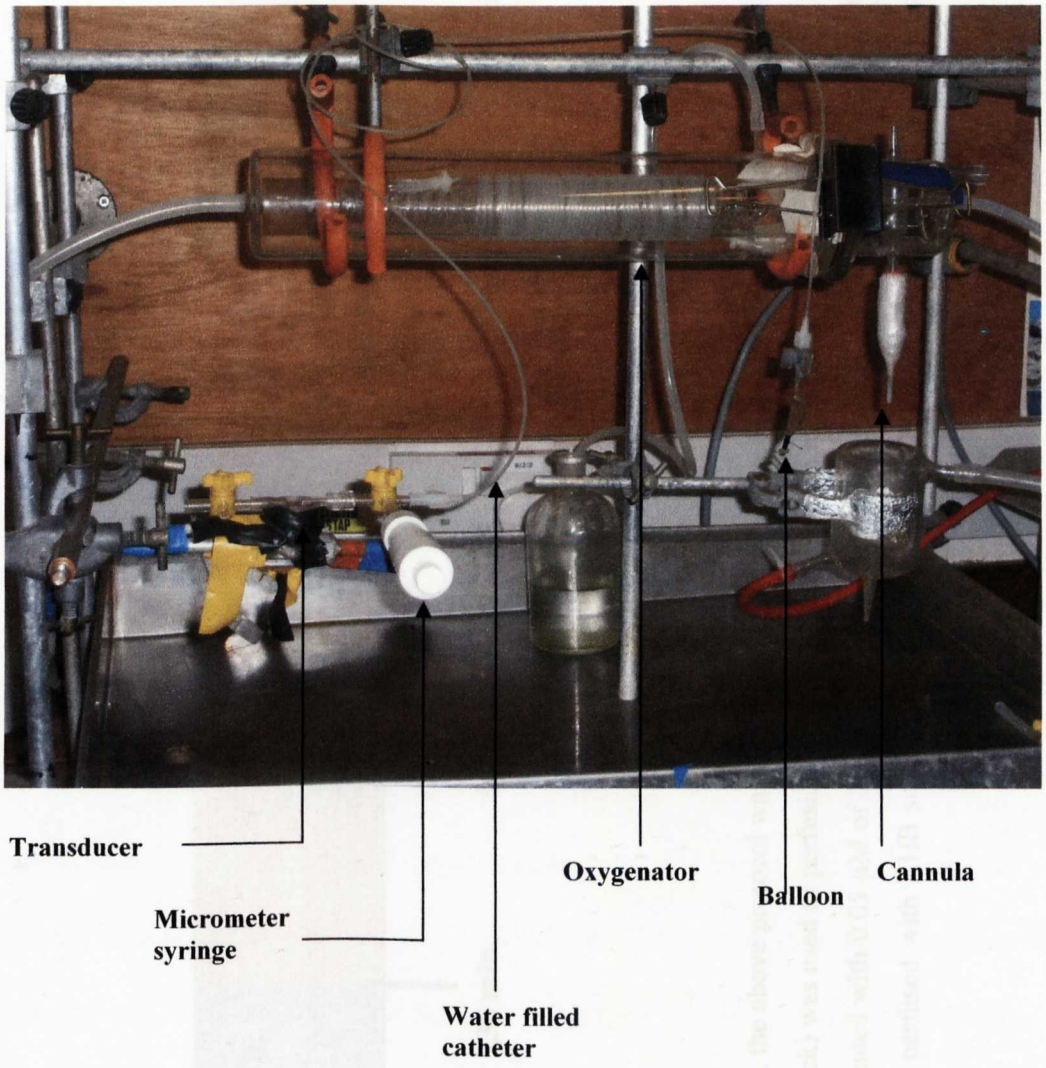

The perfusion rig assembled in the picture consists of a water filled catheter connected to the transducer and the micrometer syringe via a 3 way tap from one end and to the balloon from the other. The heart hangs from the cannula and kept at 37 °C for the duration of the experiment. The transducer picks up the electrical impulses of the heart via the water filled catheter, which are recorded using the MacLab recording system.

Figure 2.3: Experimental perfusion protocol.

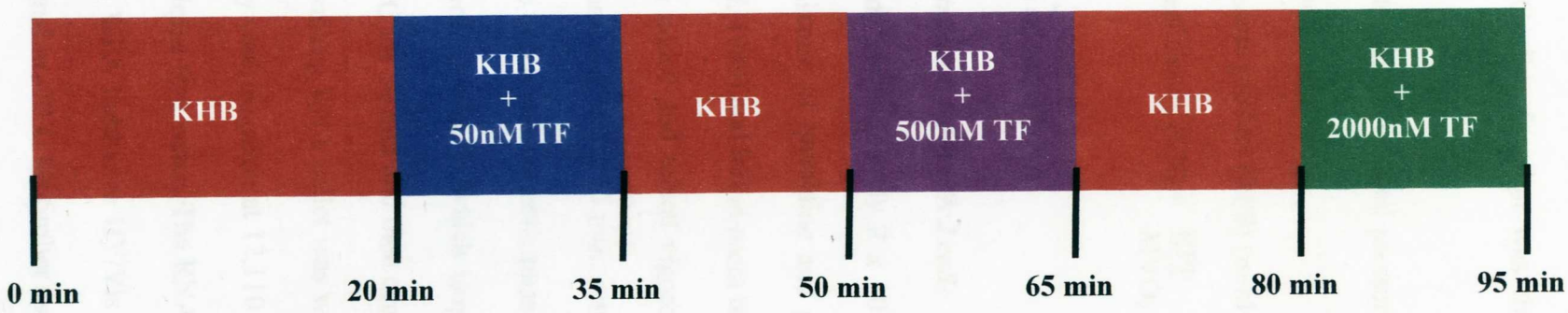

After cannulation of the heart on the perfusion rig, the above protocol was used. The heart was allowed to equilibrate for 20 min with KHB (red block). Then KHB supplemented with 0.05 μM of TF (blue block) was used as perfusion went for 15 min and then the heart was washed with KHB (red block) for 15 min. The perfusion was continued with KHB supplemented with 0.05 μM of TF (violet block) for another 15 min and a second wash with KHB (red block) took place for a further 15 min. Finally the heart was perfused with KHB supplemented with 2 μM of TF (green block) for a further 15 min and then freeze-clamped.

2.2.2.3.1 Cardiac function

Throughout the perfusion protocol, heart rate, systolic and diastolic pressures were recorded continuously and the mean values for each parameter determined (Figure 2.4a & 2.4b). Cardiac function was then assessed by calculating the following parameters:

A. Left ventricular developed pressure (LVDP) (mmHg) = End systolic pressure – End diastolic pressure

B. Rate pressure product (RPP) (mmHg/min) = LVDP x Heart rate

C. Cardiac efficiency (CE) = $\frac{RPP}{MVO_2}$ (mmHg/μmoles/g wet heart weight).

2.2.3 Isolation of total RNA

2.2.3.1 RNA extraction from H9c2 cells

Pellets containing approximately 2 x 10^4 cells were lysed by repeated pipetting in TRI-reagent (mixture of quanidine and phenol in a mono-phase solution) (200 μl) (Sambrook *et al.* 1989) and left at room temperature for 5 min. Subsequently, 40 μl of chloroform was added and mixed vigorously for 15 s. The mixture was allowed to stand at room temperature for 15 min, centrifuged at 12,110 *g* in a microcentrifuge for 15 min and the colourless aqueous phase was transferred to a nuclease free 1.5 ml Eppendorf microfuge tube to which isopropanol (100 μl) was added. This solution was left at –20°C for 30 min and then centrifuged at 12,110 *g* in a microcentrifuge for 10 min. The resulting RNA pellet was washed with 75 % nuclease free ethanol (200 μl), collected by centrifugation at 12,110 *g* for 5 min and the pellet was re-suspended in 60 μl of nuclease free water. The RNA was quantified measuring the absorption at 260 nm with a WPA lightwave UV/Vis Diobe array spectrophotometer (see section 2.2.3.4) and stored in -70°C for further use.

Figure 2.4: A representative trace of cardiac function obtained during heart perfusions.

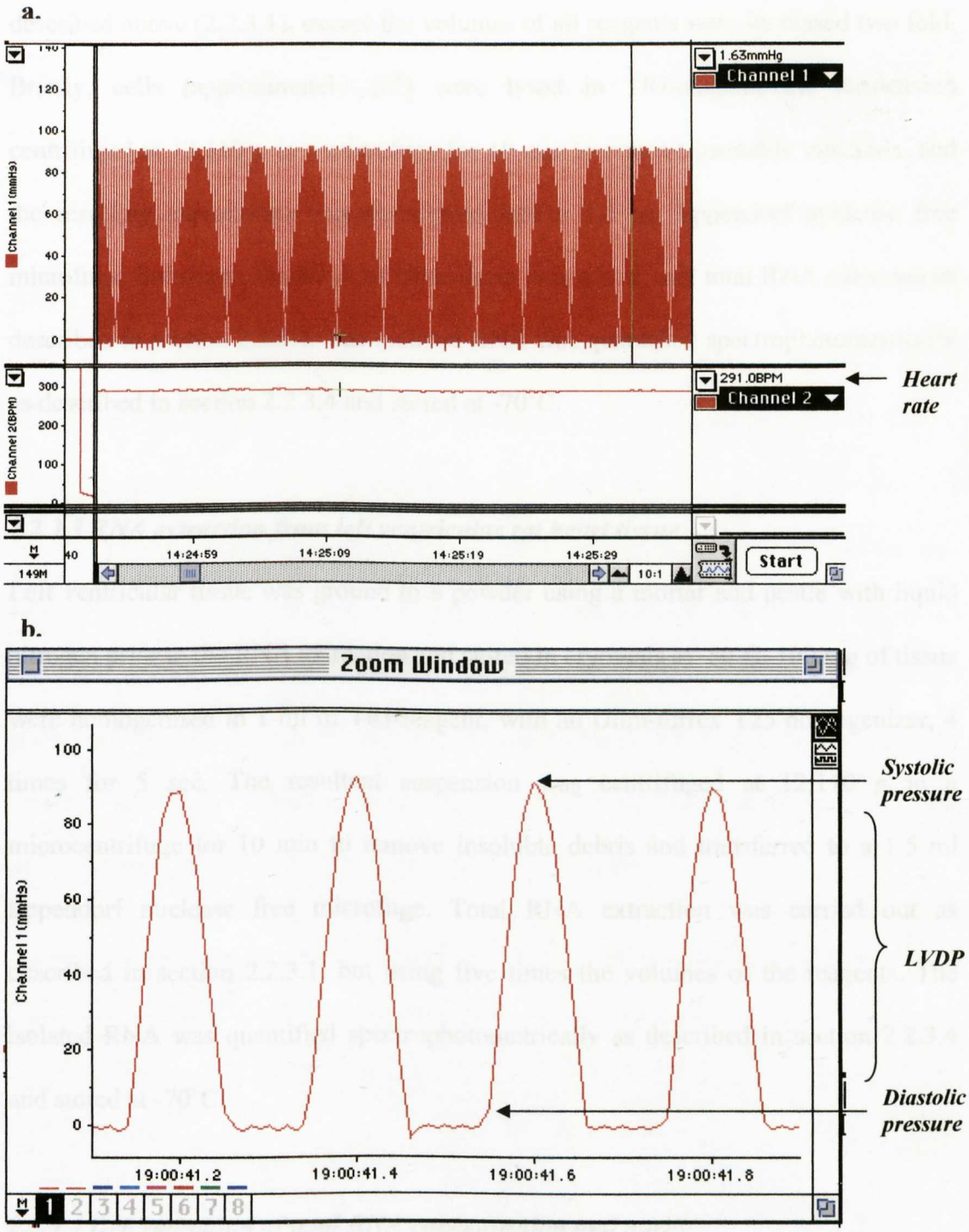

Figure (a), shows a typical trace of cardiac function obtained during the equilibration time of heart perfusion. On channel 1 the systolic and diastolic pressures were recorded and on channel 2 the heart rate. Figure (b), shows an expanded section of the trace to determine diastolic pressure and systolic pressure. The left ventricular develop pressure (LVDP) can be calculated thereafter.

2.2.3.2 RNA extraction from isolated adult ventricular rat cardiomyocytes

RNA was extracted from isolated cardiomyocytes using a similar procedure to that described above (2.2.3.1), except the volumes of all reagents were increased two fold. Briefly, cells (approximately 10^6) were lysed in TRI-reagent, the suspension centrifuged at 12,110 *g* in a microfuge for 10 min to remove insoluble materials, and the resulting supernatant was transferred into a 1.5 ml Eppendorf nuclease free microfuge. Subsequently, 80 µl of chloroform was added, and total RNA extracted as described in section 2.2.3.1. The isolated RNA was quantified spectrophotometrically as described in section 2.2.3.4 and stored at -70°C.

2.2.3.3 RNA extraction from left ventricular rat heart tissue

Left ventricular tissue was ground to a powder using a mortar and pestle with liquid nitrogen prior to the RNA extraction and stored in cryovials at -80°C. 100 mg of tissue were homogenised in 1 ml of TRI-reagent, with an Ultra-turrex T25 homogenizer, 4 times for 5 sec. The resultant suspension was centrifuged at 12,110 *g* in a microcentrifuge for 10 min to remove insoluble debris and transferred to a 1.5 ml Eppendorf nuclease free microfuge. Total RNA extraction was carried out as described in section 2.2.3.1, but using five times the volumes of the reagents. The isolated RNA was quantified spectrophotometrically as described in section 2.2.3.4 and stored at -70°C.

2.2.3.4 Determination of total RNA concentration and purity

To determine the concentration (µg/ml) and the purity of RNA, the ratio of absorbances at 260 nm and 280 nm was measured at a 10 fold dilution, using a lightwave UV/Vis Diobe array spectrophotometer. RNA samples with a ratio of 1.3 or

higher were considered to be of sufficient purity and used for experiments. The concentration (μg/ml) of the RNA per ml was determined using the following equation:

$$A_{260} \times 40\ \mu g/ml \times \text{dilution factor (10)} = \mu g/ml$$

2.2.4 Reverse transcription polymerase chain reaction (RT-PCR)

2.2.4.1 Primer design

The DNA sequences for the genes of interest were downloaded from the "NCBI" web site: "http://www.ncbi.nlm.nih.gov". The primers were designed using the "B & L Menu" computer software program avoiding primer-dimer formation. Reverse and forward primer pairs were designed for compatibility of the primer pairs and the size of the PCR product, (ideally between 400 and 800 base pairs). The primers optimised and used for the RT-PCR assessment of mRNA transcripts of glyceraldehyde-3-phosphate dehydrogenase (GAP3DH), tissue factor (TF), tissue factor pathway inhibitor (TFPI), atrial natriuretic factor (ANF), myosin heavy chain beta (MHCB) and mechano-growth factor (MGF) were as listed in table 2.2.

Table 2.2: Primer sequences for GAP3DH, TF, TFPI, ANF, MHCB and MGF

Primer name	Sequence	Product size
GAP3DH	5'-GGC ACA GTC AAG GCT GAG AAT-3'	800 bp
GAP3DH	5'-CCA GGA AAT GAG CTT CAC AAA G-3'	
TF (forward)	5'-CAC AGA GAT ATG GTC AGC AGG-3'	196 bp
TF (reverse)	5'-ATG GAG GAA CTC ACC TCA TGG-3'	
TFPI (forward)	5'-TGC AAA GCA ATG ATA CGG AG-3'	400 bp
TFPI (reverse)	5'-CTG CAC TCC TCC AAG GTC TC-3'	
ANF (forward)	5'-ATG GGC TCC TTC TCC ATC ACC-3'	397 bp
ANF (reverse)	5'-GGG CTC CAA TCC TGT CAA TCC-3'	
MHCB	5'-CAG AAG TCC TCC CTC AAG CTC C-3'	497 bp
MHCB	5'-CAG CCT CTC ATC TCG CAT CTC C-3'	
MGF (forward)	5'-GCT TGC TCA CTT TAC CAG C-3'	200 bp
MGF (reverse)	5'-AAA TGT ACT TCC TTT CCT T-3'	

The primers were synthesised by MWG-Biotech AG, reconstituted with nuclease free water at concentrations of 100 pmol/μl and kept at -20°C until use.

2.2.4.2 Analysis of mRNA transcripts by single tube RT-PCR

Ready-to-go RT-PCR beads were used for single tube RT-PCR reactions, to minimise the risk of contamination and pipetting errors by reducing the number of manipulations required. A single RT-PCR bead reconstituted in a total volume of 50 μl, provides a final concentration of ~2.0 units of Tag DNA polymerase, 10 mM Tris-HCl, 60 mM KCl, 1.5 mM $MgCl_2$, 200 μM dNTP, 200 μM Moloney murine leukaemia virus reverse transcriptase, 200 μM RNA guard ribonuclease inhibitor (porcine), 200 μM stabilizers, including RNase/DNase-free BSA (Sambrook *et al.* 1989). To initiate the reaction, 0.5 μl of 100 pmol/μl forward primer, 0.5 μl of 100 pmol/μl reverse primer and 0.1 μg of RNA template were added. Reverse transcription and PCR amplification was carried out in a continuous run in a Techgene thermal cycler according to the following programme:

Table 2.3: RT-PCR programme used for the amplification of mRNA transcripts

Program	Time	Temperature	Cycles	Event
RT step	30min	42°C	1	Transcribe mRNA to cDNA
	5min	95°C	1	RNA degradation and RTase denaturation
PCR step	1min	95°C	30	Denaturing
	1min	55-65°C		Annealing
	1min	72°C		Extension
End	10min	72°C	1	Final extension
	Hold	4°C	N/A	Cooling

The annealing temperatures for the specific test genes amplified were 61°C for GAP3DH and TFPI, 58°C for TF, ANF and MHCB; and 55°C for MGF.

2.2.4.3 Analysis of PCR products by agarose gel electrophoresis

The amplified DNA was separated and analysed on a 1.5 % (w/v) agarose gel by electrophoresis (Sambrook *et al.* 1989). 50 ml of 1.5 % (w/v) agarose gel was prepared in an electrophoresis tray with a comb and immersed in tris-borate (TBE) buffer, pH 8.3. Samples (12 µl) were mixed with loading buffer (2 µl, 0.1 % (w/v) bromophenol blue, 30 % (v/v) glycerol), and 100 x diluted Syber Green I (1 µl). 15 µl were then loaded into each well. Electrophoresis was carried out at 100 V for 1 h, the gel subsequently visualised on a UV transilluminator and the image was recorded. The amplification products were identified by comparison with a DNA ladder covering a range of 100-1000 bp. The amount of the amplified product was measured as total intensity using the "Gene Tool" computer software programme and the relative transcript expression was quantified against amplified GAP3DH mRNA as a reference gene.

2.2.5 Protein analysis

2.2.5.1 Extraction of total protein from H9c2 cells

Total protein was extracted from approximately 4 x 10^5 cells lysed in 200 µl of Laemmli buffer. An aliquot (10 µl) of cell lysate was removed and used for protein quantification (section 2.2.5.4). The remaining lysate was stored at -20°C until used.

2.2.5.2 Extraction of total protein from isolated adult ventricular rat cardiomyocytes

The isolated cardiomyocytes were homogenised in an Ultra-turrex T25 homogeniser in 1 ml of homogenisation buffer (50 mM of Tris-HCl and 1mM PMSF), 4 times each for 5 s. The homogenate was then centrifuged at 12,110 *g* in a microcentrifuge for 10 min and the remaining pellet was re-suspended in 400 µl of homogenisation buffer.

Aliquots (10 µl) of sample were used for protein quantification (section 2.2.5.4). The remaining lysate was stored at -20°C until further use.

2.2.5.3 Extraction of total protein from left ventricular rat heart tissue

Left ventricular tissue was ground as described in section 2.2.3.3. 200 mg of left ventricular tissue was homogenised in 1 ml of homogenisation buffer as described above and the protein extracted as described in section 2.2.5.2.

2.2.5.4 Estimation of protein concentration using the Bradford assay

The protein concentrations of cell and tissue extracts were determined using the method of Bradford (1976), which utilizes the principle of protein-dye interaction and is suitable for measuring µg quantities of protein. Lipid-free bovine serum albumin (BSA) was used to prepare a standard curve covering a concentration range of 0-150 µg/ml of protein. Aliquots (100 µl) of standards or samples were mixed with 900 µl of 1:1 freshly diluted Bradford reagent in water. The samples were incubated for 10 min at room temperature, and absorbance measured at 595 nm using a lightwave UV/Vis Diobe-Array spectrophotometer. Protein concentration of the cells and tissue extracts were determined from the standard curve (Figure 2.5).

2.2.5.5 SDS-polyacrylamide gel electrophoresis

A 12 % (w/v) resolving gel was prepared using 4 ml bis-acrylamide solution (30 % (w/v) acrylamide: 0.8 % (w/v) bis-acrylamide stock solution (37:5:1)), 2.6 ml resolving buffer (1.5 M Tris-HCl, pH 8.8, 0.4 % (w/v) SDS), 3.3 ml distilled water and 100 µl of 10 % (w/v) freshly made ammonium persulphate. The mixture was de-aerated by placing under vacuum for 2-3 min and polymerisation initiated by the

Figure 2.5: Protein standard curve.

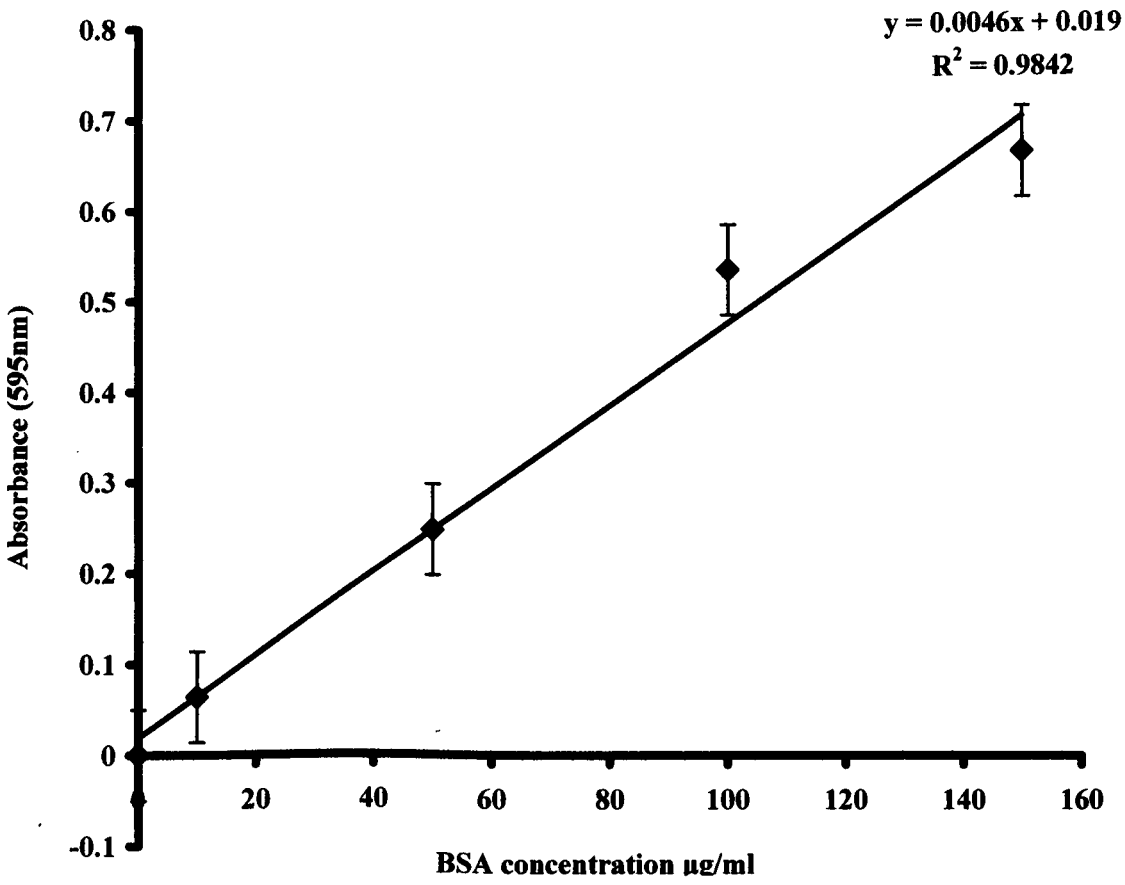

Bovine serum albumin (BSA) was used to prepare a standard curve covering a concentration range of 0-150 µg/ml of protein. Following incubation with 1:1 diluted Bradford reagent at room temperature for 10 min, the absorbance was measured at 595 nm using a lightwave UV/Vis Diobe-Array spectrophotometer. The graph represents a representative standard curve constructed on the day of the experiment with freshly made BSA standards from which the unknown concentration of protein lysates were determined ± SEM. The curve is typical of 40 experiments.

addition of 10 µl tetramethylethylenediamine (TEMED). The solution was poured into vertical sealed electrophoresis plates separated with 1 mm spacers and allowed to set for 30 min. A 4 % (w/v) stacking gel was made using 650 µl bis-acrylamide solution, 1.3 ml stacking buffer (0.5 M Tris-HCl pH 6.8, 0.4 % (w/v) SDS), 3 ml distilled water and 25 µl of 10 % (w/v) ammonium persulphate prepared as described above. The mixture was poured on top of the separating gel and an appropriate comb inserted and allowed to polymerise for 2 h. The electrophoresis plate was then placed in the electrophoresis tank with sufficient electrophoresis buffer (25 mM Tris-HCl pH 8.3, 192 mM Glycine, 0.035 % (w/v) SDS). The cell or tissue extract were denatured by boiling at 99°C for 5 min prior to electrophoresis and 20 µg of each denature sample was loaded into separate wells. Electrophoresis was carried out at 100 V until the dye front had reached the bottom of the resolving gel.

2.2.5.6 Western blot analysis of atrial natriuretic factor (ANF)

Following SDS-PAGE, the gel was transferred onto a nitrocellulose membrane, between filter paper, and positioned in the blotting tank with freshly made transfer buffer (150 mM glycine, 20 mM Tris-HCl pH 8.3, 20 % (v/v) methanol). The separated protein bands were transferred at 16 mA at 4°C overnight. Subsequently, the nitrocellulose membrane was blocked with Tris-buffered Saline Tween 20 (TBST) buffer (125 mM NaCl, 25 mM Tris-HCl, pH 8, 0.1 % (v/v)Tween-PBS) for 2 h at room temperature, washed three times with 0.1 % (v/v) Tween-PBS, each time for 10 min, and incubated with rabbit anti-rat ANF (diluted by 1:1000 in TBST), for 1.5 h at room temperature. The membrane was then washed three times with 0.1 % (v/v) Tween-PBS for 10 min each and probed with goat anti-rabbit IgG conjugated to horse radish peroxidise (HRP) antibody (diluted by 1:2000 in TBST), for 1.5 h at room

temperature. Finally, the membrane was washed twice with 0.1 % (v/v) Tween-PBS each for 10 min and a third time with PBS. The membrane was developed using 3,3',5,5'tetramethylbenzidine (TMB) stabilised substrate for horse-radish peroxidase and visualized under a white light transilluminator. The relative expression of ANF protein was quantified against GAP3DH as reference using the "Gene Tool" computer software program.

2.2.5.7 Western blot analysis of tissue factor (TF)

A similar method to that described above (section 2.2.5.6) was used for the analysis the TF protein expression. A mouse monoclonal human anti-TF diluted to 1:1000 in TBST was used as the primary antibody and developed with donkey anti-mouse IgG conjugated to HRP diluted 1:2000 in TBST.

2.2.5.8 Western blot analysis of tissue factor pathway inhibitor (TFPI)

The protein expression of TFPI expression was analysed as previously described (Section 2.2.5.6), but using a rabbit polyclonal human anti-TFPI diluted to 1:500 as the primary antibody and developed with goat anti-rabbit IgG conjugated to horse radish peroxidise (HRP) diluted 1:2000 in TBST.

2.2.5.9 Western blot analysis of glyceraldehyde-3-phosphate dehydrogenase (GAP3DH)

As reference GAP3DH protein was analysed with a similar method to that described in section 2.2.5.6. A mouse monoclonal human anti-GAP3DH diluted to 1:4000 in TBST was used as the primary antibody and developed with donkey anti-mouse IgG conjugated to HRP diluted 1:2000 in TBST.

2.2.6 Measurement of H9c2 cellular proliferation

2.2.6.1 MTS-based colorimetric assay for cellular proliferation

The CellTiter 96 AQueous One Solution reagent contains an MTS tetrazolium compound which can be reduced to a coloured formazan product by NADH and NADPH, produced by metabolically active cells. The assay is based on the production of formazan, the amount of which is proportional to the number of living cells. Post-incubation of the cells with the MTS reagent, the number of the living cells can be determined by measuring the quantity of the formazan product spectrophotometrically at 490 nm.

H9c2 cells (approximately 5 x 10^4 per well) were seeded out into a 24 well plate with complete DMEM medium and allowed to adhere overnight in a 37°C incubator in 5 % CO_2 atmosphere. The media were then removed and the cells were washed with sterile pre-warmed (37°C) PBS. Subsequently, 200 µl of fresh pre-warmed (37°C) complete DMEM media containig 40 µl of CellTiter 96 AQueous One Solution reagent was added to each well. The cells were then incubated at a 37°C humidified incubator with 5 % CO_2 atmosphere for 1-2 h. The media containing the reagent solution was transferred to 1ml cuvettes and diluted with 760 µl of distilled water (dH_2O) to a total volume of 1 ml. The cell proliferation was determined spectrophotometrically by measuring the absorption at 490 nm against a blank sample.

2.2.6.2 Preparation of a standard curve for the proliferation assay

A standard curve was constructed by preparing serial dilutions of H9c2 cells covering a range from 0-2 x 10^4 cells per well. The cells were seeded out in 24 well plate in complete DMEM media (200 µl) and allowed to adhere for 2 h without proliferating.

Subsequently, 40 µl of CellTiter 96 AQueous One Solution reagent was added to each well and the cells were incubated at 37°C under 5 % CO_2 atmosphere for 1-2 h. The absorbance was then measured at 490 nm as described in section 2.2.6.1. A standard curve was constructed by plotting the A_{490} against the $\log_{10}$ [density of the cells] (Figure 2.6).

2.2.7 Analysis of H9c2 cellular apoptosis

2.2.7.1 Determination of DNA fragmentation using the DeadEnd™ Fluorometric TUNEL assay

To determine the DNA fragmentation during cell apoptosis, the commercially available DeadEnd™ Fluorometric Tunel System was used. H9c2 cells (8×10^4) were seeded out into 8 well microscope chamberslide with complete DMEM medium and allowed to adhere overnight at 37°C in 5 % CO_2 atmosphere. The cells were then fixed with 4 % (v/v) formaldehyde solution in PBS for 25 min at 4°C and washed twice each for 5 min with PBS. The cells were then permeabilised by incubation with 0.2 % (v/v) Triton X-100 in PBS for 20 min at room temperature. Subsequently, the cells were washed twice with PBS, each for 5 min. Excess liquid was removed from each chamber and the cells were suspended with 100 µl of equilibration buffer (200 mM) potassium cacodylate, 25 mM Tris-HCl pH 6.6, 0.2 mM DTT, 0.25 mg/ml BSA, 2.5 mM $CoCl_2$), and allowed to equilibrate for 10 min at room temperature. Subsequently, 50 µl of recombinant Terminal Deoxynucleotidyl Transferase enzyme (1,500 U rTdT) incubation buffer (containing 45 µl of equilibration buffer and the addition of 50 µM fluorescein-12-dUTP, 100 µM dATP, 10 mM Tris-HCl, pH 7.6, 1 mM EDTA) was added to the cells and the slide was placed in a dark humidified chamber and incubated at 37°C for 1.5 h. The cells were then incubated with 2 x SSC

Figure 2.6: Standard curve for the cell proliferation assay.

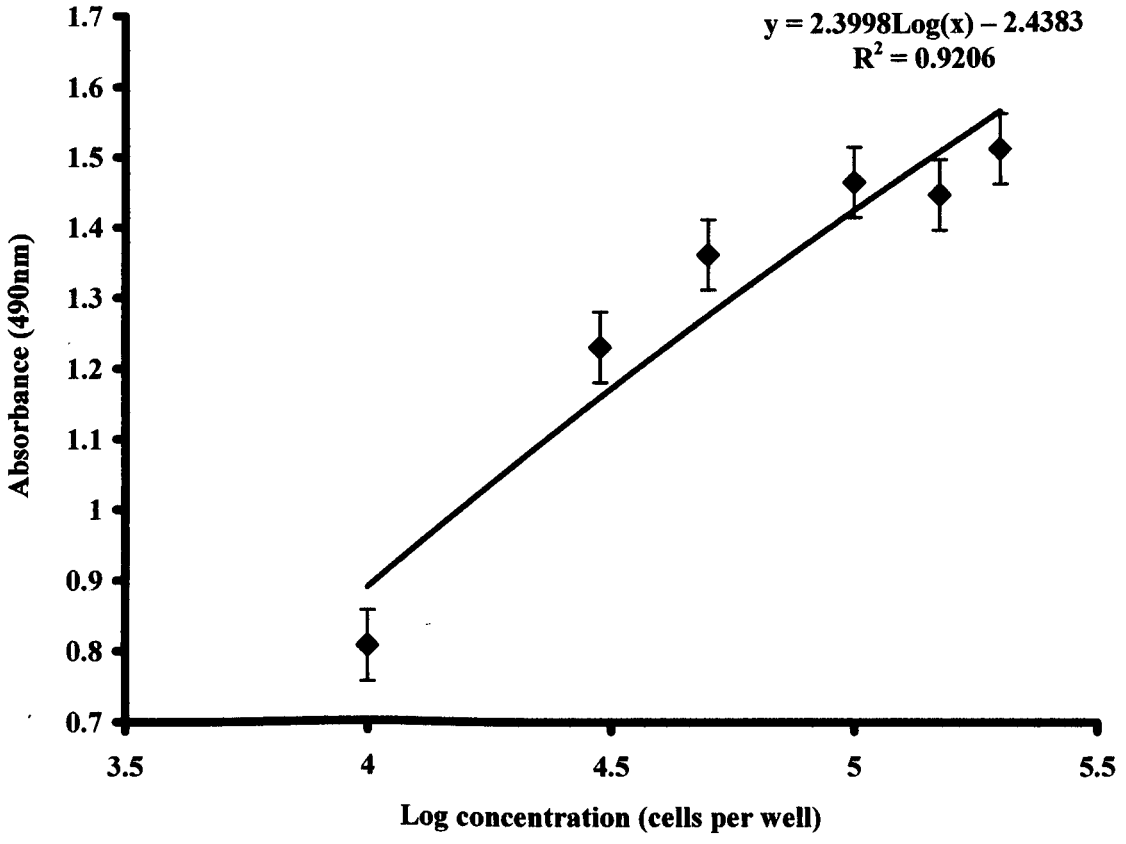

H9c2 cells were seeded out in a 24 well plate at serial dilutions covering a range of 0-2 x 10^4 in complete DMEM medium (200 µl). After incubation for 2 h on at 37°C, 40 µl of CellTiter 96 AQueous One Solution reagent was added and the cells were incubated for a further 1-2 h. Absorbance was measured at 490 nm against a water as blank and plotted against $\log_{10}$ of cell density ± SEM (n=3). The curve was prepare freshly and is typical of 20 experiments.

buffer (3 M of NaCl and 0.3 M of sodium citrate, pH 7.2) for 15 min at room temperature. Finally, the cells were washed twice with PBS, each for 5 min, and once with dH_2O for 5 min. The excess liquid was aspirated from each chamber and a coverslip was placed over the cells with fluorescent mounting medium. The cells were visualized using a Leica fluorescent microscope and images were captured using a CCD camera with ImagePro Plus software.

2.2.7.2 Determination of caspase-3 activation in H9c2 cells by flow cytometry

Flow cytometry is an automated mode of studying qualitative and quantitative changes in either cell-surface or intra-cellular markers on cells. The technique is based on labelling the cells with fluorescent tagged antibodies or peptides that can recognise specific markers on the cells (Figure 2.7). A laser excites the fluorescent tags and the signals from a population of cells (often >10,000 cells) are recorded and can be analysed. Different fluorescent tags, emit light at different wavelength. A cytometer can measure the relative amount of dye on an individual cell, generating information about the molecular properties of the cells. When cells pass through the laser beam, they disrupt and scatter the laser light, which is detected as forward scatter and side scattered. Forward scatter (FSC) light is related to cell size and side scatter (SSc) light is an indicator of cell's internal complexity (Figure 2.7). The FACSCalibur flow cytometer used here contains three channels with different band pass filters (FL1, 530+/-30nm; FL2, 585+/-42nm; FL3, 661+/-16nm) and can detect any tags within these margins.

In this study, a commercially available kit was used for detection of caspase-3 activity. This kit uses FMK as an inhibitor, which irreversibly binds to active caspase-

Figure 2.7: Schematic diagram of flow cytometry.

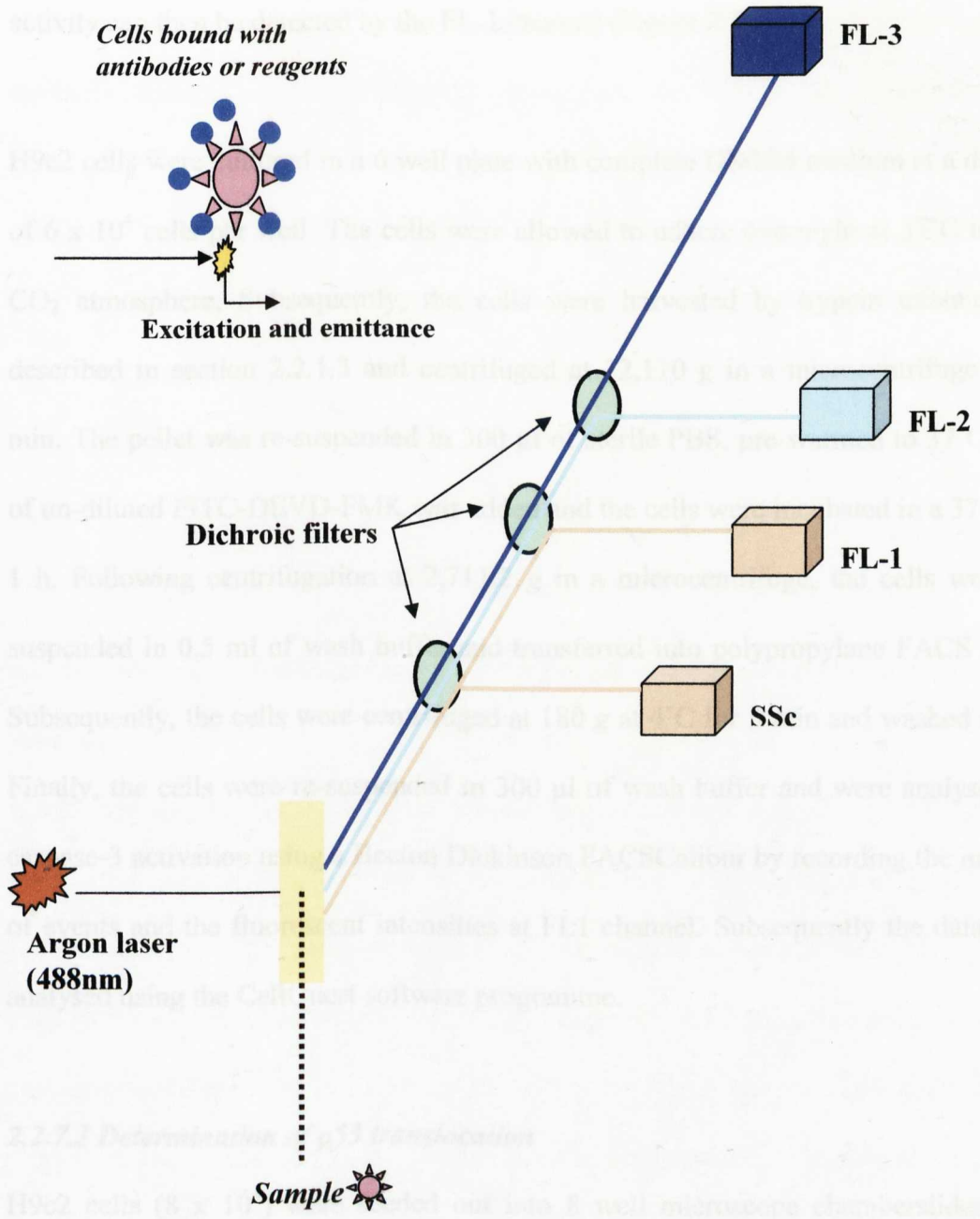

Cells bound with antibodies or reagents conjugated with different fluorescent tags can be detected in FL-1, FL-2 and FL-3 according to the fluorescent emittion of the tag. Additionally, side scatter is measured as an indication of cell granularity. In this study caspase 3 activity was detected by the FL-1 channel. *Adapted from FACSCalibur manual (BD Biosciences, U.K.).*

3. The peptide is composed of DEVD-FMK, conjugated with FITC which fluoresce on its own. After binding to the cells, the remainder is washed away. The caspase-3 activity can then be detected by the FL-1 channel (Figure 2.7).

H9c2 cells were cultured in a 6 well plate with complete DMEM medium at a density of 6 x 10^4 cells per well. The cells were allowed to adhere overnight at 37°C in 5 % CO_2 atmosphere. Subsequently, the cells were harvested by trypsin treatment as described in section 2.2.1.3 and centrifuged at 12,110 *g* in a microcentrifuge for 6 min. The pellet was re-suspended in 300 µl of sterile PBS, pre-warmed to 37°C. 1 µl of un-diluted FITC-DEVD-FMK was added and the cells were incubated in a 37°C for 1 h. Following centrifugation at 2,711.2 *g* in a microcentrifuge, the cells were re-suspended in 0.5 ml of wash buffer and transferred into polypropylane FACS tubes. Subsequently, the cells were centrifuged at 180 *g* at 4°C for 5 min and washed again. Finally, the cells were re-suspended in 300 µl of wash buffer and were analysed for caspase-3 activation using a Becton Dickinson FACSCalibur by recording the number of events and the fluorescent intensities at FL1 channel. Subsequently the data were analysed using the CellQuest software programme.

2.2.7.3 Determination of p53 translocation

H9c2 cells (8 x 10^4) were seeded out into 8 well microscope chamberslides with complete DMEM medium and allowed to adhere overnight at 37°C in 5 % CO_2 atmosphere. The cells were then washed with pre-warmed PBS (37°C) 3 times for 5 min each and fixed with 4 % (v/v) formaldehyde solution in PBS for 20 min at room temperature. Subsequently, the cells were washed 3 times with PBS for 5 min each and permeabilised with 0.2 % (v/v) Triton X-100 in PBS for 5 min at room

temperature. The cells were then washed 3 more times with PBS for 5 min each and blocked with 1 % (w/v) BSA in PBS for 2 h at room temperature. Following the blocking step, the cells were then incubated with mouse monoclonal human anti-p53 antibody (diluted 1:35 in blocking solution) for 2 h at room temperature. Subsequently, the cells were washed 4 times with PBS for 10 min each, and incubated with FITC conjugated anti-rabbit IgG (diluted 1:50 in blocking solution) for a further 2 h at room temperature. The cells were visualised using a Leica fluorescent microscope and images were captured using a CCD camera with ImagePro Plus software.

2.2.8 Immunohistochemical detection for specific antigens

2.2.8.1 Detection of neonatal myosin heavy chain (nMHC) by immunofluorescence staining

H9c2 were seeded into 8 well microscope chamber slides at a density of 10^5 cells per well with complete DMEM medium and allowed to adhere overnight at 37°C in 5 % CO_2 atmosphere. The media were removed, the cells were washed with freshly made PBS (pH 7.4) and fixed with 4 % (v/v) formaldehyde for 5 min. The cells were then permeabilised with 1 % (v/v) Triton-X in PBS for 5 min and then blocked with 1:5 diluted normal rabbit serum for 20 min at room temperature. Subsequently, the cells were incubated with mouse anti human developmental (neonatal) myosin heavy chain antibody (diluted 1:40 in blocking solution) for 1 h at room temperature. Following 2 washes with PBS (pH 7.4) for 5 min each, the cells were incubated with a rhodamine-conjugated rabbit anti-mouse IgG antibody (diluted 1:25 blocking solution) for 30 min at room temperature. The cells were then washed twice with PBS (pH 7.4) for 5 min each, and a coverslip was placed on the slide using fluorescence mounting medium.

The cells were visualised using a Leica fluorescence microscope and images were captured digitally with a CCD camera using the ImagePro Plus software.

2.2.8.2 Detection of slow myosin heavy chain β (sMHCβ) by immunofluorescence staining

Analysis of sMHCβ in H9c2 cells was carried out using the procedure described above, but with a mouse anti human slow myosin heavy chain antibody (diluted 1:400 in blocking solution). The staining was developed using the rhodamine-conjugated rabbit anti-mouse IgG antibody diluted 1:25 in blocking solution and visualised as described above.

2.2.8.3 Detection of mechano growth factor (MGF) by immunofluorescence staining

Analysis of mechano growth factor (MGF) in H9c2 cells was carried out using a similar procedure to that described above. However, the cells were blocked with 1:5 diluted normal swine serum for 20 min at room temperature. The primary antibody was a rabbit anti human MGF polyclonal antibody (kindly provided by Professor G. Goldspink from Royal Free Hospital London), used at a dilution 1:50 in blocking solution. The samples were then probed with 1:100 diluted swine anti-rabbit TRITC-conjugated antibody. The cells were visualised using a Leica fluorescence microscope and images were captured with a CCD camera using the ImagePro Plus software.

2.2.9 The one stage pro-thrombin time assay

Analysis of H9c2 cells samples for TF expression was carried out by the one-stage prothrombin time assay. All the reagents and samples were pre-warmed to 37°C.

Normal human plasma (100 µl) was in turn placed inside a coagulometer tube, followed by the addition of thromboplastin reagent (100 µl). After 30 seconds 100 µl of 25 mM $CaCl_2$was added. The clotting time was recorded using a cascade M coagulometer. The measurement was carried out up to 180 s. Samples were considered to be positive when the pro-thrombin time was less or equal to 120 s.

2.2.10 Statistical analysis

The results are presented as the mean of (n) experiments each performed in duplicates ± the standard error of the mean (SEM). Where appropriate, statistical analysis was carried out using the Statistical Package for the Social Science (SPSS Inc. Chicago, USA). One-Way ANOVA procedure was used for the analysis of variance of data against the control. Tukey's honestly significant difference test was performed as multiple comparison tests to highlight the statistical significant differences with a value of $p \leq 0.05$.

CHAPTER 3

The expression of Tissue Factor and Tissue Factor Pathway Inhibitor during the onset of cardiac hypertrophy

3. The expression of Tissue Factor and Tissue Factor Pathway Inhibitor during the onset of cardiac hypertrophy

3.1 Introduction

Cardiac hypertrophy is the adaptive response of the heart in response to chronic mechanical overload (Frey & Olson, 2003). A wide range of neuronal, hormonal and mechanical stimuli have been implicated in the induction and progression of cardiac hypertrophy, triggering a number of linked signalling pathways, transcript elements, molecular changes (Frey & Olson, 2003). Of particular interest is tissue factor (TF), a 47 kDa transmembrane glycoprotein, responsible for initiating the extrinsic pathway for blood coagulation. Recent studies have shown that TF may play a role in the remodelling of vascular and myocardial tissue (Luther & Mackman, 2001).

TF is expressed continuously at extravascular sites, playing an important role in haemostasis by minimising haemorrhage in the event of vascular injury (Drake *et al.* 1989). Loss of TF function has been shown to be incompatible with life, and more recent studies have suggested that it can also play a non-haemostatic role (Luther & Mackman, 2001). In particularly, TF is important in the development and structural maintenance of the heart (Luther & Mackman, 2001). In fact, analysis of TF mRNA levels in various tissues of mouse and rabbit, has revealed abundant expression in heart muscle (Hartzell *et al.*1989, Luther *et al.* 2000, Mackman *et al.* 1993). In the adult human myocardium, TF antigen is detectable in the intercalated discs and its content is lowest in the right atrium, with higher concentrations in the left atrium and the right ventricle, and highest in the left ventricle (Luther *et al.* 2000). Moreover, the level of TF antigen in remodelled myocardium from patients with hypertension or

ventricular hypertrophy is shown to be lower (Luther *at al.* 2000). A study, employing a transgenic rat model overexpressing the human renin and angiotensinogen genes revealed that TF mRNA levels in the heart were higher during development of cardiac hypertrophy (Muller *et al.* 2000). Although these studies appear contradictory, TF may be playing an important role in the maintenance of the heart structure since TF is localised in the intercalated discs (Luther *et al.* 2000) and in its contribution to microvascular thrombosis and microinfarction via several signalling pathways, including intergrin-matrix signalling (Cicala *et al.* 1998) and/or VLA-4/fibronectin signalling (Muller *et al.* 2000), associated with cardiac hypertrophy.

The action of TF is controlled through the expression of its inhibitor tissue factor pathway inhibitor (TFPI). The importance of TFPI has been demonstrated in knock-out transgenic animals lacking this protein (Sandset *et al.* 1991). Post-mortem examinations revealed that these animals have developed disseminated intravascular coagulation (Sandset *et al.* 1991). Further studies with homozygous mice with TFPI gene distruption of the kuniz 1 domain revealed that 60% died *in utero* during embryonic days E9.5-E11.5 with evidence of yolk sack bleeding. Mice which survived beyond this stage, exhibited signs of bleeding in the central nervous system with no survival to neonatal period (Huang *et al.* 1997). Additionally, the importance of TFPI in the heart has been shown in a transgenic mice model heterozygous for TFPI-deficiency, which was prone to the development of atherosclerosis (Westrick *et al.* 2001). Active TFPI has been found within the atherosclerotic plaque as inhibition with a TFPI polyclonal antibody resulted in an 8-fold increase in TF activity (Novotny *et al.* 1998). Moreover, patients suffering from heart disease exhibit increased circulatory levels of TFPI antigen (Falciani *et al.* 1998). These findings suggest that

an imbalance between TF and TFPI can influence the progression of both atherosclerosis and thrombosis (Doshi and Marmur, 2002). Therefore, TFPI may play a crucial protective role in the heart (Kereveur *et al.* 2001).

To date, there have been no studies investigating the role of TF and its inhibitor, TFPI, in the early phase of cardiac hypertrophy. This study aims to establish the pattern of TF and TFPI expression in adult rat ventricular cardiac myocytes and intact left ventricular tissue by analysing the mRNA and protein levels over 14 days post-surgical induction of cardiac hypertrophy. This may identify potential roles for TF and TFPI in the hypertrophied heart.

3.2 Methods

3.2.1 TF, TFPI and ANF mRNA and protein analysis in ventricular cardiomyocytes post-induction of cardiac hypertrophy

Cardiac hypertrophy was induced surgically in male Sprague Dawley rats weighing between 240-260 g (section 2.2.2) with sham operated animals as controls. Animals (controls and aortic constriction) were anaesthetised with sodium thiopentone 1, 3, 7 and 14 days post aortic constriction and hearts excised and mounted on a Langendorff apparatus. Cardiomyocyte isolation was carried out as described in section 2.2.2.1, and cells were subsequently incubated in complete pre-warmed DMEM medium in a 37°C incubator with 5 % CO_2 for 1 h to obtain a pure population of cardiomyocytes. Cells were harvested by centrifugation (section 2.2.2.1) and stored at -20 °C until further use. Total RNA was extracted from the first 3 groups of animals (section 2.2.3.2) while the remaining groups were used to extract total protein (section 2.2.5.2).

Total RNA was quantified spectrophotometrically (section 2.2.3.4) and subsequently a single tube RT-PCR analysis was performed for TF, TFPI, ANF and GAP3DH as a reference (section 2.2.4.2 & 2.2.4.3). The results were analysed by gel electrophoresis and quantified using the "Gene Tool" computer software program. The annealing temperatures of each set of primers was optimised using RNA extracts from hypertrophied heart tissue (9 weeks post surgery), kindly provided by Dr S. Richardson.

Protein analysis using SDS-PAGE electrophoresis carried out as in section 2.2.5.5 except that a 10 % (v/v) resolving gel was used to separate TF protein. Total protein concentration was estimated using the Bradford assay (section 2.2.5.4) and 20 μg protein were used for the electrophoresis. Western blot analysis for TF, TFPI, ANF and GAP3DH as reference was carried out as described previously (section 2.2.5.6-9) and results were analysed using the "Gene Tools" computer software programme.

3.2.2 TF, TFPI and ANF mRNA and protein analysis in left ventricular tissue post-induction of cardiac hypertrophy

In a separated series, 4 groups of animals underwent the aortic constriction procedure as described above. In the second series of experiments, left ventricular tissue was isolated. Briefly, the heart was rinsed with normal Krebs Hensleit Buffer (nKHB) for 10 min and the left and right ventricle dissected (section 2.2.2.2). When tissue samples were collected and powdered, half of the groups were used to extract total RNA (section 2.2.3.3) while the remaining groups were used to extract total protein from (section 2.2.5.3). RNA and protein analysis for TF, TFPI and ANF was followed.

The body weight, heart weight, kidneys weight and tibia length were also recorded from all the animals used as morphological indicators of the progression of cardiac hypertrophy.

3.3 Results

3.3.1 Morphological measurements of cardiac hypertrophy

To assess the extent of cardiac hypertrophy over the 14 days period of investigation, heart weight, body weight, left and right kidney weights and tibia length were measured at the time of cell isolation or left ventricular tissue preparation. From these data, the heart weight to tibia length ratio and the left to right kidney ratio were calculated.

Up to day 7 of the investigation, the control group exhibited a small increase in body weight relative to the aortic constriction group (Table 3.1a). By day 14 of the investigation period, the body weight of aortic constriction group was increased compared to control (Table 3.1b). Heart weight increased in both groups during the period of the investigation with a parallel increase in the heart weight to tibia length ratio (Table 3.1a and 3.1b). In the aortic constriction group the increase was higher compared to the control group, reaching significance ($p< 0.05$) by day 14 (Table 3.1a and 3.1b).

The left to right kidney ratio is a reflection of the extent of degree of constriction and thus cardiac hypertrophy, indicating successful banding (Boateng, 1997, PhD thesis). By day 14, the sham operated group had no difference in left to right kidney weight

Table 3.1: Measurement of the morphological indicators of cardiac hypertrophy.

a)

SHAM OPERATED ANIMALS					
	Body weight (g)	Heart weight (g)	Tibia length (cm)	Heart weight/Tibia length ratio	n values
Day 1	255.5 (± 8.48)	1.24 (± 0.05)	3.49 (± 0.05)	0.36 (± 0.02)	10
Day 3	264.2 (± 11.13)	1.14 (± 0.13)	3.31 (±0.10)	0.35 (± 0.04)	6
Day 7	310.6 (± 11.39)	1.36 (± 0.09)	3.59 (±0.05)	0.38 (± 0.03)	8
Day 14	310 (± 25.41)	1.70 (± 0.18)	3.76 (± 0.07)	0.45 (± 0.06)	4

b)

AORTIC CONSTRICTION ANIMALS					
	Body weight (g)	Heart weight (g)	Tibia length (cm)	Heart weight/Tibia length ratio	n values
Day 1	253 (± 6.72)	1.25 (± 0.09)	3.46 (± 0.05)	0.36 * (±0.03)	10
Day 3	247.5 (± 13.22)	1.37 (±0.10)	3.51 (± 0.07)	0.38 * (± 0.03)	6
Day 7	275 (± 15.14)	1.59 (±0.11)	3.56 (± 0.07)	0.45 * (± 0.03)	6
Day 14	357.5 (± 9.68)	1.82 (± 0.07)	3.84 (± 0.06)	0.48 * (± 0.02)	4

Table (a) shows the body weight (g), the heart weight (g), tibia length (cm) and heart weight, tibia length ratio of sham operated animals ± SEM recorded from different experiments.
Table (b) shows the body weight (g), the heart weight (g), tibia length (cm) and heart weight, tibia length ratio of aortic constriction animals ± SEM recorded from different experiments.

* $p<0.05$ aortic constriction versus sham operated animals

ratio (Table 3.2), but in the aortic constriction group, the left to right kidney ratio was significant decreased ($p<0.05$) as compared to day 1 (Table 3.2) indicative of the degree of constriction and thus successful induction of hypertrophy.

3.3.2 The expression of TF and TFPI during the onset of cardiac hypertrophy in ventricular cardiomyocytes

3.3.2.1 Primer optimisation

In order to optimise the reaction conditions for the RT-PCR amplification, total RNA was extracted from hypertrophic heart tissue and single tube RT-PCR carried out at 55°C, 58°C, 60°C and 61°C for all the transcripts (TF, TFPI, ANF, GAP3DH). The optimal annealing temperature for each set of primers was confirmed by the presence of a single band at the expected size for each gene (Figure 3.1). Amplification of GAP3DH and TFPI mRNA at 61° C resulted in a single band at 800 bp and at 400 bp respectively, while the amplification of ANF and TF mRNA at 60 ° C produced single band at 397 bp 196 bp respectively (Figure 3.1).

3.3.2.2 TF mRNA and protein expression

Analysis of TF expression by RT-PCR, revealed no TF mRNA expression in cardiomyocytes isolated either from the control or the aortic constriction group throughout the period of the investigation. Additionally, analysis of TF protein expression by SDS-PAGE confirmed the lack of TF protein expression in the isolated cardiomyocytes in agreement with the mRNA results.

Table 3.2: Left and right kidney weight during the progression of cardiac hypertrophy.

SHAM OPERATED ANIMALS				
	Left kidney (g)	Right kidney (g)	Left/Right kidney ratio	n values
Day 1	1.05 (± 0.03)	1.06 (± 0.04)	0.99 (± 0.02)	5
Day 14	1.18 (± 0.1)	1.22 (± 0.08)	0.98 (± 0.03)	4
AORTIC CONSTRICTION ANIMALS				
	Left kidney (g)	Right kidney (g)	Left/Right kidney ratio	n values
Day 1	0.97 (± 0.01)	1.03 (± 0.04)	0.94 (± 0.03)	5
Day 14	1.2 (± 0.06)	1.46 (± 0.05)	0.83 * (± 0.02)	4

The table shows the weight of the left and right kidney and the ration between left to right kidney weight of sham operated and aortic constricted animals SEM recorded from different experiments.

* $p<0.05$ aortic constriction versus sham operated animals

Figure 3.1: Optimisation of RT-PCR products following gel electrophoresis analysis.

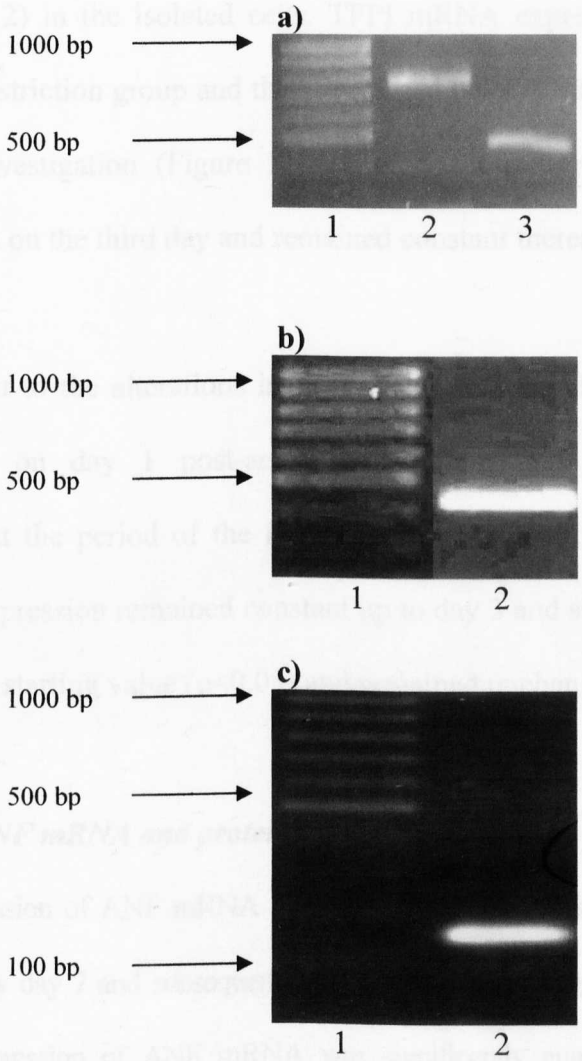

Total RNA from hypertrophied heart tissue was amplified by single tube RT-PCR at 55-61° C. The products were analysed by DNA electrophoresis on a 1.5% (w/v) agarose gel and recorded using the "Gene Tool" computer software program. The micrographs are typical of 10 experiments and show the optimal annealing temperatures for the following:

Micrograph (a) lane 1: DNA ladder, lane 2: RT-PCR product for GAP3DH at 800bp, lane 3: RT-PCR product for TFPI at 400bp, at 61° C.

Micrograph (b) lane 1: DNA ladder, lane 2: RT-PCR product for ANF at 397bp, at 60° C.

Micrograph (c) lane 1: DNA ladder, lane 2: RT-PCR product for TF at 196bp, at 60° C.

3.3.2.3 TFPI mRNA and protein expression

Induction of hypertrophy resulted in a significant increase in TFPI mRNA expression (Figure 3.2) in the isolated cells. TFPI mRNA expression peaked by day 7 in the aortic constriction group and then decreased below that of the control on the final day of the investigation (Figure 3.3). In the control group, TFPI mRNA reached a maximum on the third day and remained constant thereafter (Figure 3.3).

In contrast to the alterations in mRNA expression, TFPI protein levels (Figure 3.4) increased on day 1 post-aortic constriction and then subsequently decreased throughout the period of the investigation (Figure 3.5). In the control group, TFPI protein expression remained constant up to day 3 and significantly decreased by day 7 below the starting value ($p<0.05$) and remained unchanged thereafter (Figure 3.5).

3.3.2.4 ANF mRNA and protein expression

The expression of ANF mRNA (Figure 3.6) peaked by day 3 post surgery in both groups, declined by day 7 and subsequently reached a plateau (Figure 3.7). In the aortic constriction group, expression of ANF mRNA was significantly augmented on day 1 and 3 of the investigation ($p<0.05$) (3.5 fold on day 1 and 0.7 fold on day 3) when compared to sham operated control group and significantly increased by 0.3 fold on day 7 and day 14 (Figure 3.7).

The relative expression of ANF protein (Figure 3.8) gradually increased over the period of the investigation (Figure 3.9). Up to the seventh day of the investigation the aortic constriction group expressed increased ANF protein compared to the control group, by day 14 a significant increase in the ANF protein was observed in the control group as opposed to the aortic constriction group ($p<0.05$) (Figure 3.9).

Figure 3.2: Expression of TFPI mRNA in isolated adult ventricular rat cardiomyocytes.

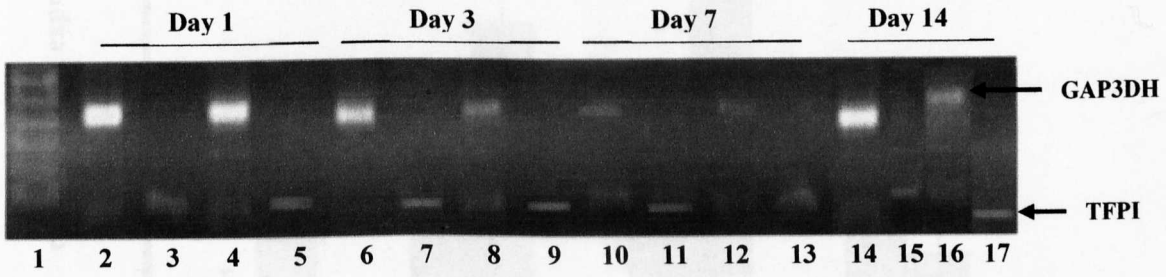

Lane 1: DNA ladder. Lanes 2, 6, 10, 14: GAP3DH mRNA expression for control group. Lanes 4, 8, 12, 16: GAP3DH mRNA expression for aortic constriction group. Lanes 3, 7, 11, 15: TFPI mRNA expression for control group. Lanes 5, 9, 13, 17: TFPI mRNA expression for aortic constriction group. The micrograph is typical of 18 gels.

Figure 3.3: Relative expression of TFPI mRNA in adult ventricular cardiomyocytes, post-induction of pressure overload cardiac hypertrophy.

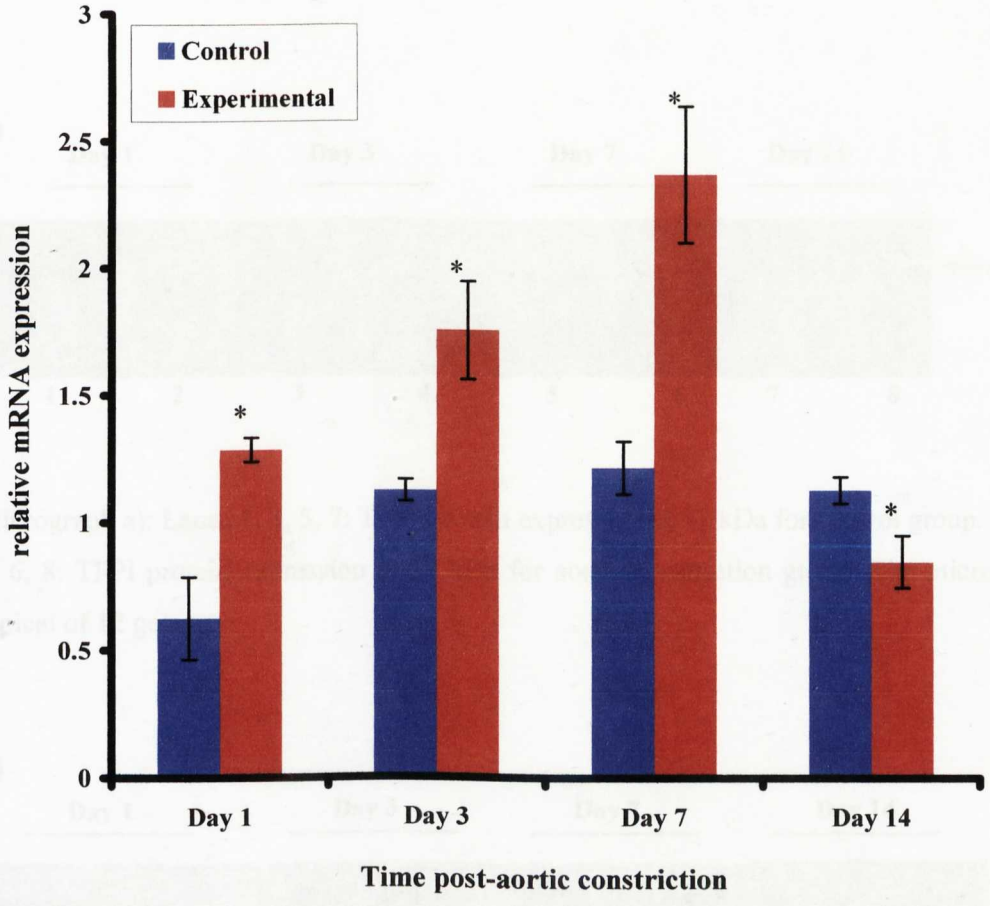

Aortic constriction procedure (■) was carried out in male Sprague Dawley rats and control animals underwent sham procedure (■).The hearts were excised at 1, 3, 7 and 14 days post-surgery and cardiomyocytes were isolated. Total RNA was extracted and a single tube RT-PCR was performed to measure TFPI mRNA expression against GAP3DH as reference. The band intensities were quantified using the "Gene Tool" software program. The data represent the mean of n=6 taken from 3 different hearts ± SEM.

* $p<0.05$ aortic constriction versus sham operated animals

Figure 3.4: Expression of TFPI protein in isolated adult ventricular rat cardiomyocytes.

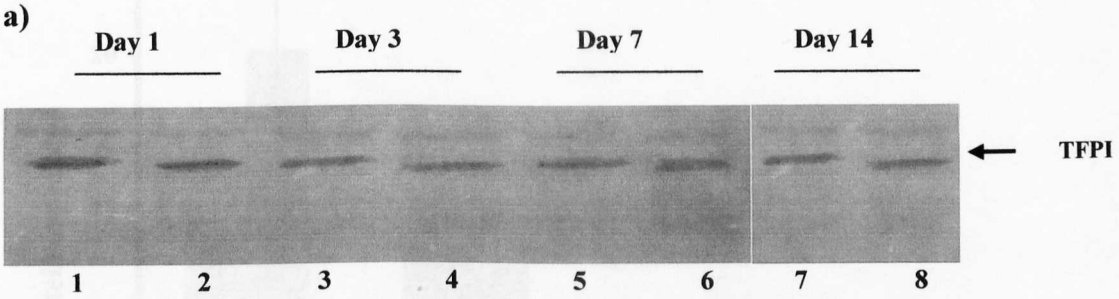

Micrograph a): Lanes 1, 3, 5, 7: TFPI protein expression at 37 kDa for control group. Lanes 2, 4, 6, 8: TFPI protein expression at 37 kDa for aortic constriction group. The micrograph is typical of 12 gels.

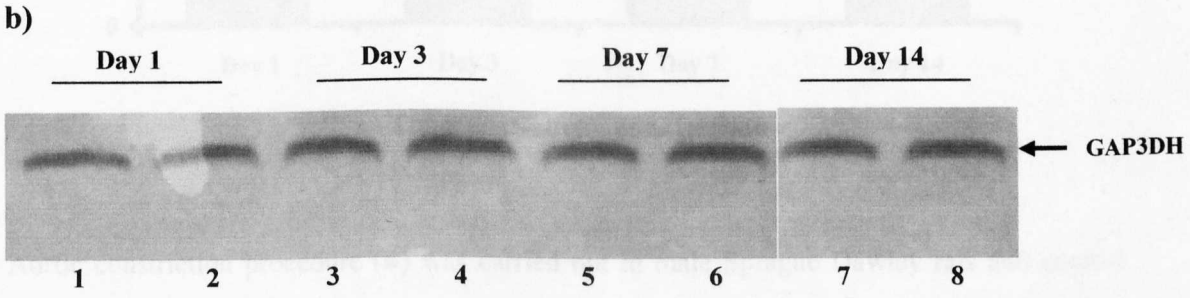

Micrograph b): Lanes 1, 3, 5, 7: GAP3DH protein expression at 38 kDa for control group. Lanes 2, 4, 6, 8: GAP3DH protein expression at 38 kDa for aortic constriction group. The micrograph is typical of 12 gels.

Figure 3.5: Relative expression of TFPI protein in adult ventricular cardiomyocytes, post-induction of pressure overload cardiac hypertrophy.

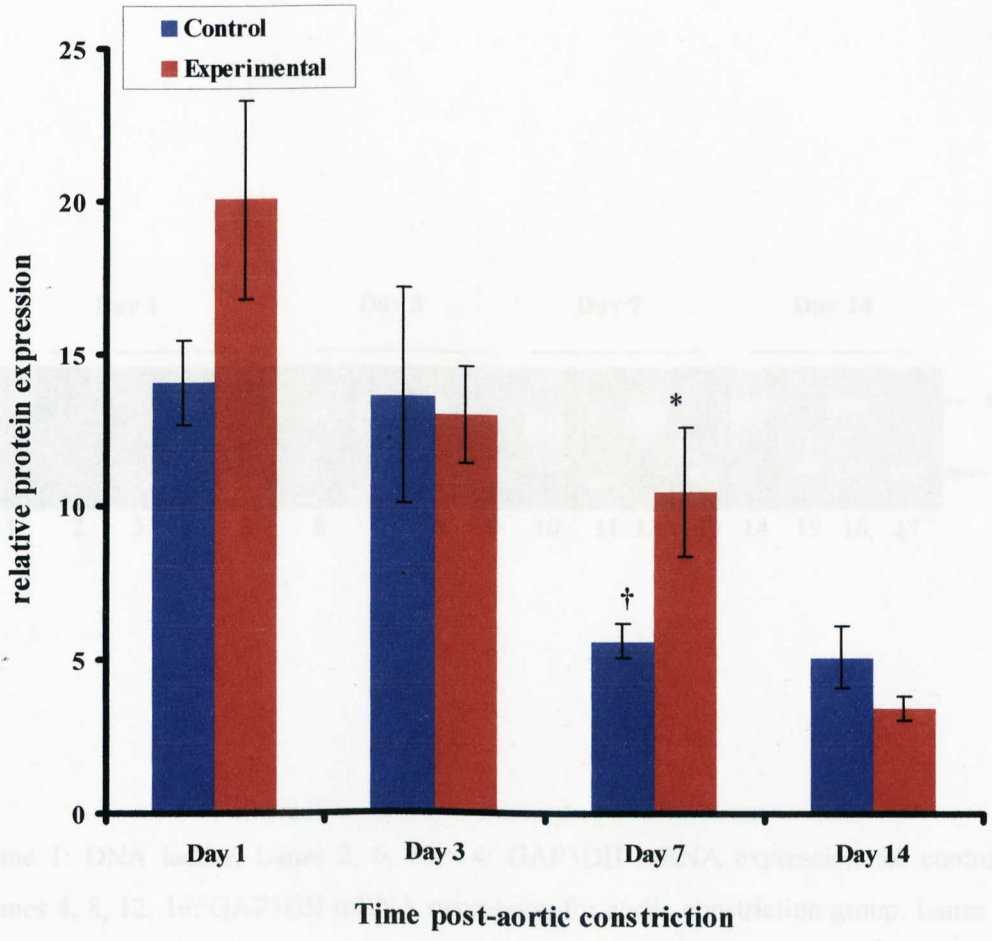

Aortic constriction procedure (■) was carried out in male Sprague Dawley rats and control animals underwent sham procedure (■). The hearts were excised at 1, 3, 7 and 14 days post-surgery and cardiomyocytes were isolated. Total protein was extracted and western blot analysis was performed to measure TFPI protein expression against GAP3DH as reference. The band intensities were quantified using the "Gene Tool" software program. The data represent the mean of n=4 taken from 2 different hearts ± SEM.

* $p<0.05$ aortic constriction versus sham operated animals

† $p<0.05$ as compared to the other days of the investigation of the same group

Figure 3.6: Expression of ANF mRNA in isolated adult ventricular rat cardiomyocytes.

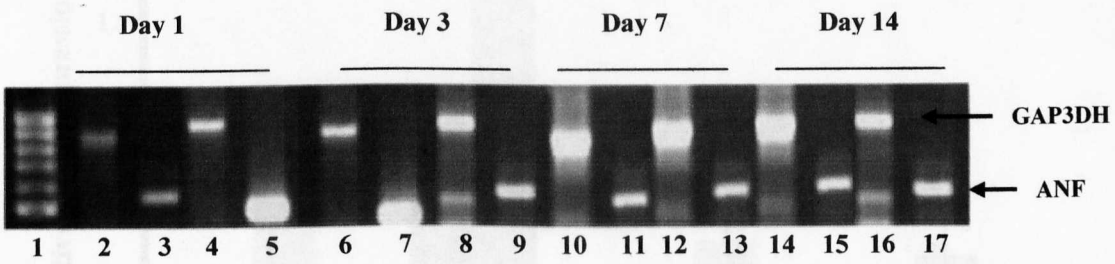

Lane 1: DNA ladder. Lanes 2, 6, 10, 14: GAP3DH mRNA expression for control group. Lanes 4, 8, 12, 16: GAP3DH mRNA expression for aortic constriction group. Lanes 3, 7, 11, 15: ANF mRNA expression for control group. Lanes 5, 9, 13, 17: ANF mRNA expression for aortic constriction group. The micrograph is typical of 18 gels.

Figure 3.7: Relative expression of ANF mRNA in adult ventricular rat cardiomyocytes, post-induction of pressure overload cardiac hypertrophy.

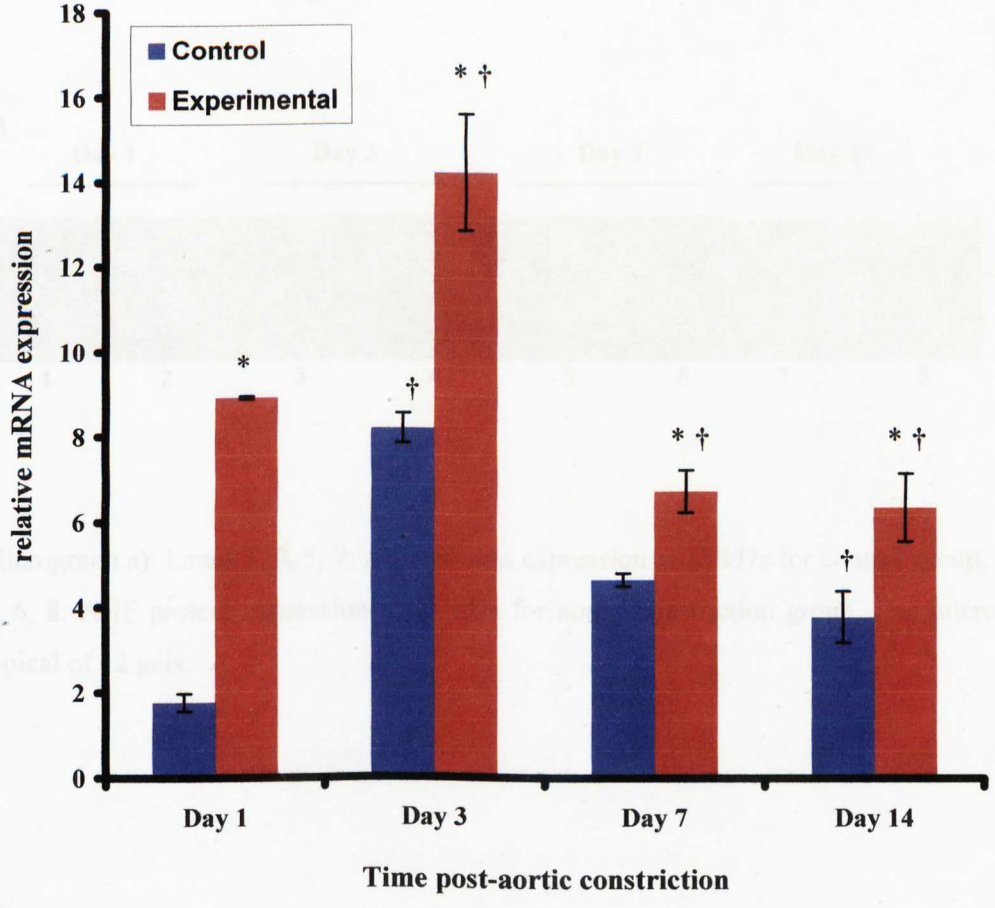

Aortic constriction procedure (■) was carried out in male Sprague Dawley rats and control animals underwent sham procedure (■). The hearts were excised at 1, 3, 7 and 14 days post-surgery and cardiomyocytes were isolated. Total RNA was extracted and a single tube RT-PCR was performed to measure ANF mRNA expression against GAP3DH as reference. The band intensities were quantified using the "Gene Tool" software program. The data represent the mean of n=6 taken from 3 different hearts ± SEM.

* $p<0.05$ aortic constriction versus sham operated animals

† $p<0.05$ as compare to the other days of the investigation of the same group

Figure 3.8: Expression of ANF protein in isolated adult ventricular rat cardiomyocytes.

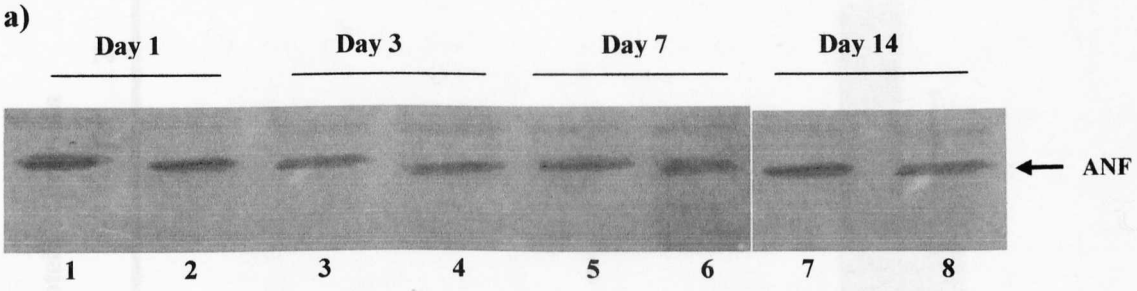

Micrograph a): Lanes 1, 3, 5, 7: ANF protein expression at 13 kDa for control group. Lanes 2, 4, 6, 8: ANF protein expression at 13 kDa for aortic constriction group. The micrograph is typical of 12 gels.

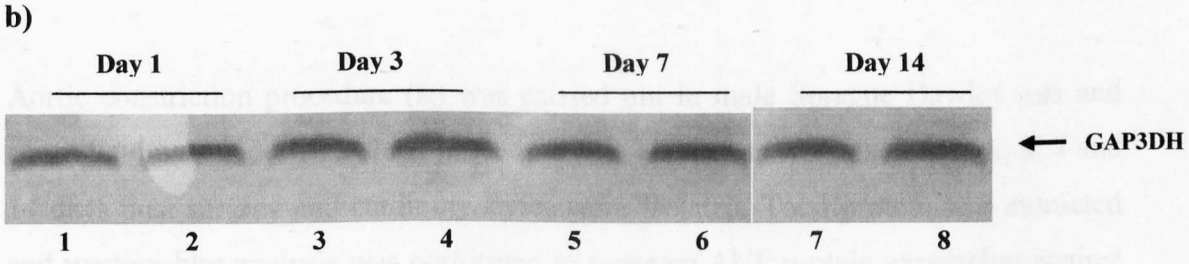

Micrograph b): Lanes 1, 3, 5, 7: GAP3DH protein expression at 38 kDa for control group. Lanes 2, 4, 6, 8: GAP3DH protein expression at 38 kDa for aortic constriction group. The micrograph is typical of 12 gels.

Figure 3.9: Relative expression of ANF protein in adult ventricular rat cardiomyocytes, post-induction of pressure overload cardiac hypertrophy.

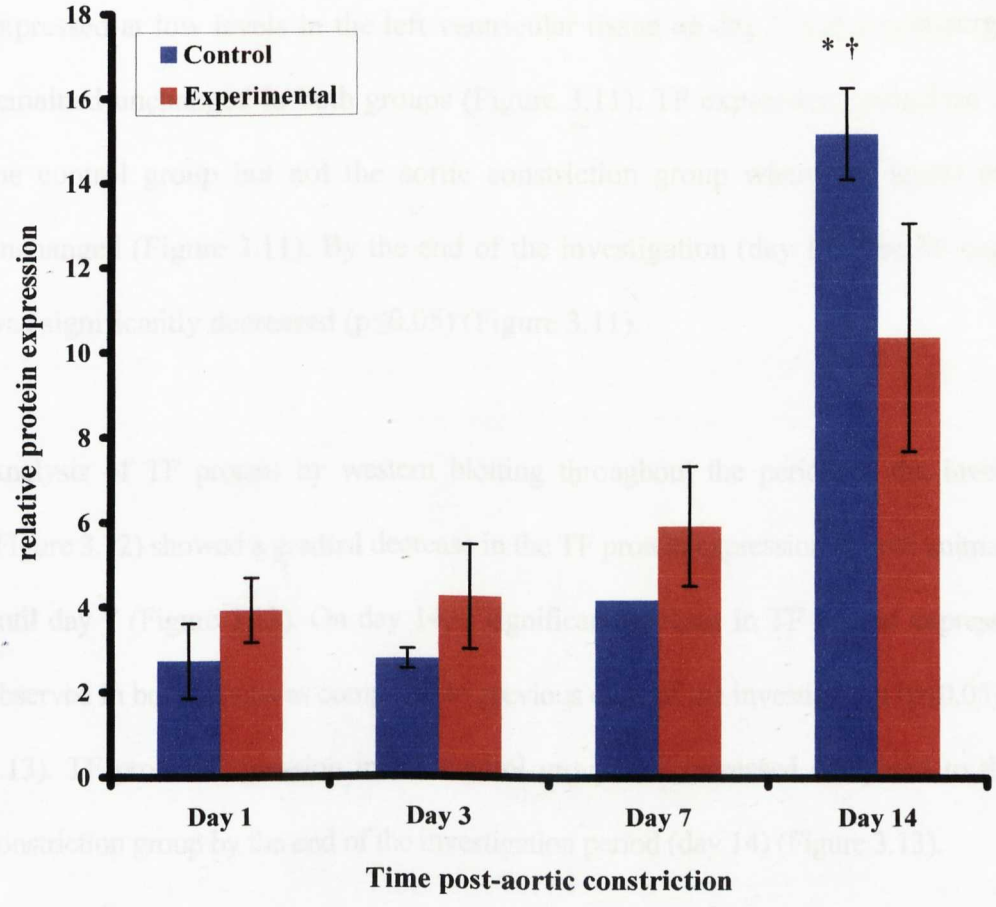

Aortic constriction procedure (■) was carried out in male Sprague Dawley rats and control animals underwent sham procedure (■). The hearts were excised at 1, 3, 7 and 14 days post-surgery and cardiomyocytes were isolated. Total protein was extracted and western blot analysis was performed to measure ANF protein expression against GAP3DH as reference. The band intensities were quantified using the "Gene Tool" software program. The data represent the mean of n=4 taken from 2 different hearts ± SEM.

* $p<0.05$ aortic constriction versus sham operated animals

† $p<0.05$ as compare to the other days of the investigation of the same group

3.3.3 The expression of TF and TFPI during the onset of cardiac hypertrophy in left ventricular tissue

3.3.3.1 TF mRNA and protein expression

Agarose gel electrophoresis analysis (Figure 3.10) showed that TF mRNA was expressed at low levels in the left ventricular tissue on day 1 and 3 post-surgery and remained unchanged in both groups (Figure 3.11). TF expression peaked on day 7 in the control group but not the aortic constriction group where TF levels remained unchanged (Figure 3.11). By the end of the investigation (day 14), the TF expression was significantly decreased ($p \leq 0.05$) (Figure 3.11).

Analysis of TF protein by western blotting throughout the period of the investigation (Figure 3.12) showed a gradual decrease in the TF protein expression in both animal groups until day 7 (Figure 3.13). On day 14, a significant increase in TF protein expression was observed in both groups as compared to previous days of the investigation ($p \leq 0.05$) (Figure 3.13). TF protein expression in the control group was increased compared to the aortic constriction group by the end of the investigation period (day 14) (Figure 3.13).

3.3.3.2 TFPI mRNA and protein expression

Expression of TFPI mRNA by RT-PCR in the left ventricular tissue was transiently increased within the first day with a second, more persistent wave on day 7 of the investigation (Figure 3.14). By day 14, TFPI relative mRNA expression remained unchanged and at the same level as day 7 (Figure 3.14).

TFPI protein expression remained unaltered in left ventricular tissue up to day 3 of the investigation (Figure 3.15). However, a decrease in both groups was observed

Figure 3.10: Expression of TF mRNA in left ventricular rat tissue.

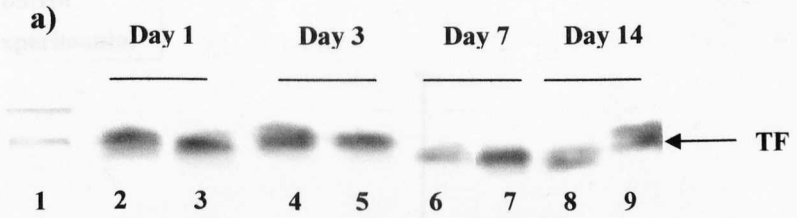

Micrograph a): Lanes 1: DNA ladder, Lanes 2, 4, 6, 8: TF mRNA expression at for control group. Lanes 3, 4, 6, 8: TF mRNA expression for aortic constriction group. The micrograph is typical of 18 gels.

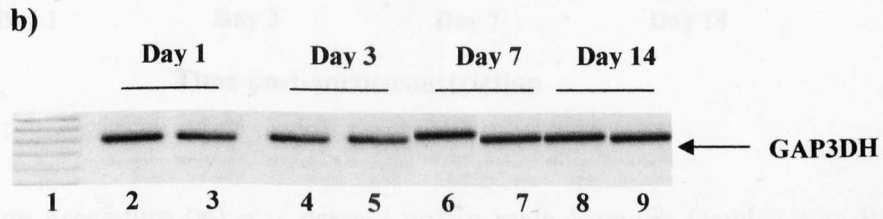

Micrograph b): Lanes 1: DNA ladder, Lanes 2, 4, 6, 8: GAP3DH mRNA expression at for control group. Lanes 3, 4, 6, 8: GAP3DH mRNA expression for aortic constriction group. The micrograph is typical of 18 gels.

Figure 3.11: Relative expression of TF mRNA in left ventricular rat tissue, post-induction of pressure overload cardiac hypertrophy.

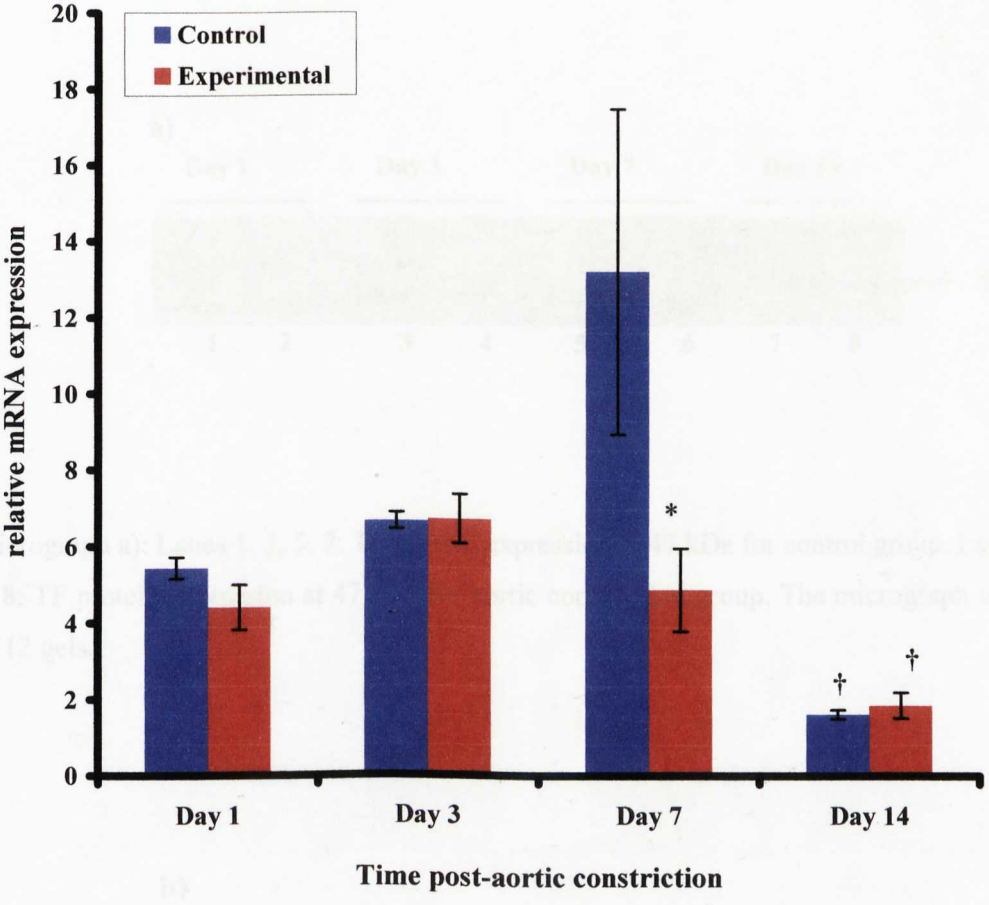

Aortic constriction procedure (■) was carried out in male Sprague Dawley rats and control animals underwent sham procedure (■). The hearts were excised at 1, 3, 7 and 14 days post-surgery and cardiomyocytes were isolated. Total RNA was extracted and a single tube RT-PCR was performed to measure TF mRNA expression against GAP3DH as reference. The band intensities were quantified using the "Gene Tool" software program. The data represent the mean of n=6 taken from 3 different hearts ± SEM.

* $p<0.05$ aortic constriction versus sham operated animals

† $p<0.05$ as compare to the other days of the investigation of the same group

Figure 3.12: Expression of TF protein in left ventricular rat tissue.

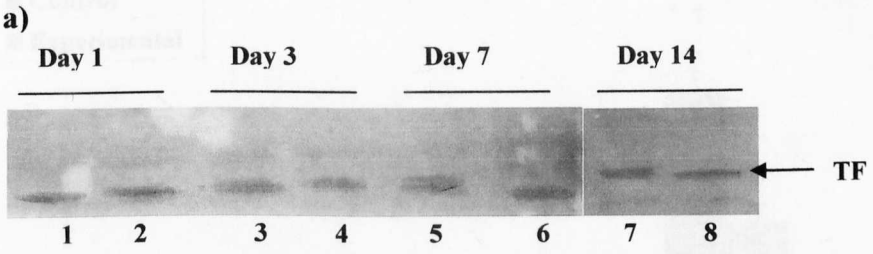

Micrograph a): Lanes 1, 3, 5, 7: TF protein expression at 47 kDa for control group. Lanes 2, 4, 6, 8: TF protein expression at 47 kDa for aortic constriction group. The micrograph is typical of 12 gels.

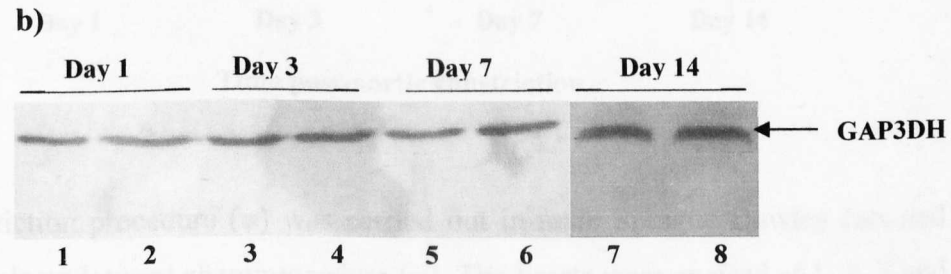

Micrograph b): Lanes 1, 3, 5, 7: GAP3DH protein expression at 38 kDa for control group. Lanes 2, 4, 6, 8: GAP3DH protein expression at 38 kDa for aortic constriction group. The micrograph is typical of 12 gels.

Figure 3.13: Relative expression of TF protein in left ventricular rat tissue, post-induction of pressure overload cardiac hypertrophy.

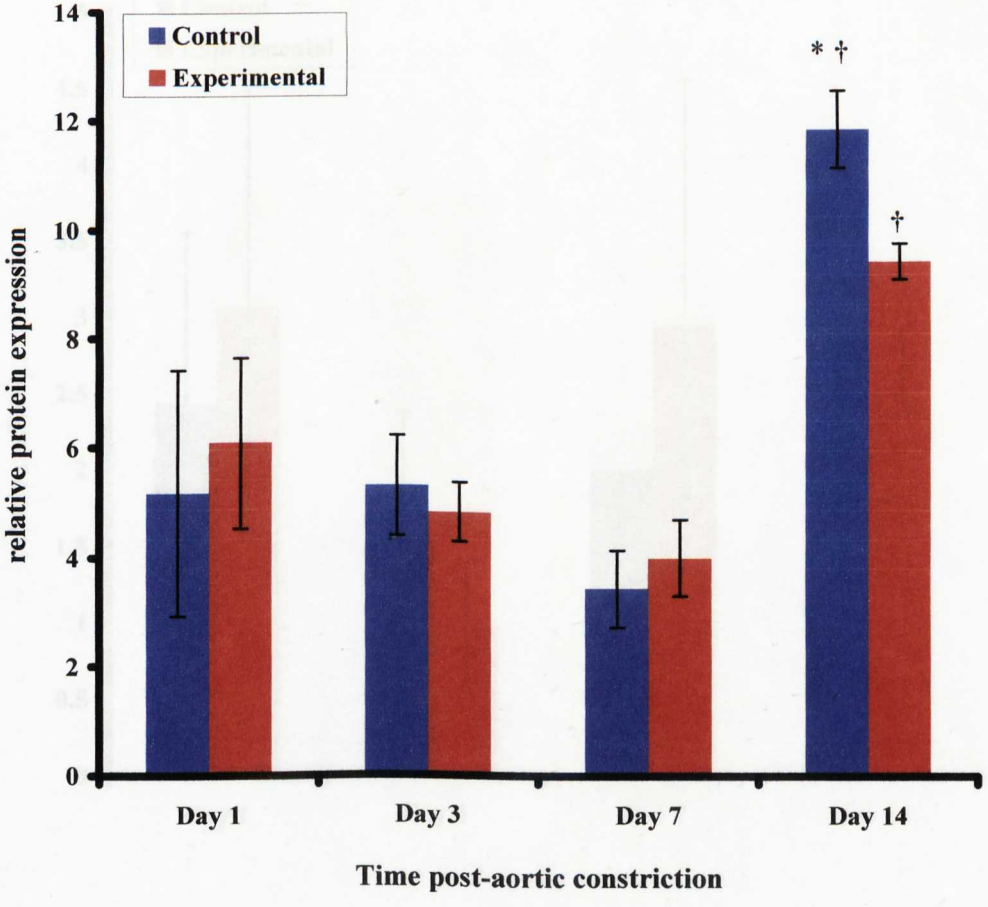

Aortic constriction procedure (■) was carried out in male Sprague Dawley rats and control animals underwent sham procedure (■). The hearts were excised at 1, 3, 7 and 14 days post-surgery and cardiomyocytes were isolated. Total protein was extracted and western blot analysis was performed to measure TF protein expression against GAP3DH as reference. The band intensities were quantified using the "Gene Tool" software program. The data represent the mean of n=4 taken from 2 different hearts ± SEM.

* $p<0.05$ aortic constriction versus sham operated animals

† $p<0.05$ as compare to the other days of the investigation of the same group

Figure 3.14: Relative expression of TFPI mRNA in left ventricular rat tissue, post-induction of pressure overload cardiac hypertrophy.

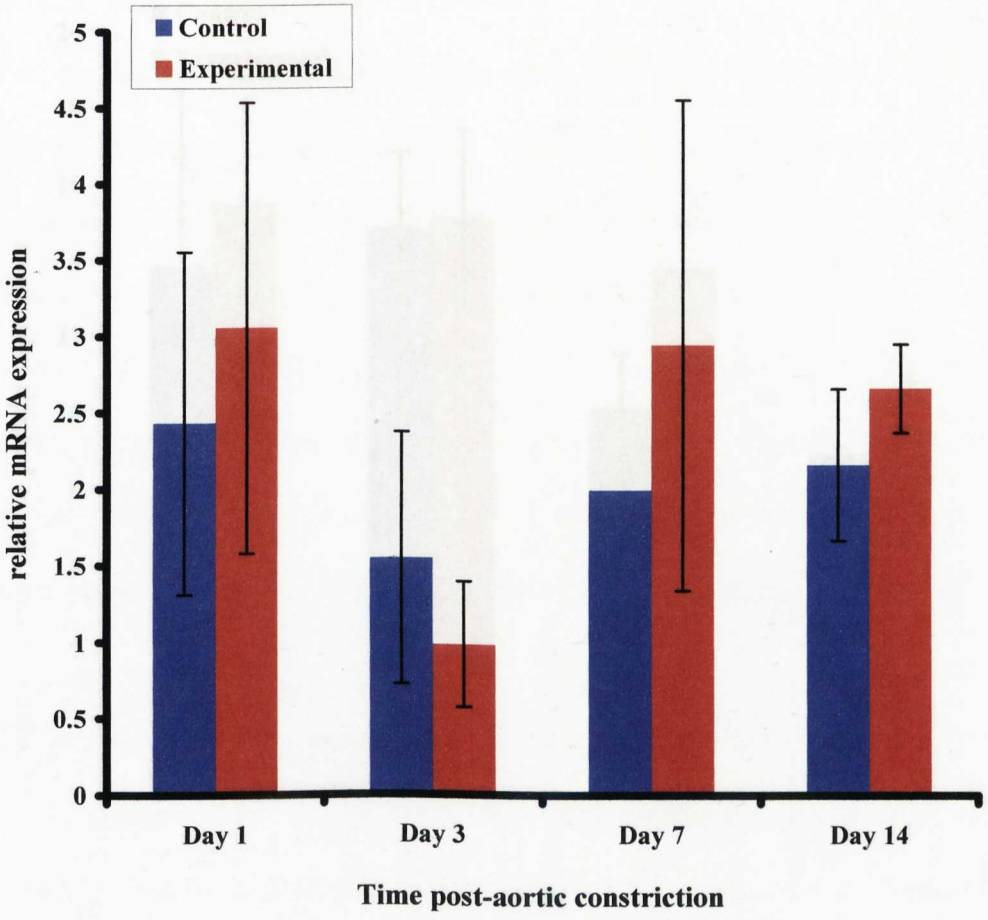

Aortic constriction procedure (■) was carried out in male Sprague Dawley rats and control animals underwent sham procedure (■). The hearts were excised at 1, 3, 7 and 14 days post-surgery and cardiomyocytes were isolated. Total RNA was extracted and a single tube RT-PCR was performed to measure TFPI mRNA expression against GAP3DH as reference. The band intensities were quantified using the "Gene Tool" software program. The data represent the mean of n=6 taken from 3 different hearts ± SEM.

Figure 3.15: Relative expression of TFPI protein in left ventricular rat tissue, post-induction of pressure overload cardiac hypertrophy.

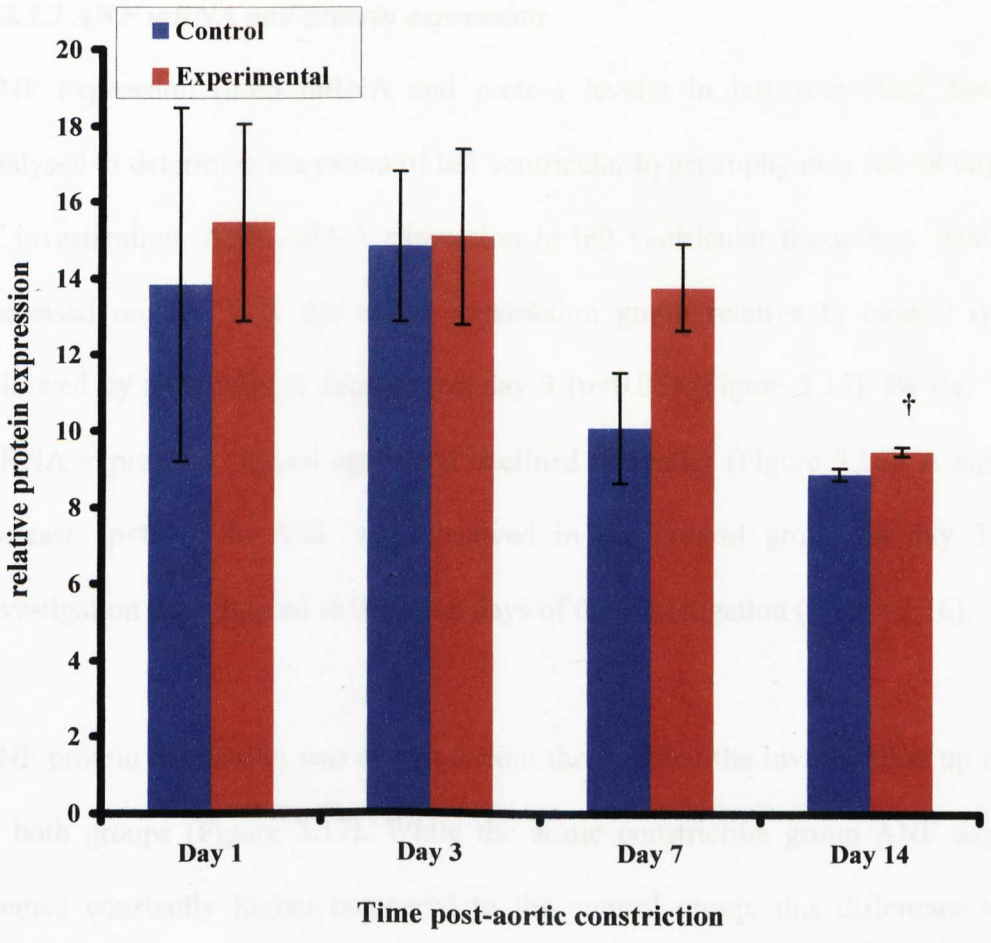

Aortic constriction procedure (■) was carried out in male Sprague Dawley rats and control animals underwent sham procedure (■). The hearts were excised at 1, 3, 7 and 14 days post-surgery and cardiomyocytes were isolated. Total protein was extracted and western blot analysis was performed to measure TFPI protein expression against GAP3DH as reference. The band intensities were quantified using the "Gene Tool" software program. The data represent the mean of n=4 taken from 2 different hearts ± SEM.

† $p<0.05$ as compare to the other days of the investigation of the same group

thereafter (Figure 3.15). In the aortic constriction group the decrease on day 14 of the investigation was significant ($p<0.05$) as compared with the values measured on days 1, 3 and 7.

3.3.3.3 ANF mRNA and protein expression

ANF expression (both mRNA and protein levels) in left ventricular tissue was analysed to determine the extent of left ventricular hypertrophy over the 14 day period of investigation. ANF mRNA expression in left ventricular tissue was significantly increased on day 1 in the aortic constriction group relative to control ($p<0.05$), followed by a significant decrease on day 3 ($p<0.05$) (Figure 3.15). By day 7, ANF mRNA expression peaked again and declined thereafter (Figure 3.16). A significant increase ($p<0.05$) in ANF was observed in the control group on day 3 of the investigation as compared to the other days of the investigation (Figure 3.16).

ANF protein expression was elevated from the onset of the investigation up to day 7 in both groups (Figure 3.17). While the aortic constriction group ANF expression seemed constantly higher compared to the control group, this difference was not significant (Figure 3.17). On day 14 of the investigation, a significant decrease in the ANF protein levels was observed in both groups as compared to the previous stage ($p<0.05$ in the control group, $p\leq0.05$ in the experimental group) but there was no difference between the two groups (Figure 3.17) .

Figure 3.16: Relative expression of ANF mRNA in left ventricular rat tissue, post-induction of pressure overload cardiac hypertrophy.

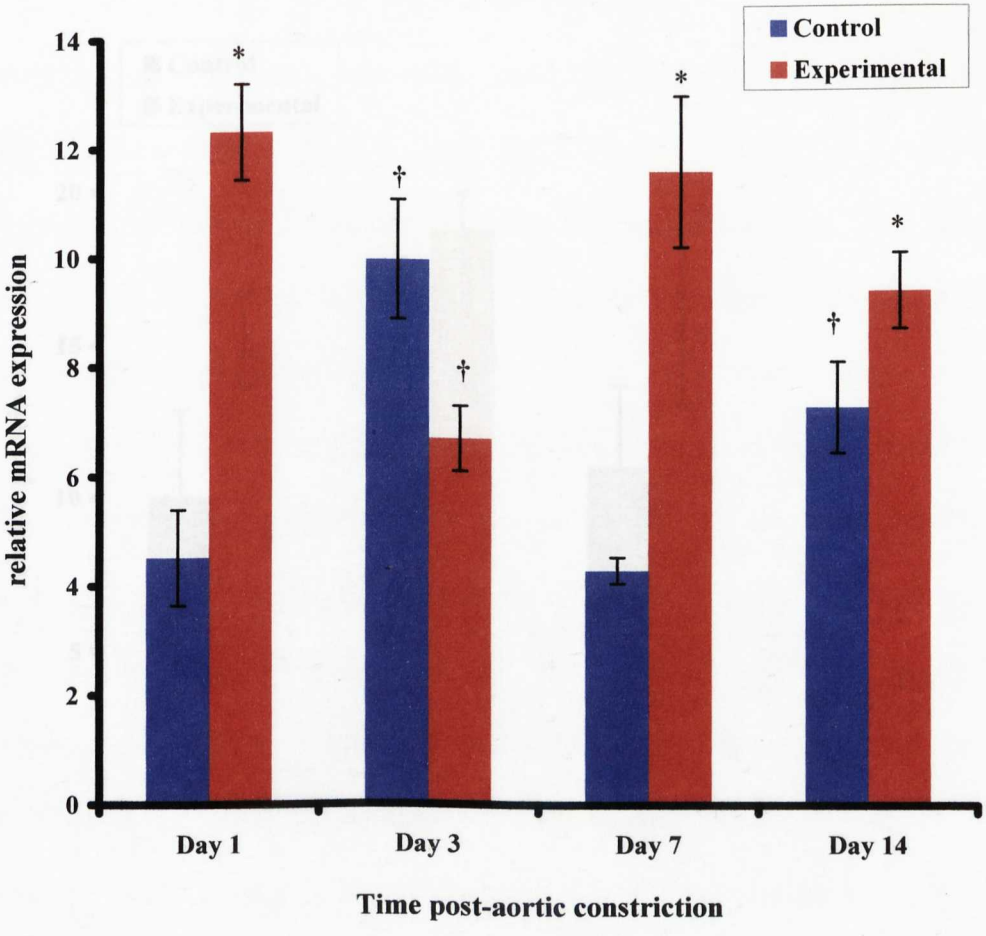

Aortic constriction procedure (■) was carried out in male Sprague Dawley rats and control animals underwent sham procedure (■). The hearts were excised at 1, 3, 7 and 14 days post-surgery and cardiomyocytes were isolated. Total RNA was extracted and a single tube RT-PCR was performed to measure ANF mRNA expression against GAP3DH as reference. The band intensities were quantified using the "Gene Tool" software program. The data represent the mean of n=6 taken from 3 different hearts ± SEM.

* $p<0.05$ aortic constriction versus sham operated animals

† $p<0.05$ as compare to the other days of the investigation of the same group

Figure 3.17: Relative expression of ANF protein in left ventricular tissue, post-induction of pressure overload cardiac hypertrophy.

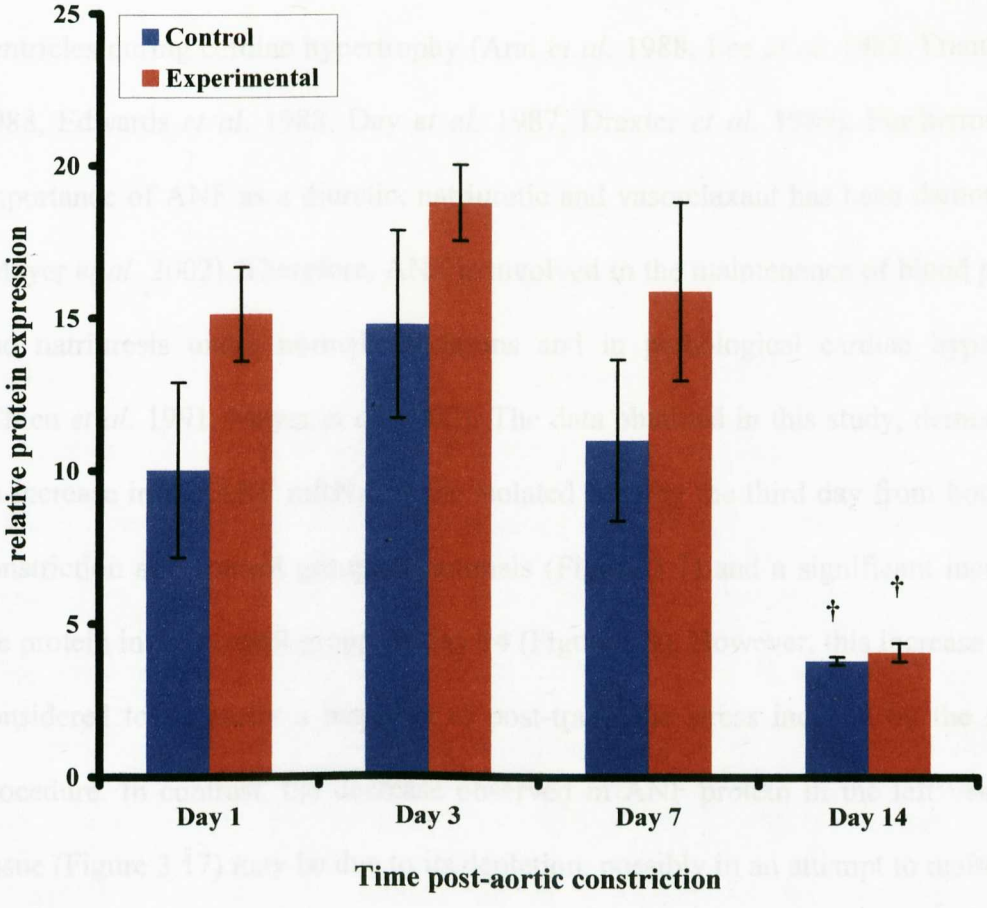

Aortic constriction procedure (■) was carried out in male Sprague Dawley rats and control animals underwent sham procedure (■). The hearts were excised at 1, 3, 7 and 14 days post-surgery and cardiomyocytes were isolated. Total protein was extracted and western blot analysis was performed to measure ANF protein expression against GAP3DH as reference. The band intensities were quantified using the "Gene Tool" software program. The data represent the mean of n=4 taken from 2 different hearts ± SEM.

† $p \leq 0.05$ as compare to the other days of the investigation of the same group

3.4 Discussion

3.4.1 Induction of cardiac hypertrophy: investigation of ANF expression

Elevated level of ventricular ANF is characteristic of cardiac hypertrophy (Ruskoaho *et al.* 1989). ANF is also a stress-related hormone which is re-expressed in the ventricles during cardiac hypertrophy (Arai *et al.* 1988, Lee *et al.* 1988, Franch *et al.* 1988, Edwards *et al.* 1988, Day *et al.* 1987, Drexter *et al.* 1989). Furthermore, the importance of ANF as a diuretic, natriuretic and vasorelaxant has been demonstrated (Mayer *et al.* 2002). Therefore, ANF is involved in the maintenance of blood pressure and natriuresis under normal conditions and in pathological cardiac hypertrophy (Chien *et al.* 1991, Mayer *et al.* 2002). The data obtained in this study, demonstrated an increase in the ANF mRNA in the isolated cells by the third day from both aortic constriction and control groups of animals (Figure 3.7) and a significant increase in the protein in the control group by day 14 (Figure 3.9). However, this increase may be considered to be partly a response to post-traumatic stress induced by the surgical procedure. In contrast, the decrease observed in ANF protein in the left ventricular tissue (Figure 3.17) may be due to its depletion, possibly in an attempt to maintain the normal blood pressure and natriuresis of the body arising from the onset of hypertrophy or stress.

Furthermore, significant increases in the heart weight to tibia length ratio (Table 3.1) and a significant decrease in the left to right kidney ratio (Table 3.2) were observed in the aortic constriction group. It is known that during the development of cardiac hypertrophy, the heart weight to tibia length ratio is increased (Yin *et al.* 1982). Also,

the decrease in the ratio between left to right kidney weight is a characteristic of the model of hypertrophy used in this study (Boateng, 1998).

The up-regulation of ANF in cardiomyocytes and left ventricular tissue, together with the significant alterations in the morphological indicators of hypertrophy by day 14 demonstrated that the aortic constriction procedure was successful as a model for early stage of cardiac hypertrophy using animals.

3.4.2 Investigation of TF expression in the hypertrophic heart

Tissue Factor (TF) is responsible for initiating the extrinsic pathway for blood coagulation but the function of TF, over many years, has been expanded and it is been found to participate in the pathophysiology of different diseases including, heart disease (Toomey *et al.* 1996, Bugge *et al.* 1996, Carmeliet *et al.* 1996, Parry *et al.* 1998, Pawlinski *et al.* 2002). Recently, the involvement of TF in cardiac hypertrophy has been suggested (Luther *et al.* 2000, Muller *et al.* 2000). However, to date, there have been no studies investigating the potential role of TF during the onset of cardiac hypertrophy. Therefore, the aim of this study was to determine alterations in the expression of tissue factor (TF) and its inhibitor, during early stages of the disease at the level of myocytes and in whole left ventricular tissue. Subsequent to aortic constriction, TF mRNA expression was undetectable throughout the period of the investigation in the isolated heart cells, whereas, in whole left ventricular tissue the expression of TF remained at basal levels (Figure 3.11). Furthermore, a similar profile of expression was seen at the protein levels the first week of the investigation with an increase on day 14 (Figure 3.13). These data suggest that in this present study, TF is not expressed in myocytes but may be expressed in other cell types, within the heart

and its expression is not a direct result of the onset of cardiac hypertrophy as shown from the control animals.

It has been shown that under normal conditions TF mRNA and protein are expressed by myocardial cells in both human and murine heart (Flossel *et al.* 1994, Drake *et al.* 1989, Fleck *et al.* 1990, Mackman *et al.* 1993). Animals that underwent sham operation showed a basal expression of TF mRNA in the whole left ventricular tissue up to the 7th day of the investigation which was decreased by day 14 (Figure 3.11). Interestingly, TF protein levels increased by 2 folds after the 7th day (Figure 3.13). TF is a transmembrane glycoprotein that is normally released upon injury (Norris 2003) and therefore its existence in the left ventricular tissue, following surgery is unsurprising. In contrast to the left ventricular tissue, isolated cardiomyocytes from sham operated animals exhibited no evidence of either TF mRNA or TF protein expression. These data indicate that other cells, apart from cardiomyocytes, are responsible for expressing TF in the heart and this expression may occur as a result of trauma. The discrepancy between the mRNA and protein levels on day 14 in the left ventricular tissue may be due to the release of TF from the cells of the myocardium followed by a feedback inhibition of mRNA (Figure 3.11 & 3.13). Therefore, in an early post-surgery phase, the expression of TF in cells other than myocytes is clearly as a result of injury. However, by day 14, hypertrophy is clearly evident both from ANF expression (see section 3.4.1) and measurement of heart weight to tibia length ratio (see section 3.4.1).

Subsequent to aortic constriction, expression of TF in isolated cells was undetectable. The presence of TF in the myocardium has been correlated with the number of

cardiomyocytes in the segments of cardiac muscle (Luther *et al.* 2000). TF antigen is detectable in the intercalated discs and co-localises with cytoskeletal proteins such as desmin and visculin (Luther *et al.* 2000). Furthermore, it has been shown that TF localises at the sarcolemma in extravascular cells, most likely to provide a haemostatic barrier in the event of injury (Flossel *et al.* 1994). In the present investigation, myocytes were isolated by digestion with type II colagenase using the Langendorff mode, where the connections between the cells were disrupted during the procedure. Therefore, during this process, TF expressed by the myocytes may be lost from these cellular junctions. Possible immuno-histological detection of TF using heart sections (Luther *et al.* 2000, Luther *et al.* 1996) may clarify that discrepancy.

After aortic constriction, TF mRNA expression in left ventricular whole tissue remained at basal levels whereas protein expression doubled by day 14 (Figure 3.11 & 3.13). Previous clinical studies have demonstrated that in a remodelled myocardium from patients with either hypertension or ventricular hypertrophy, TF antigen content was down-regulated in the cardiac muscle (Luther *et al.* 2000, Luther & Mackman 2001). This is in contrast to the results obtained in the present study. One possible explanation for the discrepancy in results between this study and that carried out by Luther *et al.* (2000) could be due to the stage of hypertrophy, the model of hypertrophy used and the species used. Luther *et al.* (2000) conducted experiment using biopsies of human hypertrophic failing hearts, whereas the present study investigated TF expression at the onset of hypertrophy in the rat aortic constriction model of hypertrophy. It is therefore conceivable that at later stages hypertrophy, the cell population has decreased and hence less TF is present in the intercalated discs as well as other cell types (Luther *et al.* 2000). In contrast, experiments conducted by

Muller *et al.* (2000) using a transgenic model of cardiac hypertrophy in rats, over-expressing the human renin and angiotensin genes, showed that the endothelial layer of coronary vessels in hypertrophied hearts have increased TF antigen, suggesting that TF is up-regulated in cardiac hypertrophy (Muller *et al.* 2000). Also, studies have shown that in infectious myocarditis, leukocytes and activated monocytes infiltrate the inflamed region of the heart and express TF within the endothelial layer (Schonbeck *et al.* 2000, Zhou *et al.* 1998). Furthermore, endothelial, smooth muscle cells and fibroblasts express TF upon stimulation (Cui *et al.* 1996, Cui *et al.* 2003, Ghrib *et al.* 2002, Carson *et al.* 1994). These studies are in agreement with the present study showing that the TF protein expression is up-regulated by day 14 (Figure 3.13). Therefore, TF appears to be up-regulated at the onset of cardiac hypertrophy although this could also be due to injury following the surgical procedure. Furthermore, TF is probably expressed by vascular and other cells within the myocardium and not by cardiomyocytes.

To conclude, this study showed that TF is not expressed in the adult cardiomyocytes and this could be due to the disruption between the connections of the cells during the isolation procedure. Furthermore, TF protein expression is up-regulated and possibly expressed by other cell types of the heart either due to injury arising from the surgical procedure or due to the induction of cardiac hypertrophy or both by the 14 day.

3.4.3 Investigation of TFPI expression in the hypertrophic heart

TFPI is the specific inhibitor of TF and is primarily expressed by endothelial cells (Bajaj *et al.* 1990, Osterub *et al.* 1995), activated monocytes (Kereveur *et al.* 2001), platelets (Novotny *et al.* 1998) and circulates in the plasma in a free state (Kokawa *et*

al. 1995) under normal conditions. The induction of hypertrophic stress in the present study resulted in a significant increase in TFPI mRNA expression peaking on day 7 of the investigation (Figure 3.3). In contrast, TFPI protein expression was increased on day 1 from the onset of the induction of hypertrophy and decreased thereafter (Figure 3.5). In left ventricular tissue, TFPI mRNA expression was transiently increased within 24 h with a second wave at day 7 (Figure 3.14). It has been shown that upon stimulation, cell types such as smooth muscle cells, fibroblasts and cardiac myocytes, can express TFPI to limit local extravascular clotting following injury (Bajaj *et al.* 1999, Kereveur *et al.* 2001, Girard *et al.* 1989). In agreement with this hypothesis, TFPI has been shown to be expressed in cardiomyocytes upon stimulation with interleukin 1 which is known to be one of the mediators of cardiac hypertrophy (Kereveur *et al.* 2001, Braunwald & Bristow 2000). Therefore, the expression of TFPI mRNA and also the release of TFPI protein, seems to increase in stress, probably to counteract the local increase of TF expressed by other cells within the myocardium.

Furthermore, the up-regulation of TFPI mRNA (Figure 3.3 & 3.14) and the gradual depletion of the protein (Figure 3.5 & 3.15) could offer protection to the heart against both the haemostatic and the homeostatic influences of TF. In other diseases such as atherosclerosis, TFPI has been shown to inhibit TF activity and to maintain a protective role (Novotny *et al.* 1998). Furthermore, genetically engineered mice heterozygous for TFPI-deficiency are more prone to atherosclerosis indicating a potential protective role for TFPI (Westrick *et al.* 2001). Disturbance in the balance between TFPI and TF expression results in altering the haemostatic balance, resulting in clot formation and further damage to the heart (Bajaj *et al.* 1999, Kereveur *et al.* 2001, Girard *et al.* 1989, Novotny *et al.* 1998, Westrick *et al.* 2001). Therefore,

increased TFPI expression demonstrated here is an essential component in regulating the activity of exogenous TF, protecting the heart from further injury.

3.5 Conclusions

This aim of this study was to establish the profile of TF and TFPI during the onset of cardiac hypertrophy. Cardiac hypertrophy was achieved by day 14 as ANF expression was up-regulated and the morphological indicators were significantly altered. Furthermore, it was shown that TF is not expressed in adult cardiomyocytes and this could be due to the disruption between the connections of the cells during the isolation procedure. Also, TF protein expression is up-regulated by other cell types of the heart either due to injury arising from the surgical procedure or due to the induction of cardiac hypertrophy or both. In addition, TFPI mRNA was up-regulated, while TFPI protein was depleted, probably to counteract the local increase of TF expressed by other cells within the myocardium. Therefore, the expression of TF and TFPI, during the onset of cardiac hypertrophy, resulting in the altered ratio of these proteins, may lead to an imbalance in haemostasis and tissue homeostasis mechanisms, much of those observed during the onset of cardiac hypertrophy or following the surgical procedures. Furthermore, it is possible that the differential expression of TFPI, between mRNA and protein in adult ventricular cardiomyocytes and left ventricular tissue in response to hypertrophic stress, may be an adaptive response to increase expression of TF from cells of the vasculature, protecting the heart against further haemostatic and homeostatic damage by TF.

CHAPTER 4

The influence of exogenous Tissue Factor on the expression of Atrial Natriuretic Factor and Mechano Growth Factor in H9c2 cardiomyocytes *in vitro*

4. The influence of exogenous Tissue Factor on the expression of Atrial Natriuretic Factor and Mechano Growth Factor in H9c2 cardiomyocytes *in vitro*

4.1 Introduction

In heart, α and/or β adrenergic stimulation, pressure overload or volume overload could lead in the expression of the immediate early genes (c-fos, c-jun) and further to this to the re-expression of the foetal phenotype, ultimately leading to increase protein expression and myocyte growth and remodelling (Sheng & Greenberg 1990, Chien *et al.* 1991). Of a great interest and one of the main characteristics of cardiac hypertrophy is the re-expression of the foetal phenotype in the ventricles (Izumo *et al.* 1987, Schwartz *et al* 1986, Izumo *et al.* 1988). Qualitative changes in hypertrophy includes, changes in the sarcomeric protein, such as skeletal actin α, myosin heavy chain β isoforms, troponin T and myosin light chain 1 isoforms (Izumo *et al.* 1987, Schwartz *et al.*1986, Izumo *et al.* 1988, Lowers *et al.* 1997, Morano *et al.* 1997 Nakao *et al.* 1997, Miyata 2000, Anderson *et al.* 1995, Hirzel *et al.* 1985). In addition, the induction of natriuretic peptides in the ventricles (ANF and BNP) plays an important role in the remodelling of the heart (Braunwald & Bristow 2000). Furthermore, quantitative changes, including the down-regulation of SERCA2a and PPARα suppress fatty acid oxidation and increases glucose utilisation in the hypertrophic myocardium (Frey & Olson 2003). These adaptations regulate and contribute to the remodelling of the hypertrophied heart (Schwartz *et al.* 1992).

ANF is a cardiac peptide that exhibits diuretic, natriuretic and vasorelaxant effects (Mayer *et al.* 2002) and can regulate cell growth (Braunwald & Bristow 2000).

Cardiac ANF expression is an important determinant of the circulating ANF peptide levels during health or heart failure (Burnett *et al.* 1986, Rascher *et al.* 1985, Shenker *et al.* 1985). Its importance is shown by maintaining blood pressure and natriuresis in health or in a pathological cardiac hypertrophy (Chien 1991, Mayer *et al.* 2002). During foetal life, ANF is expressed in both the atria and ventricles (Bloch *et al.* 1986, Wu *et al.* 1988). Following birth, the expression of ANF is down-regulated in the ventricle and the atrium becomes the main site of ANF synthesis in the adult heart (Chien 1991). Studies have shown that during cardiac hypertrophy ANF is re-expressed in the ventricles and is the most well known marker of the disorder (Arai *et al.* 1988, Lee *et al.* 1988, Franch *et al.* 1988, Edwards *et al.* 1988, Day *et al.* 1987, Drexter *et al.* 1989, Gutkowska *et al.* 1986). The potential influence of TF on the expression of ANF has not previously been explored.

During cardiac hypertrophy, muscle growth is a complex process, that involves a number of intracellular signalling pathways, including phosphatidylinositol 3-kinase (PI3K)/ Akt/ glycogen synthase kinase 3β (GSK-3β)-dependent signalling, the mitogen-activated protein kinase pathway (MAPK), the protein kinase C pathway, the calcineurin-NFAT signalling pathway and many others (Molkentin & Dorm, 2001). PI3K pathway includes a family of enzymes that exhibit both protein and lipid kinase activity (Frey & Olson, 2003). This pathway has been linked to signalling pathways involved in cellular growth and survival (Frey & Olson, 2003). The PI3K/Akt/GSK3β signalling cascade is also involved in mediating the hypertrophic response in addition to its role in insulin signalling (Selvetella *et al.* 2004). This pathway is regulated by several classes of membrane receptor, including receptor protein kinases, such as the

insulin-like growth factor I (IGF-1) as well as G protein-coupled receptors, such as α and β_2- adrenergic receptors (Figure 4.1) (Selvetella *et al.* 2004).

IGF-1 is a single-chain polypeptide that has an insulin-like short term metabolic effect and a growth factor-like long term effect (Coerper *et al.* 2001, Lloyd. 1999). IGF-1 exists in the heart in two splice variants, the mechano-growth factor (MGF) and the systemic liver type (IGF-IEa) (Figure 4.2). MGF possess a number of domains, some of which have homologous sequences to IGF-1 (Figure 4.2), and one stimulates muscle stem cells and another recognises specific binding proteins which have been found to be present in large quantities in cardiac muscle tissue (Goldspink *et al.* 1999, Harridge *et al.* 2003, Yang *et al.* 2002). However, MGF is only detectable following injury and/or following mechanical activity and its anabolic effects, including the stimulation of protein synthesis and promotion of stem cell activation, required for tissue regeneration (Harridge *et al.* 2003, Yang *et al.* 2002, Goldspink *et al.* 1999).

TF is expressed in cardiac muscle, but not in cardiomyocytes as was confirmed in the previous section (Chapter 3). However, the function of TF in the heart is not known and requires clarification. TF has been found to act as a signalling receptor and lead to alterations in the pattern of growth gene expression (Rottingen *et al.* 1995, Poulsen *et al.* 1998, Pendurthi *et al.* 1997, Camerer *et al.* 2000, Ruf *et al.* 2003). In this part of the investigation, an attempt was made to explore the mechanisms underlying the possible role of TF in the induction of cardiac hypertrophy. The effect of long-term and short-term exposure of rat cardiomyocyte cell line H9c2 to exogenous TF, on the expression of ANF was investigated. Furthermore, the influence of exogenous TF on

Figure 4.1: The PI3K signalling pathway.

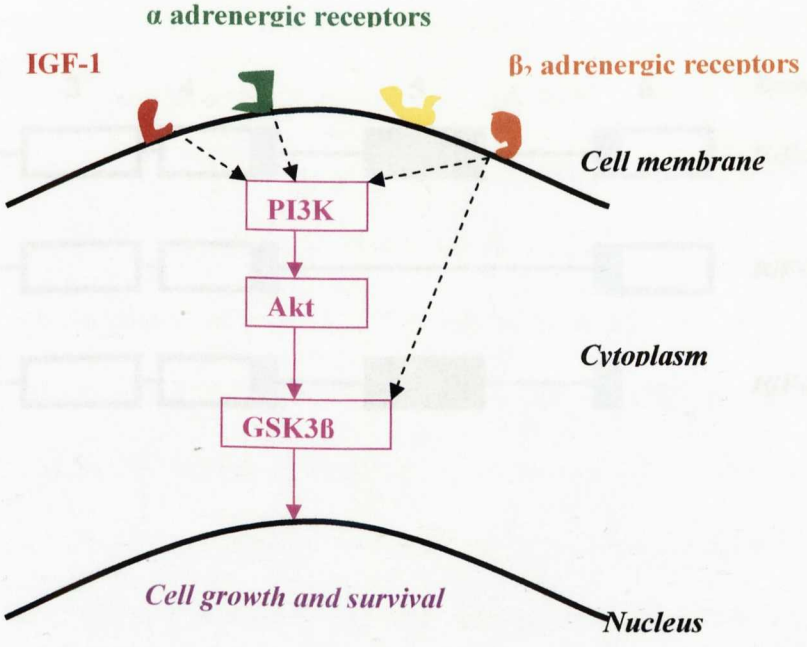

A schematic representation showing the PI3K signalling pathway promoting cell growth and survival. The PI3K pathway can be activated via IGF-1, α adrenergic receptors or β_2 adrenergic receptors. B_2 adrenergic receptors can also activate GSK3 β directly. Subsequently, a hypertrophic response is initiated, leading ultimately to heart failure.

Figure 4.2: The IGF gene and its splicing variants.

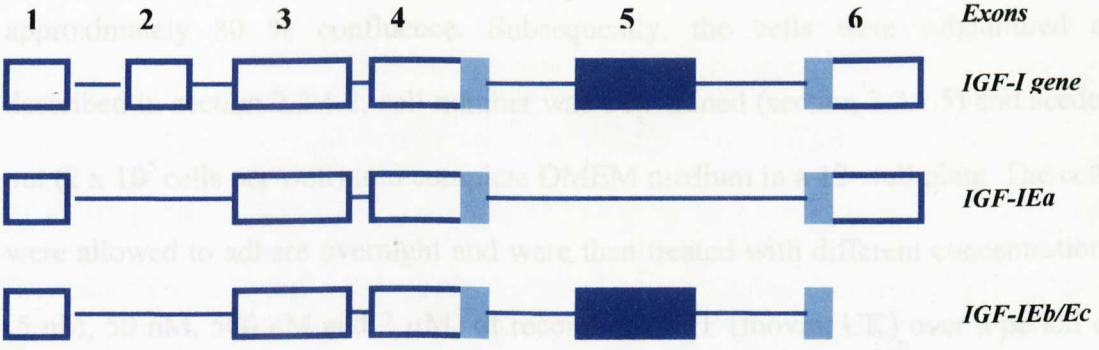

A schematic representation of the IGF gene and its locally produced splice variants. The filled blue boxes denote the insert in exon 5 (49 bp in human, 52 bp in gerbil and other species), which give rise to alternatively spliced MGF (IGF-IEb/Ec- IGF-IEb in rodents corresponds to IGF-IEc in humans) isoform. Although, IGF-1 is a simple 70 amino acid peptide, the gene is fairly large spanning a region of over 90 kb genomic DNA.

the expression of MGF and in the expression of slow myosin heavy chain β (sMHCβ) in H9c2 cardiomyocytes was examined for comparison.

4.2 Methods

4.2.1 Long-term influence of TF on ANF expression

H9c2 cells were cultured as described in section 2.1.1 and allowed to reach approximately 80 % confluence. Subsequently, the cells were subcultured as described in section 2.2.1.2, cell number was determined (section 2.2.1.5) and seeded out (2 x 10^5 cells per well) into complete DMEM medium in a 12-well plate. The cells were allowed to adhere overnight and were then treated with different concentrations (5 nM, 50 nM, 500 nM and 2 μM) of recombinant TF (Inovin, UK) over a period of 15 days. The cells were then harvested as described in section 2.2.1.3 on days 1, 2, 5, 10 and 15 and total RNA was extracted as described in sections 2.2.3.1 and 2.2.3.4. The expression of ANF was measured and analysed by semi-quantitative RT-PCR with GAP3DH as reference as previously described (section 2.2.4.2 and 2.2.4.3).

For protein expression analysis, a similar cell culture protocol that one described above was used, except that cells were seeded out (10^6 cells per flask) into a 25 cm^3 flasks. Treatment with recombinant TF was as described above and the cells were harvested on days 1, 2, 3, 5, 10 and 15. Subsequently, protein was isolated as described in section 2.2.5.1 and protein concentration was determined using the Bradford assay (section 2.2.5.4). SDS-PAGE was performed using a 12 % (w/v) resolving gel (section 2.2.5.5) and western blot analysis for ANF was followed as previously described (section 2.2.5.6).

4.2.2 Short-term influence of TF with or without FVIIa, FXa and TFPI on ANF expression

H9c2 cells were seeded out as described in section 4.2.1 in a 12-well plate and allowed to adhere overnight. The medium was replaced the following day with complete DMEM containing 5 % (v/v) FCS and incubated for 24 h. On the second day the medium was replaced with complete DMEM medium containing 3 % (v/v) FCS and cells were incubated for a further 24 h. The FCS concentration was further reduced to 1 % (v/v) on the third day and following 24 h incubation was eliminated altogether. The cells were then incubated with TF (50 and 500 nM) and combinations of FVIIa (5 nM), FXa (10 nM) and TFPI (5 pM) as described in the result section 4.3. The cells were harvested as described in section 2.2.1.3 on day 1 and 2, and analysis of ANF mRNA was performed as previously described in section 4.2.1.

Analysis of the expression of ANF protein was carried out using the same protocol as described above, except that the cells were seeded out (4×10^5 cells per well) into a 12 well plate. H9c2 cells were harvested on day 1 and 2 and ANF western blot analysis was performed as previously described in section 4.2.1.

4.2.3 Long-term influence of TF on MGF expression

H9c2 cells were seeded out into a 12-well plate at a density 4×10^5, and treated with a range of recombinant TF concentrations (50 nM, 500 nM and 2 μM) for up to 7 days. The cells were harvested as previously described (section 2.2.1.3), and total RNA was isolated and quantified (section 2.2.3.1, section 2.2.3.4 respectively) on days 1, 3 and 7. The expression of MGF was measured by semi-quantitative RT-PCR with GAP3DH as reference (section 2.2.4.2 and 2.2.4.3).

4.2.4 Long-term influence of TF on MGF, nMHC and sMHCβ antigen expression

H9c2 cells were seeded out as described in section 2.2.1.2 in an 8-well microscope chamber slide at a density of 1 x 10^5 and treated exposed to different concentrations (50 nM and 500 nM) of recombinant TF for a period of 14 days. The cells were washed with freshly made PBS (pH 7.4) and fixed with 4 % (v/v) formaldehyde for 5 min. Subsequently, cells were stained using the immunofluorescen protocol for MGF as described in section 2.2.8.3.

In a separate experiment, cells was prepared and treated with recombinant TF (50 nM and 500 nM) as described above for a period of 7 days. The cells were washed with freshly made PBS (pH 7.4) and fixed with 4 % (v/v) formaldehyde for 5 min on days 1, 3 and 7 of the investigation. Subsequently, cells were stained either for nMHC or for sMHCβ as described in sections 2.2.8.1 and 2.2.8.2, respectively.

4.3 Results

4.3.1 ANF expression following long-term treatment with TF

The mRNA expression of ANF measured on day 1 post-treatment (Figure 4.3) with exogenous TF, significantly increased to 300 %, 220 %, 120% and 150% as compared to the control (un-treated cells remained in complete DMEM medium with 10 % (v/v) foetal calf serum), when exposed to 5 nM, 50 nM, 500 nM, and 2 μM TF, respectively (Figure 4.4). However, by the second day, ANF expression was reduced to 120 % of the control in the samples treated with 5 nM and 2 μM TF respectively, 75 % of the control in the sample treated with 50 nM TF and 60 % of the control in the sample

Figure 4.3: ANF expression in H9c2 cardiomyocytes 1 day post-treatment with exogenous TF.

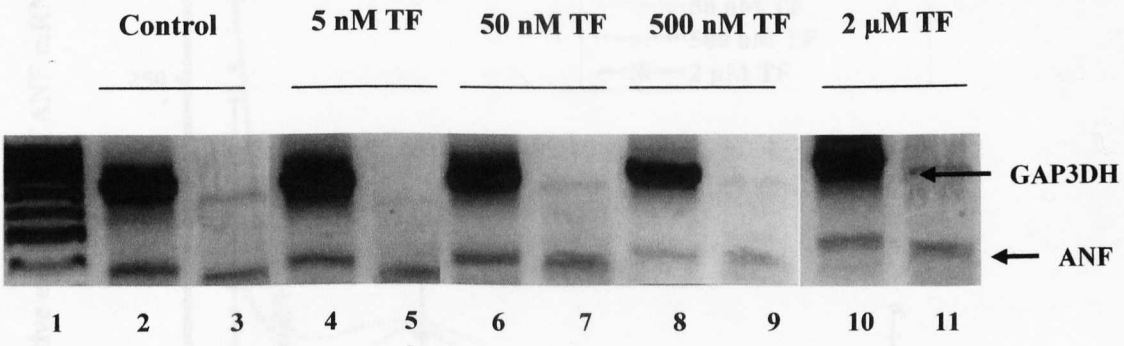

A representative agarose gel used for the analysis of ANF mRNA expression in H9c2 cells 1 day post-TF treatment. Lane 1: DNA ladder, lane 2, 4, 6, 8, 10: GAP3DH mRNA expression, lane 3, 5, 7, 9, 11: ANF mRNA expression. Similar gels were produced for subsequent days of the investigation. The micrograph is typical of 30 gels.

Figure 4.4: The percentage relative expression of ANF mRNA in H9c2 rat cardiomyocytes in response to exogenous TF.

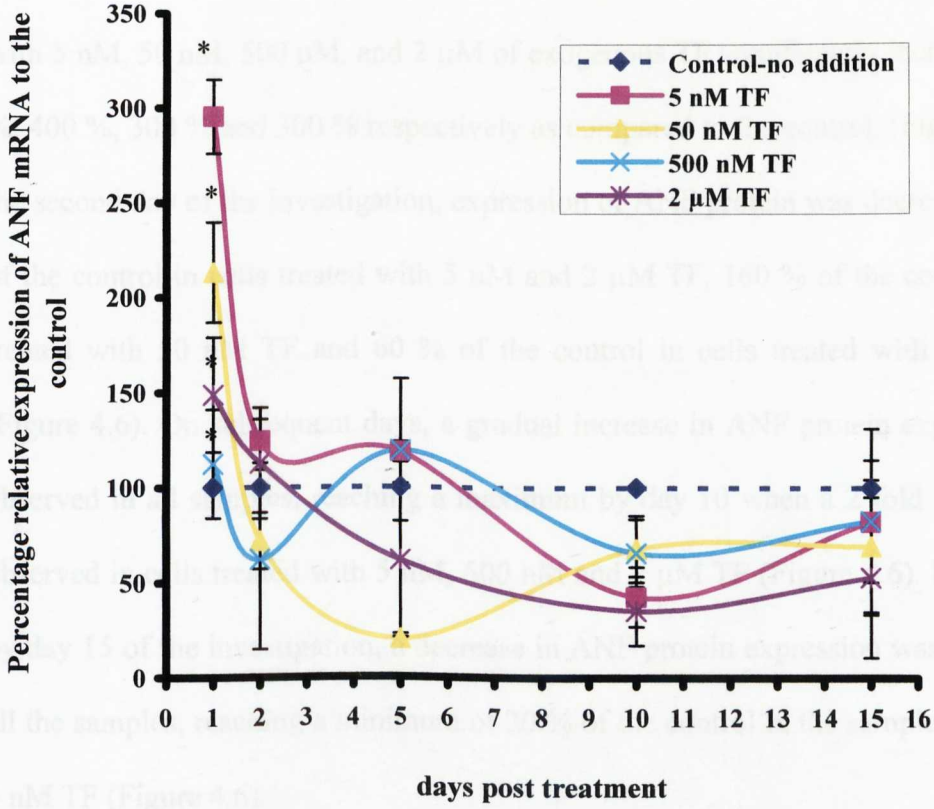

H9c2 cells were seeded out in wells at 2 x10^5/well in complete DMEM medium and treated with 5 nM of TF (■), 50 nM of TF (▲), 500 nM of TF (×) and 2 µM of TF (*), respectively. The cells were harvested on day 1, 2, 5, 10 and 15 post-treatment and total RNA was extracted. Single tube RT-PCR reaction was carried out to measure the expression of ANF mRNA was measured against GAP3DH as reference in each sample. The band intensities were quantified using the "Gene Tool" software program. The data represent the mean of n=6 for each concentration taken from 2 independent experiment and are presented as a percentage of the control (un-treated cells ◆) ± SEM, on each day of the investigation.

* $p<0.05$ as compared to the control

treated with 500 nM TF (Figure 4.4). On subsequent days of treatment, ANF expression further decreased and eventually stabilised at 50 % of the control in the samples treated with 5 nM, 50 nM and 500 nM TF and 90 % of the control in the sample treated with 2 μM of TF (Figure 4.4).

Concurrently, the expression of ANF protein (Figure 4.5) on day 1 of the treatment with 5 nM, 50 nM, 500 nM, and 2 μM of exogenous TF significantly increased to 540 %, 400 %, 300 % and 300 % respectively as compared to the control, (Figure 4.6). On the second day of the investigation, expression of ANF protein was decreased to 40 % of the control in cells treated with 5 nM and 2 μM TF, 160 % of the control in cells treated with 50 nM TF and 60 % of the control in cells treated with 500 nM TF (Figure 4.6). On subsequent days, a gradual increase in ANF protein expression was observed in all samples, reaching a maximum by day 10 when a 2 fold increase was observed in cells treated with 5 nM, 500 nM and 2 μM TF (Figure 4.6). Furthermore, by day 15 of the investigation, a decrease in ANF protein expression was observed in all the samples, reaching a minimum of 20 % of the control in the sample treated with 5 nM TF (Figure 4.6).

4.3.1.1 ANF expression in response to treatment with TF over 24 h

To determine the time-course of ANF expression in response to TF, H9c2 cell (2 x 10^4 cells per well) were cultured in a 12 well plate with complete DMEM medium and then treated with 2 μM of TF for 3, 5, 7 and 24 h. ANF mRNA expression was significantly increased 24 h post-treatment (Figure 4.7). However, after 3, 5 and 7 h with TF treatment, ANF expression remained at the same level as the control (untreated cells) (Figure 4.7).

Figure 4.5: ANF protein expression in H9c2 cardiomyocytes 1 day post treatment with exogenous TF.

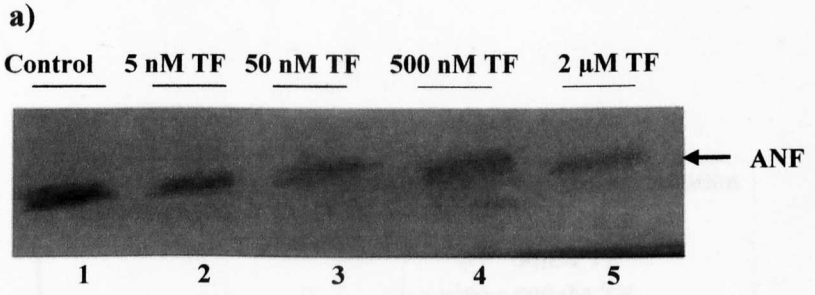

Micrograph a): ANF protein expression at 13 kDa in H9c2 cells 1 day post-treatment with exogenous TF. Similar western blots were produced for subsequent days of the experiment. The micrograph is typical of 30 gels.

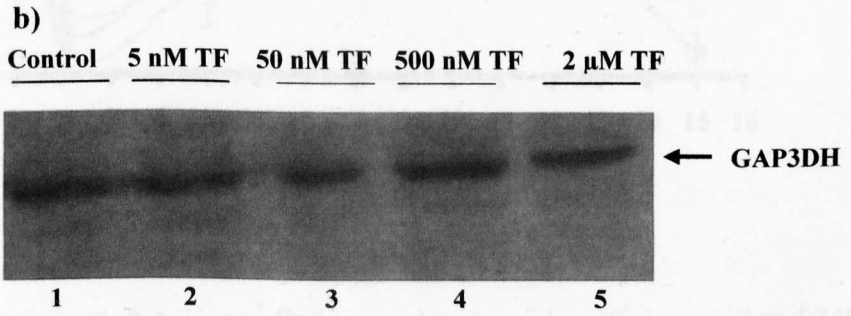

Micrograph b): GAP3DH protein expression at 38 kDa in H9c2 cells 1 day post-treatment with exogenous TF. Similar western blots were produced for subsequent days of the experiment. The micrograph is typical of 30 gels.

Figure 4.6: The percentage relative expression of ANF protein in H9c2 rat cardiomyocytes in response to treatment with exogenous TF.

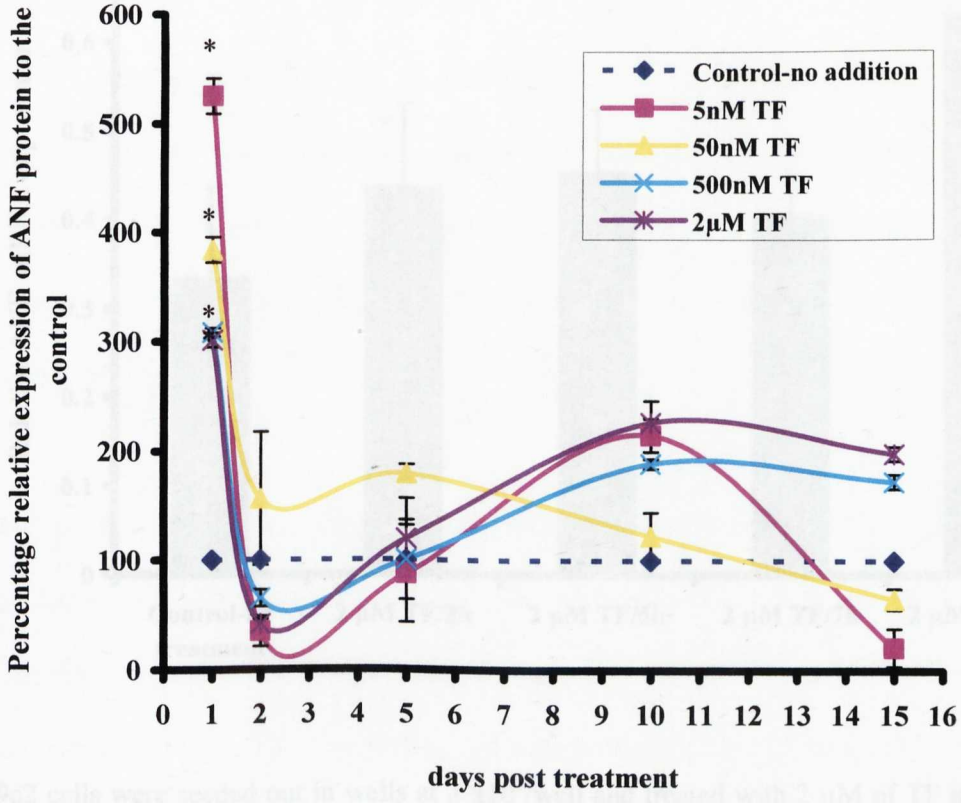

H9c2 cells were seeded out in a 25 cm^3 flasks at a density of 1 x 10^6 in complete DMEM medium and treated with 5 nM TF (■), 50 nM TF (▲), 500 nM TF (×) and 2 μM TF (*), respectively. The cells were harvested on day 1, 2, 5, 10 and 15 post-treatment and total protein was extracted. 20 μg aliquots of each sample was analysed by poly-acrylamide gel electrophoresis and subsequent western blotting using specific antibodies for ANF and also GAP3DH, as reference. The band intensities were quantified using the "Gene Tool" software program. The data represent the mean of n=6 for each concentration taken from 2 independent experiment and are presented as a percentage of the control (un-treated cells ◆) ± SEM, on each day of the investigation.

* $p<0.05$ as compared to the control

Figure 4.7: The relative expression of ANF mRNA in H9c2 rat cardiomyocytes in response to treatment with 2 μM exogenous TF after 3, 5, 7 and 24 h.

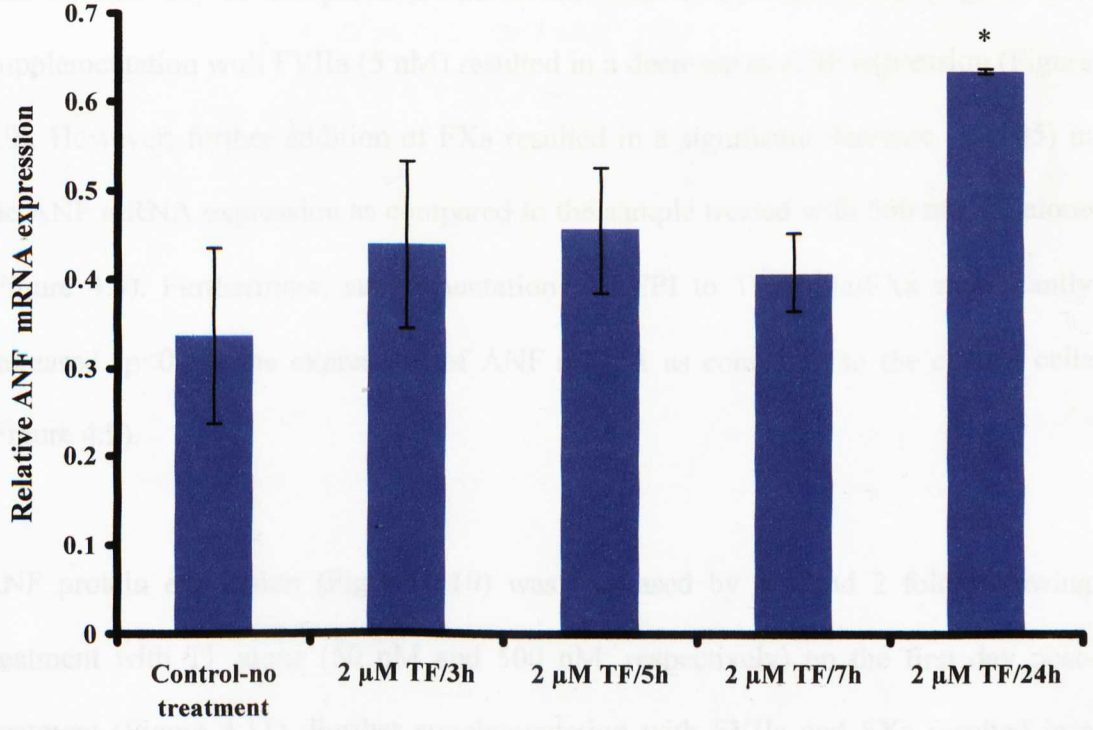

H9c2 cells were seeded out in wells at 2 x10^5/well and treated with 2 μM of TF in complete DMEM. The cells were harvested 3, 5, 7 and 24 h post-treatment. Total RNA was extracted and single-tube RT-PCR was carried out and ANF mRNA expression was measured against GAP3DH as reference. Band intensities were quantified using the "Gene Tool" software program. The data represent the mean of n= 12 taken from two separate experiments, each performed in duplicate ± SEM.

* $p<0.05$ as compared to the control

4.3.2 ANF expression following short-term treatment with TF with or without FVIIa, FXa and TFPI

The relative expression of ANF mRNA (Figure 4.8) following treatment with exogenous TF alone (50 nM and 500 nM) was significantly increased ($p<0.05$) by 2 fold on first day as compared to the control cells (un-treated cells) (Figure 4.9). Supplementation with FVIIa (5 nM) resulted in a decrease in ANF expression (Figure 4.9). However, further addition of FXa resulted in a significant decrease ($p<0.05$) in the ANF mRNA expression as compared to the sample treated with 500 nM TF alone (Figure 4.9). Furthermore, supplementation of TFPI to TF/FVIIa/FXa significantly increased ($p<0.05$) the expression of ANF mRNA as compared to the control cells (Figure 4.9).

ANF protein expression (Figure 4.10) was increased by 1.5 and 2 fold following treatment with TF alone (50 nM and 500 nM, respectively) on the first day post-treatment (Figure 4.11). Further supplementation with FVIIa and FXa resulted in a decrease in ANF protein expression, but was not significant (Figure 4.11). Moreover, addition of TFPI to TF/FVIIa/FXa resulted in a further decrease in ANF protein expression to similar levels to those observed in the control sample (Figure 4.11).

On the second day of the investigation, the ANF mRNA expression in response to TF treatment was undetectable. However, after 2 days of treatment with exogenous TF incombinations with FVIIa, FXa and TFPI, the relative protein expression of ANF in H9c2 cells, was increased in all samples as compared to the control (Figure 4.12).

Figure 4.8: The expression of ANF mRNA in H9c2 cardiomyocytes 1 day post-treatment with exogenous TF, FVIIa, FXa and TFPI.

a)

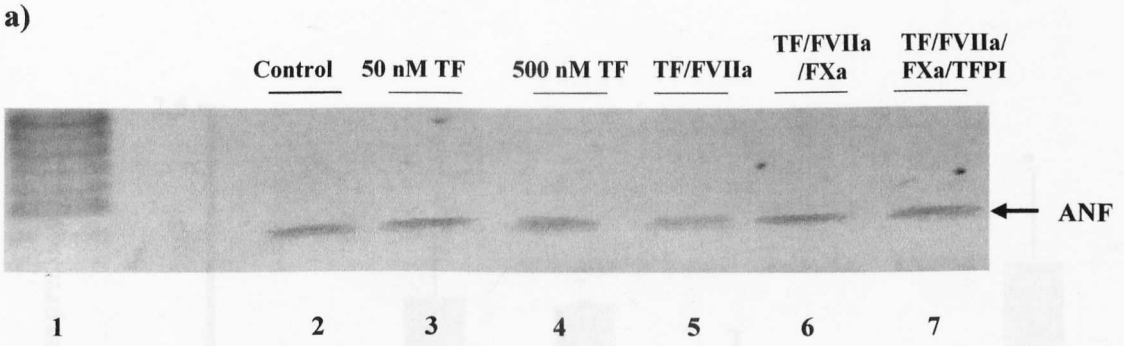

Micrograph a): Lane 1: DNA ladder, lanes 2, 3, 4, 5, 6, 7: ANF mRNA expression in H9c2 cells 1 day post-treatment with exogenous TF, FVIIa, FXa and TFPI. The micrograph is typical of 12 gels.

b)

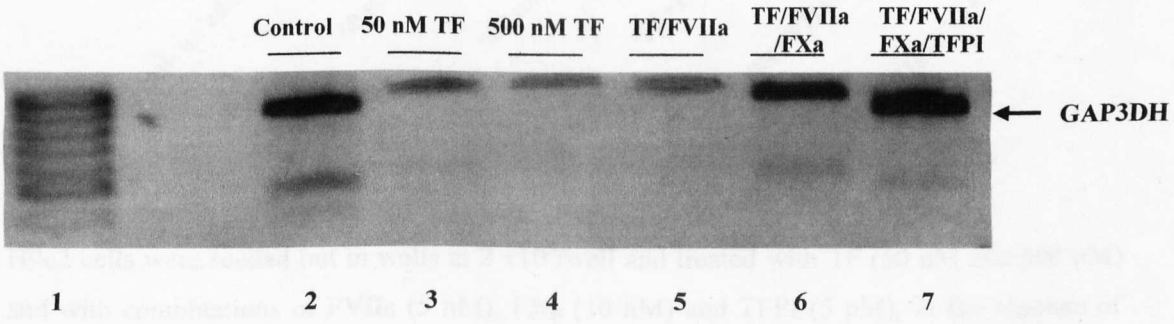

Micrograph b): Lane 1: DNA ladder, lanes 2, 3, 4, 5, 6, 7: GAP3DH mRNA expression in H9c2 cells 1 day post-treatment with exogenous TF, FVIIa, FXa and TFPI. The micrograph is typical of 12 gels.

Figure 4.9: The relative expression of ANF mRNA in H9c2 rat cardiomyocytes in response to treatment with combinations of TF, FVIIa, FXa and TFPI, 1 day post-treatment.

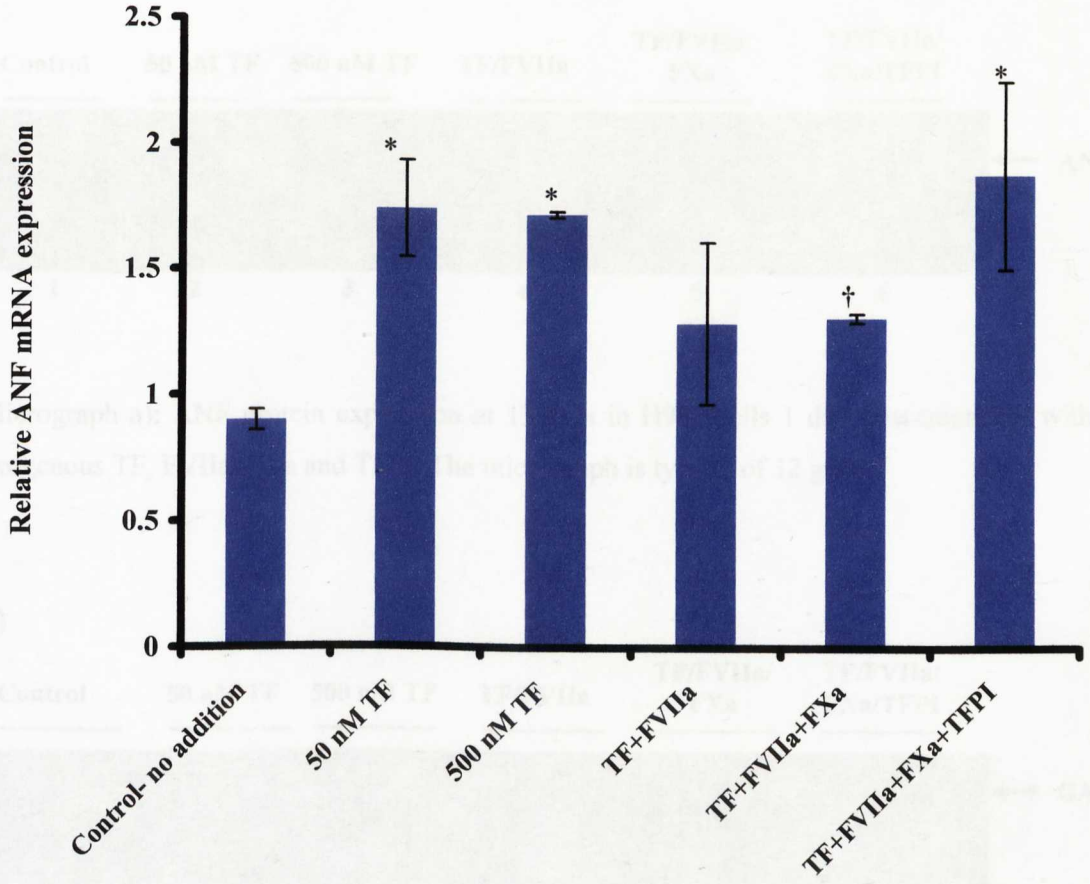

H9c2 cells were seeded out in wells at 2 x10^5/well and treated with TF (50 nM and 500 nM) and with combinations of FVIIa (5 nM), FXa (10 nM) and TFPI (5 pM), in the absence of FCS. The cells were harvested at the first day post-treatment. Total RNA was extracted and single-tube RT-PCR was carried out to measure ANF mRNA expression against GAP3DH as reference. The band intensities were quantified using the "Gene Tool" software program. The data represent the mean of n= 12 taken from two separate experiments, each performed in duplicate ± SEM.

* $p<0.05$ as compared to the control

† $p<0.05$ as compared to sample treated with 500 nM TF

Figure 4.10: The expression of ANF protein in H9c2 cardiomyocytes 1 day post-treatment with exogenous TF, FVIIa, FXa and TFPI.

a)

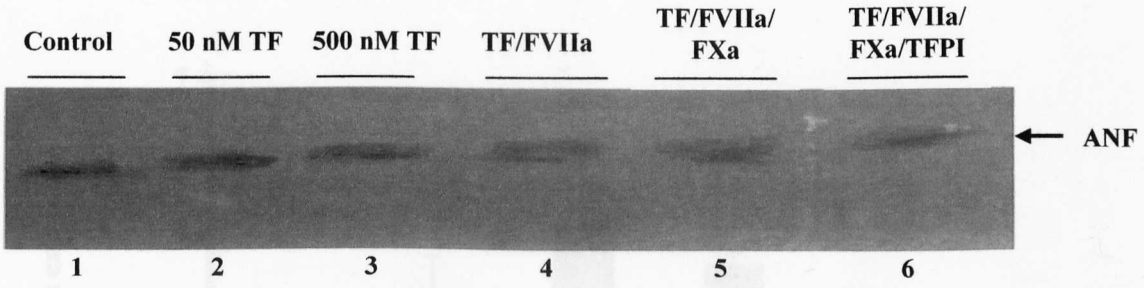

Micrograph a): ANF protein expression at 13 kDa in H9c2 cells 1 day post-treatment with exogenous TF, FVIIa, FXa and TFPI. The micrograph is typical of 12 gels.

b)

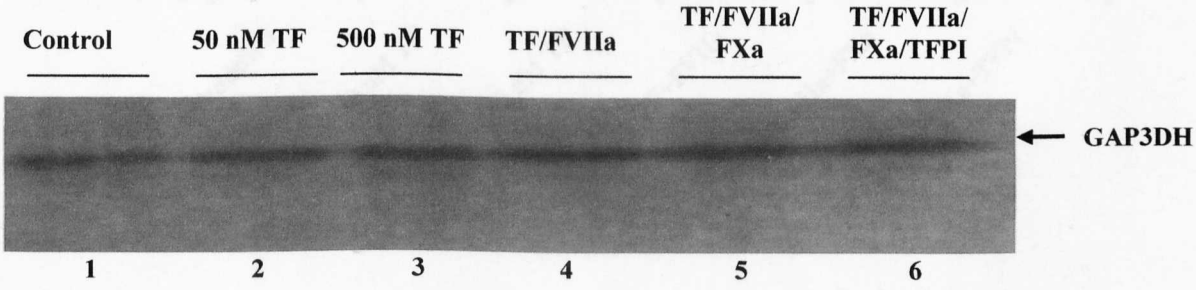

Micrograph b): GAP3DH protein expression at 38 kDa in H9c2 cells 1 day post-treatment with exogenous TF, FVIIa, FXa and TFPI. The micrograph is typical of 12 gels.

Figure 4.11: The relative expression of ANF protein in H9c2 rat cardiomyocytes in response to treatment with combinations of TF, FVIIa, FXa and TFPI, 1 day post-treatment.

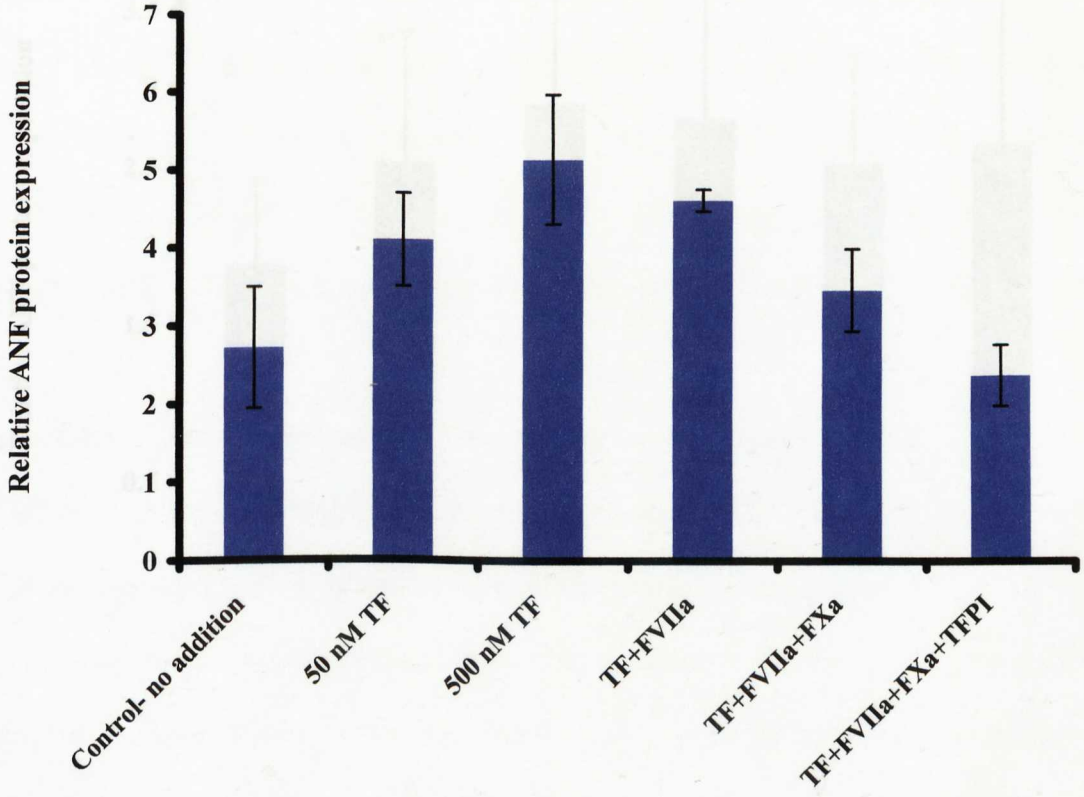

H9c2 cells were seeded out in wells at 2 x10^5/well and treated with TF (50 nM and 500 nM) and with combinations of FVIIa (5 nM), FXa (10 nM) and TFPI (5 pM), in the absence of FCS. The cells were harvested at the first day post-treatment. Total protein was extracted and western blot analysis was performed to measure ANF protein expression against GAP3DH as reference. The band intensities were quantified using the "Gene Tool" software program. The data represent the mean of n= 12 taken from two separate experiments, each performed in duplicate ± SEM.

Figure 4.12: The relative expression of ANF protein in H9c2 rat cardiomyocytes in response to treatment with combinations of TF, FVIIa, FXa and TFPI, 2 days post-treatment.

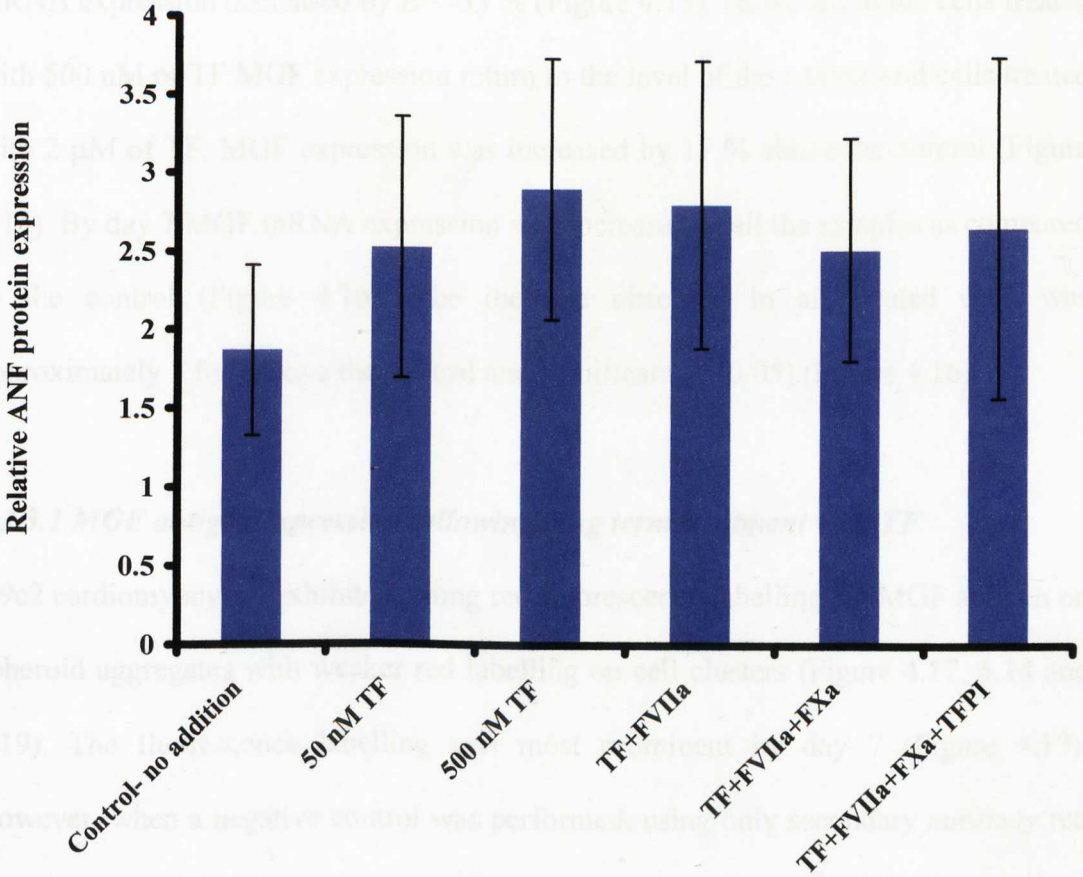

H9c2 cells were seeded out in wells at 2 x10^5/well and treated with TF (50 nM and 500 nM) and with combinations of FVIIa (5 nM), FXa (10 nM) and TFPI (5 pM), in the absence of FCS. The cells were harvested 2 days post-treatment. Total protein was extracted and western blot analysis was performed to measure ANF protein expression against GAP3DH as reference. The band intensities were quantified using the "Gene Tool" software program. The data represent the mean of n= 12 taken from two separate experiments, each performed in duplicate ± SEM.

4.3.3 MGF expression following long-term treatment with TF

After 24 h of exposure to 50 nM TF, MGF expression (Figure 4.13) was increased by approximately 30 % above the control, whereas on exposure to 500 nM and 2 μM TF, MGF expression was decreased 50 and 30 % of the control respectively (un-treated cells) (Figure 4.14). In contrast, by day 3, the cells treated with 50 nM TF MGF mRNA expression decreased by Δ= -33 % (Figure 4.15). However, in the cells treated with 500 nM of TF MGF expression return to the level of the control and cells treated with 2 μM of TF, MGF expression was increased by 17 % above the control (Figure 4.15). By day 7 MGF mRNA expression was increased in all the samples as compared to the control (Figure 4.16). The increase observed in all treated cells was approximately 3 fold above the control and significant ($p<0.05$) (Figure 4.16).

4.3.3.1 MGF antigen expression following long term treatment with TF

H9c2 cardiomyocytes, exhibited strong red fluorescence labelling for MGF antigen on spheroid aggregates with weaker red labelling on cell clusters (Figure 4.17, 4.18 and 4.19). The fluorescence labelling was most prominent by day 7 (Figure 4.19). However, when a negative control was performed, using only secondary antibody red fluorescence labelling was observed (Figure 4.20).

Figure 4.13: MGF mRNA expression in H9c2 cardiomyocytes 1 day post-treatment with exogenous TF.

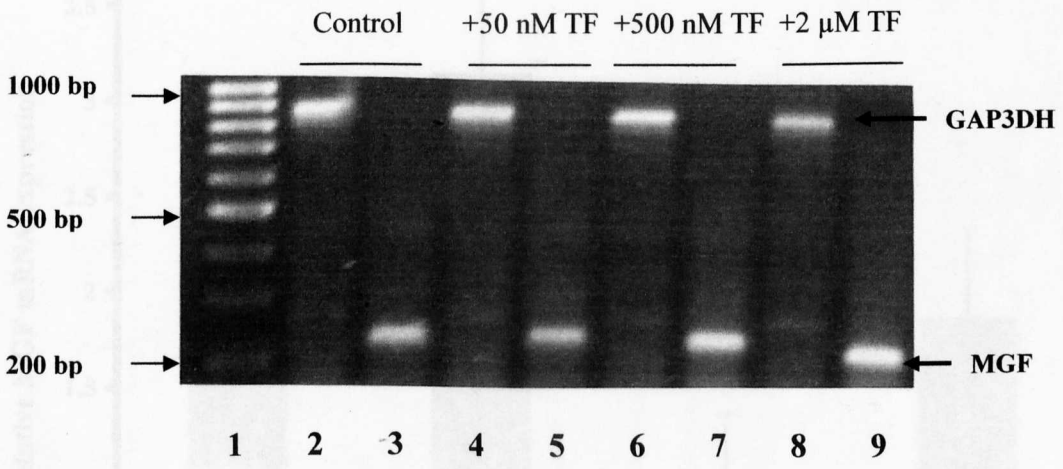

A representative agarose gel, used for measuring MGF mRNA expression, in H9c2 cells 1 day post-treatment with exogenous TF. Lane 1: DNA ladder, lanes 2, 4, 6, 8: GAP3DH mRNA expression, lanes 3, 5, 7, 9: MGF mRNA expression. The micrograph is typical of 12 gels.

Figure 4.14: The relative expression of MGF mRNA in H9c2 rat cardiomyocytes in response to treatment with exogenous TF 1day post-treatment.

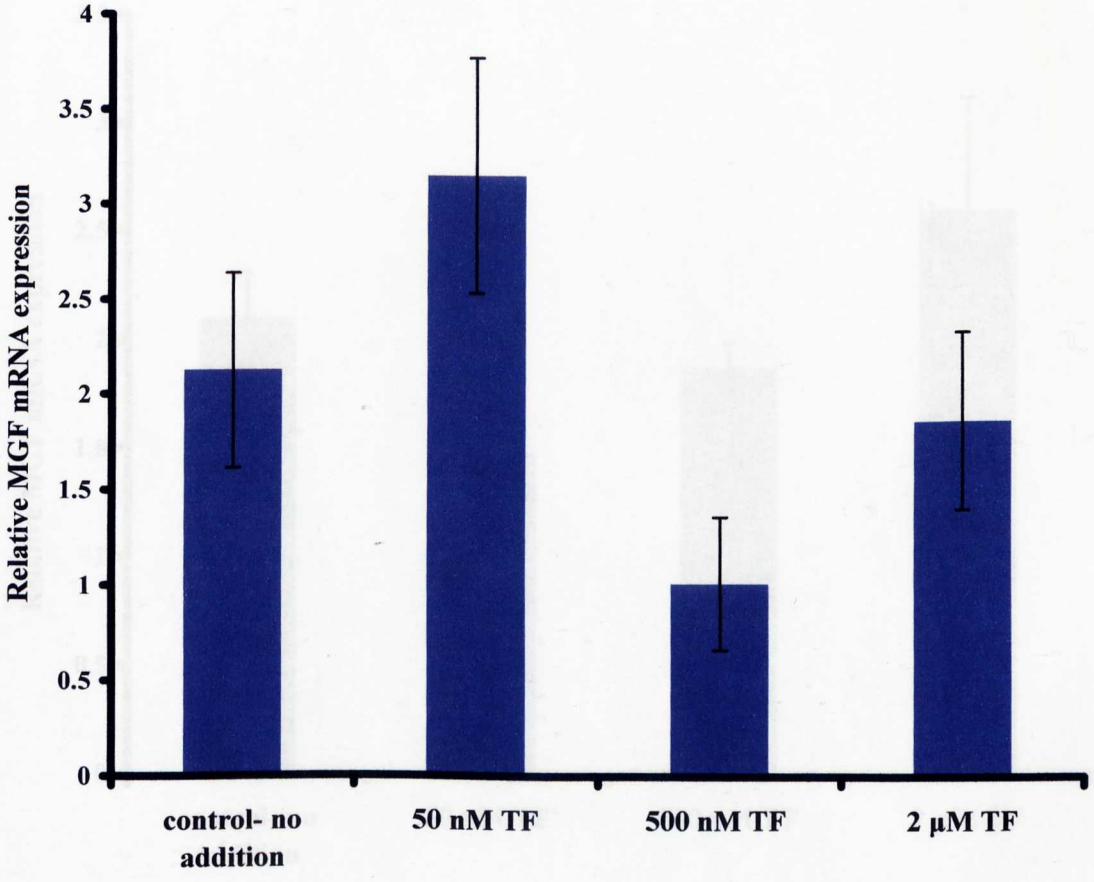

H9c2 cells were seeded out in wells at 2 x10^5/well and treated with different concentrations of exogenous TF (50 nM, 500 nM and 2µM) in the presence of serum. The cells were harvested 24 h post-treatment. Total RNA was extracted and a single tube RT-PCR was performed for MGF mRNA expression against GAP3DH as reference. The band intensities were quantified using the "Gene Tool" software program. The data represent the mean of n= 12 taken from two separate experiments, each performed in duplicate ± SEM.

Figure 4.15: The relative expression of MGF mRNA in H9c2 rat cardiomyocytes in response to treatment with exogenous TF 3 days post-treatment.

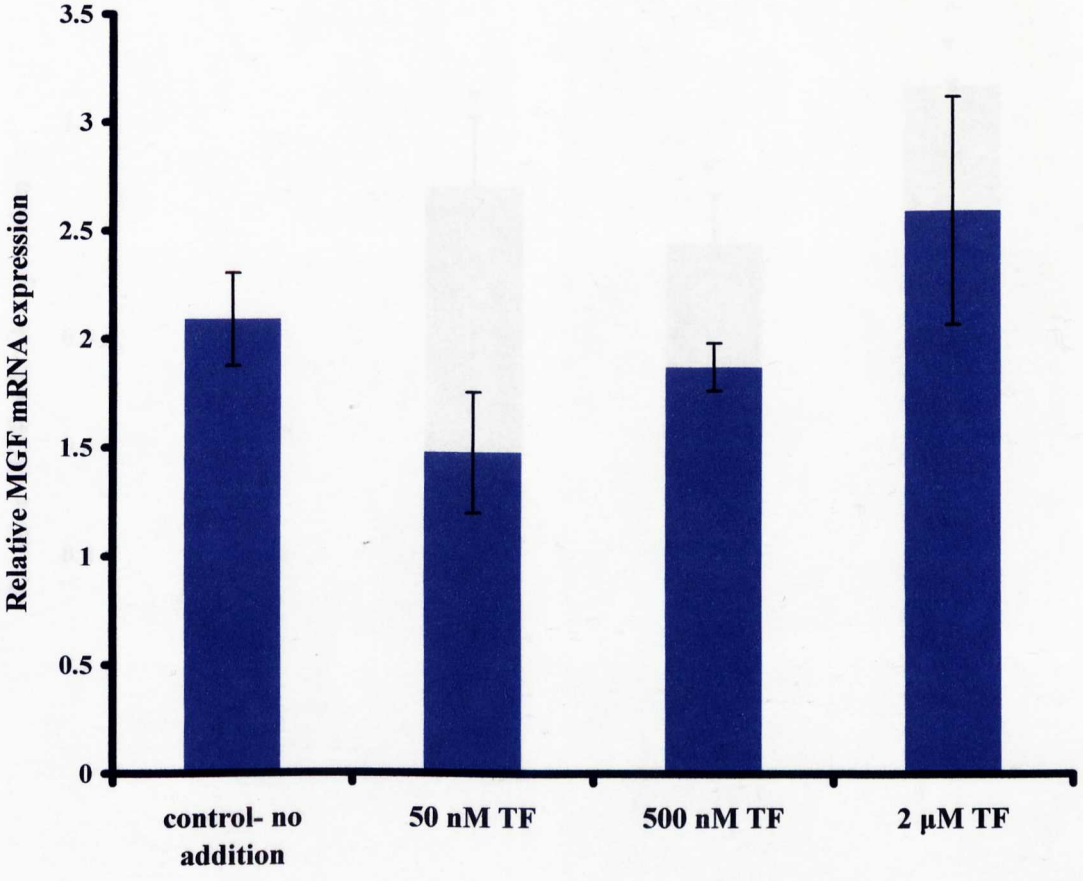

H9c2 cells were seeded out in wells at 2 x10^5/well and treated with different concentrations of exogenous TF (50 nM, 500 nM and 2 μM) in the presence of serum. The cells were harvested 72 h post-treatment. Total RNA was extracted and a single tube RT-PCR was performed for MGF mRNA expression against GAP3DH as reference. The band intensities were quantified using the "Gene Tool" software program. The data represent the mean of n= 12 taken from two separate experiments, each performed in duplicate ± SEM.

Figure 4.16: The relative expression of MGF mRNA in H9c2 rat cardiomyocytes in response to treatment with exogenous TF 7 days post-treatment.

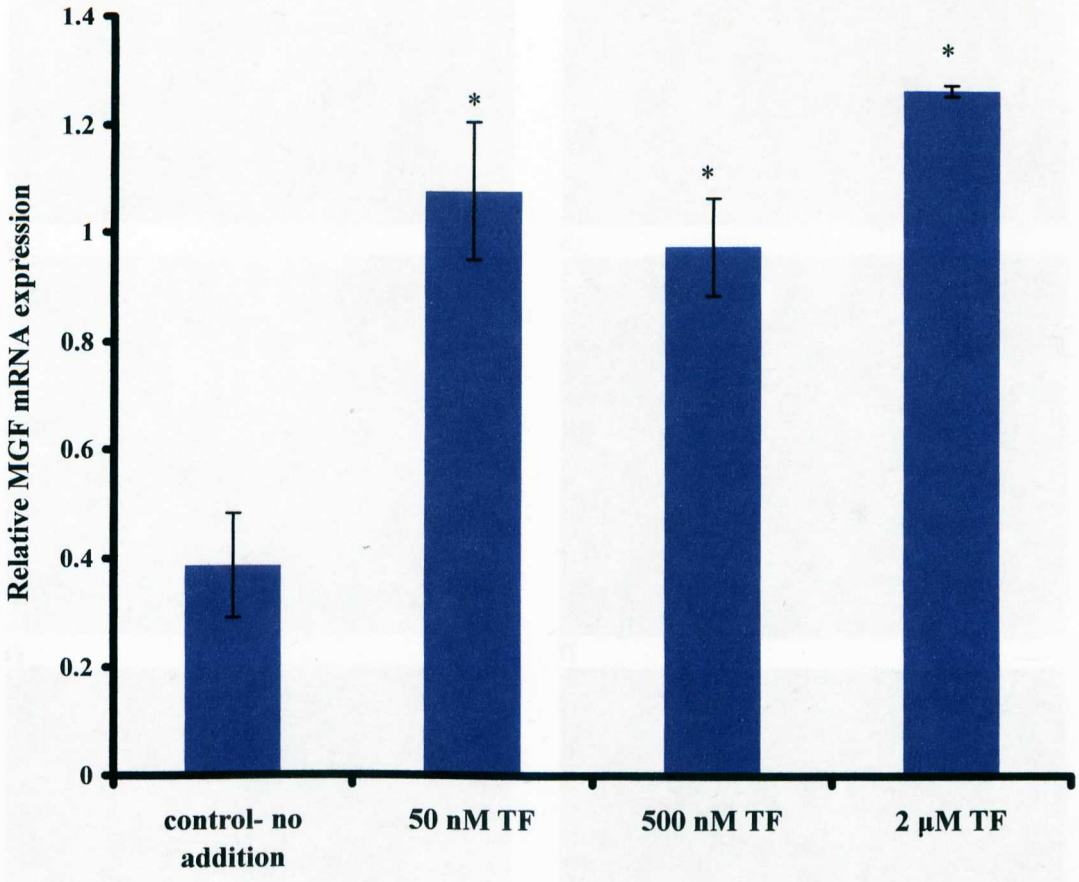

H9c2 cells were seeded out in wells at 2 x10^5/well and treated with different concentrations of exogenous TF (50 nM, 500 nM and 2 µM) in the presence of serum. The cells were harvested 168 h post-treatment. Total RNA was extracted and a single tube RT-PCR was performed for MGF mRNA expression against GAP3DH as reference. The band intensities were quantified using the "Gene Tool" software program. The data represent the mean of n= 12 taken from two separate experiments, each performed in duplicate ± SEM.

* $p<0.05$ as compared to the control

Figure 4.17: The expression of MGF antigen in H9c2 rat cardiomyocytes in response to treatment with exogenous TF 1 day post-treatment.

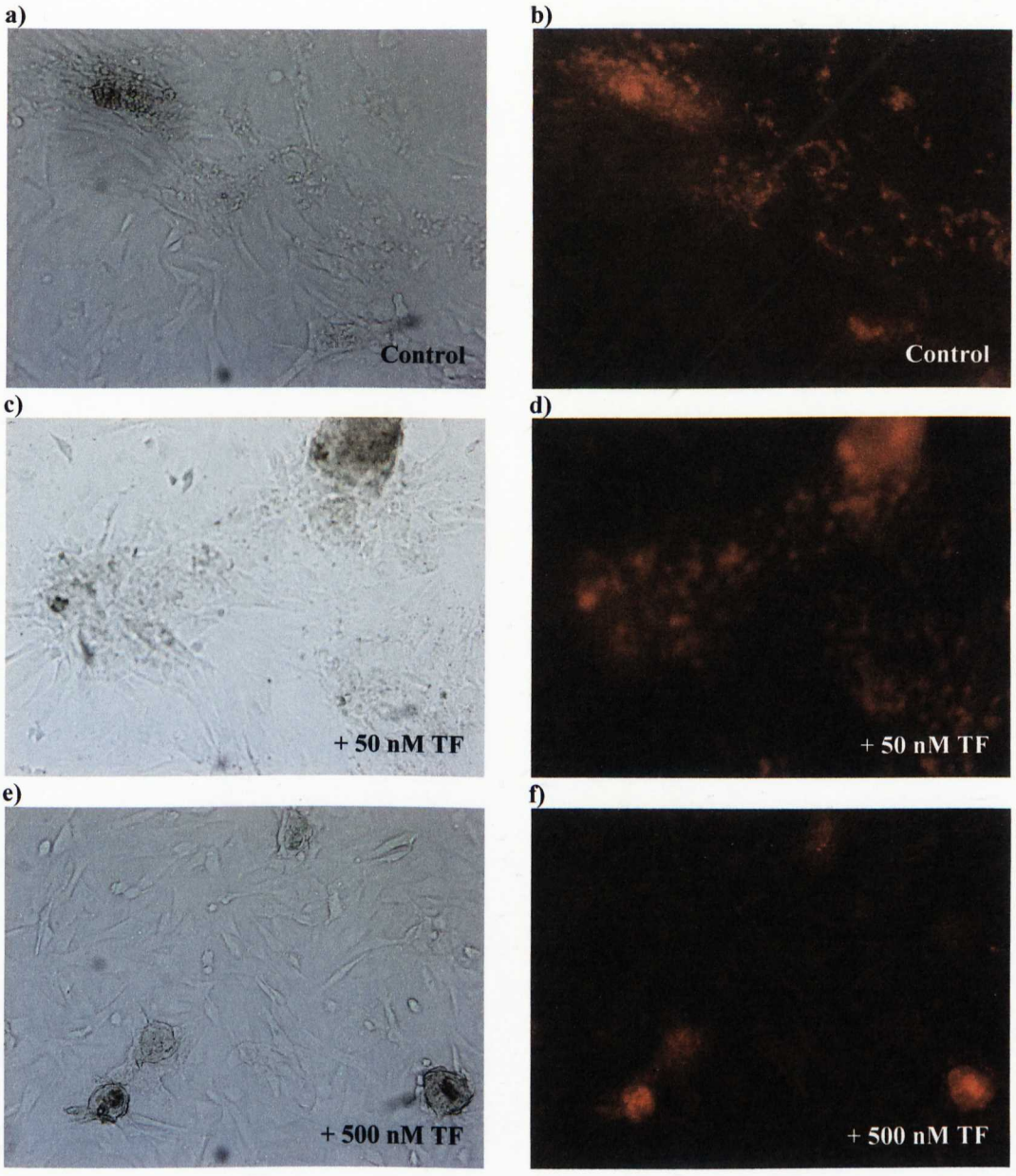

H9c2 cardiomyocytes were seeded out into an 8 well chamber slide at a density of 10^5 cells/well in complete DMEM medium and treated with 50 nM or 500 nM TF. Cells were cultured for 3 days and then stained for MGF antigen with a rabbit anti human MGF antibody. Images were captured and analysed with ImagePro software using a Leica fluorescence microscope. a) control H9c2 cells under white light, b) control H9c2 cells stained for MGF, c) H9c2 cells treated with 50 nM TF under white light, d) H9c2 cells treated with 50 nM TF stained for MGF, e) H9c2 cells treated with 500 nM TF under white, f) H9c2 cells treated with 500 nM TF stained for MGF. The micrographs are representative of 3 separate experiments performed in duplicate (Magnification x 10).

Figure 4.18: The expression of MGF antigen in H9c2 rat cardiomyocytes in response to treatment with exogenous TF 7 days post-treatment.

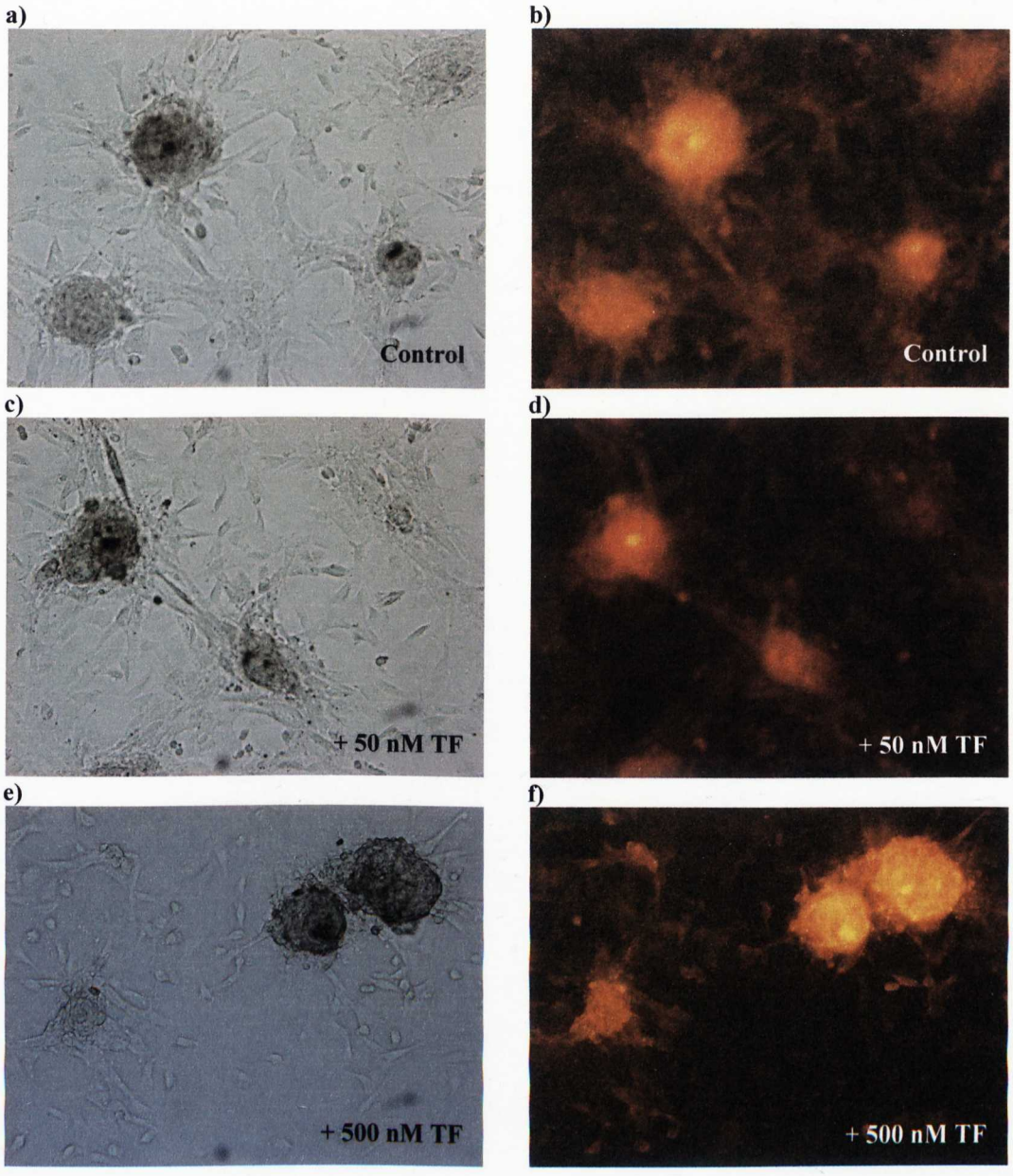

H9c2 cardiomyocytes were seeded out into an 8 well chamber slide at a density of 10^5 cells/well in complete DMEM medium and treated with 50 nM or 500 nM TF. Cells were cultured for 7 days and then stained for MGF antigen with a rabbit anti human MGF antibody. Images were captured and analysed with ImagePro software using a Leica fluorescence microscope. a) control H9c2 cells under white light, b) control H9c2 cells stained for MGF, c) H9c2 cells treated with 50 nM TF under white light, d) H9c2 cells treated with 50 nM TF stained for MGF, e) H9c2 cells treated with 500 nM TF under white, f) H9c2 cells treated with 500 nM TF stained for MGF. The micrographs are representative of 3 separate experiments performed in duplicate (Magnification x 10).

Figure 4.19: The expression of MGF antigen in H9c2 rat cardiomyocytes in response to treatment with exogenous TF 14 days post-treatment.

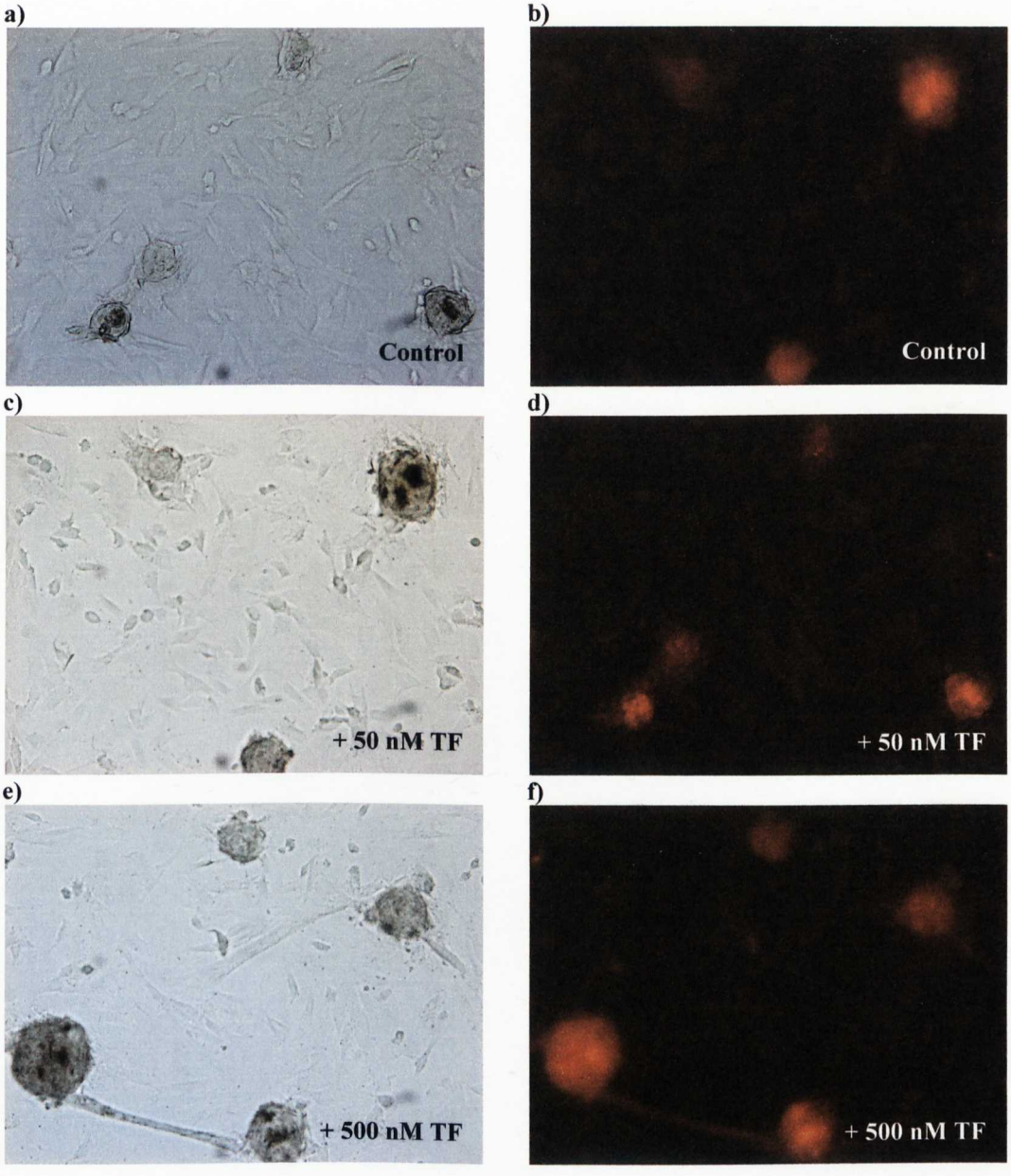

H9c2 cardiomyocytes were seeded out into an 8 well chamber slide at a density of 10^5 cells/well in complete DMEM medium and treated with 50 nM or 500 nM TF. Cells were cultured for 14 days and then stained for MGF antigen with a rabbit anti human MGF antibody. Images were captured and analysed with ImagePro software using a Leica fluorescence microscope. a) control H9c2 cells under white light, b) control H9c2 cells stained for MGF, c) H9c2 cells treated with 50 nM TF under white light, d) H9c2 cells treated with 50 nM TF stained for MGF, e) H9c2 cells treated with 500 nM TF under white, f) H9c2 cells treated with 500 nM TF stained for MGF. The micrographs are representative of 3 separate experiments performed in duplicate (Magnification x 10).

Figure 4.20: Negative control for MGF antigen expression in H9c2 rat cardiomyocytes using only secondary antibody.

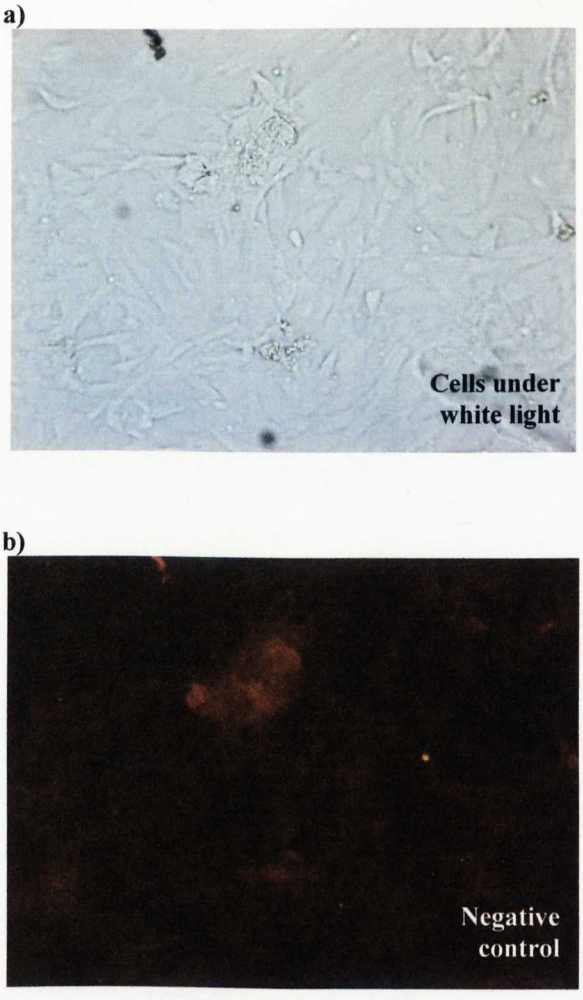

H9c2 cardiomyocytes were seeded out in an 8 well chamber slide at a density of 1 x 10^5 cells/well in complete DMEM medium. Cells were cultured for 3, 7 and 14 days and then stained for MGF antigen with a rabbit anti human MGF antibody. Images were captured and analysed with ImagePro software using a Leica fluorescence microscope. Micrograph a) H9c2 cells under white light, micrograph b) H9c2 cells stained only with secondary antibody. The micrographs are representative of 3 separate experiments performed in duplicate (Magnification x 10).

4.3.4 Expression of nMHC following long-term treatment with TF

H9c2 cells were stained for neonatal myosin heavy chain over a period of 7 days. The absence of any fluorescence labelling on either day of the investigation (day 1, 3 and 7), indicates the lack of expression of the neonatal heavy chain antigen in the cells.

4.3.5 Expression of sMHCβ following long-term treatment with TF

H9c2 cells exhibited a strong red fluorescence labelling for sMHCβ, on spheroid aggregates with weaker labelling on cell cluster on all days tested (Figure 4.21, 4.22 and 4.23). By day 1 cells treated with exogenous TF (50 nM and 500 nM), gave enhanced fluorescence labelling compared to the control (untreated cells) (Figure 4.21). By day 3, H9c2 cells treated with 50 nM of TF produce higher fluorescence label intensity (Figure 4.22d) than H9c2 cells treated with 500 nM of TF (Figure 4.22f). However, the fluorescence labelling in the treated samples was weaker than the control cells, (Figure 4.22b, 4.22d and 4.22f). By day 7, no significant differences were observed between untreated control cells and treated cells (Figure 4.23b, 4.23d and 4.23f). However, H9c2 cells treated with 50 nM of TF produced weaker fluorescence intensity on day 7 as compared to day 3 (Figure 4.22d and 4.23d). Furthermore, the cells incubated with 500 nM of TF exhibited more intense fluorescence by day 7 as compared to day 3 of the investigation (Figure 4.22f and 4.23f). Compared to day 1, fluorescence intensity was weaker on the subsequent days in all the samples (Figure 4.21, 4.22 and 4.23). Further analysis with the Image Pro Plus software showed no significant difference. A negative control was produced on each step of the investigation using only secondary antibody and no fluorescence labelling was observed (Figure 4.24a). Additionally, a positive control stained for sMHC was obtained by staining a rat heart section in each sample alongside (Figure 4.24b).

Figure 4.21: The expression of sMHCβ antigen in H9c2 rat cardiomyocytes in response to treatment with exogenous TF 1 day post-treatment.

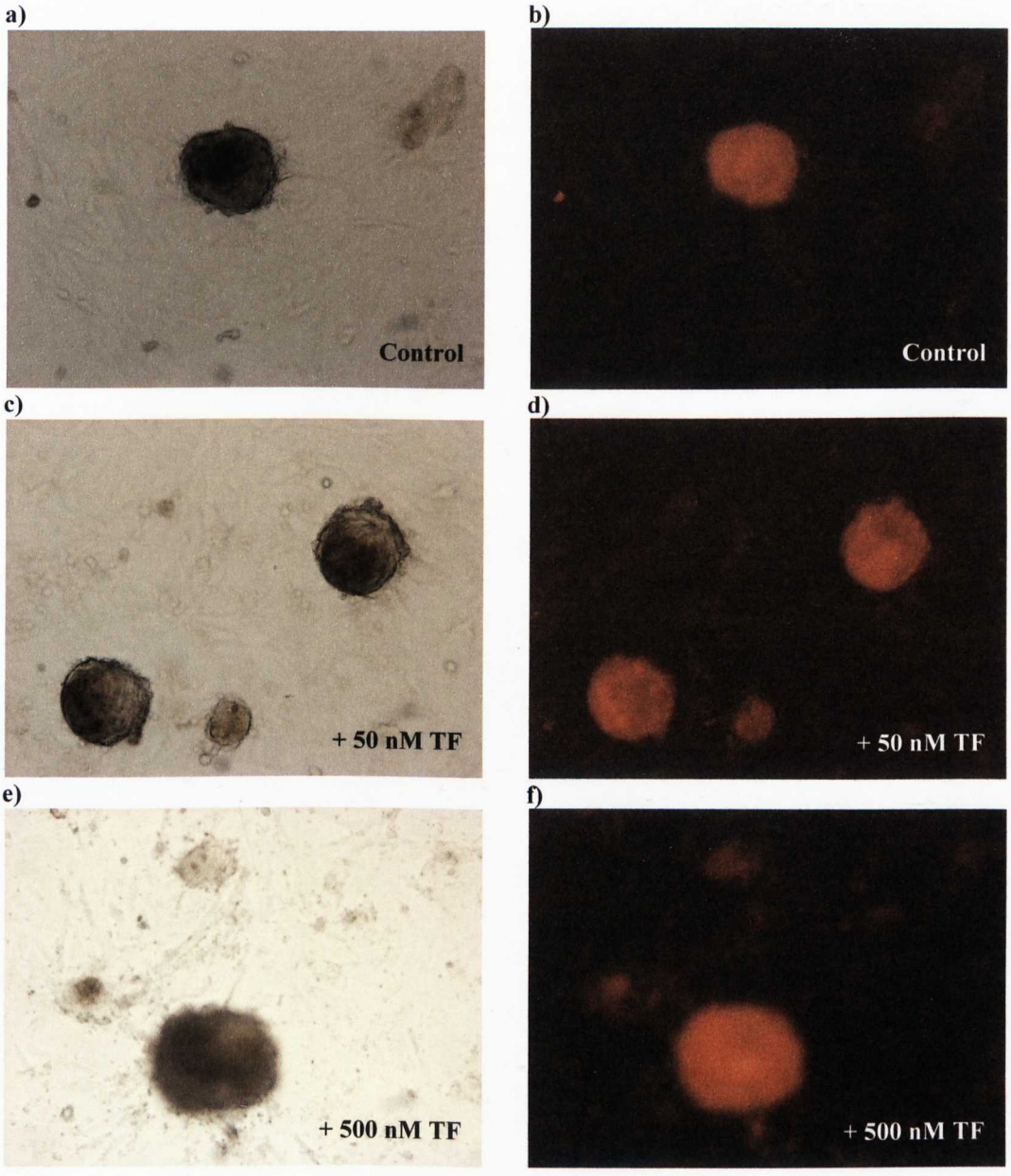

H9c2 cardiomyocytes were seeded out in an 8 well chamber slide at a density of 10^5 cells/well in complete DMEM medium and treated with 50 nM and 500 nM TF. Cells were cultured for 1 day and then stained for sMHCβ antigen with a mouse anti human sMHCβ antibody. Images were captured and analysed with ImagePro software using a Leica fluorescence microscope. Left micrographs show cells under white light microscopy and right micrographs show cells under fluoresence microscopy stained for sMHCβ. a) control H9c2 cells, b) control H9c2 cells, c) H9c2 cells treated with 50 nM TF, d) H9c2 cells treated with 50 nM TF, e) H9c2 cells treated with 500 nM TF, f) H9c2 cells treated with 500 nM TF. The micrographs are representative of 3 separate experiments performed in duplicate (Magnification x 10).

Figure 4.22: The expression of sMHCβ antigen in H9c2 rat cardiomyocytes in response to treatment with exogenous TF 3 days post-treatment.

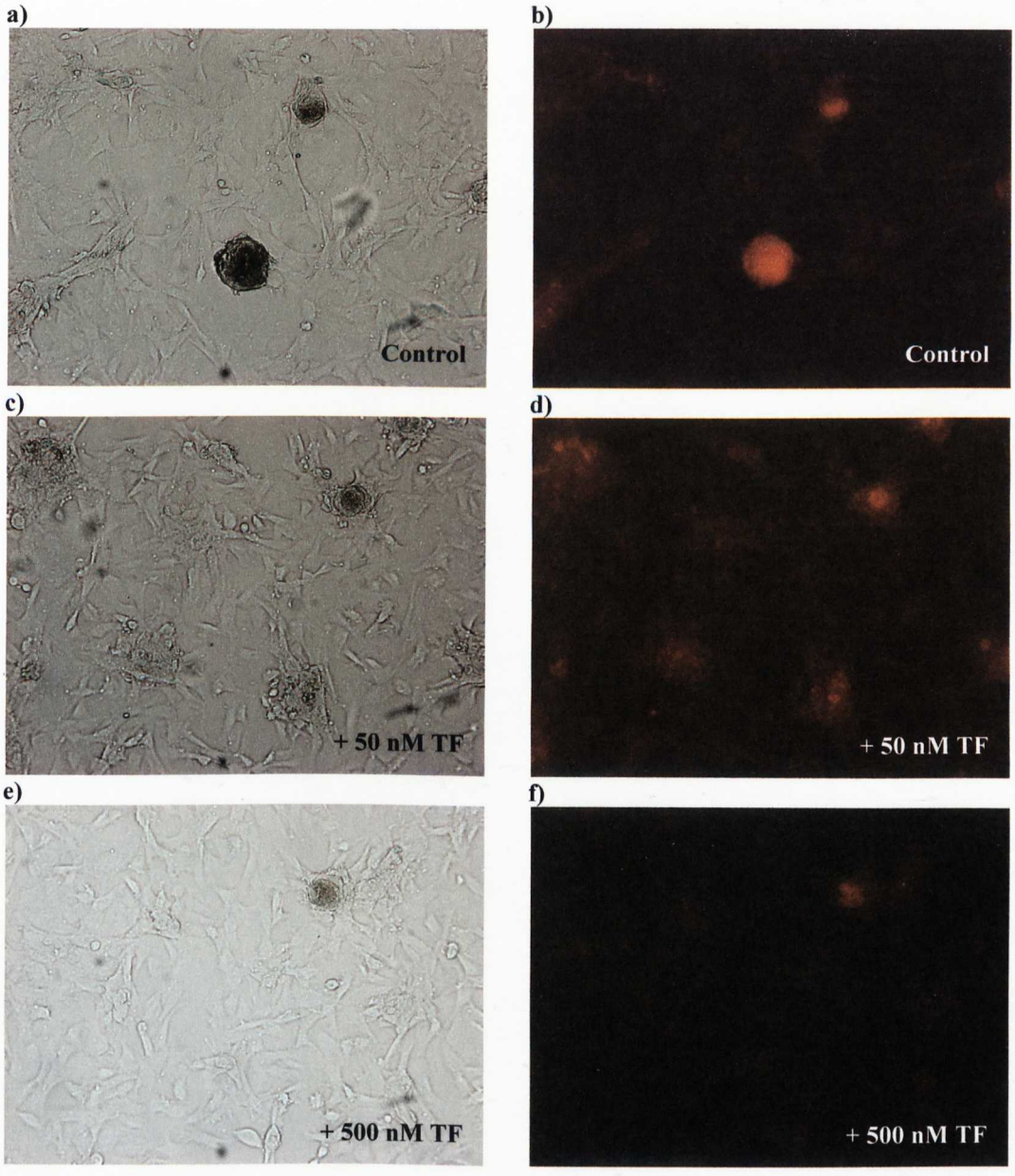

H9c2 cardiomyocytes were seeded out in an 8 well chamber slide at a density of 10^5 cells/well in complete DMEM medium and treated with 50 nM and 500 nM TF. Cells were cultured for 3 days and then stained for sMHCβ antigen with a mouse anti human sMHCβ antibody. Images were captured and analysed with ImagePro software using a Leica fluorescence microscope. Left micrographs show cells under white light microscopy and right micrographs show cells under fluoresence microscopy stained for sMHCβ. a) control H9c2 cells, b) control H9c2 cells, c) H9c2 cells treated with 50 nM TF, d) H9c2 cells treated with 50 nM TF, e) H9c2 cells treated with 500 nM TF, f) H9c2 cells treated with 500 nM TF. The micrographs are representative of 3 separate experiments performed in duplicate (Magnification x 10).

Figure 4.23: The expression of sMHCβ chain antigen in H9c2 rat cardiomyocytes in response to treatment with exogenous TF 7 days post-treatment.

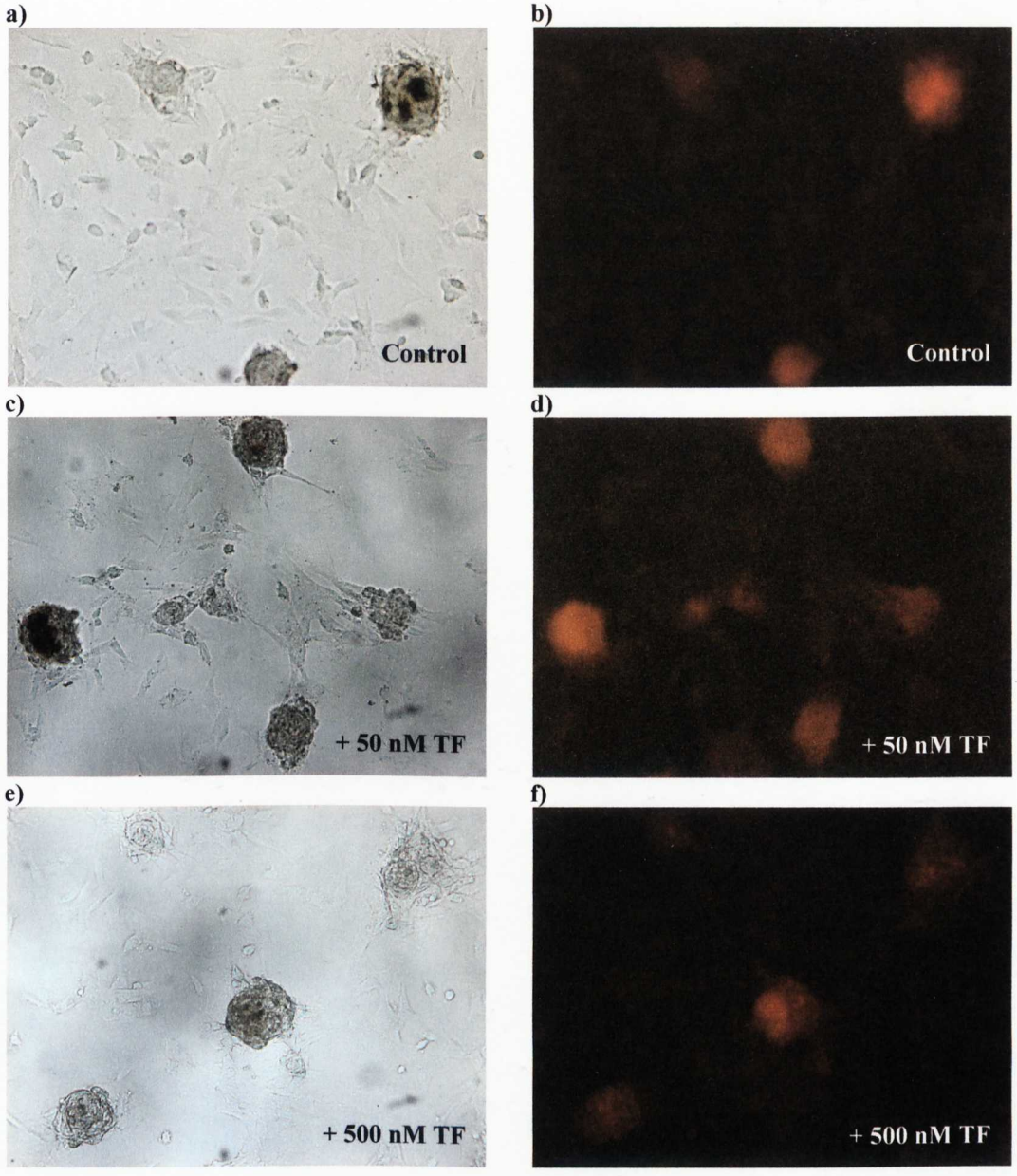

H9c2 cardiomyocytes were seeded out in an 8 well chamber slide at a density of 10^5 cells/well in complete DMEM medium and treated with 50 nM and 500 nM TF. Cells were cultured for 3 days and then stained for MHCβ antigen with a mouse anti human sMHCβ antibody. Images were captured and analysed with ImagePro software using a Leica fluorescence microscope. Left micrographs show cells under white light microscopy and right micrographs show cells under fluoresence microscopy stained for sMHCβ. a) control H9c2 cells, b) control H9c2 cells, c) H9c2 cells treated with 50 nM TF, d) H9c2 cells treated with 50 nM TF, e) H9c2 cells treated with 500 nM TF, f) H9c2 cells treated with 500 nM TF. The micrographs are representative of 3 separate experiments performed in duplicate (Magnification x 10).

Figure 4.24: Negative and positive control for sMHCβ antigen expression in H9c2 rat cardiomyocytes and rat heart section respectively.

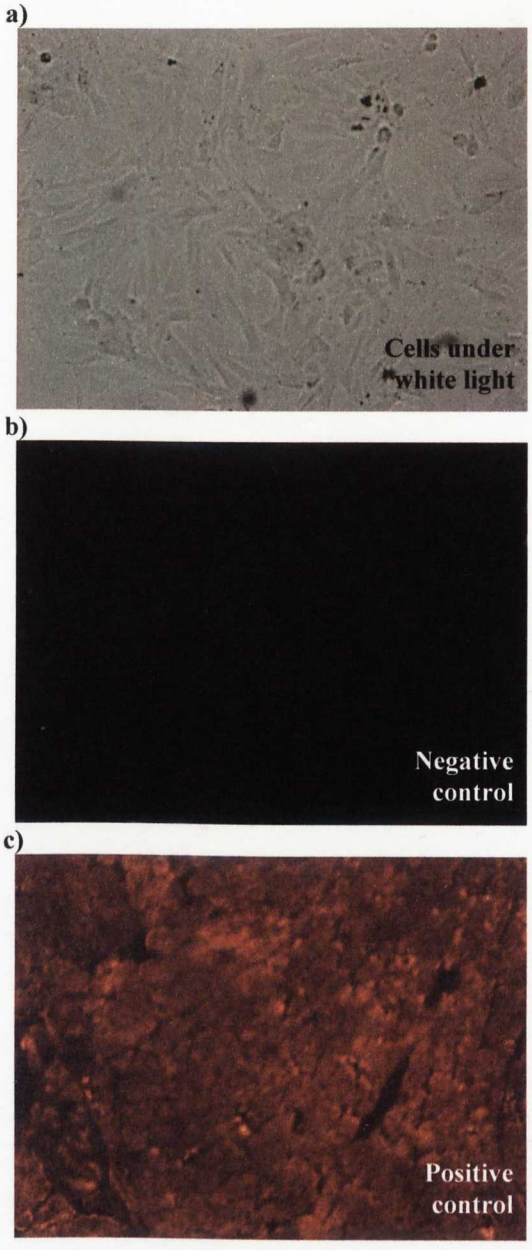

H9c2 cardiomyocytes were seeded out in an 8 well chamber slide at a density of 1 x 10^5 cells/well in complete DMEM medium. Cells were cultured for 3, 7 and 14 days and then stained for sMHCβ with a mouse anti human sMHCβ antibody. Images were captured and analysed with ImagePro software using a Leica fluorescence microscope. Micrograph a): H9c2 cells under white light, micrograph b): H9c2 cells stained only with secondary antibody, on each day of the investigation, micrograph c): is a section of rat heart stained positive for sMHCβ. The micrographs are representative of 3 separate experiments performed in duplicate (Magnification x 10).

4.4 Discussion

4.4.1 The influence of exogenous TF on ANF expression

ANF is known to be a marker of early hypertrophy in the heart (Braunwald & Bristow 2000). Furthermore, ANF is a stress-related hormone and is re-expressed in the ventricles during cardiac hypertrophy (Arai *et al.* 1988, Lee *et al.* 1988, Franch *et al.* 1988, Edwards *et al.* 1988, Day *et al.* 1987, Drexter *et al.* 1989). Over the years, the role of TF has been expanded and it has been suggested that TF can participate in the pathophysiology of heart disease including cardiac hypertrophy (Toomey *et al.* 1996, Bugge *et al.* 1996, Carmeliet *et al.* 1996, Parry *et al.* 1998, Pwlinski *et al.* 2002, Luther *et al.* 2000, Muller *et al.* 2000). The present study aimed to examine the effects of exogenous TF on the induction of cardiac hypertrophy by measuring ANF expression. For this purpose, the H9c2 cardiomyocytic cell line was used instead of freshly prepare adult cardiomyocytes as adult cardiomyoctes de-differentiate after 4 days in culture (data are not shown) and thus can cause changes in gene expression. In addition, collagenase digestion is aggressive leading to low cell yield, low viability and membrane damage, interfering with the experimental protocols (Thum & Borlak 2000). It was shown that either TF alone or in combination with serum factors, was able to increase the expression of ANF (150 % of the control) 1 day post treatment (Figure 4.4) but after 2 days, the ANF expression was decreased to below that of the control (Figure 4.4). The pattern of expression of ANF protein was similar to that observed for ANF mRNA expression (Figure 4.6). These data suggest that TF can increase ANF expression which is a marker of hypertrophic response in H9c2 cells.

TF belongs to the interferon receptor family and is an immediate early gene and is expressed during foetal life, suggesting its involvement in cell growth pathways (Taubman *et al.* 1997, Carmeliet & Collen 1998). Recently, it has been shown that TF triggers cell signalling via both protease dependent and independent mechanisms (Wiiger & Prydz 2001, Morrissey 2001). In the present study, incubation of cells with TF increased the expression of ANF under serum-free conditions, 1 day post treatment, whereas the inclusion of either FVIIa or both FVIIa and FXa, inhibited that effect (Figure 4.9 and 4.11). The expression of TF activity was specific to the proteolytic activity of these two enzymes as the inclusion of TFPI, known to inhibit both FVIIa and FXa, restored the TF-mediated ANF expression on the first day (Figure 4.9 and 4.11). It has been demonstrated that TF/FVIIa complex and FXa, can both activate protease-activated receptors 1 (PAR-1) and 2 (PAR-2) (Bromberg *et al.* 2001, Petersen *et al.* 2000, Steinberg 2005). These receptors are known to participate in the initiation of hypertrophic stimuli (Sabri *et al.* 2000, Moons *et al.* 2002). Therefore, the action of TF in combination with FVIIa and FXa may indicate the possible involvement of PARs. PARs belong to the family of G-protein-coupled receptors with a unique proteolytic activation mechanism (Streinberg, 2005). All of the members of PAR family, PAR 1-4 are widely expressed on platelets, cells of the vasculature and cardiomyocytes (Ossovskaya & Bunnet, 2004, Sabri *et al.* 2000). PAR-1 is mainly activated by thrombin and SFLLRN peptide agonist (Sabri *et al.* 2000) and has been identified as a hypertrophic stimulus, by triggering a range of events in cardiomyocytes including the activation of the extracellular signal-regulated protein kinase (ERK), the induction of atrial natriuretic factor expression and the modulation of calcium homeostasis (Steinberg *et al.* 1991, Jiang at al. 1996, Glembotski *et al.* 1993, Yasutake *et al.* 1996, Sabri *et al.* 2000). These events are

characteristic of the cardiomyocyte hypertrophic growth programme, i.e increase in protein content and cell size, increase in sarcomeric organization and induction of the immediate early genes (Streinberg 2004, Sabri *et al.* 2000). Alternatively, PAR-2 is activated by trypsin/tryptase and SLIGRL peptide (Steinberg 2005, Sabri *et al.* 2000), and recent studies have revealed that this receptor can also be activated by the SFLLRN agonist peptide (Sabri *et al.* 2000). Like PAR-1, PAR-2 activates a spectrum of biochemical and functional responses in cardiomyocytes. These responses include activation of ERK, and p38-MAPK, increase in $[Ca^{2+}]$, enhanced spontaneous automaticity and elongated/dilated hypertrophy (Sreinberg 2005, Sabri *et al.* 2000). Therefore collectively, PAR-1 and PAR-2 could alter the electrophysiological properties and contractile activity of myocytes sufficiently to induce myocyte hypertrophy (Sabri *et al.* 2000).

Although, the link between TF and the activation of PARs has been demonstrated in literature, the possible involvement of PAR-1 and 2 was not completed in this study. However an experiment to investigate the involvement of PAR-1 and 2 in ANF expression following TF treatment was designed involving the PAR-1 and PAR-2 inhibitory antibodies (WEDE-15 and ATAP-2 antibodies against PAR-1 and SAM-11 antibody against PAR-2). These antibodies were only functional for a few hours before being degraded, while the ANF expression by TF seemed to occur over a 24 h period (Figure 4.7). Therefore, due to the large quantity of the antibody required, the experiment to investigate the PAR-1 and 2 inhibition was not feasible.

In conclusion, TF can increase ANF expression *in vitro*. Furthermore, combination of TF with FVIIa or TF, FVIIa and FXa minimise ANF expression. However, the

addition of TFPI restores ANF expression possibly by inhibiting TF/FVIIa or TF/FVIIa/FXa complexes. Also, the action of TF in complex with purified supplemented FVIIa and FXa or those occurring naturally in serum (FCS) may be mediated through the activation of PAR 1 and 2. Therefore, during conditions such as infection or vascular inflammation, in which TF concentrations may be elevated, a hypertophic response may be initiated possibly via the activation of PARs.

4.4.2 The influence of exogenous TF on MGF expression

MGF is a spliced variant of IGF-1 and is only detectable following injury and/or mechanical activity in the muscles (Goldspink 2002). Furthermore, MGF has been found to act in an autocrine/ paracrine manner and is thought to be the end product of mechanotransduction signalling pathway in muscle cells (Goldspink 2002). In the present study, the involvement of TF in the expression of MGF mRNA in H9c2 cardiomyocytes was investigated. Cells treated with 50 nM TF, showed transient increases in MGF expression by day 7 (Figure 4.14, 4.15, 4.16) while the addition of 500 nM and 2 μM TF resulted in a more gradual increase in MGF expression to the final day of the investigation (Figure 4.14, 4.15, 4.16). These data suggest that the up-regulation of MGF by TF in H9c2 cells may occur in response to stress signals.

Previous studies have shown that in exercised muscles undergoing physiological hypertrophy, MGF expression is up-regulated (Goldspink *et al.* 1992, Yang *et al.* 1997). Also intramuscular injection of a plasmid, constructed to express the MGF cDNA, into mouse anterior muscle resulted in a 20 % increase in muscle mass was observed within 2 weeks of injection (Goldspink 2002). Experiments measuring muscle fibre size revealed a 25 % increase, which was due to the presence of larger

(width) fibres in the muscle treated with the plasmid and not in the surrounding muscle (Goldspink 2002). In these experiments, only some fibres take up and express the MGF cDNA and it appears that these fibres undergo hypertrophy (Goldspink 2002). The up-regulation of MGF following treatment with TF observed during the present study is in agreement with the aforementioned studies. Since Goldspink (2002), showed that muscle fibres expressing MGF cDNA have undergo hypertrophy, this provides an indirect link between TF and muscle hypertrophy.

Despite the data demonstrating the up-regulation of MGF mRNA by TF (Figure 4.14, 4.15 & 4.16), measurements of MGF antigen expression, in H9c2 cells incubated with TF were on the whole unsuccessful due to un-specific binding of the antibody. The H9c2 cardiomyocytes probed for MGF antigen, exhibited strong red fluorescence labelling on spheroid aggregates and weaker labelling on cell clusters (Figure 4.17, 4.18 and 4.19). However, similar red fluorescence intensity was produced on labelling the cells with only secondary antibody (Figure 4.20). The antibody against MGF used was an experimental polyclonal antibody provided by Professor G. Goldspink from Royal Free Hospital London was deemed not to be specific for MGF. Therefore, the up-regulation of MGF by antigen staining could not be confirmed by this procedure.

In conclusion, TF has been shown to up-regulate MGF expression, indicating that cells may possibly detect stress. Furthermore, MGF expression is known to be up-regulated following injury and during muscle hypertophy (Goldspink 2002). Thus the up-regulation of MGF by TF in H9c2 cardiomyocytes provides an indirect link between TF and a cardiac hypertrophy.

4.4.3 The influence of exogenous TF on sMHCβ expression

sMHCβ is prominent in the development of the embryonic heart (Stockdale *et al.* 2002). Study of the expression of the slow isoforms of the myosin heavy chain has contributed to our understanding of how cell diversity arises within skeletal and cardiac muscles (Stockdale *et al.* 2002, Franco *et al.* 2002) MHCβ isoforms are developmentally responsive to a number of signals provided by the nervous system, the endocrine system and, later in development, to functional demands on these developing tissues (Stockdale *et al.* 2002). Studies have shown that MHC transcripts were found to be homogeneously distributed in the myocardium of the tubular and embryonic heart of dogfish and rodents (Franco *et al.* 2002). A difference between atrial and ventricular MHC content (mRNA and protein) was also observed in the adult stage (Franco *et al.* 2002). The atrial myocardium versus the ventricular showed the highest MHC content in the adult heart in dogfish, mouse, rat, and chicken (Franco *et al.* 2002). MHCβ is known to be re-expressed and up-regulated in the ventricles during progressing hypertrophy (Braunwald & Bristow 2000, Pagani *et al.* 1988, Izumo *et al.* 1988). It has been suggested that the up-regulation of MHCβ in cardiac hypertrophy causes a decrease in the contractile cycle using less energy to initially compensate for the hypertrophic stress by normalising wall stress (Braunwald & Bristow 2000). However, the slow type of the myosin heavy chain β (sMHCβ) has been reported to be unchanged in the hypertrophic human ventricle (Schaub *et al.* 1998). In this study, any alterations in the expression of the sMHCβ in H9c2 cardiomyocytes, upon treatment with exogenous TF, were investigated. The existence of sMHCβ was confirmed in the H9c2 cells by the strong fluorescence signal in both treated and untreated cells on all the days of the investigation (Figures 4.21, 4.22 & 4.23). The third day of the investigation, cells treated with 50 nM TF produced

stronger fluorescence signal compared to those treated with 500 nM TF, but both samples appeared to have less sMHCβ when compared to the untreated control cells (Figure 4.22). Nevertheless the sMHCβ existence on day 7 was more prominent when compared to day 3 and day 1 of the investigation in all samples (Figures 4.21, 4.22 & 4.23). Although, small differences between the days of the investigation and between the control and treated cells were observed, these differences were not significant. Therefore, these data are in agreement with the study by Schaub *et al.* (1998) and suggests that TF has no effect in the expression of sMHCβ antigen in H9c2 cells.

4.5 Conclusions

The aim of this chapter was to provide evidence that exogenous TF is capable of initiating some of the mechanisms involved in hypertrophic growth *in vitro*. TF can increase ANF expression *in vitro*. Furthermore, combination of TF with FVIIa and FXa suppresses ANF expression, whereas the addition of TFPI abolishes this effect. The action of TF with unknown serum factors existing in the media or in combination with FVIIa and FXa may be mediated by the activation of PAR-1 and 2. Moreover, TF was shown to up-regulate MGF expression indicating that the cells may possibly detect stress and thus a hypertrophic response could be initiated. Also, TF was found to have no effect on the expression of sMHCβ in H9c2 cells. Therefore, TF is capable of initiating a hypertrophic response in H9c2 cardiomyocytes signified by the up-regulation of ANF expression, and possibly through the up-regulation of MGF expression (Figure 4.25). Although these results have been obtained by *in vitro* studies, potentially they may reflect events occurring *in vivo* under conditions of either inflammation, infection or vascular injury.

Figure 4.25: A schematic model showing the possible capability of TF initiating a hypertrophic response.

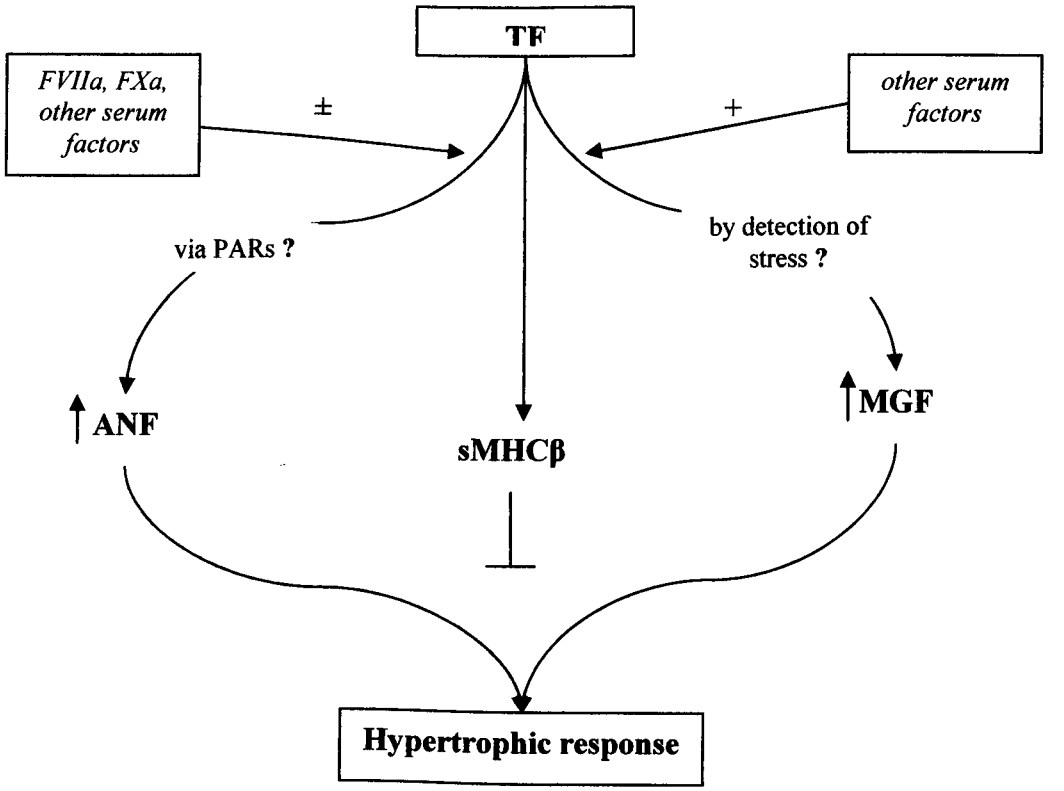

TF with or without FVIIa, FXa or other unknown serum factors that exist in media, can increase ANF expression in H9c2 cells, possibly via PARs activation, initiating a hypertrophic response. TF with other serum factors, up-regulates MGF expression possibly by the detection of injury from H9c2 cells, initiating a hypertrophic response. TF has no effect on the expression of slow myosin heavy chain (sMHCβ) and therefore a hypertrophic response is not initiated.

CHAPTER 5

The influence of exogenous Tissue Factor on the induction of proliferation and apoptosis in H9c2 cardiomyocytes *in vitro*

5. The influence of exogenous Tissue Factor on the induction of proliferation and apoptosis in H9c2 cardiomyocytes *in vitro*

5.1 Introduction

Cardiac hypertrophy results from the enlargement of pre-existing myocytes (Nadal-Ginard *et al.*, 2003). During the onset of heart disease and throughout the aging process, the rate of cell death increases (Nadal-Ginard *et al.* 2003). As a result, the number of cardiomyocytes decrease and consequently residual cells undergo hypertrophy and cellular remodelling (Nadal-Ginard *et al.* 2003). Therefore, even a moderate rate of myocyte death cause an imbalance in the heart leading to decrease in cardiac mass, remodelling of the myocardium and ultimately to chronic heart failure (Nadal-Ginard *et al.* 2003, Takemura & Fujiwara 2004).

Myocyte death can occur either via necrosis or apoptosis. On a cellular level, induction of apoptosis can be mediated either via the death receptors pathways or via the mitochondrial pathway (Figure 1.6, section 1.2.1) (Kang *et al.* 2004). The death receptor mediated pathway, also known as the extrinsic pathway, involves the binding of a death ligand such as tumour necrosis factor (TNF) to a membrane-bound death receptor, tumour necrosis factor receptor 1 (TNFR1), resulting in the activation of caspase-8 (Figure 1.6, section 1.2.1) (Nagata 1997, Takemura & Fujiwara 2004, Kang *et al.* 2004). The mitochondrial-mediated pathway, also known as the intrinsic pathway, is initiated by cellular injury or free radicals production causing the release of cytochrome c from mitochondria (Liu *et al.* 1996). Once released, cytosolic cytochrome c binds to the apoptotic protease-activating factor 1 (Apaf-1) and caspase-

9 to form an active apoptosome complex (Figure 1.6, section 1.2.1) (Li *et al.* 1997, Zou *et al.* 1997). Both these pathways activate downstream effector caspases, such as caspase-3, which eventually bring about the biochemical and structural changes observed during apoptosis (Li *et al.* 1997, Slee *et al.* 1999).

Tissue Factor (TF) is a known marker, and a suggested putative modulator of cellular signalling during apoptosis. TF signalling pathways requires FVIIa to be active so as to elicit a variety of cellular signalling events (Camerer *et al.*, 2000, Riewald and Ruf 2002). Several studies have shown that TF signalling pathways involves the mitogen activated protein kinase (MAP kinase) pathway, predominately the p44/p42 (ERK 1), the p38 pathway and JNK/SAPK pathway as well other pathways including the Src-like kinases, small GTPases and calcium signalling (Poulsen *et al.* 1998, Versteeg *et al.* 2001). These signalling pathways are known to be involved in the induction of cellular apoptosis (Han *et al.* 2004) as well as cell growth (Peppelenbosch *et al.* 2001). However, to date, it is not clear if TF alone can either mediate or induce cellular apoptosis. Studies on the coagulation factors downstream from TF, including FVIIa and FXa, have demonstrated the ability of these proteases to inhibit apoptosis in BHK cells over-expressing TF (Versteeg *et al.* 2004). Additionally, the TF inhibitor TFPI, has been shown to induce apoptosis in cultured human endothelial cells (Hamuro *et al.* 1998).

Cellular apoptosis occurs in heart tissue during cardiac hypertrophy and ageing. Although, TF in combination with FVIIa and FXa is capable on inhibiting apoptosis and promote cellular growth, the role of TF itself is less clear. The aim of this study was to investigate the influence of exogenous TF on promoting proliferation and

apoptosis in H9c2 cardiomyocytes, *in vitro*. Furthermore, the possible involvement of the associated downstream coagulation proteins, FVIIa, FXa and its inhibitor TFPI on these cellular events was also investigated for comparison.

5.2 Methods

5.2.1 Long-term influence of TF on proliferation and apoptosis

H9c2 cells were cultured as described in section 2.2.1.1 and grown until 80 % confluent. Subsequently, cells were sub-cultured as described in section 2.2.1.2, and seeded out (5 x 10^4 per well) into complete DMEM in a 24-well plate. The cells were allowed to adhere overnight and were then adapted to serum-free medium over the following 3 days as described in section 4.2.2. The cells were incubated continuously with exogenous recombinant TF (50 nM, 500 nM and 2 μM) which was supplemented over a period of 10 days. The rate of cell proliferation was measured on days 1, 3, 5, 7 and 10 as previously described in section 2.2.6.1, against a positive control containing 2 μM of anisomycin (known to induce apoptosis).

In a separate experiment, H9c2 cells were seeded out (6 x 10^4 per well) in complete DMEM medium containing 10% (v/v) foetal calf serum, 1% (v/v) antibiotic solution, 4 mM Ala-Glu solution, in a 6-well plate and allowed to adhere overnight. The cells were adapted to serum-free medium as described above and incubated continuously with a range of concentrations of exogenous recombinant TF (50 nM, 500 nM and 2 μM) which was supplemented over a period of 10 days. The extent of apoptosis was detected using a commercially available caspase-3 assay for flow cytometry on days 1, 3, 5, 7 and 10 against a positive control containing cells treated with 2 μM of

hydrogen peroxide (H_2O_2) (a known chemical that induces apoptosis via the caspase-3 pathway) for 4 h on each day of the experiment.

5.2.1.1 Long-term influence of TF in combination with FVIIa, FXa and TFPI on apoptosis

H9c2 cells were seeded out (6 x 10^4 per well) into a 6-well plate and adapted to serum free media as described in section 5.2.1. The cells were treated continuously with exogenous recombinant TF (50 nM) in combination with FVIIa (5 nM), FXa (10 nM) and TFPI (5 pM) which was supplemented over a period of 5 days. The degree of apoptosis was assessed by measuring the caspase-3 on days 1 and 5 as previously described (section 5.2.1).

5.2.2 Short-term influence of TF on proliferation and apoptosis

H9c2 cells were seeded out (5 x 10^4 per well) into a 24 well-plate and adapted to serum-free media as described in section 5.2.1. The cells were treated with a range of concentration of TF (50 nM, 500 nM and 2 μM) for 1 or 2 h. The medium was then discarded, the cells were washed with pre-warmed PBS and fresh serum-free medium was added. The cells were incubated in a humidified incubator at 37 °C under 5 % CO_2 for 10 h or 24 h and the rate of proliferation was measured, as previously described (section 2.2.6.1).

In a separate experiment H9c2 cells were seeded out (3 x 10^4 per well) into an 8 well culture slide and adapted to serum-free media. The cells were then treated with a range of TF concentrations (50 nM, 500 nM and 2 μM) for 1 or 2 h. The medium was then discarded, replaced with fresh serum-free medium and the cells were incubated

for a further 24 h. The level of apoptosis was then measured using a commercially available TUNEL assay (section 2.2.7.1).

A third set of cells were seeded out (3 x 10^4 per well) into an 8 well culture slide and adapted to serum-free media. The cells were then incubated with a range of concentrations of exogenous recombinant TF (50 nM, 500 nM and 2 μM) for 2 days. The cells were analysed by antibody staining for p53 activation on day 1 and 2 as previously described (section 2.2.7.3).

5.2.3 Short-term influence of TF with or without FVIIa, FXa and TFPI on proliferation and apoptosis

H9c2 cells were seeded out (5 x 10^4 per well) into a 24 well-plate and adapted to serum-free media as described in section 5.2.1. The cells were incubated with TF (50 and 500 nM) in combinations with FVIIa (5 nM), FXa (10 nM) and TFPI (5 pM). The cells were then incubated in a humidified incubator at 37 °C under 5 % CO_2 for 10 h or 24 h and the rate of proliferation was measured, as previously described (section 2.6.1).

In a separate experiment, H9c2 cells were seeded out (3 x 10^4 per well) into an 8 well culture slide and adapted in serum free media. The cells were then treated with TF (50 and 500 nM) in combinations with FVIIa (5 nM), FXa (10 nM) and TFPI (5 pM), incubated for 24 h and the level of apoptosis was measured using a commercially available TUNEL assay.

5.3 Results

5.3.1 The rate of proliferation and apoptosis following long-term treatment with TF

On day 1, exposure of the cells to 50 nM of TF significantly reduced the viability ($p<0.05$) by Δ= -25 % while higher concentrations of TF (500 nM and 2 μM) significantly reduced the cell viability ($p<0.05$) by Δ= -60 % and Δ= -70 % of the control respectively (Figure 5.1). By the third day, incubation of cells with 50 nM TF recovered the cell number to 95 % of the control whereas in the two higher concentrations of TF used (500 nM and 2 μM) the cell viability remained in the same level as day 1 (Figure 5.1). By day 5, sustained treatment with recombinant exogenous TF (50 nM) resulted in an increase in cell viability by Δ= +35 % (Figure 5.1). Also increases in cell viability were observed in the cells treated with the higher concentrations of TF (500 nM and 2 μM), reaching 80 % and 50 % of the control respectively (Figure 5.1). Thereafter, a progressive significant decline ($p<0.05$) in cell viability was observed in the cells treated with the higher concentrations of TF (500 nM and 2 μM) dropping to 5 % of the control on day 10 of the investigation (Figure 5.1). In the cells incubated with 50 nM TF a reduction in relative cell viability was observed on day 7 (95 % of the control) which again significantly increased ($p<0.05$) to 125 % of the control by the end of the investigation (Figure 5.1). Incubation with 2 μM of anisomycin (positive control) resulted in a reduction in cell viability to 50 % of the control on the first day and no viable cells were detected by day 3 (data not shown).

Figure 5.1: Viability of H9c2 rat cardiomyocytes following treatment with exogenous TF.

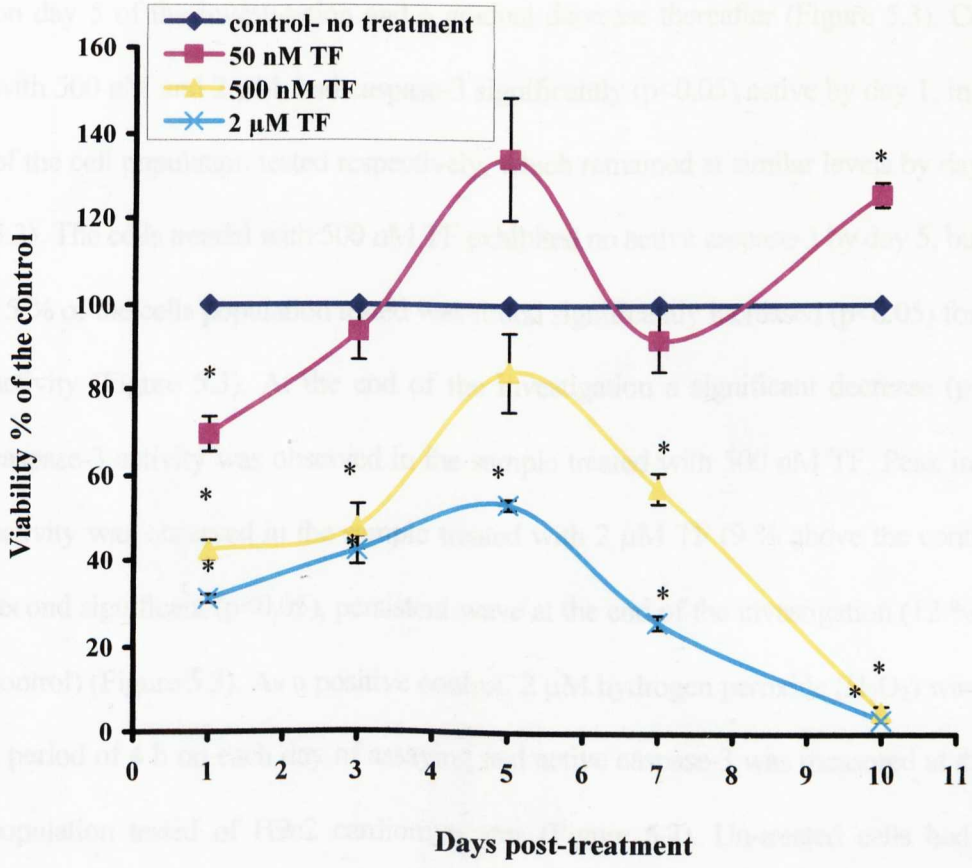

H9c2 cells were seeded out into wells at 5 x10^4/well in complete DMEM medium, adapted to serum-free medium over 4 days and incubated with 50 nM of TF (■), 500 nM of TF (▲) and 2 µM of TF (×), respectively. Cell proliferation was assessed on days 1, 3, 5, 7 and the values converted into cell numbers according a standard curve (Figure 2.6). The data represent the mean of n=9 taken form 3 separate performed in triplicate and are presented as the percentage of the control (un-treated cells) ± SEM.

* $p<0.05$ treated cells versus un-treated cells (control)

The rate of apoptosis in H9c2 cells was assessed using a flow cytometric assay for caspase-3 activity. Caspase-3 activity was detectable in the samples incubated with exogenous TF on day 1 of the investigation (Figure 5.2). In cells treated with 50 nM TF, initially (day 1) caspase-3 was significantly active ($p<0.05$) at 5 % of the cell population, with a second pick on day 5 of the investigation and a gradual decrease thereafter (Figure 5.3). Cells treated with 500 nM and 2 μM, had caspase-3 significantly ($p<0.05$) active by day 1, in 2 and 1 % of the cell population tested respectively, which remained at similar levels by day 3 (Figure 5.3). The cells treated with 500 nM TF exhibited no active caspase-3 by day 5, but on day 7, 15 % of the cells population tested was found significantly increased ($p<0.05$) for caspase-3 activity (Figure 5.3). At the end of the investigation a significant decrease ($p<0.050$) in caspase-3 activity was observed in the sample treated with 500 nM TF. Peak in caspase-3 activity was observed in the sample treated with 2 μM TF (9 % above the control) with a second significant ($p<0.05$), persistent wave at the end of the investigation (12 % above the control) (Figure 5.3). As a positive control, 2 μM hydrogen peroxide (H_2O_2) was used over a period of 4 h on each day of assaying and active caspase-3 was measured at 45 % of the population tested of H9c2 cardiomyocytes (Figure 5.2). Un-treated cells had no active caspase-3 throughout the period of the investigation (Figure 5.3).

5.3.1.1 The activity of caspase-3 following long-term treatment with TF in combination with FVIIa/FXa/TFPI

No caspase-3 activity was detectable in H9c2 cells following incubation of TF (50 nM) in combinations with FVIIa (5 nM), FXa (10 nM) and TFPI (5 pM) either on the first or the fifth day of the investigation (Figure 5.4). Caspase-3 activity in the positive control treated with 2 μM of hydrogen peroxide (H_2O_2), reached a maximum of 45 % above that of the control in H9c2 cardiomyocytes (Figure 5.4).

Figure 5.2: Caspase-3 activity profiles in H9c2 cardiomyocytes following treatment with exogenous TF.

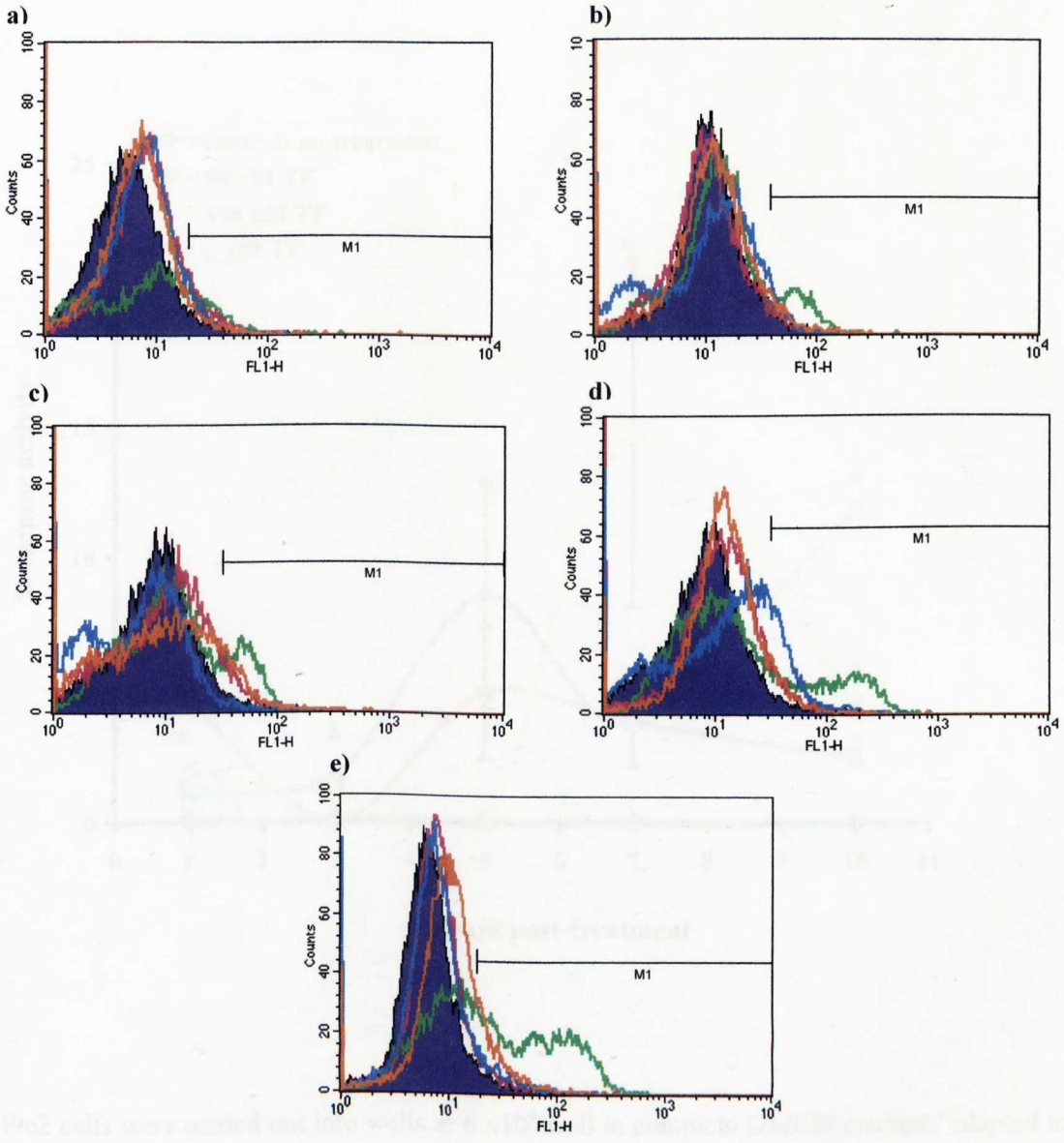

H9c2 cells were seeded out into wells at 6 x10^4/well in complete DMEM medium, adapted to serum-free medium over 4 days and treated with 50 nM (-), 500 nM (-) and 2 μM TF (-), respectively. Caspase-3 activity was measured and analysed on days 1 (panel a), 3 (panel b), 5 (panel c), 7 (panel d) and 10 (panel e) using flow cytometry. Positive (-) and negative (-) control cells were prepared by treatment with H_2O_2 (2 μM) and using un-treated cells, respectively. The percentage caspase-3 activity in the cell population tested was measured by including a 3 % of the control sample. The flow-cytometry profiles are typical of 3 separate experiments.

Figure 5.3: Activity of caspase-3 in H9c2 rat cardiomyocytes in response to treatment with exogenous TF.

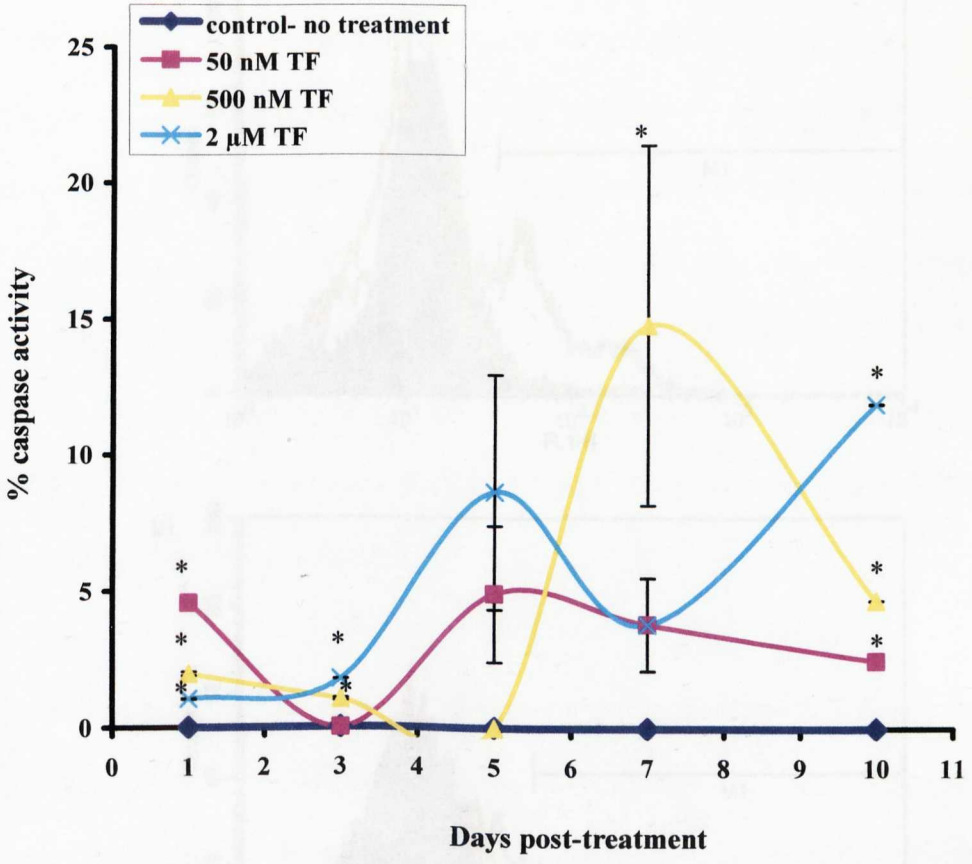

H9c2 cells were seeded out into wells at 6 x10^4/well in complete DMEM medium, adapted to serum free medium over 4 days and treated with 50 nM of TF (■), 500 nM of TF (▲) and 2 µM of TF (×), respectively. Caspase-3 activity was measured on day 1, 3, 5, 7 and 10 by flow cytometry. The data represent the mean of a 10^4 cells taken from 3 separate experiments, counted by a flowcytometer and presented as the percentage of the control ± SEM.

* $p<0.05$ treated cells versus un-treated cells (control)

Figure 5.4: Measurement of caspase-3 activity in H9c2 cardiomyocytes following treatment with exogenous TF in combination with FVIIa, FXa and TFPI.

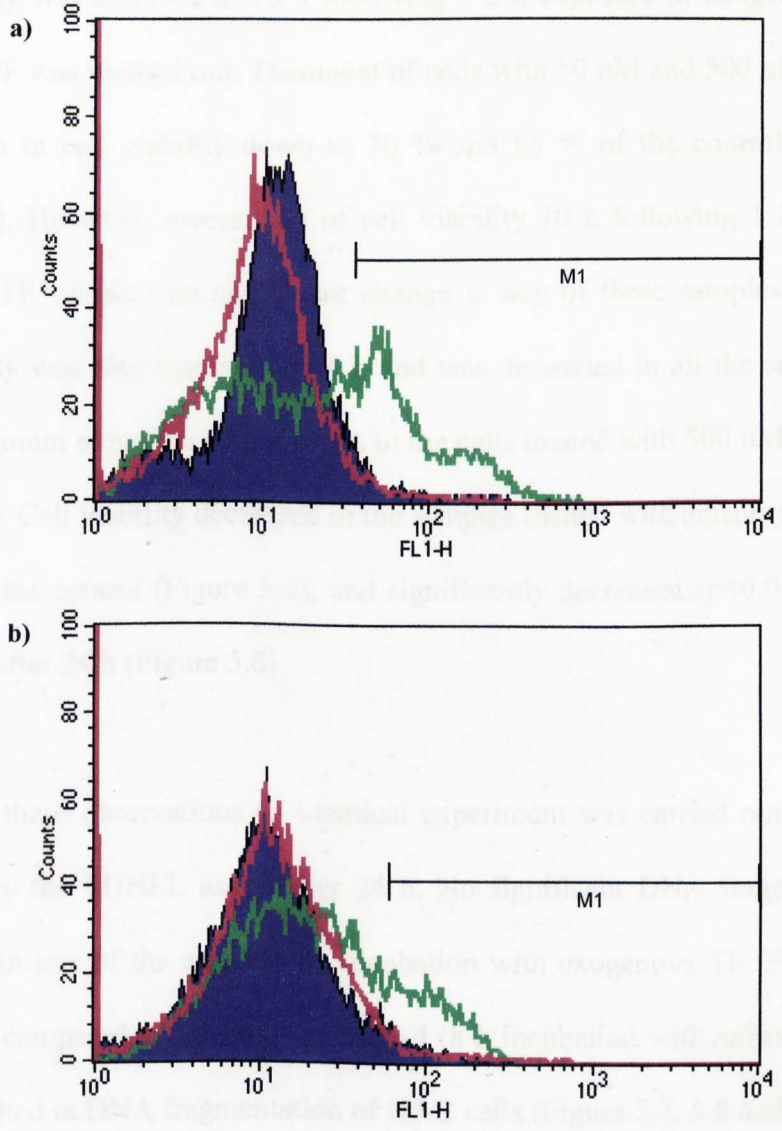

H9c2 cells were seeded out in wells at 6 x10^4/well in complete DMEM medium, adapted to serum free medium over 4 days and treated with TF (50 nM) in combination with FVIIa (5 nM), FXa (10 nM) and TFPI (5 pM) (-). On day 1 (panel a), and 5 (panel b), caspase-3 activity was measured and analysed using flow cytometry. As a positive control, cells were treated with H_2O_2 (-) had active caspase-3 in the 45 % of the cell population tested while un-treated cells (negative control) (-) exhibit no caspase-3 activity. The flow-cytometry profiles are typical of 3 separate experiments.

5.3.2 The rate of proliferation and apoptosis following short-term treatment with TF

Cell viability was assessed at 10 h following a 2 h exposure to exogenous TF after which the TF was washed out. Treatment of cells with 50 nM and 500 nM TF resulted in reduction in cell viability down to 70 % and 65 % of the control, respectively (Figure 5.5). However, assessment of cell viability 10 h following 1 h exposure to exogenous TF, showed no significant change in any of these samples (Figure 5.5). Cell viability was also assessed at 24 h and was decreased in all the samples tested, with a maximum reduction of Δ= -30 % in the cells treated with 500 nM of TF for 2 h (Figure 5.6). Cell viability decreased in the samples treated with anisomycin after 10 h to 60 % of the control (Figure 5.4), and significantly decreased ($p<0.05$) to 30 % of the control after 24 h (Figure 5.6).

To support these observations an identical experiment was carried out and the cells examined by the TUNEL assay after 24 h. No significant DNA fragmentation was observable in any of the samples on incubation with exogenous TF (Figure 5.7, 5.8 and 5.9) as compared to the positive control (8 h incubation with anisomycin) which clearly resulted in DNA fragmentation of H9c2 cells (Figure 5.7, 5.8 and 5.9).

5.3.2.1 The activation of p53 pathway following short-term treatment with TF

p53 antibody staining revealed no p53 translocation to the nucleus in any of the samples treated with exogenous TF 24 h and 48 h post-treatment (Figure 5.10 and 5.11 respectively). Incubation with 2 μM ME resulted in the translocation of p53 in the cell nucleus revealing the existence of apoptosis (Figure5.10b and 5.11b).

Figure 5.5: H9c2 rat cardiomyocytes viability on exposure to exogenous TF 2 and 1 h measured at 10 h post-treatment.

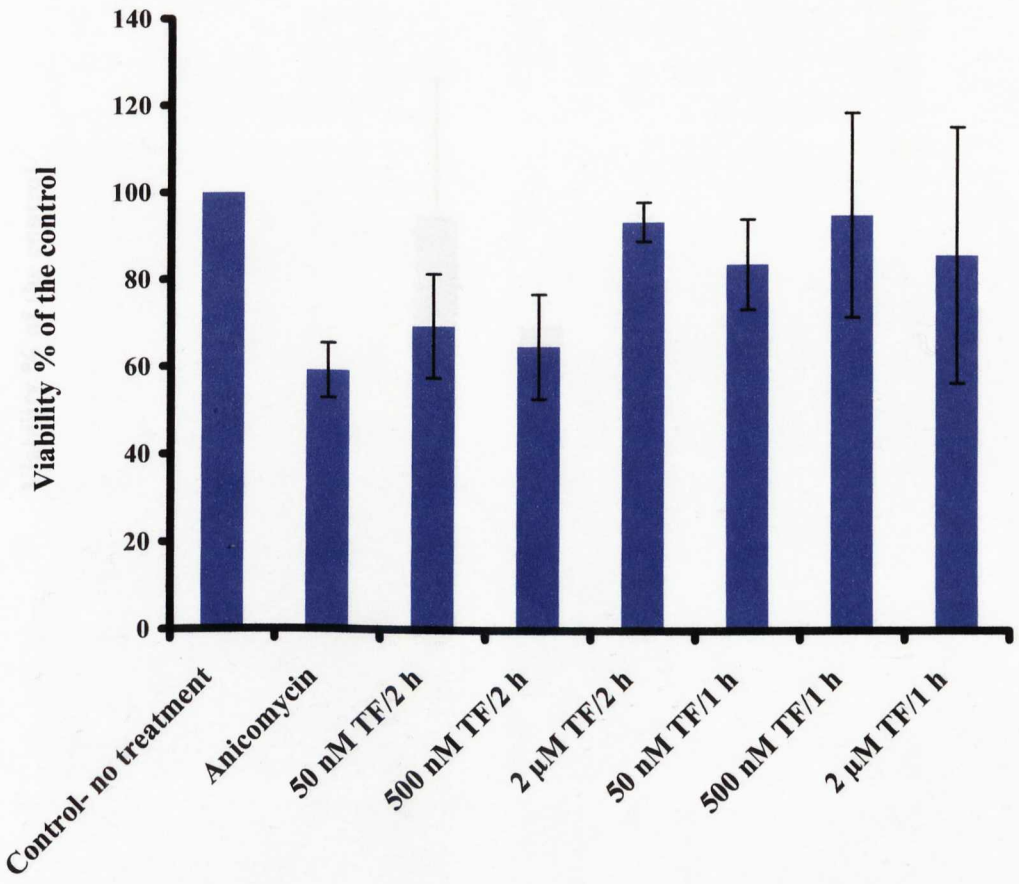

H9c2 cells were seeded out into wells at 5 x10^4/well in complete DMEM medium, adapted to serum-free medium over 4 days and treated with 50 nM, 500 nM and 2 μM of TF for 1 and 2 h respectively after which, the TF was washed out. The rate of cell proliferation was assessed after 10 h and converted to cell numbers from a standard curve. The data represent the mean of n=9 taken from 3 separate experiments, performed in triplicate and are presented as the percentage of the control ± SEM.

Figure 5.6: H9c2 rat cardiomyocyte viability, 2 and 1 h on exposure to exogenous TF measured at 24 h post-treatment.

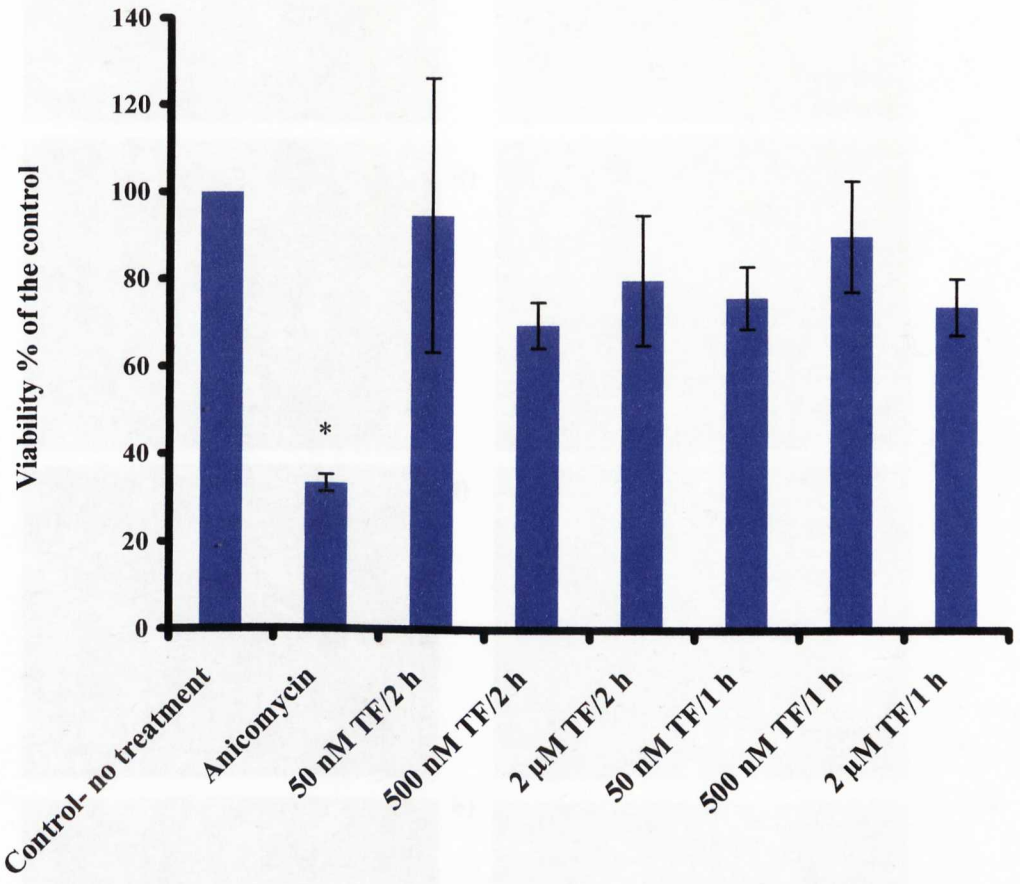

H9c2 cells were seeded out into wells at 5 x10^4/well in complete DMEM medium, adapted to serum-free medium over 4 days and treated with 50 nM, 500 nM and 2 μM of TF for 1 and 2 h respectively after which, the TF was washed out. The rate of cell proliferation was assessed after 24 h and converted to cell numbers from a standard curve. The data represent the mean of n=9 taken from 3 separate experiments, performed in triplicate and are presented as the percentage of the control ± SEM.

* $p<0.05$ treated cells versus un-treated cells (control)

Figure 5.7: Assessment of DNA fragmentation in H9c2 rat cardiomyocytes on exposure to exogenous TF for 1 and 2 h, at 24 h post-treatment.

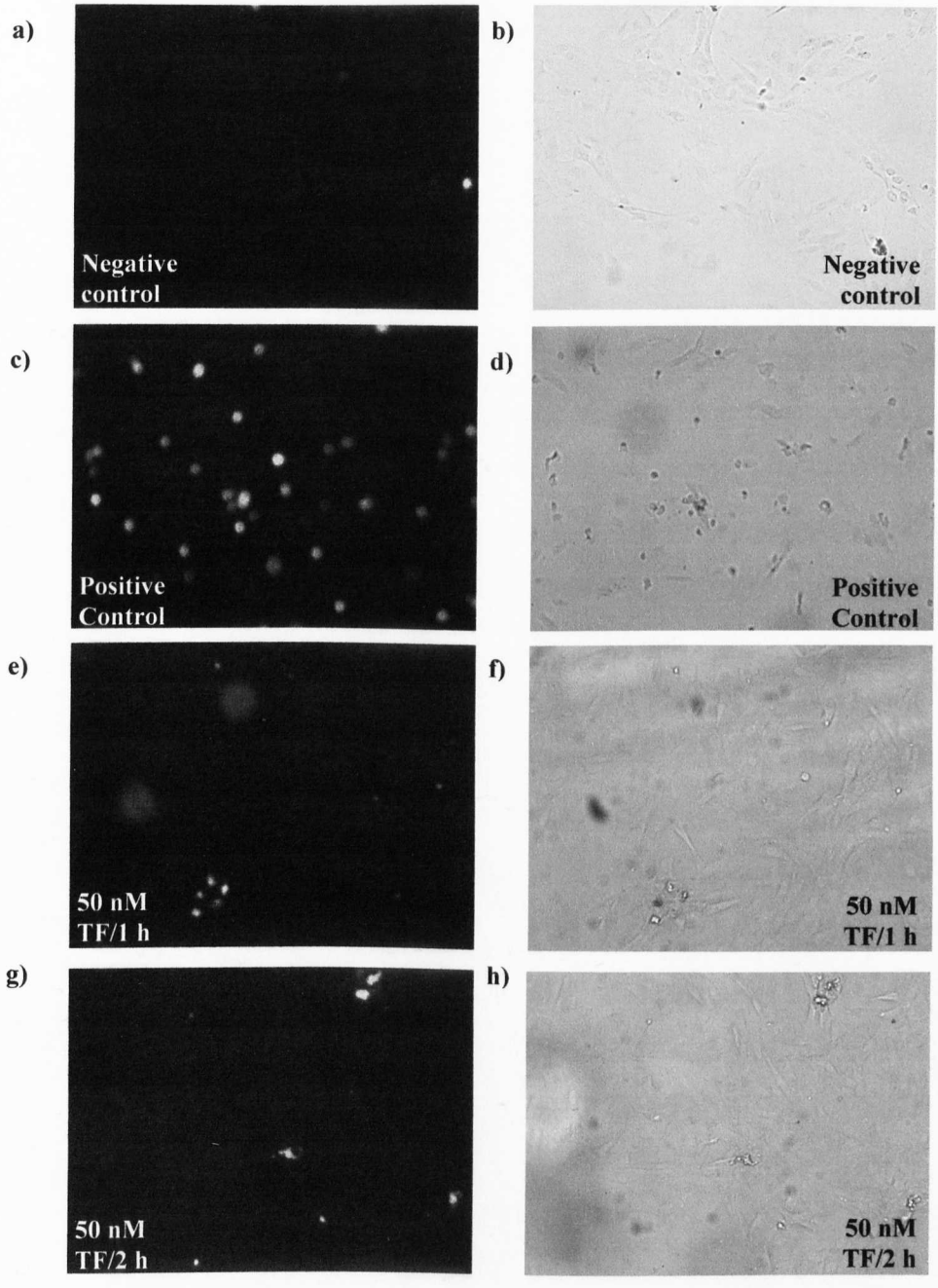

H9c2 cells were seeded out in wells at 3 x 10^4/well in complete DMEM medium, adapted to serum-free medium over 4 days and treated with 50 nM of TF for 2 h (micrograph e & f) and 50 nM of TF for 1 h (micrograph g & h). TUNEL assay was performed 24 h after treatment and the images were captured and analyzed with ImagePro software. A sample of cells remained untreated (micrograph a & b) and used as negative control. Cells treated with 2 μM of anisomycin for 8h (micrograph e & d) used as positive control. The above micrographs are representative of n=6 taken from 3 separate experiments performed in duplicate (Magnification x 10).

Figure 5.8: Assessment of DNA fragmentation in H9c2 rat cardiomyocytes on exposure to exogenous TF for 1 and 2 h, 24 h post-treatment.

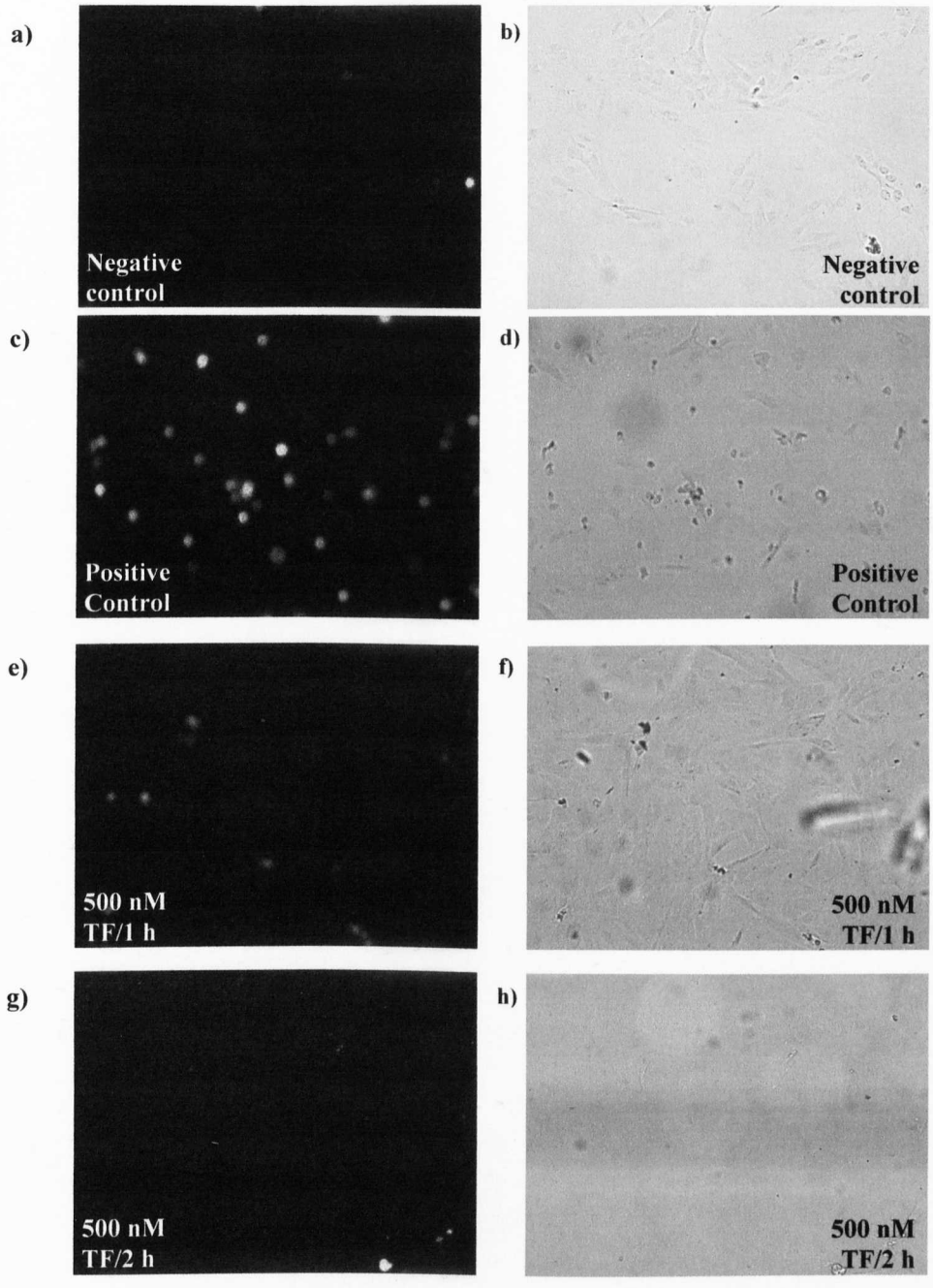

H9c2 cells were seeded out in wells at 3 x 10^4/well in complete DMEM medium, adapted to serum-free medium over 4 days and treated with 500 nM of TF for 2 h (micrograph e & f) and 500 nM of TF for 1 h (micrograph g & h). TUNEL assay was performed 24 h after treatment and the images were captured and analyzed with ImagePro software. A sample of cells remained untreated (micrograph a & b) and used as negative control. Cells treated with 2 μM of anisomycin for 8h (micrograph e & d) used as positive control. The above micrographs are representative of n=6 taken from 3 separate experiments performed in duplicate (Magnification x 10).

Figure 5.9: Assessment of DNA fragmentation in H9c2 rat cardiomyocytes on exposure to exogenous TF for 1 and 2 h, 24 h post-treatment.

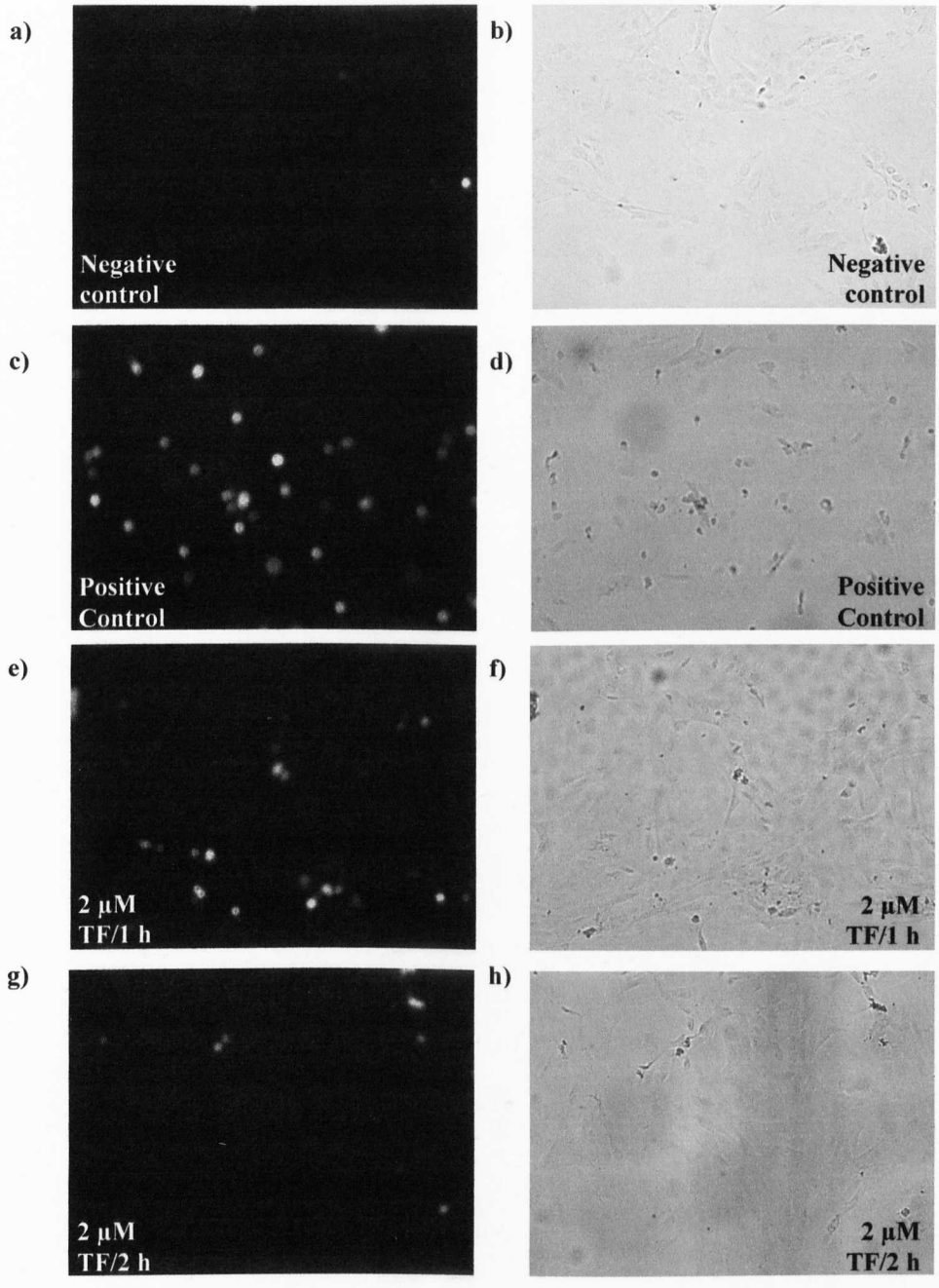

H9c2 cells were seeded out in wells at 3 x 10^4/well in complete DMEM medium, adapted to serum-free medium over 4 days and treated with 2 μM of TF for 2 h (micrograph e & f) and 2 μM of TF for 1 h (micrograph g & h). TUNEL assay was performed 24 h after treatment and the images were captured and analyzed with ImagePro software. A sample of cells remained untreated (micrograph a & b) and used as negative control. Cells treated with 2 μM of anisomycin for 8h (micrograph e & d) used as positive control. The above micrographs are representative of n=6 taken from 3 separate experiments performed in duplicate (Magnification x 10).

Figure 5.10: p53 activation pathway in H9c2 rat cardiomyocytes 24 h post-treatment with exogenous TF.

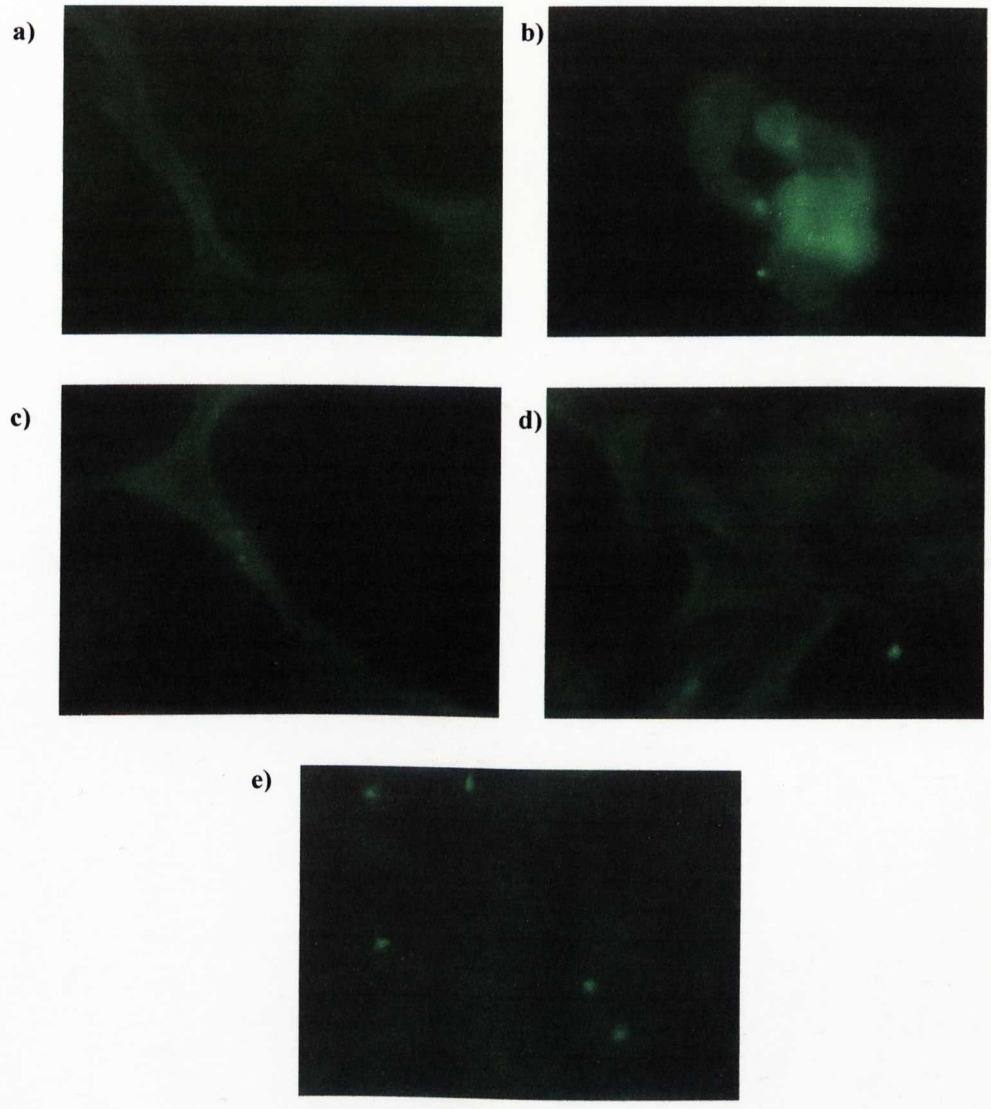

H9c2 cells were seeded out in wells at 3 x 10^4/well in complete DMEM medium, adapted to serum-free medium over 4 days and treated with 50 nM (micrograph c), 500 nM (micrograph d) and 2 μM (micrograph e) of TF. The cells were incubated for 24 h and then labelled for p53 activation using a rabbit anti-human p53 antibody. The images were captured and analyzed with ImagePro software. Untreated cells (micrograph a) were used as negative control and cells were treated with 2 μM of ME for 2h (micrograph b) were used as positive control. The above micrographs are representative of 20 cells taken from 2 separate experiments performed in duplicate (Magnification x 40).

Figure 5.11: p53 activation pathway in H9c2 rat cardiomyocytes 48 h post-treatment with exogenous TF.

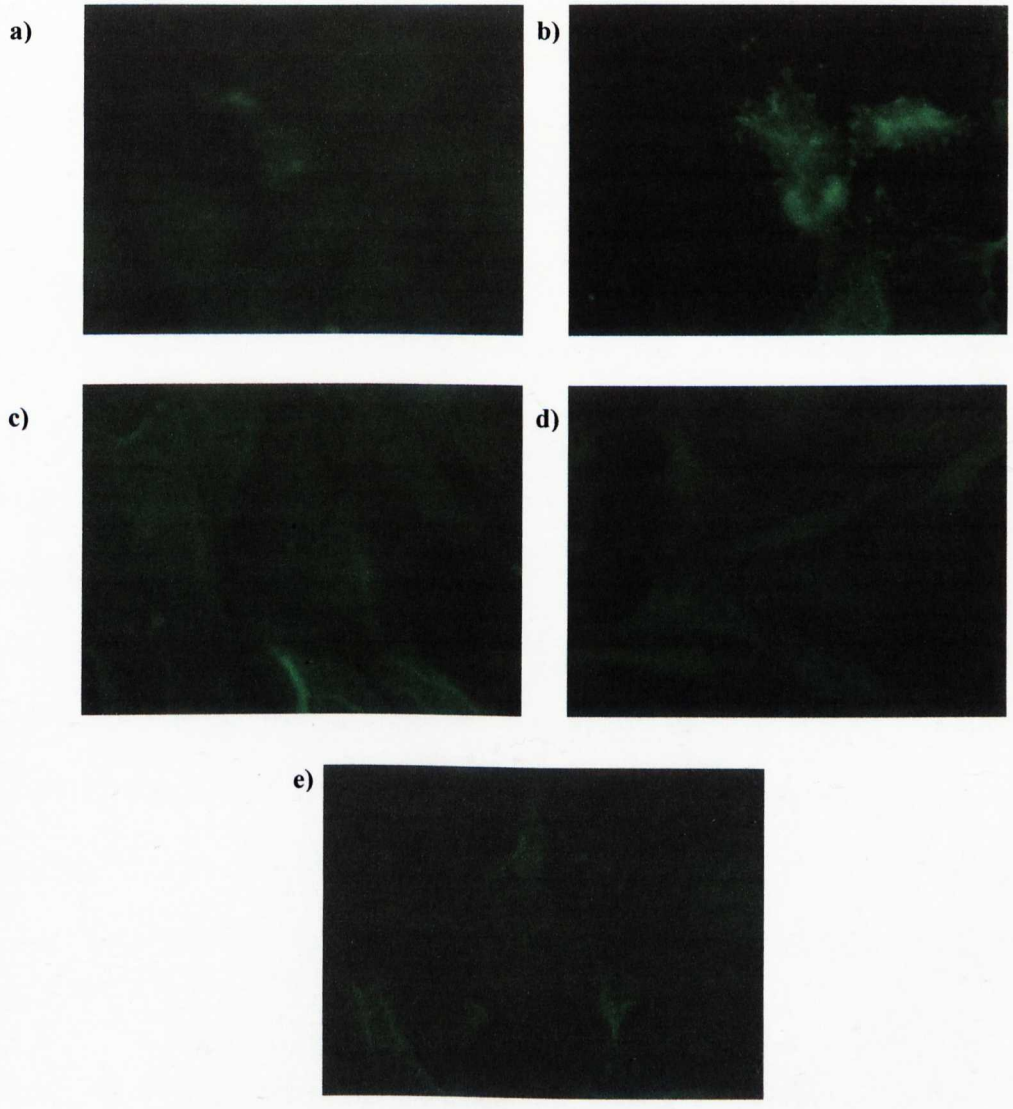

H9c2 cells were seeded out in wells at 3 x 10^4/well in complete DMEM medium, adapted to serum-free medium over 4 days and treated with 50 nM (micrograph c), 500 nM (micrograph d) and 2 μM (micrograph e) of TF. The cells were incubated for 48 h and then labelled for p53 activation using a rabbit anti-human p53 antibody. The images were captured and analyzed with ImagePro software. Untreated cells (micrograph a) were used as negative control and cells were treated with 2 μM of ME for 2h (micrograph b) were used as positive control. The above micrographs are representative of 20 cells taken from 2 separate experiments performed in duplicate (Magnification x 40).

5.3.3 The rate of proliferation and apoptosis following short-term treatment with TF with or without FVIIa, FXa and TFPI

Cell viability was reduced to 90 % of the control following short-treatment with 50 nM TF for 10 h with a further reduction to 65 % of the control in the sample treated with 500 nM TF (Figure 5.12). Combinations of TF/FVIIa or TF/FVIIa/FXa partially negated the effect of TF and restored cell viability back to 92 % of the control and 83 % of the control respectively (Figure 5.12). Supplementation of TFPI (TF/FVIIa/FXa/TFPI) resulted in no significant changes in cell viability (Figure 5.12). After 24 h incubation, cell viability decreased to 70 % of the control in the cells treated sample with 500 nM TF (Figure 5.13). Combinations of either TF/FVIIa or TF/FVIIa/FXa, both reduced the cell viability to 70 % of the control (Figure 5.13). Further supplementation with TFPI (TF/FVIIa/FXa/TFPI) resulted in a significant increase ($p<0.005$) in cell viability by 16 % above that of the control as compared with the cells treated with anicomysin, 500 nM TF, and combinations of TF/FVIIa and TF/FVIIa/FXa (Figure 5.13). The viability of cells treated with anisomycin (positive control) decreased to 60 % of the control after 10 h incubation (Figure 5.12) and became significant ($p<0.05$) after 24 h incubation reaching a value of 45 % of the control (Figure 5.13).

To support the observations obtained from performing the viability assay, the cells were examined for DNA fragmentation at 24 h post-incubation with exogenous TF in combinations with FVIIa, FXa and TFPI using the TUNEL assay. The treatment of cells supplemented with either TF alone or in combination with FXa and TFPI did not result in any significant amount of DNA fragmentation (Figure 5.14 and 5.15). However, cells treated with a combination of TF and FVIIa, exhibited positive staining of DNA fragmentation (Figure 5.15) as compared to the positive control (anisomycin treated cells-Figure 5.14).

Figure 5.12: The influence of exogenous TF in combination with FVIIa, FXa and TFPI, on H9c2 rat cardiomyocytes viability at10 h post-treatment.

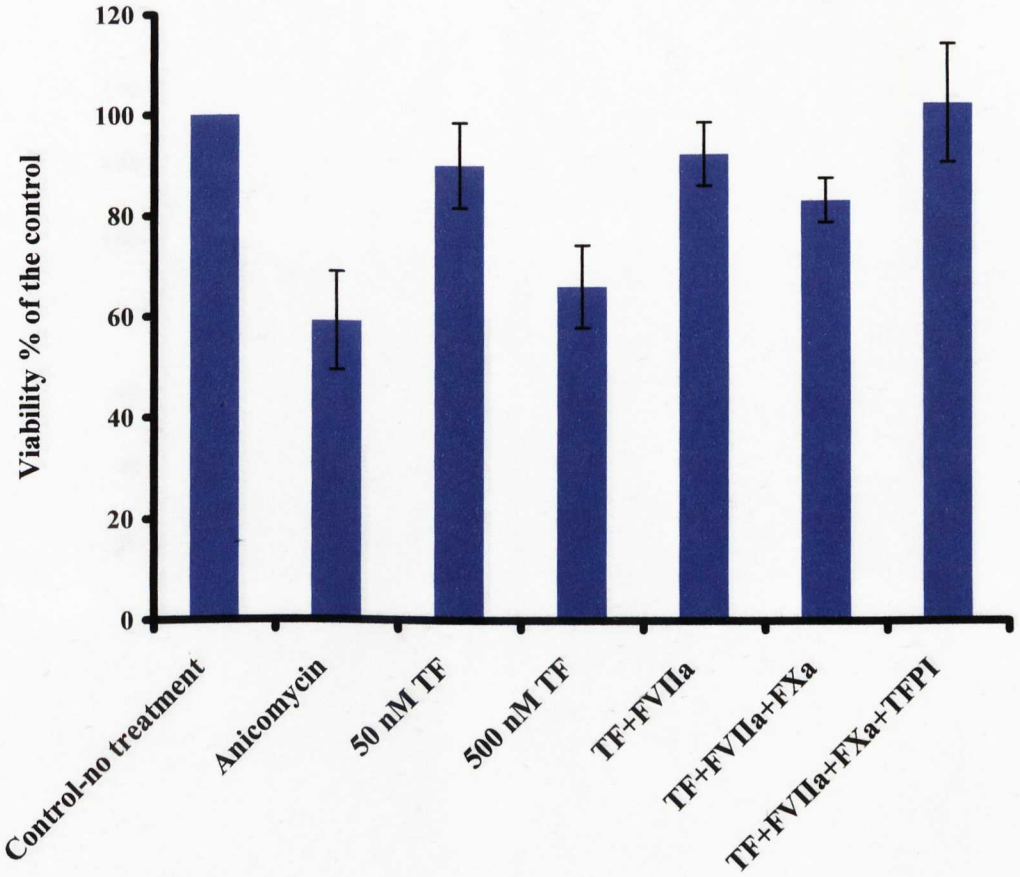

H9c2 cells were seeded out in wells at 5 x 10^4/well in complete DMEM medium, adapted to serum-free medium over 4 days and treated with 50 and 500 nM TF in combinations with FVIIa (5 nM), FXa (10 nM) and TFPI (5 pM). The rate of cell proliferation was assessed after 10 h and converted to cell number from a standard curve. The data represent the mean of n=9 taken from 3 separate experiments, performed in triplicate and are presented as the percentage of the control ± SEM.

Figure 5.13: The influence of exogenous TF in combinations with FVIIa, FXa and TFPI, on H9c2 rat cardiomyocytes viability at 24 h post-treatment.

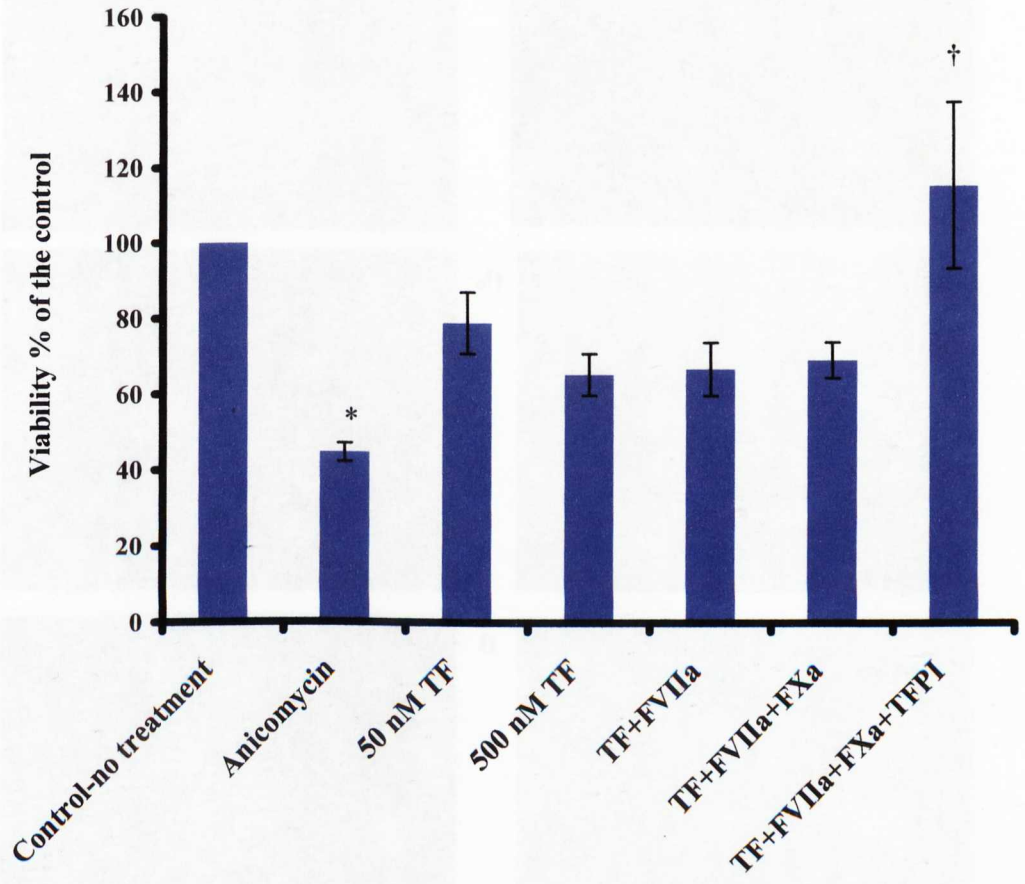

H9c2 cells were seeded out in wells at 5 x 10^4/well in complete DMEM medium, adapted to serum-free medium over 4 days and treated with 50 and 500 nM TF in combinations with FVIIa (5 nM), FXa (10 nM) and TFPI (5 pM). The rate of cell proliferation was assessed after 24 h and converted to cell number from a standard curve. The data represent the mean of n=9 taken from 3 separate experiments, performed in triplicate and are presented as the percentage of the control ± SEM.

* $p<0.05$ treated cells versus un-treated cells (control)

† $p<0.05$ as compared with cells treated with anicomycin, 500 nM TF and combinations of TF/FVIIa and TF/FVIIa/FXa

Figure 5.14: Assessment of DNA fragmentation in H9c2 rat cardiomyocytes 24 h post-treatment with exogenous TF in combinations with FVIIa, FXa and TFPI.

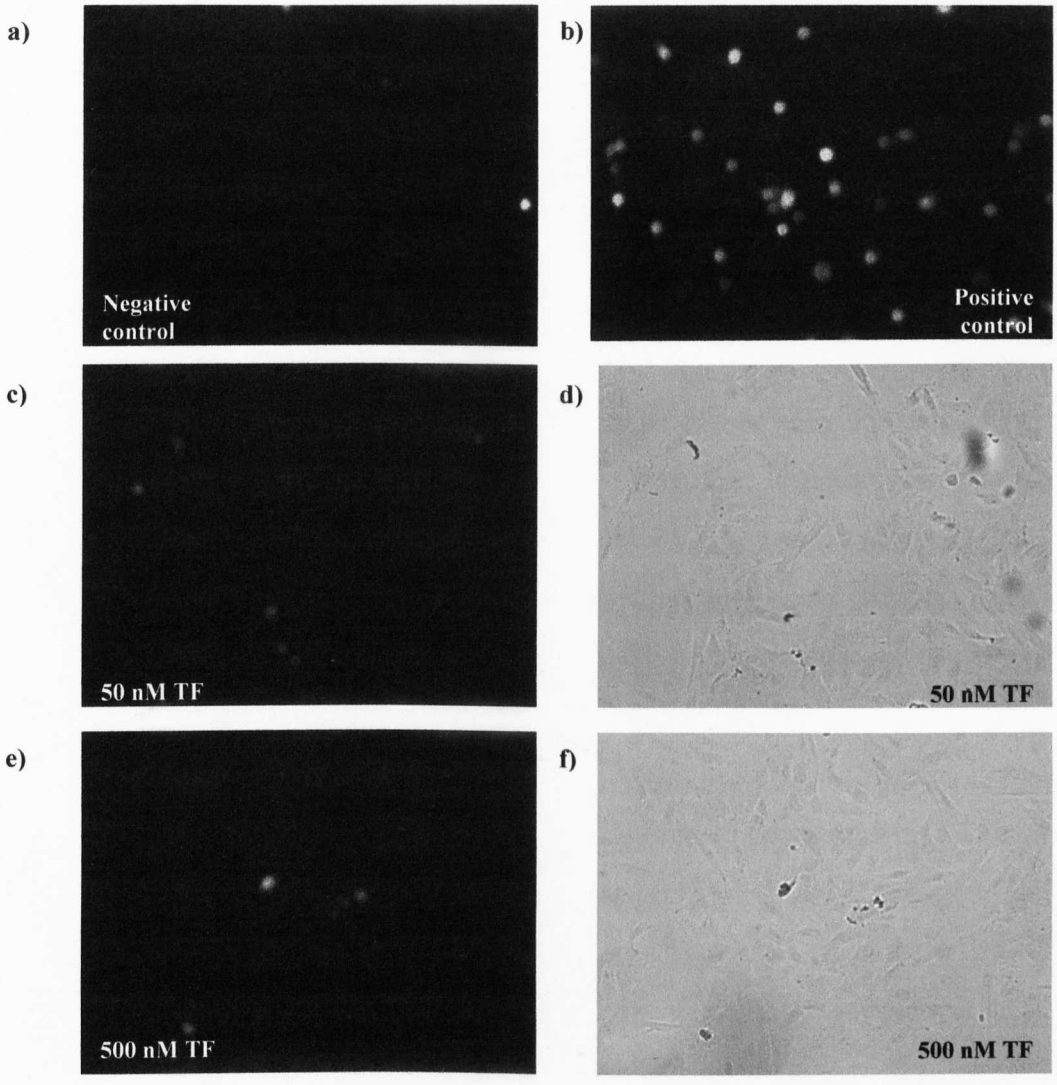

H9c2 cells were seeded out in wells at 5 x 10^4/well in complete DMEM medium, adapted to serum-free medium over 4 days and treated with 50 (micrograph c & d) and 500 nM (micrograph e & f) of TF and in combination with FVIIa (5 nM), FXa (10 nM) and TFPI (5 pM) (Figure 5.15). TUNEL assay was performed following 24 h incubation and the images were captured and analysed with ImagePro software. Untreated cells (micrograph a) were used for negative control and cells treated with 2 μM of anisomycin for 8h (micrograph b) were used as positive control. The above micrographs are representatives of n=6 taken from 3 separate experiment performed in duplicate (Magnification x 10).

Figure 5.15: Assessment of DNA fragmentation in H9c2 rat cardiomyocytes 24 h post-treatment with exogenous TF in combinations with FVIIa, FXa and TFPI.

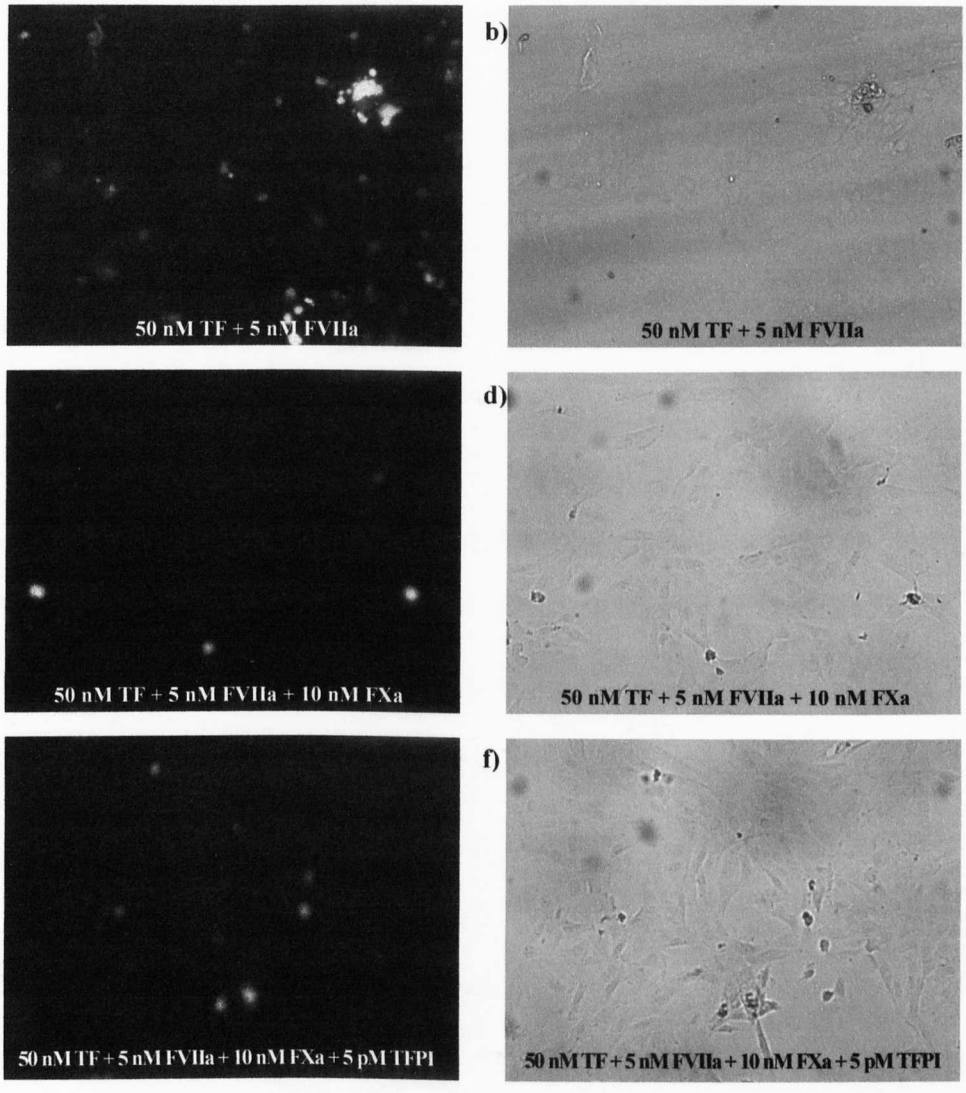

H9c2 cells were seeded out in wells at 3 x 10^4/well in complete DMEM medium, adapted to serum free medium over 4 days and treated with 50 and 500 nM (Figure 5.14) of TF and in combinations with FVIIa (5 nM) (micrograph a & b), FXa (10 nM) (micrograph c & d) and TFPI (5 pM) (micrograph e & f). TUNEL assay was performed following 24 h incubation and the images were captured and analysed with ImagePro software. Untreated cells (Figure 5.14) were used for negative control and cells treated with 2 μM of anisomycin for 8h (Figure 5.14) were used as positive control. The above micrographs are representatives of n=6 taken from 3 separate experiment performed in duplicate (Magnification x 10).

5.4 Discussion

5.4.1 The influence of exogenous TF on the rate of proliferation and apoptosis

TF is structurally similar to the class 2 cytokine receptor family (Bazan 1990). Recently, a great interest has been shown in the ability of TF to induce cellular signalling, promoting either cellular apoptosis or cellular proliferation (Han *et al.* 2004, Peppelenbosch & Versteeg 2001). In this chapter, the effect of exogenous recombinant TF on the proliferation and apoptosis of H9c2 rat cardiomyocytes was investigated. Long-term treatment of H9c2 cells with relative low concentration of TF promoted cellular proliferation, whereas higher concentrations of TF inhibited cellular proliferation (Figure 5.1). Furthermore, caspase-3 was only activated in the cells treated with higher concentrations of TF (Figure 5.3). Short-term treatment of the H9c2 cells with exogenous TF had no significant effect on cellular proliferation (Figure 5.5 & 5.6) and there was no evidence of cellular apoptosis (Figure 5.7, 5.8 & 5.9). Overall, these results indicate that TF has a dual action and at low concentrations may promote cellular growth (proliferation), whereas at high concentrations can induce cellular apoptosis possibly be the trans-activation of different signalling pathways, including the p42/44 MAP kinase, the JNK-SAPK signalling pathway (Ettelaie *et al.* 2006).

A recent study has shown that TF and active caspase-3 were both increased and co-localised in lipid-reach atherosclerotic plaques (Hutter *et al.* 2004). To date, this was the only evidence linking TF with caspase-3 activity. However, in the present study, increased TF concentration is also associated with increased caspase-3 activity (Figure

5.3). The effector caspase-3 is involved in both the intrinsic and the extrinsic apoptotic pathways (Cory & Adams 2002, Nagata 1997, Gopisetty *et al.* 2006). The intrinsic pathway is initiated mainly by the p53 activation in response to DNA damage, a common cause of which, is increased oxidative stress (Ryan *et al.* 2001). The activation of p53 results in cytocrome c release through mitochondrial activation, ultimately leading to caspase activation, DNA damage and cellular apoptosis (Cory & Adams 2002, Hockenbery *et al.* 1990). In the present study, the induction of apoptosis by TF did not involve the activation of p53 (Figure 5.10 & 5.11). Therefore, TF is unlikely to initiate apoptosis via the intrinsic pathway. The extrinsic pathway of apoptosis, also known as the death receptor mediated pathway, is initiated by cytokines that belong to the tumour necrosis factor (TNF) family (Gopisetty *et al.* 2006). The binding of a death ligand such as tumour necrosis factor (TNF) to the membrane-bound death receptor, tumour necrosis factor receptor 1 (TNFR1), results in the activation of caspase-8, leading to the activation of caspase-3 and ultimately to cell apoptosis (Nagata 1997, Takemura & Fujiwara 2004, Kang *et al.* 2004). The ability of TF to activate caspase-3 (Figure 5.3) is likely to be mediated through the activation of the extrinsic pathway of apoptosis in a death-receptor-like manner. However, there is clearly cross-talk between the two apoptotic pathways (see Figure 1.6). When activated, caspase-8 is capable of initiating the protein Bid of the third subclass (see section 1.2) of the Bcl-2 family proteins. Activation of Bid, leads to the activation of the pro-apoptotic proteins Bax and Bad, resulting in the cytochrome c release instead of activating downstream caspases of the extrinsic pathway (Gopisetty *et al.* 2006). Therefore, it is not certain if TF initiates the extrinsic pathway or induces apoptosis by activating caspase-3 via the cytochrome c release and feeding-back onto the extrinsic pathway of apoptosis.

Apoptosis, an ATP dependent process, is brought about by caspases and the apoptotic pathways mainly operate through protein-protein interactions and proteolytic cascades (Clerk *et al.* 2003). Therefore, the commitment of the cell to apoptosis is also controlled by the interaction of proteins from several signalling cascades (Clerk *et al.* 2003). Some protein kinases are involved in cytoprotection and others are promoting cell death. There are three main MAPK subfamilies, the ERKs that provides cytoprotection, and the JNK/SAPKs and p38-MAPKs that can either provide cytoprotection or promote apoptosis (Poulsen *et al.* 1998, Rao and Pendurthi 2005, Koul 2003, Kyriakis & Avruch, 2001). Other signalling pathways such as the PI3-kinase, cyclic AMP/protein kinase A and PKC are known to have a dual action, and can mediate either cell growth or cell death (Clerk *et al.* 2003). TF in complex to enzyme FVIIa have been shown to activate the MAP kinase pathways including the JNK/SAPK and p38 pathway (Poulsen *et al.* 1998, Rao and Pendurthi 2005, Koul 2003). Furthermore, it has been demonstrated that TF either alone or in combination with FVIIa can initiate the JNK/SAPK pathway in endothelial cells (Ettelaie *et al.* 2006). In this study the involvement of protein kinase cascades was not investigated and therefore, it is unknown if TF can initiate any of these signalling pathways in H9c2 cardiomyocytes.

While high concentrations of TF have been shown to activate caspase-3 and promote apoptosis in H9c2 cells (Figure 5.3), long-term incubation of the cells with low TF concentration resulted in an increase in cellular proliferation (Figure 5.1). It has been demonstrated that interaction of TF with FVIIa can induce proliferation in smooth muscle cells via the activation of p44/42 MAP kinase pathway and the JNK/SAPK pathway (Cirillo *et al.* 2004). Recently, TF/FVIIa complex has been shown to result in

proliferation of embryonic human kidney BOSC23 cells via a PAR2 dependent pathway (Fan *et al.* 2005). Furthermore, TF/FVIIa is capable of activating the p44/42 MAP kinase pathway in endothelial cells (Ettelaie *et al.* 2006). In contrast, this study ha shown that TF can increase proliferation alone in a growth-like dependent manner in H9c2 cardiomyocytes (Figure 5.3). The machinery of which TF modulate H9c2 cell proliferation was not investigated and remains poorly defined.

In conclusion, at high concentrations, TF can induce apoptosis in H9c2 cardiomyocytes *in vitro* after long-term treatment, whereas low concentration of TF was able to promote proliferation. During conditions in which TF content is elevated such as atherosclerosis, sepsis, diabetes and sickle cell disease (Mallat *et al.* 1999, Nieuwland *et al.* 2000, Diamant *et al.* 2002), TF may induce apoptosis in several cell types of the vascular system including cardiomyocytes, endothelial cells and smooth muscle cells. Consequently, as the rate of cell death increases, the remaining cells undergo hypertrophic growth to compensate for the decrease in cell number (Nadal-Ginard *et al.*, 2003). Therefore, the ability of TF to induce cell apoptosis or alternative proliferative growth in H9c2 cardiomyocyets provides an indirect link between TF and cardiac hypertrophy (Figure 5.16).

5.4.2 The influence of exogenous TF in combination with FVIIa, FXa and TFPI on proliferation and apoptosis

Interactions of TF with FVIIa and FXa have been shown to induce cellular signalling promoting cell proliferation and inhibiting apoptosis (Versteeg *et al.* 2004). Furthermore, TFPI has been shown to inhibit the above TF/FVIIa or TF/FVIIa/FXa mechanisms (Hamuro *et al.* 1998). Therefore, this section of the study was designed

Figure 5.16: A schematic representation of the dual action of TF.

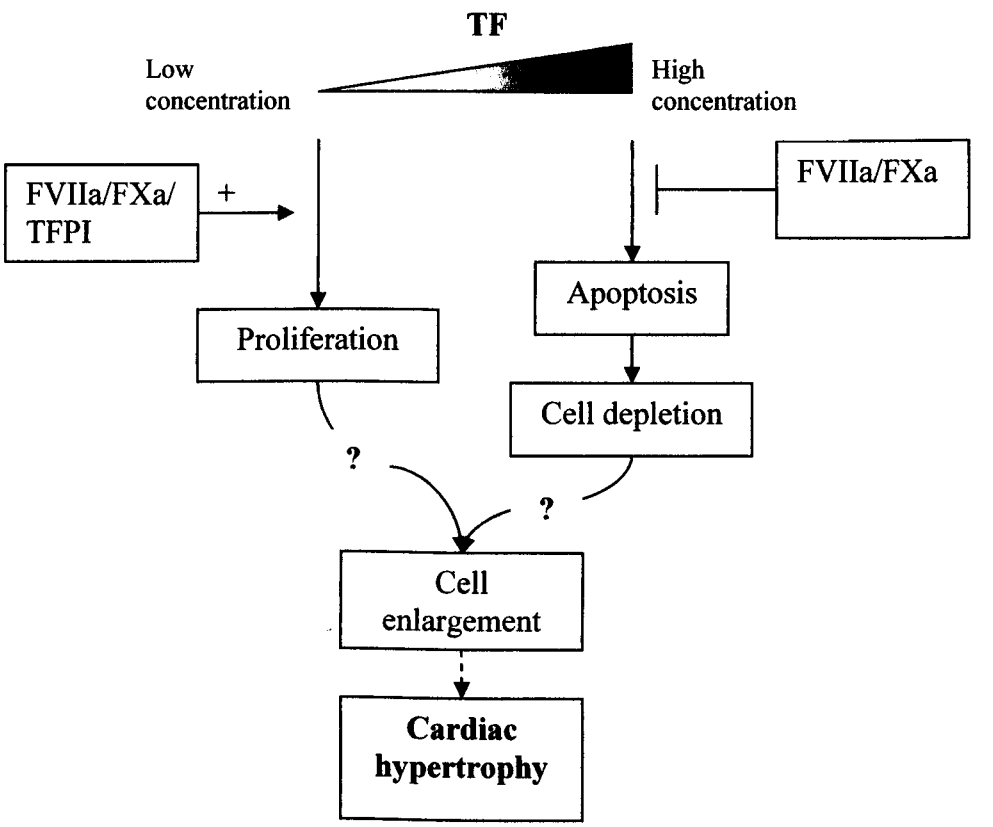

Low concentrations of TF can promote cell proliferation, the pathway of which is poorly defined. High concentration of TF can induce apoptosis on H9c2 cells, most probably via the extrinsic pathway of apoptosis. The combination of TF/FVIIa/FXa/TFPI is shown to negate the apoptotic action of TF, resulting in proliferation of H9c2 cardiomyocytes. Cellular proliferation leads to cell growth and/or cell enlargement, while apoptosis can lead to cell depletion and therefore the residual cells undergo cell growth and/or cell enlargement to compensate for the loss. Combination of proliferation and apoptosis ultimately leads to cardiac hypertrophy. Hence, TF can indirectly promote a hypertrophic response.

to investigate the influence of TF in combinations with FVIIa, FXa and TFPI on cellular proliferation and apoptosis of H9c2 cardiomyocytes.

Incubation of H9c2 cells with TF alone, resulted in inhibition of cellular proliferation after 10 h and 24 h (Figure 5.12 & 5.13), whereas, combination of TF/FVIIa and TF/FVIIa/FXa 10 h post-treatment partially restored proliferation (Figure 5.12) with a subsequent reduction after 24 h incubation (Figure 5.13). Therefore, TF alone can inhibit cellular proliferation, while combination of FVIIa and FXa could only partially reverse this effect. The binding of FVIIa to its cellular receptor TF has previously been shown to induce intracellular signalling events (Camerer *et al.*, 2000, Riewald & Ruf 2002, Sorensen *et al.* 2003). Interaction of TF with FVIIa has been shown to activate both the phosphatidylinositide-3-(OH) kinase and p42/p44 MAP kinase pathways which promote cell survival and are shown to inhibit caspase-3 activation in BHK cells over-expressing TF (Versteeg *et al.* 2003). Furthermore, FXa, generated by the formation of the TF/FVIIa complex, is capable of strongly increasing the rate of cell survival (Versteeg *et al.* 2003). The anti-apoptotic effect of TF/FVIIa is known to be mediated through activating PI3-kinase pathway, leading to the initiation of the Akt pathway, and the subsequent activation of the p44/p42 MAP kinase pathway (Sorensen *et al.* 2003). The data showing proliferation in H9c2 cells treated with TF/FVIIa and TF/FVIIa/FXa for 10 h are in consistent with those reported by Cirillo *et al.* (2004), which show that the complex forming between TF and FVIIa resulted in increase proliferation in smooth muscle cells (Figure 5.12). In contrast, treatment of H9c2 cells with TF/FVIIa and TF/FVIIa/FXa resulted in a decline in cell proliferation at 24 h (Figure 5.13). However, the underlying reason for the discrepancies observed between these set of data are at present unclear. A possible explanation is the use of

different types of culture cells, in this case H9c2 cardiomyocytes. Furthermore, the pathways of which TF/FVIIa and TF/FVIIa/FXa initially reverse the apoptotic action of TF, providing temporary cytoprotection were not investigated and are yet poorly defined.

In contrast to the influence of FVIIa and FXa on cell proliferation and apoptosis, TFPI is known to induce apoptosis in human umbilical vein endothelial cells (Hamuro *et al.* 1998). Furthermore, it has been demonstrated that the interaction of TFPI with cultured human smooth muscle cells can inhibit cell proliferation (Kamikubo *et al.* 1997). Surprisingly in this study, TFPI protected cell survival and promoted cellular proliferation in H9c2 cardiomyocytes (Figure 5.12 and 5.13) with no evidence of apoptotic cell death (Figure 5.15). Furthermore, H9c2 cardiomyocytes treated with TF/FVIIa/FXa/TFPI showed no active caspse-3 when examined for 5 days (Figure 5.4). These data indicate that TFPI inhibits the TF/FVIIa/FXa complex, suppressing the anti-proliferative action of either TF alone or TF/FVIIa or TF/FVIIa/FXa complexes.

In conclusion, either TF alone or in combination with FVIIa and FXa is capable of inhibiting proliferation in H9c2 cells (Figure 5.16). Furthermore, addition of TFPI to TF/FVIIa/FXa can restore or even promote cell proliferation probably via inhibition of TF/FVIIa/FXa complex.

5.5 Conclusions

In this study, either the influence of TF alone, or in combination with FVIIa, FXa and TFPI on proliferation and apoptosis of H9c2 cardiomyocytes was investigated. TF demonstrated a dual action; at high concentrations TF inhibited proliferation and induced apoptosis in the H9c2 cardiomyocytes, whereas at lower concentrations, TF enhanced proliferation in H9c2 cells. Furthermore, it was shown that the apoptotic action of TF was not mediated via the p53 pathway. Also, TF/FVIIa, TF/FVIIa/FXa partially negated the apoptotic action of TF. Moreover, TF/FVIIa/FXa/TFPI was capable of promoting proliferation. In disease conditions, such as atherosclerosis, diabetes, sepsis or blood disorders, TF is increased and may induce cellular apoptosis within vital organs. Cellular apoptosis is present in the heart and can lead to the hypertrophic growth of the residual cells to compensate for the extra workload. Therefore, it is suggested that TF through its dual action may be indirectly involved in the pathogenesis and/or progression of cardiac hypertrophy (Figure 5.16).

CHAPTER 6

General discussion

6. General discussion

6.1 The role of tissue factor in cardiac hypertrophy

The principle aim of this thesis was to examine the association between the initiator of the extrinsic pathway of coagulation, tissue factor (TF) and the onset of cardiac hypertrophy. Cardiac hypertrophy is the adaptive response of the heart to haemodynamic stress, occulting initially to normalise vessel wall stress and maintain normal heart function (Spann *et al.* 1967). One of the key features of cardiac hypertrophy is the increase in cardiomyocyte size in the left ventricle (Olivetti *et al.* 1995, Anversa *et al.* 1986). TF and its regulator, tissue factor pathway inhibitor (TFPI) are the major proteins involved in the extrinsic pathway of blood coagulation and have recently been implicated in the remodelling of vascular and myocardial tissue (Luther & Mackman, 2001). Several studies have shown that these changes are concurrent with alterations in the TF content of the myocardium occurring as a result of the reduction in the cellular contact sites within the heart muscle (Olivetti *et al.* 1995, Anversa *et al.* 1986). Luther *et al.* (2000) demonstrated that TF is decreased in older human males (but not females) which may correlate with the loss of myocytes and the reactive hypertrophy of the remaining cardiomyocytes that lead to a decrease in the cellular contact sites within the myocardium (Olivetti *et al.* 1995).

The initial aim of the study was to investigate the expression profile of TF and TFPI, during the induction of cardiac hypertrophy. It was demonstrated that TF was derived exogenously from other cells within the myocardium, in response to the aortic constriction and hence, elevated pressure overload to the heart. Induction of pressure overload leads to an imbalance between oxygen supply and demand, and therefore to

temporary ischemia (Keith *et al.* 1992). In normal arteries, TF is detectable predominantly in adventitial fibroblasts and also in circulating blood (Jude *et al.* 2005). However, during coronary occlusion, for example in atherosclerosis, TF expression is elevated in macrophages and vascular smooth muscle cells (Muller *et al.* 2000, Wilcox *et al.* 1989). Recently, it has been demonstrated that a significant increase in circulating TF is detectable in patients with acute coronary syndromes (Misumi *et al.* 1998). TFPI expression was found to be up-regulated in the cardiomyocytes, suggesting an opposing response by these cells to restrain the elevated TF levels. However, the increase in TFPI expression was transient indicating that the contribution of the cardiomyocytes to this control mechanism is most likely a short-term measure. Therefore, in short-term the elevation of TF activity may be controlled by release of TFPI, long-term increases in TF, such as those observed during chronic coronary occlusion (Wilcox *et al.* 1989) can overcome the response of the cardiomyocytes to defend themselves. However, the findings obtained in this study are at the onset of cardiac hypertrophy. Significant cardiac hypertrophy is observed using the abdominal aortic constriction model in rats from the tenth day post surgery and thereafter (Ganguly *et al.* 1989, Stoyanova *et al.* 2005). In addition, physiological, cellular and molecular differences are observed during the different stages of the hypertrophic process and are illustrated in Figure 6.1 (Bugaisky *et al.* 1992). Therefore, further investigation into the expression of TF and TFPI during stage II of compensatory cardiac hypertrophy (Figure 6.1) would clarify the role of these proteins in the remodelling of the heart.

As an indicator of the influence of TF on cardiac remodelling, the expression of proteins associated with cardiac hypertrophy, in response to TF were examined.

Figure 6.1: The phases of cardiac hypertrophy.

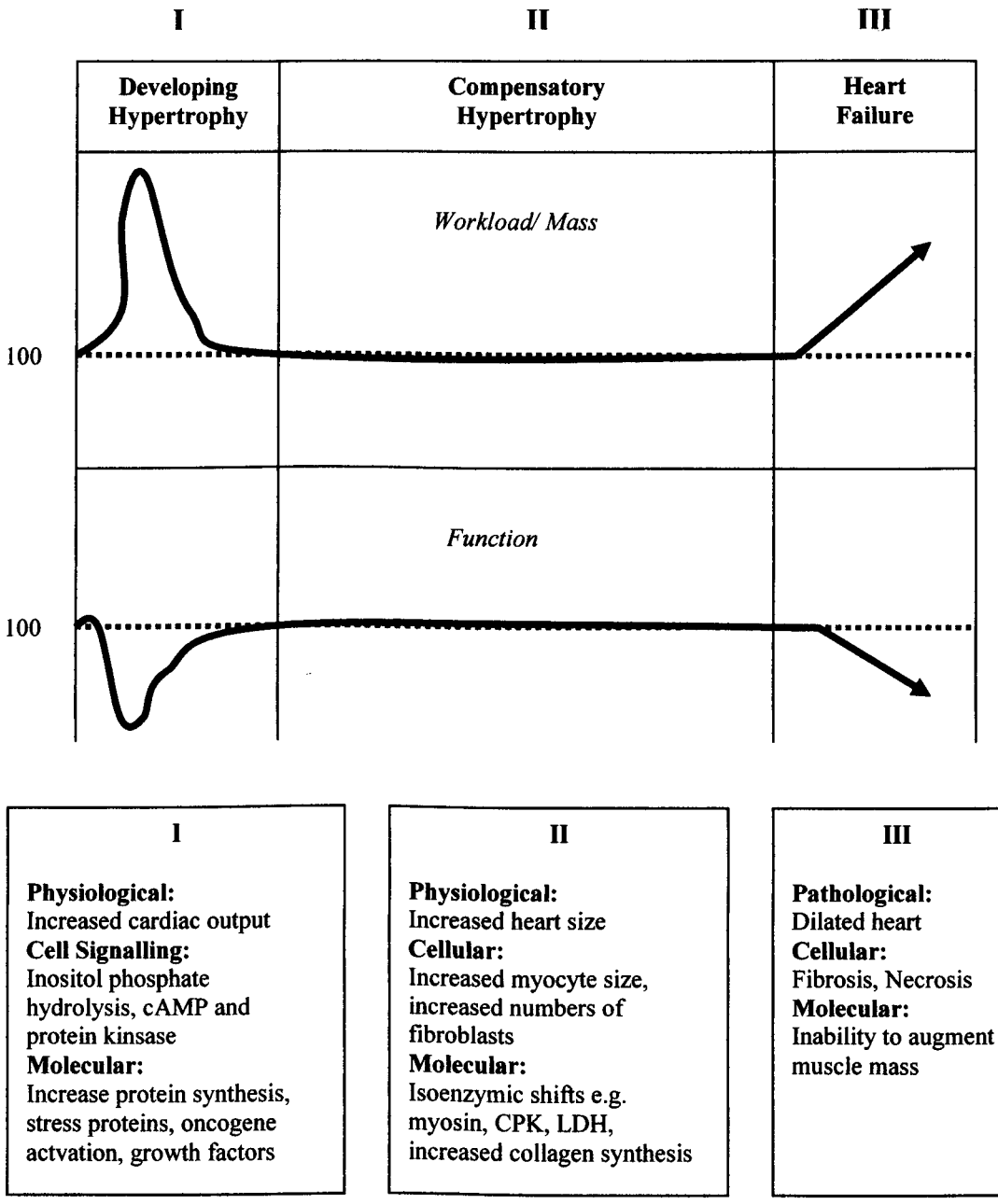

In the diagram, 100 and the dotted line indicates normal values of work load and function of the heart. The boxes include the physiological, cellular and molecular events that accompany different stages of cardiac muscle adaptation. *(Adapted from Bugaisky et al. 1992)*

Exogenous TF alone was found capable of up-regulating ANF expression. However the presence of factors FVIIa and FXa suppressed the action of TF. This suppression depended on the proteolytic activity of these enzymes, since the presence of TFPI negated this suppression. This observation suggests the possible involvement of protease activator receptors (PAR) 1 and 2. These receptors are known to participate in the initiation of hypertrophic stimuli (Sabri *et al.* 2000, Moons *et al.* 2002) and can also be activated by the TF/FVIIa complex and FXa (Bromberg *et al.* 2001, Petersen *et al.* 2000, Steinberg 2004). PAR-1 is known to trigger a range of events in cardiomyocytes including the expression of ANF (Sabri *et al.* 2000). Moreover, PAR-2 activates a spectrum of responses in cardiomyocytes, leading to dilated hypertrophy (Steinberg 2005, Sabri *et al.* 2000). An experiment to investigate the involvement of PAR 1 and 2 in ANF expression using inhibitory antibodies was considered impractical due to the large quantities of antibody required (section 4.4.1) and also lack of time. To clarify further the role of TF in the activation of the PAR receptors and ANF expression, experiments in which PAR 1 and PAR 2 activity is ablated either via short hairpin RNA (shRNA) to silence the PAR 1 or PAR 2 or both PAR 1 and PAR 2 gene, or via gene knock out would be of value.

In addition to the control of ANF expression, TF alone can also induce hypertrophy through the up-regulation of MGF. It has previously been shown that MGF expression is up-regulated in exercised skeletal muscle undergoing physiological hypertrophy (Goldspink *et al.* 1992, Yang *et al.* 1997). Furthermore, Goldspink *et al.* (2002) showed that skeletal muscle expressing MGF becomes hypertrophic. Therefore, data here suggest that TF is a mediator of MGF and consequently an inducer of hypertrophic growth in cardiomyocytes. By using specific antibodies to MGF, it could

be further investigate the influence of TF on the expression of MGF protein and thus clarify the involvement of TF in cardiac hypertrophy.

In addition to this growth effect, progression of cardiac hypertrophy is characterised by a reduction in the number of viable cells in the heart muscle (Nadal-Ginard *et al.* 2003). Therefore, the final set of investigations aimed to clarify the role of exogenous TF on cardiomyocyte cell proliferation and apoptosis. TF was shown to have a dual action; low to moderate concentrations of TF induced cellular proliferation whilst in contrast, higher concentrations of TF were capable of initiating the extrinsic pathway of apoptosis in cardiomyocytes. In early stages of coronary atheroslcerosis, TF-mediated proliferation of the cardiomyocytes may function to compensate for the increased load. Although the present belief in biology considers cardiomyocytes to be terminally differentiated cells, recent studies have shown that the heart is not a terminally differentiated organ (Beltrami *et al.* 2003). Endogenous self-renewing, clonogenic and multipotent stem cells have been identified in the adult myocardium of human, mice and rat in response to injury (Anversa & Nagal-Ginard 2002, MacLennan & Schneider 2000). These cells are capable of generating three major cell types of the myocardium: myocytes, smooth muscle cells and endothelial vascular cells (Nagal-Ginard *et al.* 2005). At early stages of the disease, expression of TF may promote the proliferation of these cell types and hence, the differentiation and depletion of the progenitor cell population. However, at later stages of heart failure, high concentrations of TF can hasten cell depletion by the induction of cellular apoptosis. As a result, the remaining viable cells undergo hypertrophic growth to compensate for the decrease in cell number (Nadal-Ginard *et al.* 2003). Therefore, in addition to the up-regulation of MGF, TF may also indirectly participate in the

progression of cardiac hypertrophy. It has been shown that TF is capable of differential activation of signalling pathways (Ettelaie *et al.* 2006), the cellular outcome of these pathways are currently unknown. Candidate pathways involved in proliferation and/or apoptosis may be the p44/42 MAP kinase pathway, the JNK/STAT kinase pathway and the p38 pathway that have previously been identified to be activated by TF alone (Ettelaie *et al.* 2006) or in combination with FVIIa (Poulsen *et al.* 1998, Rao and Pendurthi 2005, Koul 2003). Examining the association between these pathways and the cellular events described above, would help to clarify the mechanisms involved in TF-mediated proliferation and apoptosis in cardiomyocytes. This may be achieved by investigating phosphorylated components of these pathways by western blot analysis, and through the use of specific reporter vectors for key pathways. Other pathways of significance include PI3-kinase, cyclic AMP/protein kinase A and protein kinase C that are known to be involved in cell growth and/or apoptosis (Clerk *et al.* 2003) and may also be involved in TF-mediated effects.

6.2 Potential role of tissue factor in ischemia/ reperfusion injury

During an ischemic event cardiac function deteriorates (Katz 2001) and the oxygen supply is limited (Reimer & Jennings 1992). Reperfusion after a moderate ischemic event causes a prolonged impairment of systolic and diastolic function but eventually recovers requiring no further treatment (Braunwald & Kloner 1982). However, during a more severe ischemic event, function is impaired on perfusion (Ito *et al.* 1987, Buffington & Rothfield 1995, Przyklenk 2001). However, appropriate treatment with positive inotropic agents such as dobutamine, epinephrine and amrinone (a phosphodiesterase III inhibitor) can improve recovery (Ito *et al.* 1987, Buffington &

Rothfield 1995, Przyklenk 2001). As previously mentioned, TF is capable of initiating the apoptotic pathway. Following an ischemic event, 80 % of the affected cardiomyocytes are apoptotic (Bardales *et al.* 1996). However, the fundamental consequences of exposure to TF in the heart have not been demonstrated.

To determine the potential role of TF in moderating cardiac function and thus its potential as an injurious agent, a preliminary experiment was carried out. Hearts from male Sprague-Dawely rats were perfused with a range of concentrations of TF (section 2.2.2.3) and myocardial function was recorded. The activity of TF, before and after circulation in the perfusions apparatus, was determined using the one-step prothrombin assay to ensure that the correct level of activity was being delivered to the heart. There was no evidence of the protein adhering to the apparatus. Exogenous TF appears to have a chronotropic effect in the heart rate, increasing rate to 302 bpm following administration of 50 nM TF (Figure 6.2a, Appendix A), and an inotropic effect in the left ventricular pressure of the healthy heart (Figure 6.2b, Appendix A). The mean oxygen consumption (MVO_2) was 2.5 μmoles per min per g of wet heart weight during the equilibration period, which did not change significantly with increasing TF concentrations (table 6.1, Appendix A). The rate pressure product (RPP) of the heart stabilised at 25 x 10^3 mmHg/min during the equilibration time and gradually increased with administration of TF (Figure 6.2c, Appendix A). These preliminary data indicates that low to moderate concentrations of TF, can act as a positive inotropic agent.

The degree of imbalance of oxygen supply and demand during an ischemic event is variable and thus can classify ischemia as mild, moderate or severe (Reimer &

Jennings 1992). The complete abolition of the blood flow to the myocardium results in irreversible injury in cardiomyocytes and subsequently to the death of the cells (Reimer & Jennings 1992). Hypoxia also leads to cardiomyocyte depletion as the supply of oxygen is insufficient to meet the requirement of the heart tissue (Keith Reimer & Jennings 1992). TF is expressed upon injury and, during myocardial ischemia, is shown to be up-regulated (Ikonomidis *et al.* 2005) in cells of the vasculature, including circulating monocytes, vascular endothelial cells, machrophages and smooth muscle cells (Nahara *et al.* 1994, Yesner *et al.* 1996, Chong *et al.* 2003). Up-regulation of TF expression has been associated with the increased expression of the proangiogenic molecule VEGF, and the decreased expression of the antiangiogenic molecule thrombospondin-1 (Pawlinski *et al.* 2004, Zhang *et al.* 1994). Therefore, during chronic mild or moderate ischemia, TF up-regulation in response to injury could be potentially beneficial by triggering angiogenesis with the intention of supplying the heart tissue with oxygen. Nevertheless its impact on apoptosis and cell preservation warrants further investigation.

The experiment outlined above was intended to provide preliminary data on the effect of TF in the function of the healthy adult heart. It is clearly apparent that TF has an inotropic effect and could be beneficial for the heart in case of injury or damage. Furthermore, a potential role of TF during ischemia arises through its ability to promote angiogenesis. Further experimentation could involve the use of experimental models and the TF effect during ischemia, ischemia pre-conditioning, reperfusion and post-conditioning (Downey & Cohen 2006). In addition, expression studies for VEGF

pre, during and post ischemia would be beneficial to understand the role of TF during coronary disease.

6.3 Limitations of the study

One of the limitations of this study was the use of the isolated adult cardiomyocytes. Aggressive enzyme digestions can results in low cell yield and viability and therefore a balance between digestion of the connective tissue but non-aggressive preparation is needed (Thum & Borlak 2000). Unfortunately, membrane damage cannot be determine in culture and thus changes in the pattern of the structural genes of the cells can occur, interfering with the experimental protocols (Thum & Borlak 2000), thus the discrepancy in the TF expression results in chapter 3. Furthermore, the cells cannot be maintained for prolonged periods as the process of cellular differentiations starts as early as on the fourth day in culture leading to the loss of rod-shaped morphology and changes in the cytoskeleton (Thum & Borlak 2000). Therefore freshly isolated cardiomycytes could not be used for long term expression studies.

The H9c2 cardiomyocytic cell line was used for experiments in chapter 4 and 5 since were easy to manipulate and use for long term experiments. However, H9c2 cells are not "true" cardiomyocytes, but a sub-clone of the original clonal cell line derived from the embryonic BD1X rat heart tissue by B. Kimes & B. Brandt, exhibiting many of the properties of skeletal muscle and also demonstrating some characteristics of cardiomyocytes including ANF expression and the slow type of myosin heavy chain. However, they are lucking structural gene expression like other isotopes of myosin heavy chain and spontaneous contractility, therefore are not suitable for morphological and physiological studies.

6.4 Scope for future experiments

In the present study, it was shown that increase in the pressure overload in rat harts, resulted in the increase in the expression of TF. It was found that the source of TF within the myocardium was not cardiomyocytes themselves but other cells (Chapter 3). At this stage, it would be beneficial to identify the source of cardiac-associated TF by using the aortic constriction model. Hearts from control and hypertrophic animals could be subjected to cell isolation, and cell separation to cardiomyocytes, fibroblasts and endothelial cells using the MACS cell isolation system. Further to this, the different cell types could be examined for TF expression by RT-PCR, western blot and ELISA. Moreover, co-localisation studies using heart sections subjected to paraffin fixation and probed for TF and structural proteins of the heart like visculin and desmin could provide further information in the TF expression and role within the hypertrophic myocardium.

The increase in TF concentration was found to have proliferative, differentiative and apoptotic influences on H9c2 cells (Chapter 4 and 5). More specific, TF has the ability in low concentrations to promote cellular proliferation and in higher concentrations to promote cellular apoptosis and also up-regulating the pro-differentiative gene MGF. Based on the above, further examination on the changes in the rate of cellular turnover in response to TF and the mechanism involved would be beneficial. The H9c2 cardiomyocytic cell line could be used and upon stimulation with TF the cells could be examine for activation of several signalling pathways, including the p44/42 MAPK pathway, the JNK-SAPK pathway and the p38 pathway. That could be achieved by measuring the level of phosphorylation of appropriate markers of the above pathways by western blot and through the use of specific reporter vectors. Furthermore,

beneficial would be the development of a specific antibody for MGF using phage display technology could further elucidate in the expression of MGF upon TF treatment in the H9c2 cells or other cells of the myocardium.

6.5 Final conclusion: "The influence and role of tissue factor in the pathogenesis of myocardial hypertrophy?"

In conclusion, pressure overload due to aortic constriction can result in an increase in TF expression in the heart. The expression of TFPI by cardiomyocytes in response to increased TF acts to contain the influence of TF. However, progressive elevation of TF can result in cellular proliferation as well as hypertrophic growth. In latter stages of heart failure, substantial elevation in TF results in cardiomyocyte depletion through cellular apoptosis which in turn may further exacerbate hypertrophic growth in the remaining cells. Therefore, TF plays an influential role during the progression of cardiac hypertrophy and the pathogenesis of heart disease.

APPENDIX A

Preliminary results

Appendix A: Preliminary results

Figure 6.2: The effect of exogenous TF in the heart rate, left ventricular developed pressure and the rate pressure product of the healthy heart.

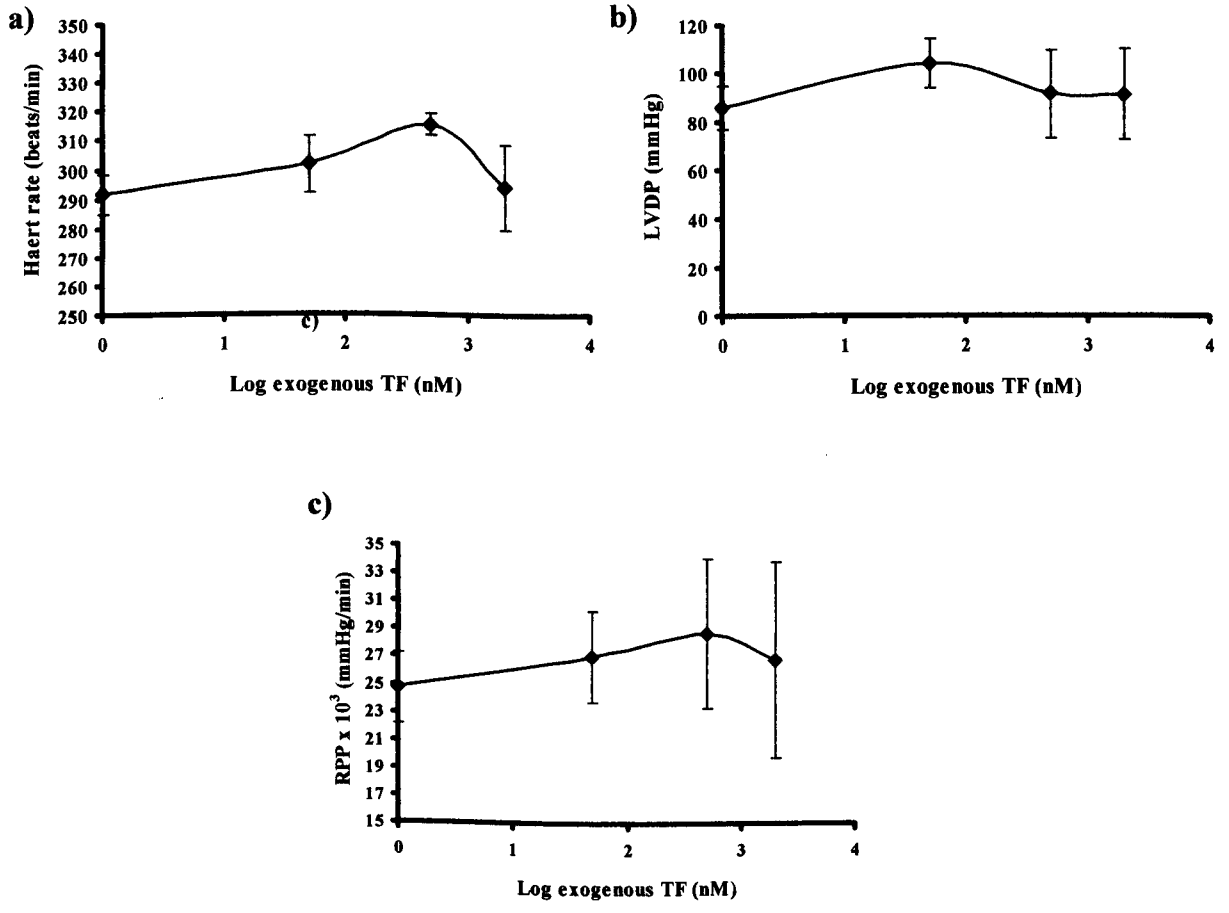

Four hearts were excised and cannulated via the aorta and subjected to retrograde perfusion by a modified isovolumic Langendorff method, using a range of exogenous TF concentrations (0.05, 0.5 and 2 μM). The heart rate (a) was recorded using a SensoNor 840 transducer connected to the MacLab recording system and then the LVDP (b) and the rate pressure product (c) was calculated as previously described in section 2.2.2.3.1. The data are presented as mean of n=16 taken from 4 different heart for each TF concentration ± SEM.

Table 6.1: Oxygen consumption during heart perfusions with different concentrations of exogenous TF.

	Equilibration period	**50 nM TF**	**500 nM TF**	**2 μM TF**
MVO_2 (μmoles O_2/min/g wet heart weight)	2.5 (±0.4)	2.6 (±0.9)	2.7 (±1.3)	2.4 (±0.7)

The mean oxygen consumption was calculated during perfusion with TF. There was no significant difference observed in the oxygen consumption upon perfusion with TF. The data are presented as mean of n=16 taken from 4 different heart for each TF concentration ± SEM.

REFERENCES

References

ABE, K., SHOJI, M., CHEN, J., BIERHAUS, A., DANAVE, I., MICKO, C., CASPER, K., DILLEHAY, D. L., NAWROTH, P. P. & RICKLES, F. R. (1999). Regulation of vascular endothelial growth factor production and angiogenesis by the cytoplasmic tail of tissue factor. *Proc Natl Acad Sci U S A* **96,** 8663-8668.

ALPERT, N. R., MULIERI, L. A. & LITTEN, R. Z. (1979). Functional significance of altered myosin adenosine triphosphatase activity in enlarged hearts. *Am J Cardiol* **44,** 946-953.

ANDERSON, P. A., GREIG, A., MARK, T. M., MALOUF, N. N., OAKELEY, A. E., UNGERLEIDER, R. M., ALLEN, P. D. & KAY, B. K. (1995). Molecular basis of human cardiac troponin T isoforms expressed in the developing, adult, and failing heart. *Circ Res* **76,** 681-686.

ANTOS, C. L. MCKINSEY, T. A., FREY N., KUTSCHKE W., MCANALLY J., SHELTON J. M., RICHARDSON J. A., HILL J. A., OLSON, E. N. (2002). Activated glycogen synthase-3β suppresses cardiac hypertrophy *in vivo*. *Proc. Natl. Acad. Sci. USA* **99**, 907-912.

ANVERSA, P., HILER, B., RICCI, R., GUIDERI, G. & OLIVETTI, G. (1986). Myocyte cell loss and myocyte hypertrophy in the aging rat heart. *J Am Coll Cardiol* **8,** 1441-1448.

ANVERSA, P. & NADAL-GINARD, B. (2002). Cardiac chimerism: methods matter. *Circulation* **106,** e129-31; author reply e129-131.

ANVERSA, P., OLIVETTI, G., LI, P., HERMAN, M. V. & CAPASSO, J. M. (1993). Myocardial infarction, cardiac anatomy and ventricular loading. *Cardioscience* **4,** 55-62.

ARAI, H., NAKAO, K., SAITO, Y., MORII, N., SUGAWARA, A., YAMADA, T., ITOH, H., SHIONO, S., MUKOYAMA, M., OHKUBO, H. & ET AL. (1988). Augmented

expression of atrial natriuretic polypeptide gene in ventricles of spontaneously hypertensive rats (SHR) and SHR-stroke prone. *Circ Res* **62,** 926-930.

ARBER, S., HUNTER, J. J., ROSS, J., JR., HONGO, M., SANSIG, G., BORG, J., PERRIARD, J. C., CHIEN, K. R. & CARONI, P. (1997). MLP-deficient mice exhibit a disruption of cardiac cytoarchitectural organization, dilated cardiomyopathy, and heart failure. *Cell* **88,** 393-403.

ARDISSINO, D., MERLINI, P. A., ARIENS, R., COPPOLA, R., BRAMUCCI, E. & MANNUCCI, P. M. (1997). Tissue-factor antigen and activity in human coronary atherosclerotic plaques. *Lancet* **349,** 769-771.

BACHMAIER, K., NEU, N., PUMMERER, C., DUNCAN, G. S., MAK, T. W., MATSUYAMA, T. & PENNINGER, J. M. (1997). iNOS expression and nitrotyrosine formation in the myocardium in response to inflammation is controlled by the interferon regulatory transcription factor 1. *Circulation* **96,** 585-591.

BAJAJ, M. S., KUPPUSWAMY, M. N., SAITO, H., SPITZER, S. G. & BAJAJ, S. P. (1990). Cultured normal human hepatocytes do not synthesize lipoprotein-associated coagulation inhibitor: evidence that endothelium is the principal site of its synthesis. *Proc Natl Acad Sci U S A* **87,** 8869-8873.

BAJAJ, M. S., STEER, S., KUPPUSWAMY, M. N., KISIEL, W. & BAJAJ, S. P. (1999). Synthesis and expression of tissue factor pathway inhibitor by serum-stimulated fibroblasts, vascular smooth muscle cells and cardiac myocytes. *Thromb Haemost* **82,** 1663-1672.

BARDALES, R. H., HAILEY, L. S., XIE, S. S., SCHAEFER, R. F. & HSU, S. M. (1996). In situ apoptosis assay for the detection of early acute myocardial infarction. *Am J Pathol* **149,** 821-829.

BARRESI, R., DI BLASI, C., NEGRI, T., BRUGNONI, R., VITALI, A., FELISARI, G., SALANDI, A., DANIEL, S., CORNELIO, F., MORANDI, L. & MORA, M. (2000). Disruption of heart sarcoglycan complex and severe cardiomyopathy caused

by beta sarcoglycan mutations. *J Med Genet* **37,** 102-107.

BAZAN, J. F. (1990). Structural design and molecular evolution of a cytokine receptor superfamily. *Proc Natl Acad Sci U S A* **87,** 6934-6938.

BELTING, M., DORRELL, M. I., SANDGREN, S., AGUILAR, E., AHAMED, J., DORFLEUTNER, A., CARMELIET, P., MUELLER, B. M., FRIEDLANDER, M. & RUF, W. (2004). Regulation of angiogenesis by tissue factor cytoplasmic domain signaling. *Nat Med* **10,** 502-509.

BELTRAMI, A. P., BARLUCCHI, L., TORELLA, D., BAKER, M., LIMANA, F., CHIMENTI, S., KASAHARA, H., ROTA, M., MUSSO, E., URBANEK, K., LERI, A., KAJSTURA, J., NADAL-GINARD, B. & ANVERSA, P. (2003). Adult cardiac stem cells are multipotent and support myocardial regeneration. *Cell* **114,** 763-776.

BENNETT, M. R., GIBSON, D. F., SCHWARTZ, S. M. & TAIT, J. F. (1995). Binding and phagocytosis of apoptotic vascular smooth muscle cells is mediated in part by exposure of phosphatidylserine. *Circ Res* **77,** 1136-1142.

BERRY, C., TOUYZ, R., DOMINICZAK, A. F., WEBB, R. C. & JOHNS, D. G. (2001). Angiotensin receptors: signaling, vascular pathophysiology, and interactions with ceramide. *Am J Physiol Heart Circ Physiol* **281,** H2337-2365.

BEUCKELMANN, D. J., NABAUER, M. & ERDMANN, E. (1992). Intracellular calcium handling in isolated ventricular myocytes from patients with terminal heart failure. *Circulation* **85,** 1046-1055.

BICKNELL, K. A., COXON, C. H., BROOKS, G. (2007). Can the cardiomyocyte cell cycle be reprogrammed? *J Mol Cell Cardiol* ***in press.***

BLOCH, K. D., SEIDMAN, J. G., NAFTILAN, J. D., FALLON, J. T. & SEIDMAN, C. E. (1986). Neonatal atria and ventricles secrete atrial natriuretic factor via tissue-specific secretory pathways. *Cell* **47,** 695-702.

BOATENG, S. Y., SEYMOUR, A. M., BHUTTA, N. S., DUNN, M. J., YACOUB, M. H. & BOHELER, K. R. (1998). Sub-antihypertensive doses of ramipril normalize sarcoplasmic reticulum calcium ATPase expression and function following cardiac hypertrophy in rats. *J Mol Cell Cardiol* **30,** 2683-2694.

BOWLING, N., WALSH, R. A., SONG, G., ESTRIDGE, T., SANDUSKY, G. E., FOUTS, R. L., MINTZE, K., PICKARD, T., RODEN, R., BRISTOW, M. R., SABBAH, H. N., MIZRAHI, J. L., GROMO, G., KING, G. L. & VLAHOS, C. J. (1999). Increased protein kinase C activity and expression of Ca2+-sensitive isoforms in the failing human heart. *Circulation* **99,** 384-391.

BRADFORD, M. M. (1976). A rapid and sensitive method for the quantification of microgram quantities of protein utilizing the principle of protein-dye binding. *Anal Biochem* **72,** 248-254.

BRAUNWALD, E. & BRISTOW, M. R. (2000). Congestive heart failure: fifty years of progress. *Circulation* **102,** IV14-23.

BRAUNWALD, E. & KLONER, R. A. (1982). The stunned myocardium: prolonged, postischemic ventricular dysfunction. *Circulation* **66,** 1146-1149.

BRAZ, J. C., BUENO, O. F., LIANG, Q., WILKINS, B. J., DAI, Y. S., PARSONS, S., BRAUNWART, J., GLASCOCK, B. J., KLEVITSKY, R., KIMBALL T. F., HEWETT, T. E., MOLKENTIN, J. D. (2003). Targeted inhibition of p38 MAPK promotes hypertrophic cardiomyopathy through upregulation of calcineurin-NFAT signaling. *J. Clin. Invest.* **111**, 1475-1486.

BRENNER, B. M., BALLERMANN, B. J., GUNNING, M. E. & ZEIDEL, M. L. (1990). Diverse biological actions of atrial natriuretic peptide. *Physiol Rev* **70,** 665-699.

BRISTOW, M. R. (2000). beta-adrenergic receptor blockade in chronic heart failure. *Circulation* **101,** 558-569.

BRODSKY, G. L., MUNTONI, F., MIOCIC, S., SINAGRA, G., SEWRY, C. & MESTRONI, L. (2000). Lamin A/C gene mutation associated with dilated cardiomyopathy with variable skeletal muscle involvement. *Circulation* **101,** 473-476.

BROMBERG, M. E., BAILLY, M. A. & KONIGSBERG, W. H. (2001). Role of protease-activated receptor 1 in tumor metastasis promoted by tissue factor. *Thromb Haemost* **86,** 1210-1214.

BROMBERG, M. E., KONIGSBERG, W. H., MADISON, J. F., PAWASHE, A. & GAREN, A. (1995). Tissue factor promotes melanoma metastasis by a pathway independent of blood coagulation. *Proc Natl Acad Sci U S A* **92,** 8205-8209.

BROMBERG, M. E., SUNDARAM, R., HOMER, R. J., GAREN, A. & KONIGSBERG, W. H. (1999). Role of tissue factor in metastasis: functions of the cytoplasmic and extracellular domains of the molecule. *Thromb Haemost* **82,** 88-92.

BROMME, H. J. & HOLTZ, J. (1996). Apoptosis in the heart: when and why? *Mol Cell Biochem* **163-164,** 261-275.

BROZE, G. J., JR. (1992). The role of tissue factor pathway inhibitor in a revised coagulation cascade. *Semin Hematol* **29,** 159-169.

BROZE, G. J., JR. (1995). Tissue factor pathway inhibitor. *Thromb Haemost* **74,** 90-93.

BROZE, G. J., JR., LEYKAM, J. E., SCHWARTZ, B. D. & MILETICH, J. P. (1985). Purification of human brain tissue factor. *J Biol Chem* **260,** 10917-10920.

BROZE, G. J., JR. & MILETICH, J. P. (1987). Isolation of the tissue factor inhibitor produced by HepG2 hepatoma cells. *Proc Natl Acad Sci U S A* **84,** 1886-1890.

BUFFINGTON, C. W. & ROTHFIELD, K. P. (1995). Effects of intracoronary calcium chloride on the postischemic heart in pigs. *Ann Thorac Surg* **59,** 1448-1455.

BUGAISKY, E., GUPTA, M., GUPTA, M. P. & ZAK, R. (1992). *Cellular and molecular mechanisms of cardiac hypertrophy*, 2nd edition. Raven Press Ltd., New York.

BUGGE, T. H., XIAO, Q., KOMBRINCK, K. W., FLICK, M. J., HOLMBACK, K., DANTON, M. J., COLBERT, M. C., WITTE, D. P., FUJIKAWA, K., DAVIE, E. W. & DEGEN, J. L. (1996). Fatal embryonic bleeding events in mice lacking tissue factor, the cell-associated initiator of blood coagulation. *Proc Natl Acad Sci U S A* **93,** 6258-6263.

BURNETT, J. C., JR., KAO, P. C., HU, D. C., HESER, D. W., HEUBLEIN, D., GRANGER, J. P., OPGENORTH, T. J. & REEDER, G. S. (1986). Atrial natriuretic peptide elevation in congestive heart failure in the human. *Science* **231,** 1145-1147.

CALDERONE, A., THAIK, C. M., TAKAHASHI, N., CHANG, D. L. & COLUCCI, W. S. (1998). Nitric oxide, atrial natriuretic peptide, and cyclic GMP inhibit the growth-promoting effects of norepinephrine in cardiac myocytes and fibroblasts. *J Clin Invest* **101,** 812-818.

CAMERER, E., GJERNES, E., WIIGER, M., PRINGLE, S. & PRYDZ, H. (2000). Binding of factor VIIa to tissue factor on keratinocytes induces gene expression. *J Biol Chem* **275,** 6580-6585.

CAMERER, E., HUANG, W. & COUGHLIN, S. R. (2000). Tissue factor- and factor X-dependent activation of protease-activated receptor 2 by factor VIIa. *Proc Natl Acad Sci U S A* **97,** 5255-5260.

CAMERER, E., KOLSTO, A. B. & PRYDZ, H. (1996). Cell biology of tissue factor, the principal initiator of blood coagulation. *Thromb Res* **81,** 1-41.

CAMERER, E., ROTTINGEN, J. A., GJERNES, E., LARSEN, K., SKARTLIEN, A. H., IVERSEN, J. G. & PRYDZ, H. (1999). Coagulation factors VIIa and Xa induce cell signaling leading to up-regulation of the egr-1 gene. *J Biol Chem* **274,** 32225-32233.

CAMERER, E., ROTTINGEN, J. A., IVERSEN, J. G. & PRYDZ, H. (1996). Coagulation factors VII and X induce Ca2+ oscillations in Madin-Danby canine. *J Biol*

Chem **271,** 29034-29042.

CAO, L. & GARDNER, D. G. (1995). Natriuretic peptides inhibit DNA synthesis in cardiac fibroblasts. *Hypertension* **25,** 227-234.

CAREY, R. M., HOWELL, N. L., JIN, X. H. & SIRAGY, H. M. (2001). Angiotensin type 2 receptor-mediated hypotension in angiotensin type-1 receptor-blocked rats. *Hypertension* **38,** 1272-1277.

CARMELIET, P. & COLLEN, D. (1998). Molecules in focus tissue factor. *Int J Biochem Cell Biol* **30,** 661-667.

CARMELIET, P., MACKMAN, N., MOONS, L., LUTHER, T., GRESSENS, P., VAN VLAENDEREN, I., DEMUNCK, H., KASPER, M., BREIER, G., EVRARD, P., MULLER, M., RISAU, W., EDGINGTON, T. & COLLEN, D. (1996). Role of tissue factor in embryonic blood vessel development. *Nature* **383,** 73-75.

CARSON, S. D., PERRY, G. A. & PIRRUCCELLO, S. J. (1994). Fibroblast tissue factor: calcium and ionophore induce shape changes, release of membrane vesicles, and redistribution of tissue factor antigen in addition to increased procoagulant activity. *Blood* **84,** 526-534.

CHANG, K. C., FIGUEREDO, V. M., SCHREUR, J. H., KARIYA, K., WEINER, M. W., SIMPSON, P. C. & CAMACHO, S. A. (1997). Thyroid hormone improves function and Ca2+ handling in pressure overload hypertrophy. Association with increased sarcoplasmic reticulum Ca2+-ATPase and alpha-myosin heavy chain in rat hearts. *J Clin Invest* **100,** 1742-1749.

CHAVRIER, P., ZERIAL, M., LEMAIRE, P., ALMENDRAL, J., BRAVO, R. & CHARNAY, P. (1988). A gene encoding a protein with zinc fingers is activated during G0/G1 transition in culture cells. *EMBO J* **7,** 29-35.

CHEN, Y. F., DURAND, J. & CLAYCOMB, W. C. (1997). Hypoxia stimulates atrial natriuretic peptide gene expression in cultured atrial cardiocytes. *Hypertension*

29, 75-82.

CHIEN, K. R. (1992). Signaling mechanism for the activation of an embryonic gene program during the hypertrophy of cardiac ventricular muscle. *Basic Res Cardiol* **87Suppl 2,** 49-58.

CHIEN, K. R., KNOWLTON, K. U., ZHU, H. & CHIEN, S. (1991). Regulation of cardiac gene expression during myocardial growth and hypertrophy: molecular studies of an adaptive physiological response. *Faseb J* **5,** 3037-3046.

CHIEN, K. R., ZHU, H., KNOWLTON, K. U., MILLER-HANCE, W., VAN-BILSEN, M., O'BRIEN, T. X. & EVANS, S. M. (1993). Transcriptional regulation during cardiac growth and development. *Annu Rev Physiol* **55,** 77-95.

CHINKERS, M. & GARBERS, D. L. (1991). Signal transduction by guanylyl cyclases. *Annu Rev Biochem* **60,** 553-575.

CHONG, A. J., POHLMAN, T. H., HAMPTON, C. R., SHINAMOTO, A., MACKMAN, N. & VERRIER, E. D. (2003). Tissue factor and thrombin mediated myocardial ishemia-reperfusion injury. *Ann Thorac Surg* **75,** S649-655.

CHRISTY, B. A., LAU, L. F. & NATHANS, D. (1988). A gene activated in mouse 3T3 cells by serum growth factors encodes a protein with "zinc finger" sequences. *Proc Natl Acad Sci U S A* **85,** 7857-7861.

CICALA, C. & CIRINO, G. (1998). Linkage between inflammation and coagulation: an update on the molecular vasis of the crosstalk. *Life Sci* **62,** 1817-1824.

CIRILLO, P., CALI, G., GOLINO, P., CALABRO, P., FORTE, L., DE ROSA, S., PACILEO, M., RAGNI, M., SCOPACASA, F., NITSCH, L. & CHIARIELLO, M. (2004). Tissue factor binding of activated factor VII triggers smooth muscle cell proliferation via extracellular signal-regulated kinase activation. *Circulation* **109,** 2911-2916.

CLERK, A. (2003). The radical balance between life and death. *J Mol Cell Cardiol* **35,**

599-602.

COERPER, S., WOLF, S., VON KIPARSKI, S., THOMAS, S., ZITTEL, T. T., RANKE, M. B., HUNT, T. K. & BECKER, H. D. (2001). Insulin-like growth factor I accelerates gastric ulcer healing by stimulating cell proliferation and by inhibiting gastric acid secretion. *Scand J Gastroenterol* **36,** 921-927.

CORY, S. & ADAMS, J. M. (2002). The Bcl2 family: regulators of the cellular life-or-death switch. *Nat Rev Cancer* **2,** 647-656.

CUI, M. Z., PARRY, G. C., OETH, P., LARSON, H., SMITH, M., HUANG, R. P., ADAMSON, E. D. & MACKMAN, N. (1996). Transcriptional regulation of the tissue factor gene in human epithelial cells is mediated by Sp1 and EGR-1. *J Biol Chem* **271,** 2731-2739.

CUI, M. Z., ZHAO, G., WINOKUR, A. L., LAAG, E., BYDASH, J. R., PENN, M. S., CHISOLM, G. M. & XU, X. (2003). Lysophosphatidic acid induction of tissue factor expression in aortic smooth muscle cells. *Arterioscler Thromb Vasc Biol* **23,** 224-230.

D'ANGELO, D. D., SAKATA, Y., LORENZ, J. N., BOIVIN, G. P., WALSH, R. A., LIGGETT, S. B. & DORN, I. I. G. W. N. (1997). Transgenic Galphaq overexpression induces cardiac contractile failure in mice. *Proc Natl Acad Sci U S A* **94,** 8121-8126.

DAVIS, R. J. (2000). Signal transduction by the JNK group of MAP kinases. *Cell* **103,** 239-252.

DAY, M. L., SCHWARTZ, D., WIEGAND, R. C., STOCKMAN, P. T., BRUNNERT, S. R., TOLUNAY, H. E., CURRIE, M. G., STANDAERT, D. G. & NEEDLEMAN, P. (1987). Ventricular atriopeptin. Unmasking of messenger RNA and peptide synthesis by hypertrophy or dexamethasone. *Hypertension* **9,** 485-491.

DE BOLD, A. J., MA, K. K., ZHANG, Y., DE BOLD, M. L., BENSIMON, M. &

KHOSHBATEN, A. (2001). The physiological and pathophysiological modulation of the endocrine function of the heart. *Can J Physiol Pharmacol* **79,** 705-714.

DIAMANT, M., NIEUWLAND, R., PABLO, R. F., STURK, A., SMIT, J. W. & RADDER, J. K. (2002). Elevated numbers of tissue-factor exposing microparticles correlate with components of the metabolic syndrome in uncomplicated type 2 diabetes mellitus. *Circulation* **106,** 2442-2447.

DIPLA, K., MATTIELLO, J. A., JEEVANANDAM, V., HOUSER, S. R. & MARGULIES, K. B. (1998). Myocyte recovery after mechanical circulatory support in humans with end-stage heart failure. *Circulation* **97,** 2316-2322.

DONG, F., ESBERG, L. B., ROUGHEAD, Z. K., REN, J. & SAARI, J. T. (2005). Increased contractility of cardiomyocytes from copper-deficient rats is associated with upregulation of cardiac IGF-1 receptor. *Am J Physiol Heart Circ Physiol* **289,** H78-84.

DOSHI, S. N. & MARMUR, J. D. (2002). Evolving role of tissue factor and its pathway inhibitor. *Crit Care Med* **30,** S241-250.

DOWNEY, J. M. & COHEN, M. V. (2006). Reducing infarct size in the setting of acute myocardial infarction. *Prog Cardiovasc Dis* **48,** 363-371.

DRAKE, T. A., MORRISSEY, J. H. & EDGINGTON, T. S. (1989). Selective cellular expression of tissue factor in human tissues. Implications for disorders of hemostasis and thrombosis. *Am J Pathol* **134,** 1087-97.

DREXLER, H., HANZE, J., FINCKH, M., LU, W., JUST, H. & LANG, R. E. (1989). Atrial natriuretic peptide in a rat model of cardiac failure. Atrial and ventricular mRNA, atrial content, plasma levels, and effect of volume loading. *Circulation* **79,** 620-633.

EDGINGTON, T. S., MACKMAN, N., BRAND, K. & RUF, W. (1991). The structural biology of expression and function of tissue factor. *Thromb Haemost* **66,** 67-

79.

EDWARDS, B. S., ACKERMANN, D. M., LEE, M. E., REEDER, G. S., WOLD, L. E. & BURNETT, J. C., JR. (1988). Identification of atrial natriuretic factor within ventricular tissue in hamsters and humans with congestive heart failure. *J Clin Invest* **81,** 82-86.

EICHHORN, E. J. & BRISTOW, M. R. (1996). Medical therapy can improve the biological properties of the chronically failing heart. Anew era in the treatment of heart failure. *Circulation* **94,** 2285-2296.

ENGEL, A. M. & LOWE, D. G. (1995). Characterization of the hormone binding site of natriuretic peptide receptor-C. *FEBS Lett* **360,** 169-172.

ENTMAN, M. L., MICHAEL, L., ROSSEN, R. D., DREYER, W. J., ANDERSON, D. C., TAYLOR, A. A. & SMITH, C. W. (1991). Inflammation in the course of early myocardial ischemia. *Faseb J* **5,** 2529-2537.

ETTELAIE, C., LI, C., COLLIER, M. E. W., PRADIER, A., FRENTZOU, G. A., WOOD, C. G., CHETTER, I. C., MCCOLLUM, P. T., BRIUCKDORFER, K. R. & JAMES, N. J. (2006). Differential functions of cellular signalling pathways. *Atherosclerosis* ***in press.***

FALCIANI, M., GORI, A. M., FEDI, S., CHIARUGI, L., SIMONETTI, I., DABIZZI, R. P., PRISCO, D., PEPE, G., ABBATE, R., GENSINI, G. F. & NERI SERNERI, G. G. (1998). Elevated tissue factor and tissue factor pathway inhibitor circulating levels in ischaemic heart disease patients. *Thromb Haemost* **79,** 495-499.

FAN, L., YOTOV, W. V., ZHU, T., ESMAILZADEH, L., JOYAL, J. S., SENNLAUB, F., HEVEKER, N., CHEMTOB, S. & RIVARD, G. E. (2005). Tissue factor enhances protease-activated receptor-2-mediated factor VIIa cell proliferative properties. *J Thromb Haemost* **3,** 1056-1063.

FATKIN, D., MACRAE, C., SASAKI, T., WOLFF, M. R., PORCU, M., FRENNEAUX, M.,

ATHERTON, J., VIDAILLET, H. J., JR., SPUDICH, S., DE GIROLAMI, U., SEIDMAN, J. G., SEIDMAN, C., MUNTONI, F., MUEHLE, G., JOHNSON, W. & MCDONOUGH, B. (1999). Missense mutations in the rod domain of the lamin A/C gene as causes of dilated cardiomyopathy and conduction-system disease. *N Engl J Med* **341,** 1715-1724.

FELDMAN, A. M., WEINBERG, E. O., RAY, P. E. & LORELL, B. H. (1993). Selective changes in cardiac gene expression during compensated hypertrophy and the transition to cardiac decompensation in rats with chronic aortic banding. *Circ Res* **73,** 184-192.

FLECK, R. A., RAO, L. V., RAPAPORT, S. I. & VARKI, N. (1990). Localization of human tissue factor antigen by immunostaining with monospecific, polyclonal anti-human tissue factor antibody. *Thromb Res* **59,** 421-437.

FLOSSEL, C., LUTHER, T., MULLER, M., ALBRECHT, S. & KASPER, M. (1994). Immunohistochemical detection of tissue factor (TF) on paraffin sections of routinely fixed human tissue. *Histochemistry* **101,** 449-453.

FRANCH, H. A., DIXON, R. A., BLAINE, E. H. & SIEGL, P. K. (1988). Ventricular atrial natriuretic factor in the cardiomyopathic hamster model of congestive heart failure. *Circ Res* **62,** 31-36.

FRANCO, D., GALLEGO, A., HABETS, P. E., SANS-COMA, V. & MOORMAN, A. F. (2002). Species-specific differences of myosin content in the developing cardiac chambers of fish, birds, and mammals. *Anat Rec* **268,** 27-37.

FREY, N. & OLSON, E. N. (2003). Cardiac hypertrophy: the good, the bad, and the ugly. *Annu Rev Physiol* **65,** 45-79.

FREY, N. BARRIENTOS, T., SHELTON, J. M., FRANK, D., RUTTEN, H., GEHRING, D., KUHN, C., LUTZ, M., ROTHERMEL, B., BASSEL-DUBY, R., RICHARDSON, J. A., KATUS, H. A., HILL, J. A., OLSON, E. N. (2004). Mice lacking calsarcin-1 are sensitized to calcineurin signalling and show accelerated cardiomyopathy in

response to pathological biomechanical stress. *Nat Med* **10**, 1336-1343.

GANGULY, P. K., LEE, S. L., BEAMISH, R. E. & DHALLA, N. S. (1989). Altered sympathetic system and adrenoceptors during the development of cardiac hypertrophy. *Am Heart J* **118,** 520-525.

GARDNER, D. G. (2003). Natriuretic peptides: markers or modulators of cardiac hypertrophy? *Trends Endocrinol Metab* **14,** 411-416.

GERDES, A. M., KELLERMAN, S. E., MOORE, J. A., MUFFLY, K. E., CLARK, L. C., REAVES, P. Y., MALEC, K. B., MCKEOWN, P. P. & SCHOCKEN, D. D. (1992). Structural remodeling of cardiac myocytes in patients with ischemic cardiomyopathy. *Circulation* **86,** 426-430.

GHRIB, F., BRISSET, A. C., DUPOUY, D., TERRISSE, A. D., NAVARRO, C., CADROY, Y., BONEU, B. & SIE, P. (2002). The expression of tissue factor and tissue factor pathway inhibitor in aortic smooth muscle cells is up-regulated in synthetic compared to contractile phenotype. *Thromb Haemost* **87,** 1051-1056.

GIRARD, T. J., WARREN, L. A., NOVOTNY, W. F., LIKERT, K. M., BROWN, S. G., MILETICH, J. P. & BROZE, G. J., JR. (1989). Functional significance of the Kunitz-type inhibitory domains of lipoprotein-associated coagulation inhibitor. *Nature* **338,** 518-520.

GLEMBOTSKI, C. C., IRONS, C. E., KROWN, K. A., MURRAY, S. F., SPRENKLE, A. B. & SEI, C. A. (1993). Myocardial alpha-thrombin receptor activation induces hypertrophy and increases atrial natriuretic factor gene expression. *J Biol Chem* **268,** 20646-20652.

GOLDSPINK, D. F. & GOLDSPINK, G. (1986). *Electrical stimulation neuromuscular disorders*. Springer-Verlag, London.

GOLDSPINK, G. (1999). Changes in muscle mass and phenotype and the expression of autocrine and systemic growth factors by muscle in response to stretch and

overload. *J Anat* **194 (Pt 3),** 323-334.

GOLDSPINK, G. (2002). Gene expression in skeletal muscle. *Biochem Soc Trans* **30,** 285-290.

GOLDSPINK, G., SCUTT, A., LOUGHNA, P. T., WELLS, D. J., JAENICKE, T. & GERLACH, G. F. (1992). Gene expression in skeletal muscle in response to stretch and force generation. *Am J Physiol* **262,** R356-363.

GOPISETTY, G., RAMACHANDRAN, K. & SINGAL, R. (2006). DNA methylation and apoptosis. *Mol Immunol* **43,** 1729-1740.

GRIFFIN, G. E., WILLIAMS, P. E. & GOLDSPINK, G. (1971). Region of longitudinal growth in striated muscle fibres. *Nat New Biol* **232,** 28-29.

GROSSMAN, W., JONES, D. & MCLAURIN, L. P. (1975). Wall stress and patterns of hypertrophy in the human left ventricle. *J Clin Invest* **56,** 56-64.

GWATHMEY, J. K. & MORGAN, J. P. (1985). Altered calcium handling in experimental pressure-overload hypertrophy in the ferret. *Circ Res* **57,** 836-843.

HAMADA, K., KURATSU, J., SAITOH, Y., TAKESHIMA, H., NISHI, T. & USHIO, Y. (1996). Expression of tissue factor in glioma. *Noshuyo Byori* **13,** 115-118.

HAMURO, T., KAMIKUBO, Y., NAKAHARA, Y., MIYAMOTO, S. & FUNATSU, A. (1998). Human recombinant tissue factor pathway inhibitor induces apoptosis in cultured human endothelial cells. *FEBS Lett* **421,** 197-202.

HAN, X., TU, Z., WANG, X., SHEN, S. & HOU, Y. (2004). Nonylphenol induced apoptosis in rat testis through the Fas/FasL pathway. *Bull Environ Contam Toxicol* **73,** 620-627.

HANGARTNER, J. R., MARLEY, N. J., WHITEHEAD, A., THOMAS, A. C. & DAVIES, M. J. (1985). The assessment of cardiac hypertrophy at autopsy. *Histopathology* **9,** 1295-1306.

HARRIDGE, S. D. (2003). Ageing and local growth factors in muscle. *Scand J Med Sci Sports* **13,** 34-39.

HART, G. (2003). Exercise-induced hypertrophy: a substrate for sudden death in athletes? *Exp. Physiol.* **88,** 639-644.

HARTZELL, S., RYDER, K., LANAHAN, A., LAU, L. F. & NATHAN, D. (1989). A growth factor-responsive gene of murine BALB/c 3T3 cells encodes a protein homologous to human tissue factor. *Mol Cell Biol* **9,** 2567-2573.

HAUNSTETTER, A. & IZUMO, S. (1998). Apoptosis: basic mechanisms and implications for cardiovascular disease. *Circ Res* **82,** 1111-1129.

HAZEL, T. G., NATHANS, D. & LAU, L. F. (1988). A gene inducible by serum growth factors encodes a member of the steroid and thyroid hormone receptor superfamily. *Proc Natl Acad Sci U S A* **85,** 8444-8448.

HEIN, S., KOSTIN, S., HELING, A., MAENO, Y. & SCHAPER, J. (2000). The role of the cytoskeleton in heart failure. *Cardiovasc Res* **45,** 273-278.

HEINEKE, J. & MOLKENTIN, J. D. (2006). Regulation of cardiac hypertrophy by intracellular signaling pathways. *Nature* **7,** 589-600.

HIRZEL, H. O., TUCHSCHMID, C. R., SCHNEIDER, J., KRAYENBUEHL, H. P. & SCHAUB, M. C. (1985). Relationship between myosin isoenzyme composition, hemodynamics, and myocardial structure in various forms of human cardiac hypertrophy. *Circ Res* **57,** 729-740.

HJORTOE, G. M., PETERSEN, L. C., ALBREKTSEN, T., SORENSEN, B. B., NORBY, P. L., MANDAL, S. K., PENDURTHI, U. R. & RAO, L. V. (2004). Tissue factor-factor VIIa-specific up-regulation of IL-8 expression in MDA-MB-231 cells is mediated by PAR-2 and results in increased cell migration. *Blood* **103,** 3029-3037.

HOCKENBERY, D., NUNEZ, G., MILLIMAN, C., SCHREIBER, R. D. & KORSMEYER, S. J. (1990). Bcl-2 is an inner mitochondrial membrane protein that blocks programmed cell death. *Nature* **348,** 334-336.

HOFFMAN, M. (2003). Remodeling the blood coagulation cascade. *J Thromb Thrombolysis* **16,** 17-20.

HOLSCHERMANN, H., BOHLE, R. M., SCHMIDT, H., ZELLER, H., FINK, L., STAHL, U., GRIMM, H., TILLMANNS, H. & HABERBOSCH, W. (2000). Hirudin reduces tissue factor expression and attenuates graft arteriosclerosis in rat cardiac allografts. *Circulation* **102,** 357-363.

HOLSCHERMANN, H., BOHLE, R. M., ZELLER, H., SCHMIDT, H., STAHL, U., FINK, L., GRIMM, H., TILLMANNS, H. & HABERBOSCH, W. (1999). In situ detection of tissue factor within the coronary intima in rat cardiac allograft vasculopathy. *Am J Pathol* **154,** 211-220.

HOLTWICK, R., GOTTHARDT, M., SKRYABIN, B., STEINMETZ, M., POTTHAST, R., ZETSCHE, B., HAMMER, R. E., HERZ, J. & KUHN, M. (2002). Smooth muscle-selective deletion of guanylyl cyclase-A prevents the acute but not chronic effects of ANP on blood pressure. *Proc Natl Acad Sci U S A* **99,** 7142-7147.

HORIO, T., NISHIKIMI, T., YOSHIHARA, F., MATSUO, H., TAKISHITA, S. & KANGAWA, K. (2000). Inhibitory regulation of hypertrophy by endogenous atrial natriuretic peptide in cultured cardiac myocytes. *Hypertension* **35,** 19-24.

HORIUCHI, M., AKISHITA, M. & DZAU, V. J. (1999). Recent progress in angiotensin II type 2 receptor research in the cardiovascular system. *Hypertension* **33,** 613-621.

HOUSER, S. R. & MARGULIES, K. B. (2003). Is depressed myocyte contractility centrally involved in heart failure? *Circ Res* **92,** 350-358.

HUANG, Z. F., HIGUCHI, D., LASKY, N. & BROZE, G. J., JR. (1997). Tissue factor pathway inhibitor gene disruption produces intrauterine lethality in mice. *Blood* **90,** 944-951.

HUANG, Z. F., WUN, T. C. & BROZE, G. J., JR. (1993). Kinetics of factor Xa inhibition by tissue factor pathway inhibitor. *J Biol Chem* **268,** 26950-26955.

HUTTER, R., VALDIVIEZO, C., SAUTER, B. V., SAVONTAUS, M., CHERESHNEV, I., CARRICK, F. E., BAURIEDEL, G., LUDERITZ, B., FALLON, J. T., FUSTER, V. & BADIMON, J. J. (2004). Caspase-3 and tissue factor expression in lipid-rich plaque macrophages: evidence for apoptosis as link between inflammation and atherothrombosis. *Circulation* **109,** 2001-2008.

ICHIHARA, S., SENBONMATSU, T., PRICE, E., JR., ICHIKI, T., GAFFNEY, F. A. & INAGAMI, T. (2001). Angiotensin II type 2 receptor is essential for left ventricular hypertrophy and cardiac fibrosis in chronic angiotensin II-induced hypertension. *Circulation* **104,** 346-351.

IHLE, J. N., WITTHUHN, B. A., QUELLE, F. W., YAMAMOTO, K. & SILVENNOINEN, O. (1995). Signaling through the hematopoietic cytokine receptors. *Annu Rev Immunol* **13,** 369-398.

IKONOMIDIS, I., ATHANASSOPOULOS, G., LEKAKIS, J., VENETSANOU, K., MARINOU, M., STAMATELOPOULOS, K., COKKINOS, D. V. & NIHOYANNOPOULOS, P. (2005). Myocardial ischemia induces interleukin-6 and tissue factor production in patients with coronary artery disease: a dobutamine stress echocardiography study. *Circulation* **112,** 3272-3279.

ITO, B. R., TATE, H., KOBAYASHI, M. & SCHAPER, W. (1987). Reversibly injured, postischemic canine myocardium retains normal contractile reserve. *Circ Res* **61,** 834-846.

ITOH, G., TAMURA, J., SUZUKI, M., SUZUKI, Y., IKEDA, H., KOIKE, M., NOMURA, M., JIE, T. & ITO, K. (1995). DNA fragmentation of human infarcted myocardial cells demonstrated by the nick end labeling method and DNA agarose gel

electrophoresis. *Am J Pathol* **146,** 1325-1331.

IZUMO, S., LOMPRE, A. M., MATSUOKA, R., KOREN, G., SCHWARTZ, K., NADAL-GINARD, B. & MAHDAVI, V. (1987). Myosin heavy chain messenger RNA and protein isoform transitions during cardiac hypertrophy. Interaction between hemodynamic and thyroid hormone-induced signals. *J Clin Invest* **79,** 970-977.

IZUMO, S., NADAL-GINARD, B. & MAHDAVI, V. (1988). Protooncogene induction and reprogramming of cardiac gene expression produced by pressure overload. *Proc Natl Acad Sci U S A* **85,** 339-343.

JAMES, T. N. (1994). Normal and abnormal consequences of apoptosis in the human heart. From postnatal morphogenesis to paroxysmal arrhythmias. *Circulation* **90,** 556-573.

JAMES, T. N., ST MARTIN, E., WILLIS, P. W., 3RD & LOHR, T. O. (1996). Apoptosis as a possible cause of gradual development of complete heart block and fatal arrhythmias associated with absence of the AV node, sinus node, and internodal pathways. *Circulation* **93,** 1424-1438.

JIANG, T., KUZNETSOV, V., PAK, E., ZHANG, H., ROBINSON, R. B. & STEINBERG, S. F. (1996). Thrombin receptor actions in neonatal rat ventricular myocytes. *Circ Res* **78,** 553-563.

JOSEPH, L. J., LE BEAU, M. M., JAMIESON, G. A. J., ACHARYA, S., SHOWS, T. B., ROWLEY, J. D. & SUKHATME, V. P. (1988). Molecular cloning, sequencing, and mapping of EGR2, a human early growth response gene encoding a protein with "zinc-binding" structure. *Proc Natl Acad Sci U S A* **85,** 7164-7168.

JUDE, B., ZAWADZKI, C., SUSEN, S. & CORSEAUX, D. (2005). Relevance of tissue factor in cardiovascular disease. *Arch Mal Coeur Vaiss* **98,** 667-671.

KAMIKUBO, Y., NAKAHARA, Y., TAKEMOTO, S., HAMURO, T., MIYAMOTO, S. &

FUNATSU, A. (1997). Human recombinant tissue-factor pathway inhibitor prevents the proliferation of cultured human neonatal aortic smooth muscle cells. *FEBS Lett* **407,** 116-120.

KANG, Y. H., LEE, E., CHOI, M. K., KU, J. L., KIM, S. H., PARK, Y. G. & LIM, S. J. (2004). Role of reactive oxygen species in the induction of apoptosis by alpha-tocopheryl succinate. *Int J Cancer* **112,** 385-392.

KANG, Y. H., YI, M. J., KIM, M. J., PARK, M. T., BAE, S., KANG, C. M., CHO, C. K., PARK, I. C., PARK, M. J., RHEE, C. H., HONG, S. I., CHUNG, H. Y., LEE, Y. S. & LEE, S. J. (2004). Caspase-independent cell death by arsenic trioxide in human cervical cancer cells: reactive oxygen species-mediated poly(ADP-ribose) polymerase-1 activation signals apoptosis-inducing factor release from mitochondria. *Cancer Res* **64,** 8960-8967.

KATZ, A. M. (1994). The cardiomyopathy of overload: an unnatural growth response in the hypertrophied heart. *Ann Intern Med* **121,** 363-371.

KATZ, A. M. (2000). Cytoskeletal abnormalities in the failing heart: out on a LIM? *Circulation* **101,** 2672-2683.

KATZ, A. M. (2001). A growth of ideas: role of calcium as activator of cardiac contraction. *Cardiovasc Res* **52,** 8-13.

KATZ, A. M. (2003). Heart failure: a hemodynamic disorder complicated by maladaptive proliferative responses. *J Cell Mol Med* **7,** 1-10.

KELLY, R. & STRUTHERS, A. D. (2001). Are natriuretic peptides clinically useful as markers of heart failure? *Ann Clin Biochem* **38,** 575-583.

KENNEDY, S. G., WAGNER, A. J., CONZEN, S. D., JORDAN, J., BELLACOSA, A., TSICHLIS, P. N. & HAY, N. (1997). The PI 3-kinase/Akt signaling pathway delivers an anti-apoptotic signal. *Genes Dev* **11,** 701-713.

KEREVEUR, A., ENJYOJI, K., MASUDA, K., YUTANI, C. & KATO, H. (2001). Production

of tissue factor pathway inhibitor in cardiomyocytes and its upregulation by interleukin-1. *Thromb Haemost* **86,** 1314-1319.

KIRCHHOFER, D. & NEMERSON, Y. (1996). Initiation of blood coagulation: the tissue factor/factor VIIa complex. *Curr Opin Biotechnol* **7,** 386-391.

KLINGER, J. R., WARBURTON, R. R., PIETRAS, L., OLIVER, P., FOX, J., SMITHIES, O. & HILL, N. S. (2002). Targeted disruption of the gene for natriuretic peptide receptor-A worsens hypoxia-induced cardiac hypertrophy. *Am J Physiol Heart Circ Physiol* **282,** H58-65.

KLINGER, J. R., WARBURTON, R. R., PIETRAS, L. A., SMITHIES, O., SWIFT, R. & HILL, N. S. (1999). Genetic disruption of atrial natriuretic peptide causes pulmonary hypertension in normoxic and hypoxic mice. *Am J Physiol* **276,** L868-874.

KNOLL, R. HOSHIJIMA, M., HOFFMAN, H. M., PERSON, V., LORENZEN-SCHMIDT, I., BANG, M. L., HAYASHI, T., SHIGA, N., YASUKAWA, H., SCHAPER, W., MCKENNA, W., YOKOYAMA, M., SCHORK, N. J., OMENS, J. H., MCCULLOCH, A. D., KIMURA, A., GREGORIO, C. C., POLLER, W., SCHAPER, J., SCHULTHEISS, H. P., CHIEN, K. R. (2002). The cardiac mechanical stretch sensor machinery involves a Z disc complex that is defective in a subset of human cardiomyopathy. *Cell* **111,** 943-955.

KNOWLTON, K. U., BARACCHINI, E., ROSS, R. S., HARRIS, A. N., HENDERSON, S. A., EVANS, S. M., GLEMBOTSKI, C. C. & CHIEN, K. R. (1991). Co-regulation of the atrial natriuretic factor and cardiac myosin light chain-2 genes during alpha-adrenergic stimulation of neonatal rat ventricular cells. Identification of cis sequences within an embryonic and a constitutive contractile protein gene which mediate inducible expression. *J Biol Chem* **266,** 7759-7768.

KOCKX, M. M., CAMBIER, B. A., BORTIER, H. E., DE MEYER, G. R., DECLERCQ, S. C., VAN CAUWELAERT, P. A. & BULTINCK, J. (1994). Foam cell replication and smooth muscle cell apoptosis in human saphenous vein grafts. *Histopathology* **25,** 365-371.

KOIDE, M., NAGATSU, M., ZILE, M. R., HAMAWAKI, M., SWINDLE, M. M., KEECH, G., DEFREYTE, G., TAGAWA, H., COOPER, G. T. & CARABELLO, B. A. (1997). Premorbid determinants of left ventricular dysfunction in a novel model of gradually induced pressure overload in the adult canine. *Circulation* **95,** 1601-1610.

KOKAWA, T., ABUMIYA, T., KIMURA, T., HARADA-SHIBA, M., KOH, H., TSUSHIMA, M., YAMAMOTO, A. & KATO, H. (1995). Tissue factor pathway inhibitor activity in human plasma. Measurement of lipoprotein-associated and free forms in hyperlipidemia. *Arterioscler Thromb Vasc Biol* **15,** 504-510.

KOMURO, I. & YAZAKI, Y. (1994). Molecular mechanism of cardiac hypertrophy and failure. *Clin Sci (Lond)* **87,** 117-126.

KOUL, H. K. (2003). Role of p38 MAP kinase signal transduction in apoptosis and survival of renal epithelial cells. *Ann N Y Acad Sci* **1010,** 62-65.

KULIK, G., KLIPPEL, A. & WEBER, M. J. (1997). Antiapoptotic signalling by the insulin-like growth factor I receptor, phosphatidylinositol 3-kinase, and Akt. *Mol Cell Biol* **17,** 1595-1606.

KYRIAKIS, J. M. & AVRUCH, J. (2001). Mammalian mitogen-activated protein kinase signal transduction pathways activated by stress and inflammation. *Physiol Rev* **81,** 807-869.

LAMORTE, V. J., THORBURN, J., ABSHER, D., SPIEGEL, A., BROWN, J. H., CHIEN, K. R., FERAMISCO, J. R. & KNOWLTON, K. U. (1994). Gq- and ras-dependent pathways mediate hypertrophy of neonatal rat ventricular myocytes following alpha 1-adrenergic stimulation. *J Biol Chem* **269,** 13490-13496.

LEE, H. R., HENDERSON, S. A., REYNOLDS, R., DUNNMON, P., YUAN, D. & CHIEN, K. R. (1988). Alpha 1-adrenergic stimulation of cardiac gene transcription in neonatal rat myocardial cells. Effects on myosin light chain-2 gene expression. *J Biol Chem* **263,** 7352-7358.

LEE, R. T., BLOCH, K. D., PFEFFER, J. M., PFEFFER, M. A., NEER, E. J. & SEIDMAN, C. E. (1988). Atrial natriuretic factor gene expression in ventricles of rats with spontaneous biventricular hypertrophy. *J Clin Invest* **81,** 431-434.

LEMAIRE, P., REVELANT, O., BRAVO, R. & CHARNAY, P. (1988). Two mouse genes encoding potential transcription factors with identical DNA-binding domains are activated by growth factors in cultured cells. *Proc Natl Acad Sci U S A* **85,** 4691-4965.

LEVIN, E. R., GARDNER, D. G. & SAMSON, W. K. (1998). Natriuretic peptides. *N Engl J Med* **339,** 321-328.

LEVY, B. I. (2005). How to explain the differences between renin angiotensin system modulators. *Am J Hypertens* **18,** 134S-141S.

LI, D., TAPSCOFT, T., GONZALEZ, O., BURCH, P. E., QUINONES, M. A., ZOGHBI, W. A., HILL, R., BACHINSKI, L. L., MANN, D. L. & ROBERTS, R. (1999). Desmin mutation responsible for idiopathic dilated cardiomyopathy. *Circulation* **100,** 461-464.

LI, Q., LI, B., WANG, X., LERI, A., JANA, K. P., LIU, Y., KAJSTURA, J., BASERGA, R. & ANVERSA, P. (1997). Overexpression of insulin-like growth factor-1 in mice protects from myocyte death after infarction, attenuating ventricular dilation, wall stress, and cardiac hypertrophy. *J Clin Invest* **100,** 1991-1999.

LI, Y. Y., FELDMAN, A. M., SUN, Y. & MCTIERNAN, C. F. (1998). Differential expression of tissue inhibitors of metalloproteinases in the failing human heart. *Circulation* **98,** 1728-1734.

LIANG, Q. BUENO, O. F., WILKINS, B. J., KUAN, C. Y., XIA, Y., MOLKENTIN, J. D. c-jun N-terminal kinases (JNK) antagonize cardiac growth through cross-talk with calcineurin-NFAT signaling (2003). *EMBO J.* **22**, 5079-5089.

LIM, H. W., DE WINDT, L. J., STEINBERG, L., TAIGEN, T., WITT, S. A., KIMBALL, T. R. & MOLKENTIN, J. D. (2000). Calcineurin expression, activation, and function in cardiac pressure-overload hypertrophy. *Circulation* **101,** 2431-2437.

LIN, M. C., ALMUS-JACOBS, F., CHEN, H. H., PARRY, G. C., MACKMAN, N., SHYY, J. Y. & CHIEN, S. (1997). Shear stress induction of the tissue factor gene. *J Clin Invest* **99,** 737-744.

LIU, X., KIM, C. N., YANG, J., JEMMERSON, R. & WANG, X. (1996). Induction of apoptotic program in cell-free extracts: requirement for dATP and cytochrome c. *Cell* **86,** 147-157.

LLOYD, R. V., ERICKSON, L. A., NASCIMENTO, A. G. & KLOPPEL, G. (1999). Neoplasms Causing Nonhyperinsulinemic Hypoglycemia. *Endocr Pathol* **10,** 291-297.

LOHMANN, S. M., VAANDRAGER, A. B., SMOLENSKI, A., WALTER, U. & DE JONGE, H. R. (1997). Distinct and specific functions of cGMP-dependent protein kinases. *Trends Biochem Sci* **22,** 307-312.

LOUGHNA, P., GOLDSPINK, G. & GOLDSPINK, D. F. (1986). Effect of inactivity and passive stretch on protein turnover in phasic and postural rat muscles. *J Appl Physiol* **61,** 173-179.

LOWES, B. D., MINOBE, W., ABRAHAM, W. T., RIZEQ, M. N., BOHLMEYER, T. J., QUAIFE, R. A., RODEN, R. L., DUTCHER, D. L., ROBERTSON, A. D., VOELKEL, N. F., BADESCH, D. B., GROVES, B. M., GILBERT, E. M. & BRISTOW, M. R. (1997). Changes in gene expression in the intact human heart. Downregulation of alpha-myosin heavy chain in hypertrophied, failing ventricular myocardium. *J Clin Invest* **100,** 2315-2324.

LUTHER, T., DITTERT, D. D., KOTZSCH, M., ERLICH, J., ALBRECHT, S., MACKMAN, N. & MULLER, M. (2000). Functional implications of tissue factor localization to cell-cell contacts in myocardium. *J Pathol* **192,** 121-130.

LUTHER, T., FLOSSEL, C., MACKMAN, N., BIERHAUS, A., KASPER, M., ALBRECHT, S., SAGE, E. H., IRUELA-ARISPE, L., GROSSMANN, H., STROHLEIN, A., ZHANG, Y., NAWROTH, P. P., CARMELIET, P., LOSKUTOFF, D. J. & MULLER, M. (1996). Tissue factor expression during human and mouse development. *Am J Pathol* **149,** 101-113.

LUTHER, T. & MACKMAN, N. (2001). Tissue factor in the heart. Multiple roles in hemostasis, thrombosis, and inflammation. *Trends Cardiovasc Med* **11,** 307-312.

MACKMAN, N. (1995). Regulation of the tissue factor gene. *Faseb J* **9,** 883-889.

MACKMAN, N., MORRISSEY, J. H., FOWLER, B. & EDGINGTON, T. S. (1989). Complete sequence of the human tissue factor gene, a highly regulated cellular receptor that initiates the coagulation protease cascade. *Biochemistry* **28,** 1755-1762.

MACKMAN, N., SAWDEY, M. S., KEETON, M. R. & LOSKUTOFF, D. J. (1993). Murine tissue factor gene expression in vivo. Tissue and cell specificity and regulation by lipopolysaccharide. *Am J Pathol* **143,** 76-84.

MCMULLEN, J. R. & IZUMO, S. (2006). Role of the insulin-like growth factor 1 (IGF1)/phosphoinositide-3-kinase (PI3K) pathway mediating physiological cardiac hypertrophy. *Novartis Found. Symp.* **274,** 90-111.

MAJNO, G. & JORIS, I. (1995). Apoptosis, oncosis, and necrosis. An overview of cell death. *Am J Pathol* **146,** 3-15.

MALLAT, Z., HUGEL, B., OHAN, J., LESECHE, G., FREYSSINET, J. M. & TEDGUI, A. (1999). Shed membrane microparticles with procoagulant potential in human atherosclerotic plaques: a role for apoptosis in plaque thrombogenicity. *Circulation* **99,** 348-353.

MALLAT, Z., TEDGUI, A., FONTALIRAN, F., FRANK, R., DURIGON, M. & FONTAINE, G. (1996). Evidence of apoptosis in arrhythmogenic right ventricular dysplasia. *N*

Engl J Med **335,** 1190-1196.

MARIN-GREZ, M., FLEMING, J. T. & STEINHAUSEN, M. (1986). Atrial natriuretic peptide causes pre-glomerular vasodilation and post-glomerular vasoconstriction in rat kidney. *Nature* **324,** 473-476.

MARMUR, J. D., ROSSIKHINA, M., GUHA, A., FYFE, B., FRIEDRICH, V., MENDLOWITZ, M., NEMERSON, Y. & TAUBMAN, M. B. (1993). Tissue factor is rapidly induced in arterial smooth muscle after balloon injury. *J Clin Invest* **91,** 2253-2259.

MARMUR, J. D., THIRUVIKRAMAN, S. V., FYFE, B. S., GUHA, A., SHARMA, S. K., AMBROSE, J. A., FALLON, J. T., NEMERSON, Y. & TAUBMAN, M. B. (1996). Identification of active tissue factor in human coronary atheroma. *Circulation* **94,** 1226-1232.

MARTIN, S. J. & GREEN, D. R. (1995). Protease activation during apoptosis: death by a thousand cuts? *Cell* **82,** 349-352.

MARUTSUKA, K., HATAKEYAMA, K., SATO, Y., YAMASHITA, A., SUMIYOSHI, A. & ASADA, Y. (2002). Protease-activated receptor 2 (PAR2) mediates vascular smooth muscle cell migration induced by tissue factor/factor VIIa complex. *Thromb Res* **107,** 271-276.

MASASHI, A. (1999). Function and regulation of sarcoplasmic reticulum Ca^{2+}-ATPase. *Jpn. Heart J.* 1-13.

MATSUKAWA, N., GRZESIK, W. J., TAKAHASHI, N., PANDEY, K. N., PANG, S., YAMAUCHI, M. & SMITHIES, O. (1999). The natriuretic peptide clearance receptor locally modulates the physiological effects of the natriuretic peptide system. *Proc Natl Acad Sci U S A* **96,** 7403-7408.

MATTHEWS, D. R., BOWN, E., BECK, T. W., PLOTKIN, E., LOCK, L., GOSDEN, E. & WICKHAM, M. (1988). An amperometric needle-type glucose sensor tested in rats and man. *Diabet Med* **5,** 248-252.

MATTIAZZI, A., MUNDINA-WEILENMANN, C., GUOXIANG, C., VITTONE, L., KRANIAS, E. (2005). Role of phospholamban phosphorylation on Thr^{17} in cardiac physiological and pathological conditions. *Cardiolvasc. Res.* **68**, 366-375.

MAYER, B., KAISER, T., KEMPT, P., CORNELIUS, T., HOLMER, S. R. & SCHUNKERT, H. (2002). Molecular cloning and functional characterization of the upstream rat atrial natriuretic peptide promoter. *J Hypertens* **20,** 219-228.

MEERSON, F. Z. (1969). The myocardium in hyperfunction, hypertrophy and heart failure. *Circ Res* **25,** Suppl 2:1-163.

MEYER, M., SCHILLINGER, W., PIESKE, B., HOLUBARSCH, C., HEILMANN, C., POSIVAL, H., KUWAJIMA, G., MIKOSHIBA, K., JUST, H., HASENFUSS, G. & ET AL. (1995). Alterations of sarcoplasmic reticulum proteins in failing human dilated cardiomyopathy. *Circulation* **92,** 778-784.

MILBRANDT, J. (1987). A nerve growth factor-induced gene encodes a possible transcriptional regulatory factor. *Science* **238,** 797-799.

MISUMI, K., OGAWA, H., YASUE, H., SOEJIMA, H., SUEFUJI, H., NISHIYAMA, K., TAKAZOE, K., KUGIYAMA, K., TSUJI, I. & KUMEDA, K. (1998). Circadian variation in plasma levels of free-form tissue factor pathway inhibitor antigen in patients with coronary spastic angina. *Jpn Circ J* **62,** 419-424.

MIYATE, S., MINOBE, W., BRISTOW, M. R. & LEINWAND, L. A. (2000). Myosin heavy chain isoform expression in the failing and nonfailing human heart. *Circ Res* **86,** 386-390.

MODY, R. S. & CARSON, S. D. (1997). Tissue factor cytoplasmic domain peptide is multiply phosphorylated *in vitro*. *Biochemistry* **36,** 7869-7875.

MOLKENTIN, J. D. & DORN, I. I. G. W. N. (2001). Cytoplasmic signaling pathways that regulate cardiac hypertrophy. *Annu Rev Physiol* **63,** 391-426.

MOLKENTIN, J. D., LU, J. R., ANTOS, C. L., MARKHAM, B., RICHARDSON, J., ROBBINS,

J., GRANT, S. R. & OLSON, E. N. (1998). A calcineurin-dependent transcriptional pathway for cardiac hypertrophy. *Cell* **93,** 215-228.

MOONS, A. H., LEVI, M. & PETERS, R. J. (2002). Tissue factor and coronary artery disease. *Cardiovasc Res* **53,** 313-325.

MORANO, I., HADICKE, K., HAASE, H., BOHM, M., ERDMANN, E. & SCHAUB, M. C. (1997). Changes in essential myosin light chain isoform expression provide a molecular basis for isometric force regulation in the failing human heart. *J Mol Cell Cardiol* **29,** 1177-1187.

MORISCO, C., ZEBROWSKI, D., CONDORELLI, G., TSICHLIS, P., VATNER, S. F. & SADOSHIMA, J. (2000). The Akt-glycogen synthase kinase 3beta pathway regulates transcription of atrial natriuretic factor induced by beta-adrenergic receptor stimulation in cardiac myocytes. *J Biol Chem* **275,** 14466-14475.

MORRISSEY, J. H. (2001). Tissue factor: an enzyme cofactor and a true receptor. *Thromb Haemost* **86,** 66-74.

MUELLER, B. M. & RUF, W. (1998). Requirement for binding of catalytically active factor VIIa in tissue factor-dependent experimental metastasis. *J Clin Invest* **101,** 1372-1378.

MUKOYAMA, M., NAKAO, K., HOSODA, K., SUGA, S., SAITO, Y., OGAWA, Y., SHIRAKAMI, G., JOUGASAKI, M., OBATA, K., YASUE, H. & ET AL. (1991). Brain natriuretic peptide as a novel cardiac hormone in humans. Evidence for an exquisite dual natriuretic peptide system, atrial natriuretic peptide and brain natriuretic peptide. *J Clin Invest* **87,** 1402-1412.

MULLER, D. N., MERVAALA, E. M., DECHEND, R., FIEBELER, A., PARK, J. K., SCHMIDT, F., THEUER, J., BREU, V., MACKMAN, N., LUTHER, T., SCHNEIDER, W., GULBA, D., GANTEN, D., HALLER, H. & LUFT, F. C. (2000). Angiotensin II (AT(1)) receptor blockade reduces vascular tissue factor in angiotensin II-induced cardiac vasculopathy. *Am J Pathol* **157,** 111-122.

NADAL-GINARD, B., ANVERSA, P., KAJSTURA, J. & LERI, A. (2005). Cardiac stem cells and myocardial regeneration. *Novartis Found Symp* **265,** 142-154; discussion 155-157, 204-211.

NADAL-GINARD, B., KAJSTURA, J., LERI, A. & ANVERSA, P. (2003). Myocyte death, growth, and regeneration in cardiac hypertrophy and failure. *Circ Res* **92,** 139-150.

NADAL-GINARD, B. & MAHDAVI, V. (1989). Molecular basis of cardiac performance. Plasticity of the myocardium generated through protein isoform switches. *J Clin Invest* **84,** 1693-1700.

NAGATA, S. (1997). Apoptosis by death factor. *Cell* **88,** 355-365.

NAGAYASU, T., SAADI, S., HOLZKNECHT, R. A., PLUMMER, T. B. & PLATT, J. L. (2000). Induction of tissue factor mRNA in acute vascular rejection: localization by in situ reverse transcriptase polymerase chain reaction. *Transplant Proc* **32,** 970.

NAKAO, K., MINOBE, W., RODEN, R., BRISTOW, M. R. & LEINWAND, L. A. (1997). Myosin heavy chain gene expression in human heart failure. *J Clin Invest* **100,** 2362-2370.

NARAHARA, N., ENDEN, T., WIIGER, M. & PRYDZ, H. (1994). Polar expression of tissue factor in human umbilical vein endothelial cells. *Arterioscler Thromb* **14,** 1815-1820.

NIEUWLAND, R., BERCKMANS, R. J., MCGREGOR, S., BOING, A. N., ROMIJN, F. P., WESTENDORP, R. G., HACK, C. E. & STURK, A. (2000). Cellular origin and procoagulant properties of microparticles in meningococcal sepsis. *Blood* **95,** 930-935.

NORRIS, L. (2003). Blood coagulation. *Best Pract Res Clin Obst Gynaecol* **17,** 369-383.

NOVOTNY, W. F., GIRARD, T. J., MILETICH, J. P. & BROZE, G. J., JR. (1988). Platelets secrete a coagulation inhibitor functionally and antigenically similar to the lipoprotein associated coagulation inhibitor. *Blood* **72,** 2020-2025.

OGAWA, Y., ITOH, H. & NAKAO, K. (1995). Molecular biology and biochemistry of natriuretic peptide family. *Clin Exp Pharmacol Physiol* **22,** 49-53.

OGINO, H., SMOLENSKI, R. T., M., Z., SEYMOUR, A. M. & YACOUB, M. H. (1996). Influence of preconditioning on rat hearts subjected to prolonged cardioplegic arrest. *Ann Thorac Surg* **62,** 496-474.

OLIVETTI, G., ABBI, R., QUAINI, F., KAJSTURA, J., CHENG, W., NITAHARA, J. A., QUAINI, E., DI LORETO, C., BELTRAMI, C. A., KRAJEWSKI, S., REED, J. C. & ANVERSA, P. (1997). Apoptosis in the failing human heart. *N Engl J Med* **336,** 1131-1141.

OLIVETTI, G., GIORDANO, G., CORRADI, D., MELISSARI, M., LAGRASTA, C., GAMBERT, S. R. & ANVERSA, P. (1995). Gender differences and aging: effects on the human heart. *J Am Coll Cardiol* **26,** 1068-1079.

OSSOVSKAYA, V. S. & BUNNETT, N. W. (2004). Protease-activated receptors: contribution to physiology and disease. *Physiol Rev* **84,** 579-621.

OSTERUD, B., BAJAJ, M. S. & BAJAJ, S. P. (1995). Sites of tissue factor pathway inhibitor (TFPI) and tissue factor expression under physiologic and pathologic conditions. On behalf of the Subcommittee on Tissue factor Pathway Inhibitor (TFPI) of the Scientific and Standardization Committee of the ISTH. *Thromb Haemost* **73,** 873-875.

OTSUKA, S., SUGANO, M., MAKINO, N., SAWADA, S., HATA, T. & NIHO, Y. (1998). Interaction of mRNAs for angiotensin II type 1 and type 2 receptors to vascular remodeling in spontaneously hypertensive rats. *Hypertension* **32,** 467-472.

PAGANI, E. D., ALOUSI, A. A., GRANT, A. M., OLDER, T. M., DZIUBAN, S. W., JR. & ALLEN, P. D. (1988). Changes in myofibrillar content and Mg-ATPase activity in ventricular tissues from patients with heart failure caused by coronary artery disease, cardiomyopathy, or mitral valve insufficiency. *Circ Res* **63,** 380-385.

PARRY, G. C., ERLICH, J. H., CARMELIET, P., LUTHER, T. & MACKMAN, N. (1998). Low levels of tissue factor are compatible with development and hemostasis in mice. *J Clin Invest* **101,** 560-569.

PAWLINSKI, R., FERNANDES, A., KEHRLE, B., PEDERSEN, B., PARRY, G., ERLICH, J., PYO, R., GUTSTEIN, D., ZHANG, J., CASTELLINO, F., MELIS, E., CARMELIET, P., BARETTON, G., LUTHER, T., TAUBMAN, M., ROSEN, E. & MACKMAN, N. (2002). Tissue factor deficiency causes cardiac fibrosis and left ventricular dysfunction. *Proc Natl Acad Sci U S A* **99,** 15333-15338.

PAWLINSKI, R., PEDERSEN, B., ERLICH, J. & MACKMAN, N. (2004). Role of tissue factor in haemostasis, thrombosis, angiogenesis and inflammation: lessons from low tissue factor mice. *Thromb Haemost* **92,** 444-450.

PENDURTHI, U. R., ALLEN, K. E., EZBAN, M. & RAO, L. V. (2000). Factor VIIa and thrombin induce the expression of Cyr61 and connective tissue growth factor, extracellular matrix signaling proteins that could act as possible downstream mediators in factor VIIa x tissue factor-induced signal transduction. *J Biol Chem* **275,** 14632-14641.

PENDURTHI, U. R., ALOK, D. & RAO, L. V. (1997). Binding of factor VIIa to tissue factor induces alterations in gene expression in human fibroblast cells: up-regulation of poly(A) polymerase. *Proc Natl Acad Sci U S A* **94,** 12598-12603.

PEPPELENBOSCH, M. P. & VERSTEEG, H. H. (2001). Cell biology of tissue factor, an unusual member of the cytokine receptor family. *Trends Cardiovasc Med* **11,** 335-339.

PETERSEN, L. C., FRESKGARD, P. & EZBAN, M. (2000). Tissue factor-dependent factor VIIa signaling. *Trends Cardiovasc Med* **10,** 47-52.

PETIT, P. X., LECOEUR, H., ZORN, E., DAUGUET, C., MIGNOTTE, B. & GOUGEON, M. L. (1995). Alterations in mitochondrial structure and function are early events of dexamethasone-induced thymocyte apoptosis. *J Cell Biol* **130,** 157-167.

POULSEN, L. K., JACOBSEN, N., SORENSEN, B. B., BERGENHEM, N. C., KELLY, J. D., FOSTER, D. C., THASTRUP, O., EZBAN, M. & PETERSEN, L. C. (1998). Signal transduction via the mitogen-activated protein kinase pathway induced by binding of coagulation factor VIIa to tissue factor. *J Biol Chem* **273,** 6228-6232.

PRZYKLENK, K. (2001). Pharmacologic treatment of the stunned myocardium: the concepts and the challenges. *Coron Artery Dis* **12,** 363-369.

RANGNEKAR, V. M., APLIN, A. C. & SUKHATME, V. P. (1990). The serum and TPA responsive promoter and intron-exon structure of EGR2, a human early growth response gene encoding a zinc finger protein. *Nucleic Acids Res* **18,** 2749-2757.

RAO, L. V. & PENDURTHI, U. R. (2005). Tissue factor-factor VIIa signaling. *Arterioscler Thromb Vasc Biol* **25,** 47-56.

RASCHER, W., TULASSAY, T. & LANG, R. E. (1985). Atrial natriuretic peptide in plasma of volume-overloaded children with chronic renal failure. *Lancet* **2,** 303-305.

REDONDO, J., BISHOP, J. E. & WILKINS, M. R. (1998). Effect of atrial natriuretic peptide and cyclic GMP phosphodiesterase inhibition on collagen synthesis by adult cardiac fibroblasts. *Br J Pharmacol* **124,** 1455-1462.

REINER, K. A. & JENNINGS, R. B. (1992). *Myocardial ischemia, hypoxia and infarction*, 2nd edition. Raven Press Ltd., New York.

RIEWALD, M. & RUF, W. (2002). Orchestration of coagulation protease signaling by tissue factor. *Trends Cardiovasc Med* **12,** 149-154.

ROTTINGEN, J. A., ENDEN, T., CAMERER, E., IVERSEN, J. G. & PRYDZ, H. (1995). Binding of human factor VIIa to tissue factor induces cytosolic Ca2+ signals in J82 cells, transfected COS-1 cells, Madin-Darby canine kidney cells and in human endothelial cells induced to synthesize tissue factor. *J Biol Chem* **270,** 4650-4660.

RUF, W., DORFLEUTNER, A. & RIEWALD, M. (2003). Specificity of coagulation factor signaling. *J Thromb Haemost* **1,** 1495-1503.

RUSKOAHO, H. (1992). Atrial natriuretic peptide: synthesis, release, and metabolism. *Pharmacol Rev* **44,** 479-602.

RUSKOAHO, H., KINNUNEN, P., TASKINEN, T., VUOLTEENAHO, O., LEPPALUOTO, J. & TAKALA, T. E. (1989). Regulation of ventricular atrial natriuretic peptide release in hypertrophied rat myocardium. Effects of exercise. *Circulation* **80,** 390-400.

RYAN, K. M., PHILLIPS, A. C. & VOUSDEN, K. H. (2001). Regulation and function of the p53 tumor suppressor protein. *Curr Opin Cell Biol* **13,** 332-337.

SABRI, A., MUSKE, G., ZHANG, H., PAK, E., DARROW, A., ANDRADE-GORDON, P. & STEINBERG, S. F. (2000). Signaling properties and functions of two distinct cardiomyocyte protease-activated receptors. *Circ Res* **86,** 1054-1061.

SAKAMOTO, A., ONO, K., ABE, M., JASMIN, G., EKI, T., MURAKAMI, Y., MASAKI, T., TOYO-OKA, T. & HANAOKA, F. (1997). Both hypertrophic and dilated cardiomyopathies are caused by mutation of the same gene, delta-sarcoglycan, in hamster: an animal model of disrupted dystrophin-associated glycoprotein complex. *Proc Natl Acad Sci U S A* **94,** 13873-13878.

SAMBROOK, J., FRITSCH, E. F. & MANIATIS, T. (1989). *Molecular cloning: A*

laboratory manual, 2nd edition. Cold Sprink Harbour Laboratory Press, New York.

SANDSET, P. M., WARN-CRAMER, B. J., MAKI, S. L. & RAPAPORT, S. I. (1991). Immunodepletion of extrinsic pathway inhibitor sensitizes rabbits to endotoxin-induced intravascular coagulation and the generalized Shwartzman reaction. *Blood* **78,** 1496-1502.

SANDSET, P. M., WARN-CRAMER, B. J., RAO, L. V., MAKI, S. L. & RAPAPORT, S. I. (1991). Depletion of extrinsic pathway inhibitor (EPI) sensitizes rabbits to disseminated intravascular coagulation induced with tissue factor: evidence supporting a physiologic role for EPI as a natural anticoagulant. *Proc Natl Acad Sci U S A* **88,** 708-712.

SAWADA, Y., SUDA, M., YOKOYAMA, H., KANDA, T., SAKAMAKI, T., TANAKA, S., NAGAI, R., ABE, S. & TAKEUCHI, T. (1997). Stretch-induced hypertrophic growth of cardiomyocytes and processing of brain-type natriuretic peptide are controlled by proprotein-processing endoprotease furin. *J Biol Chem* **272,** 20545-20554.

SCHAUB, M. C., HEFTI, M. A., ZUELLIG, R. A. & MORANO, I. (1998). Modulation of contractility in human cardiac hypertrophy by myosin essential light chain isoforms. *Cardiovasc Res* **37,** 381-404.

SCHONBECK, U., MACH, F., SUKHOVA, G. K., HERMAN, M., GRABER, P., KEHRY, M. R. & LIBBY, P. (2000). CD40 ligation induces tissue factor expression in human vascular smooth muscle cells. *Am J Pathol* **156,** 7-14.

SCHWARTZ, K., BOHELER, K. R., DE LA BASTIE, D., LOMPRE, A. M. & MERCADIER, J. J. (1992). Switches in cardiac muscle gene expression as a result of pressure and volume overload. *Am J Physiol* **262,** R364-369.

SCHWARTZ, K., DE LA BASTIE, D., BOUVERET, P., OLIVIERO, P., ALONSO, S. & BUCKINGHAM, M. (1986). Alpha-skeletal muscle actin mRNA's accumulate in hypertrophied adult rat hearts. *Circ Res* **59,** 551-555.

SCHWINGER, R. H., MUNCH, G., BOLCK, B., KARCZEWSKI, P., KRAUSE, E. G. & ERDMANN, E. (1999). Reduced Ca(2+)-sensitivity of SERCA 2a in failing human myocardium due to reduced serin-16 phospholamban phosphorylation. *J Mol Cell Cardiol* **31,** 479-491.

SELVETELLA, G., HIRSCH, E., NOTTE, A., TARONE, G. & LEMBO, G. (2004). Adaptive and maladaptive hypertrophic pathways: points of convergence and divergence. *Cardiovasc Res* **63,** 373-380.

SHANNON, T. R. & BERS, D. M. (2004). Integrated Ca2+ management in cardiac myocytes. *Ann N Y Acad Sci* **1015,** 28-38.

SHENG, M. & GREENBERG, M. E. (1990). The regulation and function of c-fos and other immediate early genes in the nervous system. *Neuron* **4,** 477-485.

SHENKER, Y., SIDER, R. S., OSTAFIN, E. A. & GREKIN, R. J. (1985). Plasma levels of immunoreactive atrial natriuretic factor in healthy subjects and in patients with edema. *J Clin Invest* **76,** 1684-1687.

SHIRWANY, A. & WEBER, K. T. (2006). Extracellular matrix remodeling in hypertensive heart disease. *J Am Coll Cardiol* **48,** 97-108.

SILBERBACH, M., GORENC, T., HERSHBERGER, R. E., STORK, P. J., STEYGER, P. S. & ROBERTS, C. T., JR. (1999). Extracellular signal-regulated protein kinase activation is required for the anti-hypertrophic effect of atrial natriuretic factor in neonatal rat ventricular myocytes. *J Biol Chem* **274,** 24858-24864.

SIRAGY, H. M. (2000). The role of the AT2 receptor in hypertension. *Am J Hypertens* **13,** 62S-67S.

SLEE, E. A., ADRAIN, C. & MARTIN, S. J. (1999). Serial killers: ordering caspase activation events in apoptosis. *Cell Death Differ* **6,** 1067-1074.

SMOLENSKI, R. T., SCHRADER, J., DE GROOT, H. & DEUSSEN, A. (1991). Oxygen partial pressure and free intracellular adenosine of isolated cardiomyocytes. *Am J Physiol* **260,** C708-714.

SODERLING, S. H. & BEAVO, J. A. (2000). Regulation of cAMP and cGMP signaling: new phosphodiesterases and new functions. *Curr Opin Cell Biol* **12,** 174-179.

SORENSEN, B. B., FRESKGARD, P. O., NIELSEN, L. S., RAO, L. V., EZBAN, M. & PETERSEN, L. C. (1999). Factor VIIa-induced p44/42 mitogen-activated protein kinase activation requires the proteolytic activity of factor VIIa and is independent of the tissue factor cytoplasmic domain. *J Biol Chem* **274,** 21349-21354.

SORENSEN, B. B., RAO, L. V., TORNEHAVE, D., GAMMELTOFT, S. & PETERSEN, L. C. (2003). Antiapoptotic effect of coagulation factor VIIa. *Blood* **102,** 1708-1715.

SPANN, J. F., JR., BUCCINO, R. A., SONNENBLICK, E. H. & BRAUNWALD, E. (1967). Contractile state of cardiac muscle obtained from cats with experimentally produced ventricular hypertrophy and heart failure. *Circ Res* **21,** 341-354.

SPRENKLE, A. B., MURRAY, S. F. & GLEMBOTSKI, C. C. (1995). Involvement of multiple cis elements in basal- and alpha-adrenergic agonist-inducible atrial natriuretic factor transcription. Roles for serum response elements and an SP-1-like element. *Circ Res* **77,** 1060-1069.

STANLEY, W. C., RECCHIA, F. A. & LOPASCHUK, G. D. (2005). Myocardial substrate metabolism in the normal and failing heart. *Physiol Rev* **85,** 1093-1129.

STEIN, B. C. & LEVIN, R. I. (1998). Natriuretic peptides: physiology, therapeutic potential, and risk stratification in ischemic heart disease. *Am Heart J* **135,** 914-923.

STEINBERG, S. F. (2005). The cardiovascular actions of protease-activated receptors. *Mol Pharmacol* **67,** 2-11.

STEINBERG, S. F., ROBINSON, R. B., LIEBERMAN, H. B., STERN, D. M. & ROSEN, M. R. (1991). Thrombin modulates phosphoinositide metabolism, cytosolic calcium, and impulse initiation in the heart. *Circ Res* **68,** 1216-1229.

STOCKDALE, F. E., NIKOVITS, W., JR. & ESPINOZA, N. R. (2002). Slow myosins in muscle development. *Results Probl Cell Differ* **38,** 199-214.

STOYANOVA, V. K., ZHELEV, N. Z., YANEV, I. B., GHENEV, E. D. & NACHEV, C. K. (2005). Time course and progression of pressure overload-induced cardiac hypertrophy in rats. *Folia Med (Plovdiv)* **47,** 52-57.

SUKHATME, V. P., CAO, X. M., CHANG, L. C., TSAI-MORRIS, C. H., STAMENKOVICH, D., FERREIRA, P. C., COHEN, D. R., EDWARDS, S. A., SHOWS, T. B., CURRAN, T. & ET AL. (1988). A zinc finger-encoding gene coregulated with c-fos during growth and differentiation, and after cellular depolarization. *Cell* **53,** 37-43.

SWYNGHEDAUW, B. (1986). Developmental and functional adaptation of contractile proteins in cardiac and skeletal muscles. *Physiol Rev* **66,** 710-771.

SZABOLCS, M., MICHLER, R. E., YANG, X., AJI, W., ROY, D., ATHAN, E., SCIACCA, R. R., MINANOV, O. P. & CANNON, P. J. (1996). Apoptosis of cardiac myocytes during cardiac allograft rejection. Relation to induction of nitric oxide synthase. *Circulation* **94,** 1665-1673.

TAKEMURA, G. & FUJIWARA, H. (2004). Role of apoptosis in remodeling after myocardial infarction. *Pharmacol Ther* **104,** 1-16.

TAUBMAN, M. B., FALLON, J. T., SCHECTER, A. D., GIESEN, P., MENDLOWITZ, M., FYFE, B. S., MARMUR, J. D. & NEMERSON, Y. (1997). Tissue factor in the pathogenesis of atherosclerosis. *Thromb Haemost* **78,** 200-204.

THUM T. & BORLAK J. (2000). Isolation and cultivation of Ca2+ tolerant cardiomyocytes from the adult rat: improvements and applications *Xenobiotica* **30**, 1063-1077.

TOOMEY, J. R., KRATZER, K. E., LASKY, N. M., STANTON, J. J. & BROZE, G. J., JR. (1996). Targeted disruption of the murine tissue factor gene results in embryonic lethality. *Blood* **88,** 1583-1587.

TOSCHI, V., GALLO, R., LETTINO, M., FALLON, J. T., GERTZ, S. D., FERNANDEZ-ORTIZ, A., CHESEBRO, J. H., BADIMON, L., NEMERSON, Y., FUSTER, V. & BADIMON, J. J. (1997). Tissue factor modulates the thrombogenicity of human atherosclerotic plaques. *Circulation* **95,** 594-599.

TOWBIN, J. A. (1998). The role of cytoskeletal proteins in cardiomyopathies. *Curr Opin Cell Biol* **10,** 131-139.

TSUTSUI, H., TAGAWA, H., KENT, R. L., MCCOLLAM, P. L., ISHIHARA, K., NAGATSU, M. & COOPER, G. T. (1994). Role of microtubules in contractile dysfunction of hypertrophied cardiocytes. *Circulation* **90,** 533-555.

URBANOVA, D. (1983). Assessment of left and right ventricular hypertrophy by various macroscopic techniques. *Cor Vasa* **25,** 450-458.

VANGHELUWE, P., SIPIDO, K. R. RAEYMAEKERS, L., WUYTACK, F. (2006). New perspectives on the role of SERCA2's Ca^{2+} affinity in cardiac function. *Biochim. Biophys. Acta* **1763**, 1216-1228.

VERSTEEG, H. H., BRESSER, H. L., SPEK, C. A., RICHEL, D. J., VAN DEVENTER, S. J. & PEPPELENBOSCH, M. P. (2003). Regulation of the p21Ras-MAP kinase pathway by factor VIIa. *J Thromb Haemost* **1,** 1012-1018.

VERSTEEG, H. H., HOEDEMAEKER, I., DIKS, S. H., STAM, J. C., SPAARGAREN, M., VAN BERGEN EN HENEGOUWEN, P. M., VAN DEVENTER, S. J. & PEPPELENBOSCH, M. P. (2000). Factor VIIa/tissue factor-induced signaling via activation of Src-like kinases, phosphatidylinositol 3-kinase, and Rac. *J Biol Chem* **275,** 28750-28756.

VERSTEEG, H. H., PEPPELENBOSCH, M. P. & SPEK, C. A. (2001). The pleiotropic effects of tissue factor: a possible role for factor VIIa-induced intracellular signalling? *Thromb Haemost* **86,** 1353-1359.

VERSTEEG, H. H., SORENSEN, B. B., SLOFSTRA, S. H., VAN DEN BRANDE, J. H., STAM, J. C., VAN BERGEN EN HENEGOUWEN, P. M., RICHEL, D. J., PETERSEN, L. C. & PEPPELENBOSCH, M. P. (2002). VIIa/tissue factor interaction results in a tissue factor cytoplasmic domain-independent activation of protein synthesis, p70, and p90 S6 kinase phosphorylation. *J Biol Chem* **277,** 27065-27072.

VERSTEEG, H. H., SPEK, C. A., RICHEL, D. J. & PEPPELENBOSCH, M. P. (2004). Coagulation factors VIIa and Xa inhibit apoptosis and anoikis. *Oncogene* **23,** 410-417.

VILES-GONZALEZ, J. F. & BADIMON, J. J. (2004). Atherothrombosis: the role of tissue factor. *Int J Biochem Cell Biol* **36,** 25-30.

WAKASAKI, H., KOYA, D., SCHOEN, F. J., JIROUSEK, M. R., WAYS, D. K., HOIT, B. D., WALSH, R. A. & KING, G. L. (1997). Targeted overexpression of protein kinase C beta2 isoform in myocardium causes cardiomyopathy. *Proc Natl Acad Sci U S A* **94,** 9320-9325.

WAKATSUKI, T., SCHLESSINGER, J., ELSON, E. L. (2004). The biochemical response of the heart to hypertension and exercise. *Trends Biochem. Sci.* **29**, 609-617.

WEBER, K. T. (2005). Are myocardial fibrosis and diastolic dysfunction reversible in hypertensive heart disease? *Congest Heart Fail* **11,** 322-324; quiz 325.

WEI, C. M., HEUBLEIN, D. M., PERRELLA, M. A., LERMAN, A., RODEHEFFER, R. J., MCGREGOR, C. G., EDWARDS, W. D., SCHAFF, H. V. & BURNETT, J. C., JR. (1993). Natriuretic peptide system in human heart failure. *Circulation* **88,** 1004-1009.

WESTRICK, R. J., BODARY, P. F., XU, Z., SHEN, Y. C., BROZE, G. J. & EITZMAN, D. T. (2001). Deficiency of tissue factor pathway inhibitor promotes atherosclerosis

and thrombosis in mice. *Circulation* **103,** 3044-3046.

The World Healt Organisation, (WHO) (2002). Caediovascular disease: prevention and control. www.who.int/dietphysicalactivity/publications/facts/cvd/en/

WIIGER, M. T. & PRYDZ, H. (2000). Cellular effects of initiation of the extrinsic pathway of blood coagulation. *Trends Cardiovasc Med* **10,** 360-365.

WILCOX, J. N., SMITH, K. M., SCHWARTZ, S. M. & GORDON, D. (1989). Localization of tissue factor in the normal vessel wall and in the atherosclerotic plaque. *Proc Natl Acad Sci U S A* **86,** 2839-2843.

WILKINS, B. J. & MOLKENTIN, J. D. (2004). Calcium-calcineurin signaling in the regulation of cardiac hypertrophy. *Biochem. Biophys. Res. Commun.* **322,** 1178-1191

WILKINS, B. J. DE WINDT, L. J., BUENO, O. F., BRAZ, J. C., GLASCOCK, B. J., KIMBALL, T. F., MOLKENTIN, J.D. (2002). Targeted disruption of NFATc3, but not NFATc4, reveals an intrinsic defect in calcineurin-mediated cardiac hypertrophic growth. *Mol Cell Biol* **22,** 7603-7613.

WILLIAMS, P. E. & GOLDSPINK, G. (1971). Longitudinal growth of striated muscle fibres. *J Cell Sci* **9,** 751-767.

WU, F., YAN, W., PAN, J., MORSER, J. & WU, Q. (2002). Processing of pro-atrial natriuretic peptide by corin in cardiac myocytes. *J Biol Chem* **277,** 16900-16905.

WU, J. P., DESCHEPPER, C. F. & GARDNER, D. G. (1988). Perinatal expression of the atrial natriuretic factor gene in rat cardiac tissue. *Am J Physiol* **255,** E388-396.

YAN, W., WU, F., MORSER, J. & WU, Q. (2000). Corin, a transmembrane cardiac serine protease, acts as a pro-atrial natriuretic peptide-converting enzyme. *Proc Natl Acad Sci U S A* **97,** 8525-8529.

YANG, H., ALNAQEEB, M., SIMPSON, H. & GOLDSPINK, G. (1997). Changes in muscle fibre type, muscle mass and IGF-I gene expression in rabbit skeletal muscle subjected to stretch. *J Anat* **190 (Pt 4),** 613-622.

YANG, S., ALNAQEEB, M., SIMPSON, H. & GOLDSPINK, G. (1996). Cloning and characterization of an IGF-1 isoform expressed in skeletal muscle subjected to stretch. *J Muscle Res Cell Motil* **17,** 487-495.

YANG, S. Y. & GOLDSPINK, G. (2002). Different roles of the IGF-I Ec peptide (MGF) and mature IGF-I in myoblast proliferation and differentiation. *FEBS Lett* **522,** 156-160.

YANG-FENG, T. L., FLOYD-SMITH, G., NEMER, M., DROUIN, J. & FRANCKE, U. (1985). The pronatriodilatin gene is located on the distal short arm of human chromosome 1 and on mouse chromosome 4. *Am J Hum Genet* **37,** 1117-1128.

YAP, L. B., ASHRAFIAN, H., MUKERJEE, D., COGHLAN, J. G. & TIMMS, P. M. (2004). The natriuretic peptides and their role in disorders of right heart dysfunction and pulmonary hypertension. *Clin Biochem* **37,** 847-856.

YASUTAKE, M., HAWORTH, R. S., KING, A. & AVKIRAN, M. (1996). Thrombin activates the sarcolemmal Na(+)-H+ exchanger. Evidence for a receptor-mediated mechanism involving protein kinase C. *Circ Res* **79,** 705-715.

YESNER, L. M., HUH, H. Y., PEARCE, S. F. & SILVERSTEIN, R. L. (1996). Regulation of monocyte CD36 and thrombospondin-1 expression by soluble mediators. *Arterioscler Thromb Vasc Biol* **16,** 1019-1025.

YIN, F. C., SPURGEON, H. A., RAKUSAN, K., WEISFELDT, M. L. & LAKATTA, E. G. (1982). Use of tibial length to quantify cardiac hypertrophy: application in the aging rat. *Am J Physiol* **243,** H941-947.

ZAMZAMI, N., MARCHETTI, P., CASTEDO, M., DECAUDIN, D., MACHO, A., HIRSCH, T., SUSIN, S. A., PETIT, P. X., MIGNOTTE, B. & KROEMER, G. (1995). Sequential

reduction of mitochondrial transmembrane potential and generation of reactive oxygen species in early programmed cell death. *J Exp Med* **182,** 367-377.

ZHANG, Y., DENG, Y., LUTHER, T., MULLER, M., ZIEGLER, R., WALDHERR, R., STERN, D. M. & NAWROTH, P. P. (1994). Tissue factor controls the balance of angiogenic and antiangiogenic properties of tumor cells in mice. *J Clin Invest* **94,** 1320-1327.

ZHOU, L., STORDEUR, P., DE LAVAREILLE, A., THIELEMANS, K., CAPEL, P., GOLDMAN, M. & PRADIER, O. (1998). CD40 engagement on endothelial cells promotes tissue factor-dependent procoagulant activity. *Thromb Haemost* **79,** 1025-1028.

ZHU, W., ZOU, Y., SHIOJIMA, I., KUDOH, S., AIKAWA, R., HAYASHI, D., MIZUKAMI, M., TOKO, H., SHIBASAKI, F., YAZAKI, Y., NAGAI, R. & KOMURO, I. (2000). Ca2+/calmodulin-dependent kinase II and calcineurin play critical roles in endothelin-1-induced cardiomyocyte hypertrophy. *J Biol Chem* **275,** 15239-15245.

ZIONCHECK, T. F., ROY, S. & VEHAR, G. A. (1992). The cytoplasmic domain of tissue factor is phosphorylated by a protein kinase C-dependent mechanism. *J Biol Chem* **267,** 3561-3564.

ZOLK, O., CARONI, P. & BOHM, M. (2000). Decreased expression of the cardiac LIM domain protein MLP in chronic human heart failure. *Circulation* **101,** 2674-2677.

ZOU, H., HENZEL, W. J., LIU, X., LUTSCHG, A. & WANG, X. (1997). Apaf-1, a human protein homologous to C. elegans CED-4, participates in cytochrome c-dependent activation of caspase-3. *Cell* **90,** 405-413.